Investigation of molecular pathways associated with Parkin

Hsiu-Chuan Wu

UCL Institute of Neurology

Thesis submitted in fulfilment of

the degree of Doctor of Philosophy (UCL)

Declaration:

I, Hsiu-Chuan Wu, confirm that the work presented in this thesis is my own. Where information has been derived from other sources, I confirm that this has been indicated in the thesis.

Abstract:

Parkinson's disease (PD) is an incurable neurodegenerative disease. Although the majority of PD cases are sporadic, 5-10% of cases are inherited. Studies of sporadic and genetic forms of PD suggest shared pathogenesis such as mitochondrial dysfunction. Mutations in the gene encoding Parkin are the most common cause of autosomal recessive, young-onset PD. Parkin has been shown to regulate mitochondrial quality control (mitophagy), however the molecular pathways that regulate Parkin activity remain poorly characterised. MEKK3/p38, MAPK/ERK, and PI3K/Akt signalling pathways have been described in association with Parkin regulation. In this thesis, I have investigated whether activation of any of these pathways could lead to Parkin phosphorylation by utilising inducible cell lines overexpressing MEKK3-ER, Raf-ER or Akt-ER genes. I found that Parkin was not phosphorylated following the activation of the p38, ERK and Akt pathways. In an attempt to depolarise mitochondria in neuroblastoma SH-SY5Y cells lines by mitochondrial uncoupler carbonyl cyanide m-chlorophenyl hydrazone (CCCP), I found that Parkin was phosphorylated at serine 101 (S101). In order to investigate the role of phosphorylation of Parkin S101 in mitochondrial quality control, I established SH-SY5Y clones stably expressing wild type (WT), non-phosphorylatable (S101A), or phosphomimetic (S101D) FLAG-Parkin. I found that this phosphorylation is associated with increased Parkin's E3 ligase activity. S101A cells showed deficiencies in translocation of Parkin to depolarised mitochondria, ubiquitination of outer mitochondrial membrane proteins, p62 (an autophagy adaptor) recruitment, perinuclear mitochondrial clustering and mitophagy. Overall the work presented in this thesis demonstrates that Parkin is activated during mitochondrial depolarisation, and that the regulation of Parkin function via phosphorylation at S101 plays an important role in mitochondrial quality control associated with PD pathophysiology.

Acknowledgement:

I'm deeply grateful to the many people I've come to know throughout these years in the lab. I would like to sincerely thank my supervisor, Hélène Plun-Favreau, for giving me this great opportunity to learn to be a scientist and offering her guidance, expertise and most important of all, endless support throughout my PhD and during the preparation of this thesis. I'm also grateful to John Hardy, who's always be there giving me invaluable suggestions and encouragement. I want to express my gratitude to Julia Fitzgerald for patiently guiding me to learn all the techniques I need since my first day in the lab. Thanks to Vikki Burchell for providing assistance in setting up qPCR and confocal imaging acquisition. I am grateful to Claudia Manzoni and Marc Soutar for their willingness to share their expertise in all the protein work, to Fernando Bartolome and Kira Holmström for helping me in live cell imaging, to Michael Devine and Selina Wray for technical support in stem cell work, to Una-Marie Sheerin for obtaining patient's skin biopsy, to Niccolo Mancacci and the genetic lab for the help in PCR and sequencing work, to Marta Delgado Camprubi for the contribution of data in chapter 3, and to Wolfdieter Springer for the contribution of data in chapter 5.

I'd especially like to thank all the postdocs and PhD students, past and present, who made my PhD an enjoyable experience. I'm truly blessed to share the same office with Claudia Manzoni, Daniah Trabzuni, Sybille Dihanich, Marc Soutar, Fernando Bartolome, Suran Nethisinghe, Boniface Mok, and Arianna Tucci. I'll really miss you and all those crazy talks about science, food, travel, culture, and so much more. An enormous thank you to Marc for reading this thesis many times and giving me invaluable feedbacks. I also need to thank Daniah and Boniface for helping the preparation of this thesis.

Last, I'd like to thank my family and friends for their support, especially my husband who shared all the housework with me while he was also doing a PhD same time as me, my two children who draw countless pictures every day to make me smile, and my parents who always encourage me to fly and follow my dream.

Table of Contents

Table of Figures

Table of Tables

Abbreviations

˚C	Degrees Celcius
4OH-Tx	4-hydroxytamoxifen
AMP	Adenosine monophosphate
AMPK	Adenosine monophosphate-activated protein kinase
ATP	Adenosine triphosphate
ATPase	Adenosine triphosphatase
ATP13A2	ATPase type 13A2
BAC	Bacterial artificial chromosome
CCCP	Carbonyl cyanide m-chlorophenyl hydrazone
Cdk5	Cyclin-dependent kinase-5
CK	Casein kinase
COR	C-terminal of Ras of complex protein
CREB	cAMP response element-binding protein
CT	Computed tomography
CNV	Copy number variation
DLB	Dementia with Lewy body
DNA	Deoxyribonucleic acid
DMSO	Dimethyl sulfoxide
DUB	Deubiquitinating enzyme
DTT	Dithiothreitol
E. coli	Escherichia coli
ECL	Enhanced chemiluminescence
EDTA	Ethylenediaminetetraacetic acid
EGFR	Epidermal growth factor receptor
EOPD	Early-onset Parkinson's disease
ETC	electron transport chain
ER	Endoplasmic reticulum
ERK	extracellular signal-regulated kinase
g/mg/ug/ng	Gram/milligram/microgram/nanogram (respectively)
GBA	Gene encoding glucocerebrosidase

GFP	Green florescence protein
GTPase	Guanosine triphosphatase
GWAS	Genome-wide association study
h/min/s	Hour/minute/second (respectively)
HECT	Homologous to the E6-AP Carboxyl Terminus (catalytic domain of E3 ubiquitin ligase)
HLA	Human leukocyte antigen
HRP	Horse radish peroxidase
HtrA2	Heat temperature requirement protein A2
IAP	Inhibitor of apoptosis
IBR	In-between-RING
IKK	IκB kinase
IMM	Inner mitochondrial membrane
iNOS	Inducible nitric oxide synthetase
iPSC	Induced pluripotent stem cell
JNK	Jun N-terminal kinases
kDa	Kilodalton
KO	Knockout
L/mL/uL	Litre/millilitre/microliter (respectively)
LB	Luria Broth
LB	Lewy bodies
LC	Locus coeruleus
LRRK2	leucine-rich repeat kinase 2
M/mM/uM/nM	Molar/millimolar/micromolar/nanomolar (respectively)
MAPK	Mitogen-activated protein kinase
MAPT	Gene encoding tau
Mb/kb	Megabase/kilobase (respectively)
MEF	Mouse embryonic fibroblast
MEKK	MAPK/ERK kinase kinase kinase
Mfn	mitofusin
MIRO1	Mitochondrial Rho GTPase 1
MLPA	Multiplex ligation-dependent probe amplification
MPP+	1-methyl-4-phenylpyridinium

MPTP	1-methyl-4-phenyl-1,2,3,6-tetrahydropyrindine
MRI	Magnetic resonance imaging
MSA	Multiple system atrophy
mtDNA	Mitochondrial deoxyribonucleic acid
mTOR	Mammalian target of rapamycin
NaCl	Sodium chloride
NCBI	National Center for Biotechnology Information
NEMO	NF-κB essential modifier
NF-κB	nuclear factor kappa-light-chain-enhancer of activated B cells
NHNN	National Hospital for Neurology and Neurosurgery
NIH	National Institute of Health
nNOS	Neuronal nitric oxide synthetase
NO	Nitric oxide
OMM	outer mitochondrial membrane
OXPHOS	Oxidative phosphorylation
PARL	Presenilins-associated rhomboid-like protein
PBS	Phosphate buffered saline
PCR	Polymerase chain reaction
PI3K	Phosphatidylinositide 3-kinase
PKA	protein kinase A
PD	Parkinson's disease
PET	Positron emission topography
pH	Potential of hydrogen, $-\log_{10}$ [H+]
PINK1	PTEN Induced putative Kinase-1
PTEN	Phosphatase and tensin homologue
PTM	Post-translational modification
PVDF	Polyvinylidene fluoride
qPCR	Quantative PCR
RBR	RING-in-between-RING
REP	Repressor element of Parkin
RING	Really Interesting New Gene (catalytic domain of E3 ubiquitin ligase)
RNA	Ribonucleic acid

ROC	Ras of complex proteins
ROS	Reactive oxygen species
rpm	Rotations per minute
RT	Room temperature
RT-PCR	Reversed transcription-PCR
s.e.m	standard error of mean
SDS	Sodium dodecyl sulfate
SDS-PAGE	Sodium dodecyl sulfate – polyacrylamide gel electrophoresis
shRNA	Small hairpin RNA
siRNA	Small interfering RNA
SNc	Substantia nigra pars compacta
SNCA	Gene encoding alpha-synuclein
SPECT	Single photon emission computed tomography
$STEP_{61}$	Striatal-enriched protein tyrosine phosphatase 61
SUMO	Small ubiquitin-related modifier
TFAM	Mitochondrial transcription factor A
TNF	tumor necrosis factor
TRAF2	tumor necrosis factor (TNF) receptor-associated factor 2
TRAP1	tumor necrosis factor (TNF) receptor-associated protein 1
Ub	ubiquitin
Ubl	ubiquitin-like
UBS	Ubiquitin proteasome system
UIM	Ubiquitin-interacting motif
VCP	Valosin-containing protein
VDAC	Voltage-dependent anion channel
WT	Wild type
βME	2-Mercaptoethanol

Three- and single-letter codes for amino acids

Side group	Amino acid	Three-letter code	Single-letter code
hydrophobic	Valine	val	V
	Leucine	leu	L
	Isolucien	ile	I
	Methionine	met	M
	Phenylalanine	phe	F
hydrophilic	Asparagine	asn	N
	Aspartic acid	asp	D
	Glutamine	gln	Q
	Glutamic acid	glu	E
	Histidine	his	H
	Lysine	lys	K
	Arginine	arg	R
In between hydrophobic and hydrophilic	Glycine	gly	G
	Alanine	ala	A
	Serine	ser	S
	Threonine	thr	T
	Tyrosine	try	Y
	Tryptophan	trp	W
	Cysteine	cys	C
	Proline	pro	P

Publications arising from this thesis:

Wu H-C, Caulfield TR, Manzoni C, Wang H-H, Soutar MPM, Wood NW, Hardy J, Springer W, Plun-Favreau H. *Parkin phosphorylation at serine 101 modulates mitophagy*. (Manuscript in preparation for resubmission)

Birsa N, Norkett R, Wauer T, Mevissen TET, **Wu H-C**, Foltynie T, Bhatia K, Hirst WD, Komander D, Plun-Favreau H, Kittler JT. *Lysine 27 ubiquitination of the mitochondrial transport protein Miro is dependent on serine 65 of the Parkin ubiquitin ligase.* J. Biol. Chem. 2014; 289(21): 14569-82

Bartolome F, **Wu H-C**, Burchell VS, Preza E, Wray S, Mahoney CJ, Fox NC, Calvo A, Canosa A, Moglia C, Mandrioli J, Chio A, Orrell RW, Houlden H, Hardy J, Abramov AY, Plun-Favreau H. *Pathogenic VCP mutations induce mitochondrial uncoupling and reduced ATP levels.* Neuron 2013; 78: 57-64

Fitzgerald JC, Camprubi MD, Dunn L, **Wu H-C**, Ip NY, Kruger R, Martins LM, Wood NW, Plun-Favreau H. *Phosphorylation of HtrA2 by cyclin-dependent kinase-5 is important for mitochondrial function.* Cell Death and Differentiation. 2012; 19: 257-66

Chapter 1 Introduction

1.1 Parkinson's disease

Parkinson's disease (PD) is the second most common neurodegenerative disorder, affecting about 2% of the population above 65 years old. The prevalence of PD increases with age (de Lau and Breteler, 2006). When the symptoms present before the age of 40, the disorder is called young-onset Parkinson's disease (YOPD) (Quinn et al., 1987).

The clinical presentations of the disease were first described in 1817 by James Parkinson, whose monograph ''An Essay on the Shaking Palsy'' portrayed the principal clinical symptoms of the disease, such as involuntary tremor in rest, stooped posture and festinating gait (Parkinson, 1817). The intellects and senses were not affected. The French neurologist Jean Martin Charcot brought the term 'Parkinson's disease' into describing these associated symptoms in 1877 in order to conferring the honour to Parkinson (Lees, 2007). According to the criteria established by UK Parkinson's Disease Society Brain Bank, PD is diagnosed with presentation of bradykinesia plus at least one of the following symptoms: rigidity, resting tremor at between 4-6 Hz, or postural instability (Table 1-1 summary of clinical diagnosis of PD).

Brain computed tomography (CT) and magnetic resonance imaging (MRI) scans of PD patients are usually normal, the measurement of dopaminergic function in basal ganglia by positron emission topography (PET) or single-photon emission computed tomography (SPECT) scan can aid in diagnosing PD when dopamine

activity is decreased (Brooks, 2010; Brooks et al., 2003). The definite diagnosis of idiopathic PD, however, requires histological demonstration of Lewy bodies (LB) inclusions in surviving neurons of the substantia nigra compacta (SNc), which is one of the main characteristics of the disease (Hughes et al., 1992). The main component of LB is α-synuclein, and many other molecules such as ubiquitin and tubulin have also been found in these eosinophilic cytoplasmic inclusions (Shults, 2006). Another prominent neuropathological hallmark of PD is a progressive loss of dopaminergic neurons in SNc and locus coeruleus (LC), and these pathological changes could present preclinically (Hughes et al., 1992). By the time PD symptoms appear, at least 50% of dopaminergic neurons are dead, along with an 80% reduction of dopamine levels (Marsden, 1990).

The aetiology of PD remains elusive; both environmental and genetic risk factors have been identified. Environmental factors such as rural residency (Behari et al., 2001; Rajput and Uitti, 1988; Rajput et al., 1986), agricultural industry (Barbeau et al., 1987; Fall et al., 1999; Gorrell et al., 1996), or consumption of well water (Tanner and Goldman, 1996) have been reported to increase the risk of PD. In addition, exposure to some herbicides, organochloride pesticides, paraquat, annonacin, manganese, 1-methyl-4-phenyl-1,2,3,6-tetrahydropyridine (MPTP) , or rotenone has been found to associate with PD (Schapira, 2006). Rapid onset of parkinsonism was first discovered in uses of illegal drugs containing MPTP (Langston et al., 1984). Although MPTP is not toxic itself, its metabolite cation, 1-methyl-4-phenylpyridinium (MPP+), interferes with Complex I of electron transport chain (ETC) in mitochondria (Schapira et al., 1990). This results in gross dopaminergic neuronal death. Rotenone, another Complex I inhibitor, also produces parkinsonism in experimental animals by causing dopaminergic neuronal death (Schapira et al., 1990). Conversely, two environmental factors have been reported to reduce the risk of PD: caffeine (Ascherio et al., 2001) (Ascherio et al., 2001) and smoking (Baron, 1986; Quik, 2004). The molecular mechanism by which these factors modify the risk of PD is unclear.

Over the last two decades, the role of genetic factors in PD pathogenesis has been unravelled by studies such as linkage analysis and genome–wide association studies. The details will be described in the next section. Genetic advances have enormous impact on the understanding of molecular pathways implicated in PD pathogenesis, such as mitochondrial dysfunction, oxidative stress, and misfolded proteins accumulation (reviewed in (Dawson and Dawson, 2010; Devine and Lewis, 2008; Exner et al., 2012; Fitzgerald and Plun-Favreau, 2008; Martin et al., 2011; Shulman et al., 2011)). Notably, there is increasing evidence that mitochondrial dysfunction may be a common pathogenic mechanism for both sporadic and familial PD. As mentioned above, the two ETC Complex I inhibitors, MPTP and rotenone, cause parkinsonian pathology in animal models (Schapira et al., 1990). Reduced Complex I activity in the SNc and frontal cortex of PD patients at autopsy further supports the role of Complex I dysfunction in sporadic PD (Schapira et al., 1989). Additionally, a dopaminergic neuron-specific deletion of the mitochondrial DNA (mtDNA) transcription factor TFAM in mice cause parkinsonian features. In the SNc of post mortem human brain, there is also an age-dependent increase in mtDNA deletion (Bender et al., 2006). Although there is no strong evidence that mtDNA mutations are major risk for PD, Complex I is particularly vulnerable to mtDNA damage (Exner et al., 2012). When mtDNA mutations surpass a critical threshold, the respiratory deficiency may contribute to dopaminergic neuronal death.

Diagnosis of Parkinsonian syndrome
Bradykinesia and at least one of the following: 1. muscular rigidity; 2. 4-6 Hz resting tremor; 3. postural instability not caused by primary visual, vestibular cerebellar, or proprioceptive dysfunction.
Exclusion criteria for Parkinson's disease
History of: 1. repeated strokes with stepwise progression of parkinsonian features, 2. repeated head injury 3. definite encephalitis Oculogyric crises Neuroleptic treatment at onset of symptoms More than one affected relative Sustained remission Strictly unilateral features after 3 years Supranuclear gaze palsy Cerebellar signs Early severe autonomic involvement Early severe dementia with disturbance of memory, language and prexia Babinski sign Presence of cerebral tumour or communicating hydrocephalus on computed tomography scan Negative response to large doses of levodopa (if malabsorption excluded) 1-methyl-4-phenyl1,2,3,6-tetrahydropyridine hydrochloride (MPTP) exposure
Supportive prospective positive criteria for Parkinson's disease (three or more required for diagnosis of definite Parkinson's disease)
Unilateral onset Resting tremor present Progressive disorder Persistent symmetry affecting side of onset most Excellent response (70-100%) to levodopa Severe levodopa-induced chorea Levodopa response for 5 years or more Clinical course of 10 years or more

Table 1-1 UK Parkinson's Disease Society Brain Bank Clinical Diagnostic Criteria.

(Adapted from (Twelves et al., 2003))

1.2 Genetics of Parkinson's disease

PD has long been considered as a sporadic disease. Over the past two decades, however, a number of genes have been identified to be associated with PD (Table 1-2), and these familial PD cases account for about 5-10% of all PD cases (Gasser, 2001). The genes with conclusive evidence of disease association are *SNCA*, *LRRK2 (leucine-rich repeat kinase 2)*, *Parkin*, *PINK1 (phosphatase and tensin homologue (PTEN)-induced putative kinase 1)*, *DJ-1* and *ATP13A2 (ATPase type 13A2)*. The first reported gene, *SNCA*, is associated with to autosomal dominant PD. It encodes α-synuclein which is found abundantly in LB (Polymeropoulos et al., 1997; Singleton et al., 2003). Mutations in *LRKK2*, which encodes a large protein with a kinase and a GTPase function, also lead to autosomal dominant early-onset PD (EOPD) (Paisan-Ruiz et al., 2004; Zimprich et al., 2004). The four other PD genes are inherited in an autosomal recessive fashion. *Parkin* encodes an E3 ubiquitin ligase (Kitada et al., 1998), *PINK1* encodes a mitochondrial kinase (Valente et al., 2004), *DJ-1* encodes a redox sensor (Bonifati et al., 2003), and *ATP13A2* encodes lysosomal pump (Ramirez et al., 2006)

Several genes or loci have also been identified as susceptibility factors for PD (Table 1-3). A multicentre study demonstrated that mutations in *GBA*, which encodes a lysosomal glycosylceramidase, is strongly associated with PD (odds ratio 5.43) (Bras et al., 2008; Sidransky et al., 2009). Genome-wide association studies (GWASs), on the other hand, identified several common, low risk variants (odds ratio < 2) in association with sporadic PD. These loci locate in *SNCA*, *MAPT*, and *HLA* (Hamza et al., 2010; Simon-Sanchez et al., 2009). The association between *LRRK2* and sporadic PD seen in GWAS remains unclear (Hardy, 2010). The investigation on the functions of these PD-associated genes has considerably improved our understanding of PD pathogenesis.

Park locus	Map position	Gene	Functions	Forms of PD	Reference
Autosomal dominant					
PARK1/4	4q21	*SNCA*	Synaptic protein	LOPD	(Polymeropoulos et al., 1997; Singleton et al., 2003)
PARK3	2p13	unknown	unknown	LOPD	(Gasser et al., 1998)
PARK5	4p14	*UCHL-1*	Ubiquitin C-terminal hydroxylase	LOPD	(Leroy et al., 1998)
PARK8	12q12	*LRRK2*	Kinase / GTPase	LOPD	(Paisan-Ruiz et al., 2004; Zimprich et al., 2004)
PARK11	2q36-37	*GIGYF2*	Regulation of tyrosine receptor kinase signalling?	LOPD	(Lautier et al., 2008)
Autosomal recessive					
PARK2	6q25-27	*Parkin*	E3 ubiquitin ligase	Juvenile and EOPD	(Kitada et al., 1998)
PARK6	1p35-36	*PINK1*	Mitochondrial kinase	EOPD	(Valente et al., 2004)
PARK7	1p36	*DJ-1*	Redox sensor	EOPD	(Bonifati et al., 2003)
PARK9	*1p36*	*ATP13A2*	*Lysosomal ATPase*	*Juvenile Kufor-Rakeb syndrome and EOPD*	*(Ramirez et al., 2006)*
PARK14	22q13.1	*PLA2G6*	A2 phospholipase	Juvenile levodopa-responsive dystonia- parkinsonism	(Paisan-Ruiz et al., 2009)

PARK15	22q12-13	*FBXO7*	E3 ubiquitin ligase	EO parkinsonism-pyramidal syndrome	(Di Fonzo et al., 2009b; Shojaee et al., 2008)
Unclear					
PARK10	1p32	Unknown	Unknown	LOPD	(Li et al., 2002)
PARK12	Xq21-25	Unknown	Unknown	Not clear	(Pankratz et al., 2002)
PARK13	2p13	*Omi/HtrA2*	Mitochondrial protease	Not clear	(Bogaerts et al., 2008; Strauss et al., 2005)
PARK16	1q32	unknown	unknown	Not clear	(Satake et al., 2009)

Table 1-2 Genes and loci associated with monogenic parkinsonism

PARK Locus	Gene	Map Position	Risk variants	Approximate Odds Ratio for PD	Reference
Not assigned	*GBA*	1q21	>300 mutations including; N370S and L444P	5.4	(Sidransky et al., 2009)
PARK1/ PARK4	*SNCA*	4q21	REP1 repeat polymorphism, multiple SNPs in 3' half of gene	1.2-1.4	(Simon-Sanchez et al., 2009)
Not assigned	*MAPT*	17q21.1	H1 haplotype	1.4	(Simon-Sanchez et al., 2009)
PARK18	*HLA-DRA*	6p21.3	Multiple SNPs from GWASs	1.3	(Hamza et al., 2010)
PARK8	*LRRK2*	12q12	G2385R, R1628P	2.0-2.2	(Kachergus et al., 2005)

Table 1-3 Susceptibility genes/loci for Parkinson's disease

1.2.1 Autosomal dominant PD: α-synuclein and LRRK2

Mutations in *SNCA*, the gene encoding α-synuclein, was the first gene locus found to associate with dominantly inherited EOPD (Polymeropoulos et al., 1997). Both missense mutations and genomic multiplications in *SNCA* cause EOPD and lead to dementia (Kruger et al., 1998; Polymeropoulos et al., 1997; Ross et al., 2008a; Zarranz et al., 2004). A gain of toxic function mechanism was suggested by the dominant inheritance pattern of *SNCA* mutations, although the precise function of α-synuclein remains poorly understood. The finding of α-synuclein as a major component of LB suggests an important role of α-synuclein in the pathogenesis of sporadic PD (Spillantini et al., 1997). Studies in sporadic and familial PD patients have revealed susceptibility variants located in the *SNCA* gene (Dickson et al., 2009; Ross et al., 2007). Several recent studies suggest that the accumulation of mutant α-synuclein alters mitochondrial morphology or fission/fusion process (Banerjee et al., 2010; Calì et al., 2012; Devi et al., 2008; Kamp et al., 2010; Nakamura et al., 2011; Xie and Chung, 2012). However, the precise relationship between aggregation, mitochondrial dysfunction and cell death caused by mutant α-synuclein remains largely unknown.

Mutations in *LRRK2* also cause EOPD with clinical features indistinguishable from the sporadic form of PD. The encoded multidomain protein, has 2527 amino acids. More than 40 different *LRRK2* mutations have been reported. To date, six missense mutations (R1441C, R1441G, R1441H. Y1699C, G2019S and I2020T) have been identified as pathogenic and all are highly penetrant (Li et al., 2014; Manzoni et al., 2013; Wider et al., 2010). Amongst them, kinase domain-located G2019S is the most common disease linked mutation in European (Kachergus et al., 2005). Both R1629P (Ross et al., 2008b) and G2385R (Di Fonzo et al., 2006) have been described as risk factors associated with PD in eastern Asian populations. Mutations in the kinase domain has been consistently associated with an increased kinase activity (Greggio et al., 2006), whereas mutations in ROC (Ras of complex proteins) or COR (C-terminal of ROC) domains display a reduced GTPase activity (Daniels et al., 2011; Greggio and

Cookson, 2009; Lewis et al., 2007; Li et al., 2007; West et al., 2005). LRRK2 has been implicated in several cellular process , including the neurite branching regulation, autophagy , protein synthesis through the mTOR (mammalian target of rapamycin) pathway, and mitochondrial quality control (Alegre-Abarrategui et al., 2009; Cherra et al., 2013; Cookson, 2010; Manzoni et al., 2013).

1.2.2 Autosomal recessive PD: PINK1, Parkin, DJ-1, ATP13A2, FBXO7 and HtrA2

Mutation in *Parkin* are the most common cause of EOPD (Kitada et al., 1998), particularly in patient with recessive inheritance (Lucking et al., 2000). Parkin is a cytosolic E3 ubiquitin ligase (Shimura et al., 2000) with multiple functions. In addition to facilitating proteasomal degradation of target proteins, recent studies have suggested that Parkin acts downstream of PINK1 in the common pathway of mitochondrial quality control process (Clark et al., 2006; Exner et al., 2007; Park et al., 2006; Poole et al., 2008; Yang et al., 2006; Yang et al., 2008), indicating the important role of mitochondrial dysfunction in PD pathogenesis. Details of Parkin will be further described in 1.3.

Mutations in *PINK1*, although much rarer than *Parkin*, also causes autosomal recessive EOPD with clinical features indistinguishable to those caused by *Parkin* mutations (Valente et al., 2004). The neuropathological investigation of persons with homozygous pathogenic mutations has never been reported, although heterozygous cases reported demonstrate LB pathology of unclear pathogenic relevance (Gandhi et al., 2006). The majority of PINK1 mutations occur in the kinase domain or otherwise impair kinase activity (Deas et al., 2009). PINK1 is a protein kinase located in mitochondrial membranes (Gandhi et al., 2006). In healthy mitochondria where membrane potential is high, PINK1 is imported into inner mitochondrial membrane (IMM) where it is cleaved by presenilins-associated rhomboid-like protein (PARL) and the ~53kDa cleaved-form PINK1 is cleared from the outer mitochondrial membrane (OMM) (Deas et al., 2011b). In damaged mitochondria where membrane potential is low, the 63 kDa full-length PINK1 is accumulated on OMM to recruit Parkin for the

subsequent mitophagy process (Narendra et al., 2008). The exact activators of PINK1 are currently unknown. PINK1 has been shown to phosphorylate TNF receptor-associated protein 1 (TRAP1) (Pridgeon et al., 2007), High temperature requirement protein A2 (HtrA2) (Plun-Favreau et al., 2007), and Parkin (Kondapalli et al., 2012; Shiba-Fukushima et al., 2012), further supporting its important role in maintaining mitochondrial integrity.

Mutations in *DJ-1* are a rare cause of autosomal recessive EOPD (Abou-Sleiman et al., 2003; Bonifati et al., 2003; Haque et al., 2008; Hedrich et al., 2004). No neuropathological examination of homozygous pathogenic DJ-1 patient has been described yet, so it is uncertain whether this is a LB disorder or not. The precise function of the protein is not clear, although it translocates to mitochondria in response to oxidative stress (Canet-Aviles et al., 2004). Mitochondrial oxidative damage, depolarisation and fragmentation have been associated with *DJ-1* loss-of-function mutations (Irrcher et al., 2010; Thomas et al., 2011), suggesting a protective function of DJ-1 to safeguard neurons from oxidative stress (Zhou et al., 2006). However, its physiological function and the mechanism by which it exerts this protective effect remain to be determined (Cookson and Bandmann, 2010).

Mutations in *ATP13A2* have been found in families with Kufor-Rakeb syndrome, characterised by atypical juvenile-onset parkinsonism with pyramidal degeneration and cognitive dysfunction (Ramirez et al., 2006). A homozygous mutation was later described in a sporadic patient presenting juvenile-onset parkinsonism, impaired upward gaze and moderate brain atrophy (Di Fonzo et al., 2007). This gene encodes a lysosomal ATPase, but it is not clear what its substrate is. Since α-synuclein aggregates are cleared by lysosomal degradation, it is likely that lysosomal dysfunction caused by mutations in *ATP13A2* or other PD-associated lysosomal gene *GBA* contributes to the pathogenesis of parkinsonism (Pan et al., 2008).

Mutations in *FBXO7* cause parkinsonism with the combination of extrapyramidal and pyramidal symptoms. A number of mutations haven been

reported in families from Europe and Asia (Di Fonzo et al., 2009a; Paisán-Ruiz et al., 2010; Shojaee et al., 2008). FBXO7 is a member of the F-box family of proteins that functions as adaptors for E3 ubiquitin ligase complex named SCF (Skp1-Cul1-F-box) complex (Skowyra et al., 1997). Pathogenic mutations in *FBXO7* have been reported to affect mitophagy process, thereby reducing Parkin recruitment to depolarised mitochondria and mitofusin 1 (Mfn1) ubiquitination for subsequent mitophagy (Burchell et al., 2013).

Mutations in *HtrA2* have been reported to associate with PD since a heterozygous mutation has been found in four patients and a genetic polymorphism has been associated with PD (Strauss et al., 2005). *HtrA2* encodes a mitochondria-located protease (Bogaerts et al., 2008; Strauss et al., 2005). It was first described as a pro-apoptotic factor when few groups reported that HtrA2 is released from mitochondrial intermembrane space where it binds a number of inhibitors of apoptosis (IAPs) (Jones et al., 2003; Martins et al., 2002; Verhagen et al., 2002). This releases the inhibitory effects of IAPs on caspases and induces subsequent cell death. On the contrary, HtrA2 knockout (KO) mice or mice carrying a loss-of-function mutation were found to exhibit severe neurodegeneration, supporting an neuroprotective role for HtrA2 (Jones et al., 2003; Martins et al., 2004). As described earlier, upon activation of the p38 signalling pathway, HtrA2 is phosphorylated by PINK1 at S142 (Plun-Favreau et al., 2007) whereby protease activity is enhanced, as well as by cyclin-dependent kinase-5 (Cdk5) at S400 (Fitzgerald et al., 2012) whereby mitochondrial health is maintained. However, the downstream function of HtrA2 remains largely unclear. Due to the genetic association study has not been reproducible, mutations in HtrA2 are likely to be a risk factor for PD.

1.3 Parkin: an E3 ubiquitin ligase

1.3.1 Gene structure and pathogenic mutations

Parkin is encoded by a gene of 12 exons that spans 1.38 Mb in the long arm of chromosome 6 (6q25.2-q27) (Kitada et al., 1998). Mutations in *Parkin* are most commonly identified in early onset Parkinson's disease (EOPD) (Hedrich et al., 2002; Lucking et al., 2000). About 50% of EOPD patients with a family history of autosomal recessive inheritance carry mutations in the *Parkin* gene (Lucking et al., 2000). Mutations in this gene have also been identified in 15% to 18% of sporadic EOPD cases (Broussolle et al., 2000; Hedrich et al., 2002; Periquet et al., 2003), suggesting that Parkin plays an important role in the pathogenesis of both familial and sporadic PD.

A large number of mutations, including exonic copy number variations (deletions/duplications), sequence substitutions, and insertions, have been reported in *Parkin* (Marder et al., 2010; West et al., 2002). Copy number variation (CNV) mutations commonly occur between exons 2 and 7 (Marder et al., 2010; West et al., 2002). The exon rearrangements in *Parkin* gene are summarised in Figure 1-1 (Figure 1-1 A), whist the missense and nonsense mutations are summarised in Figure 1-1(Figure 1-1B) (Mizuno et al., 2006). The pathogenic mutations in *Parkin* are usually homozygous or compound heterozygous, whilst the role of heterozygous mutations in increasing the risk for PD remains controversial (Klein et al., 2007). Hypotheses that support the heterozygous mutations as a risk of PD include haploinsufficiency (Foroud et al., 2003; Sun et al., 2006), and a subclinical reduction in dopamine metabolism in sporadic PD patients with heterozygous mutations in *Parkin* (Hilker et al., 2001).

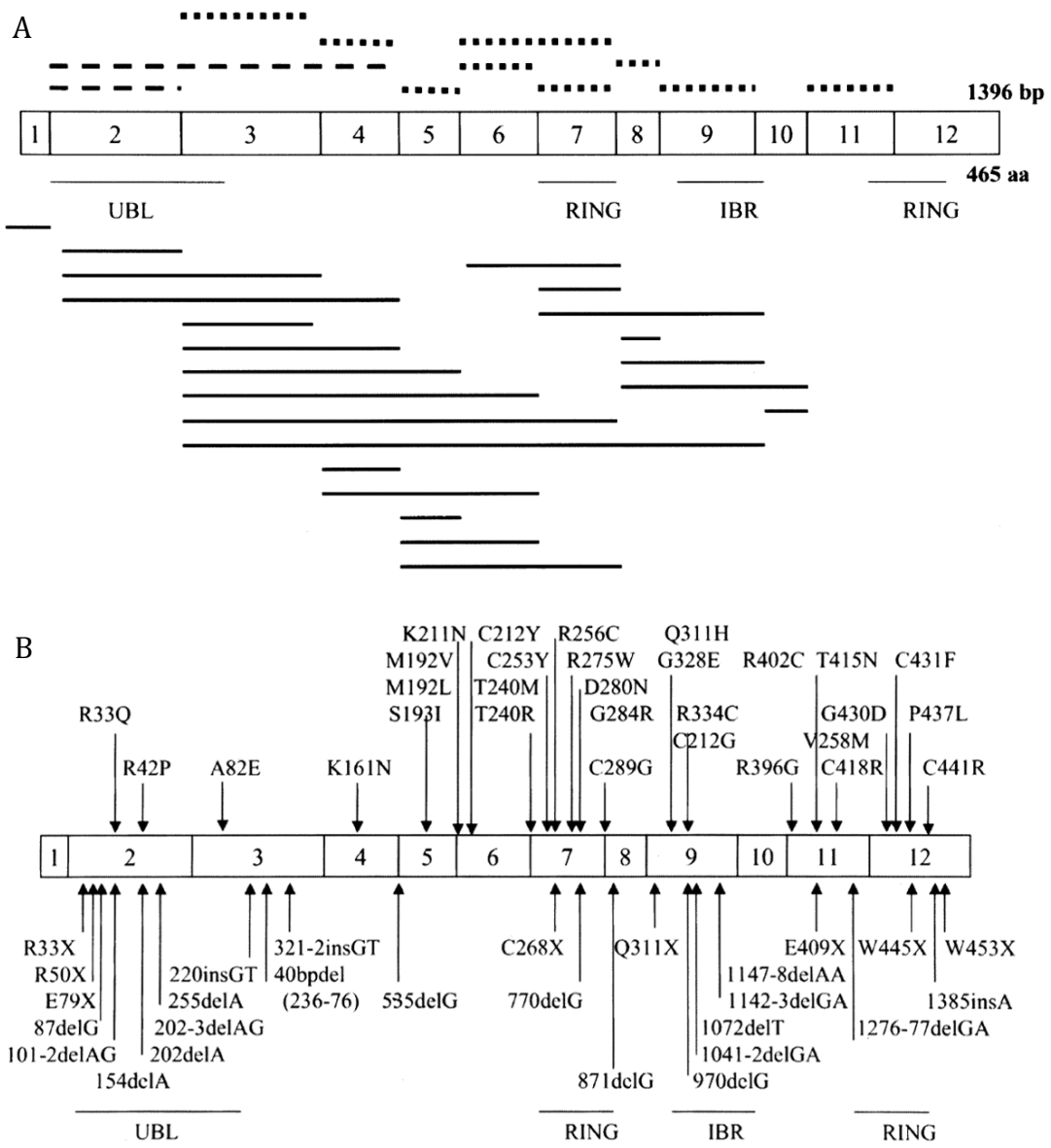

Figure 1-1 Parkin gene structure

(A) Schematic presentation of exons of *Parkin* and its exon rearrangement. (B) Schematic presentation of exons of *Parkin* and missense mutations, nonsense mutations, and small deletions (Figures adapted from (Mizuno et al., 2006))

1.3.2 Protein structure and localisation

Parkin is a 465-amino acid RING (Really Interesting New Gene)-in-between-RING (RBR) type E3 ubiquitin ligase that consists of an N-terminus ubiquitin-like (Ubl) domain, a linker and four RING finger domains, namely RING0, RING1, in-between-RING (IBR), and RING2 (Kitada et al., 1998; Trempe et al., 2013) (Figure 1-2 A). Recent resolution of full-length Parkin crystal structure reveals that RING1 is the only domain with classical C3HC4 (C: cysteine, H: histidine) cross-brace zinc-coordination topology characteristic of a canonical RING. RING0 demonstrates an atypical hairpin topology, and IBR and RING2 display sequential topologies (Trempe et al., 2013) (Figure 1-2 B).

Parkin is expressed abundantly in the brain, heart, skeletal muscles, testis (http://www.uniprot.org/uniprot/O60260), and at lower level in fibroblasts and peripheral leukocytes (Kasap et al., 2009; Nakaso et al., 2006). Although the Parkin subcellular localisation is mainly cytosolic (Shimura et al., 2000), Parkin was observed in Golgi apparatus (Huynh et al., 2007; Kubo et al., 2001), endoplasmic reticulum (ER) (Imai et al., 2001), mitochondria (Darios et al., 2003; Narendra et al., 2008), aggresomes (Muqit et al., 2004), neurites (Huynh et al., 2001), and synaptic vesicles (Kubo et al., 2001; Zhang et al., 2000). Some pathogenic mutations in Parkin, of which the catalytic activity is retained, have been reported to alter Parkin localisation, thereby forming aggresome-like structures (Cookson et al., 2003; Sriram et al., 2005; Wang et al., 2005b).

A

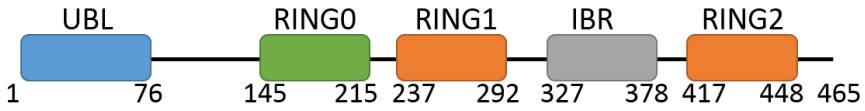

B

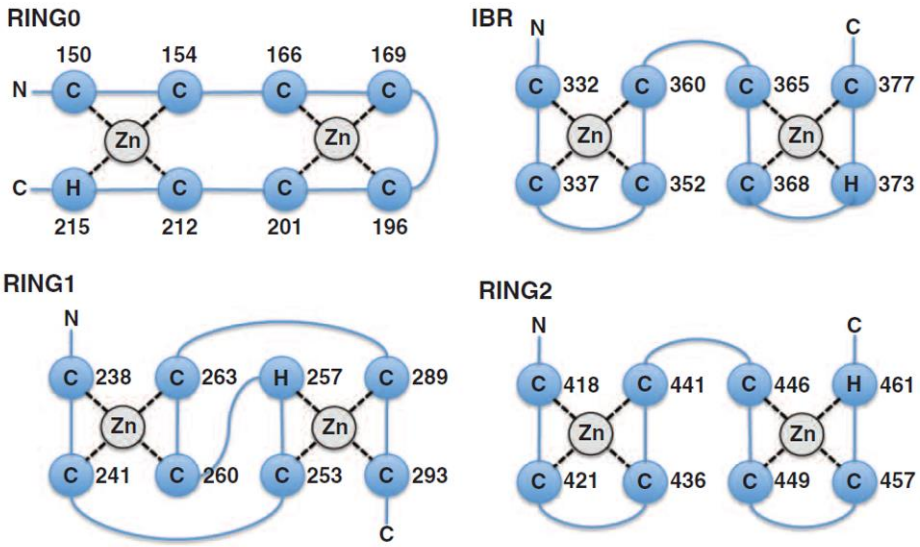

Figure 1-2 Domains of full-length Parkin and topology of its zinc-finger domains.

(A) Diagram of Parkin domains with domain names on the top and amino acid numbers for domain boundary at the bottom. (B) Cysteine (C) or Histidine (H) zinc-finger domains are shown in blue circles connecting by lines from the N- to the C-terminus. (Figure 1-2 B adapted from (Wauer and Komander, 2013))

1.3.2.1 Effects of protein domains on Parkin's E3 ubiquitin ligase activity

A number of studies have also shown that Parkin is tightly folded, hence auto-inhibited (Chaugule et al., 2011; Trempe et al., 2013; Wauer and Komander, 2013). This is suggested by two major structural features: first the RING0:RING2 interface that buries the catalytic Cys431 on RING2, and second the REP (Repressor element of Parkin):RING1 interface that occludes E2 ubiquitin-conjugating enzyme binding site on RING1 (Trempe et al., 2013; Wauer and Komander, 2013) (Figure 1-3 A&B). Large-scale conformational changes appear to be required to open up these two interfaces and further activate Parkin.

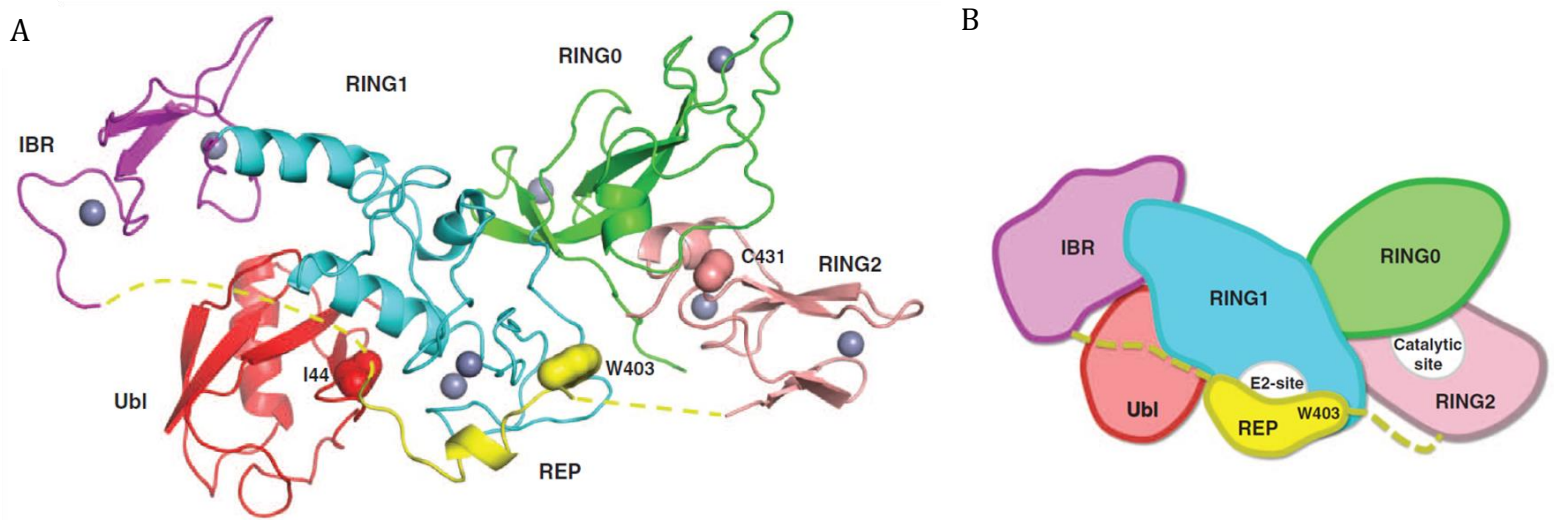

Figure 1-3 Structure of Parkin.

(A) Full-length Parkin domain structures are rendered in ribbon with colour by domain. Ubl: red. REP: yellow. RING0: green. RING1: blue. IBR: purple. RING2: pink. Zinc atoms: grey spheres. The REP α-helix is flanked by unstructured regions (yellow dashed lines). (B) Schematic representation of full-length Parkin in the same colour scheme as (A), showing the occluded E2 binding site on RING1 and catalytic site on RING2. (Figures adapted from (Wauer and Komander, 2013))

1.3.2.2 Alteration of protein characteristics by pathogenic mutations

Mutations in Parkin change its solubility, subcellular localisation, and activity (Hampe et al., 2006; Henn et al., 2005; Matsuda et al., 2006; Sriram et al., 2005; Wang et al., 2005b). Altered parkin solubility has been suggested as a potential mechanism of parkin dysfunction in both familial and sporadic PD. For instance, deletion of Parkin N-terminal Ubl domain has been shown to reduce Parkin stability, whereas C-terminal deletion either induce misfolding and aggregation of Parkin or impair the association of parkin with cellular membranes, hence changing its cellular localization (Henn et al., 2005). Similarly, pathogenic mutations in the Ubl domain were shown to cause rapid degradation of parkin (Finney et al., 2003; Henn et al., 2005). Parkin solubility is reduced by several pathogenic mutations, most of which have been reported to reside in the RING domains (Cookson et al., 2003; Hampe et al., 2006; Henn et al., 2005; Sriram et al., 2005) (Figure 1-4) . Several studies show that oxidative stress also reduces parkin solubility (Jensen et al., 2006; Wang et al., 2005a; Wong et al., 2007).

Whilst most pathogenic Parkin point mutations reduce or abolish its catalytic activity, point mutations in the RING0 (F146A) or RING2 (F463A) potentially interrupt the RING0:RING2 interface, thus increasing Parkin autoubiquitination activity (Trempe et al., 2013; Wauer and Komander, 2013). Similarly, a W403A mutation in the REP increases Parkin mitochondrial recruitment, which is likely due to a reduced auto-inhibition by REP (Trempe et al., 2013).

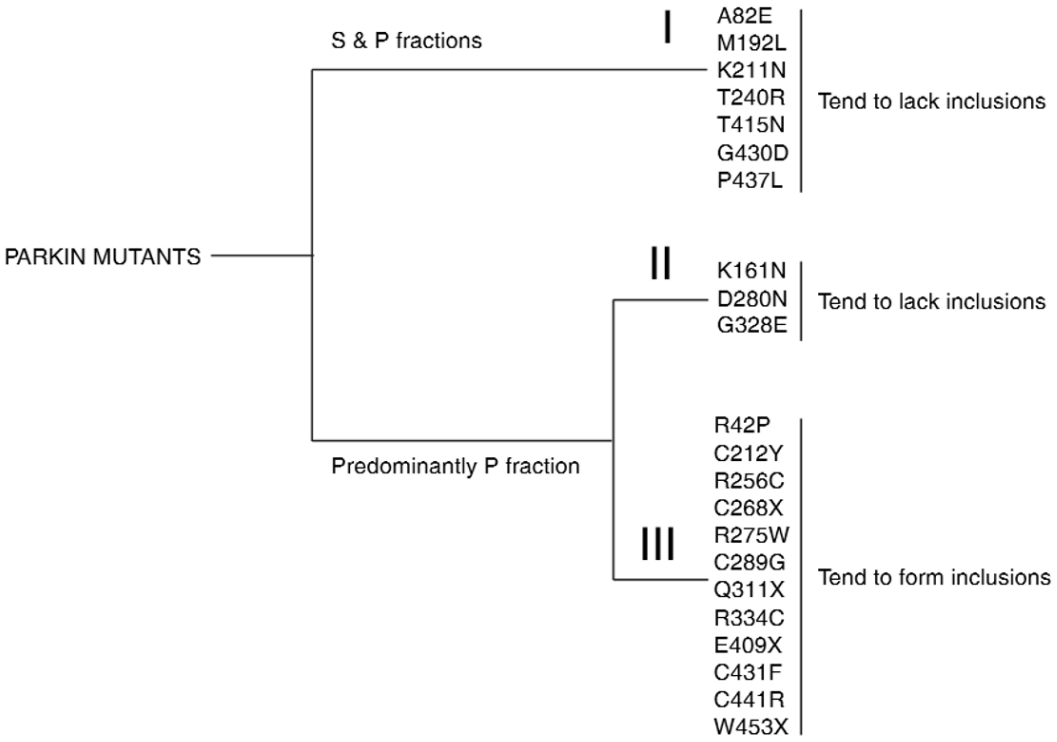

Figure 1-4 Altered Parkin solubility in pathogenic Parkin mutation.

Parkin mutants examined can be categorized into 3 groups: Group I – Soluble; II – Insoluble with low tendency to form inclusions; and III – Insoluble with high tendency to form inclusions. S and P fractions refer to Triton-X-100 and SDS extractable fractions, respectively. (Figure adapted from (Wang et al., 2005b))

1.3.3 Functions of Parkin

1.3.3.1 E3 ubiquitin ligase

The E3 ubiquitin ligase Parkin, as described earlier, is a component of the ubiquitin proteasome system (UPS) (Figure 1-5). Parkin is involved in the ubiquitin-dependent degradation of proteins by assembling lysine48- (K48)-linked polyubiquitin chains (Pickart and Fushman, 2004). Parkin can also catalyse K63 polyubiquitination or multiple monoubiquitination, which are implicated in various cellular processes including signal transduction, membrane trafficking, DNA repair, histone regulation or endocytosis (Doss-Pepe et al., 2005; Fallon et al., 2006; Winklhofer, 2007). Upon mitochondria depolarisation, Parkin catalyses K27 ubiquitination of voltage-dependent anion channel 1 (VDAC1) and Miro1 (Birsa et al., 2014; Geisler et al., 2010). An absolute quantitative proteomics study recently demonstrates that mitochondrial depolarisation leads to the assembly of K6, K11, K48, and K63 ubiquitin chains on damaged mitochondria in a manner that requires phosphorylation of Parkin S65 and Parkin's catalytic activity (Ordureau et al., 2014). USP30, which is a type of mitochondrion-localised deubiquitinating enzymes (DUBs), has been shown to preferentially remove Parkin-catalysed K6- and K11-linked ubiquitin chains on depolarised mitochondria (Cunningham et al., 2015). It is not as yet clear how Parkin-mediated noncanonical ubiquitination (K6 and K11) is relevant to the PD pathogenesis.

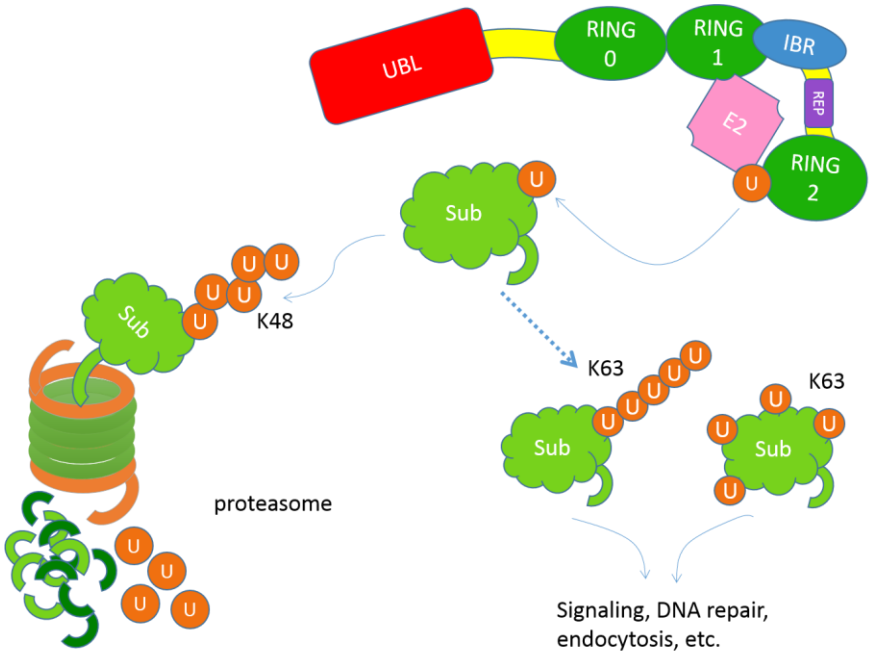

Figure 1-5 Parkin as an E3 ubiquitin ligase.

Schematic cartoon of Parkin binds to E2 to mediate ubiquitination of its substrate. K48-linked ubiquitination leads to proteasomal degradation of the substrate. K63-linked ubiquitination functions in subsequent signal transduction, DNA repair, or endocytosis.

Overview of UPS:

Ubiquitin is a highly conserved peptide of 76 amino acids. The covalent binding of chains of ubiquitin molecules to cytoplasmic or nuclear proteins elicits a signal that directs these ubiquitinated proteins to the 26S proteasome for further degradation (Wilkinson, 1995). This cellular process, named ubiquitination, is an enzymatic cascade involving three classes of enzymes: E1s (ubiquitin-activating enzymes), E2s (ubiquitin-conjugating enzymes), and E3s (ubiquitin ligases) (Hochstrasser, 1996). The E1 activates ubiquitin by forming a thiol-ester bond between the carboxyl terminus of ubiquitin and the E1. This ATP-dependent process is then followed by the transfer of the activated ubiquitin from the E1 to the E2. The E3 ligase then interacts with its specific substrate and ubiquitin-linked E2 and facilitates the transferral of ubiquitin from the E2 to the substrate. The specificity of substrate recognition depends largely on the E3 level or the E2-E3 interaction (Hershko and Ciechanover, 1998; Weissman, 1997). Ubiquitin can be attached to target proteins as a single molecule on one or multiple sites, yielding mono- and multi-monoubiquitinated proteins, respectively. Polyubiquitination refers to the formation of an ubiquitin chain on target proteins by multiple ubiquitin molecules that are linked through one of the seven ubiquitin lysine (K) residues (which are K6, K11, K27, K29, K33, K48 and K63) or through the ubiquitin amino terminal methionine1 residue (which generates linear chains) (Figure 1-6 A). Linkage types have been classified as having either 'compact' (K6-, K11-, and K48-linked) (Bremm et al., 2010; Bremm and Komander, 2011; Cook et al., 1992; Eddins et al., 2007; Matsumoto et al., 2010; Virdee et al., 2010) or 'open' (K63- and Met1-linked) (Datta et al., 2009; Komander et al., 2009) conformations. In the compact conformations the distal (that is, linked via its C terminus) and the next proximal (that is, linked via its Lys residue) ubiquitin moieties form an intramolecular interface, whereas in the open conformation the linkage point is the only contact (Kulathu and Komander, 2012) (Figure 1-6 B).

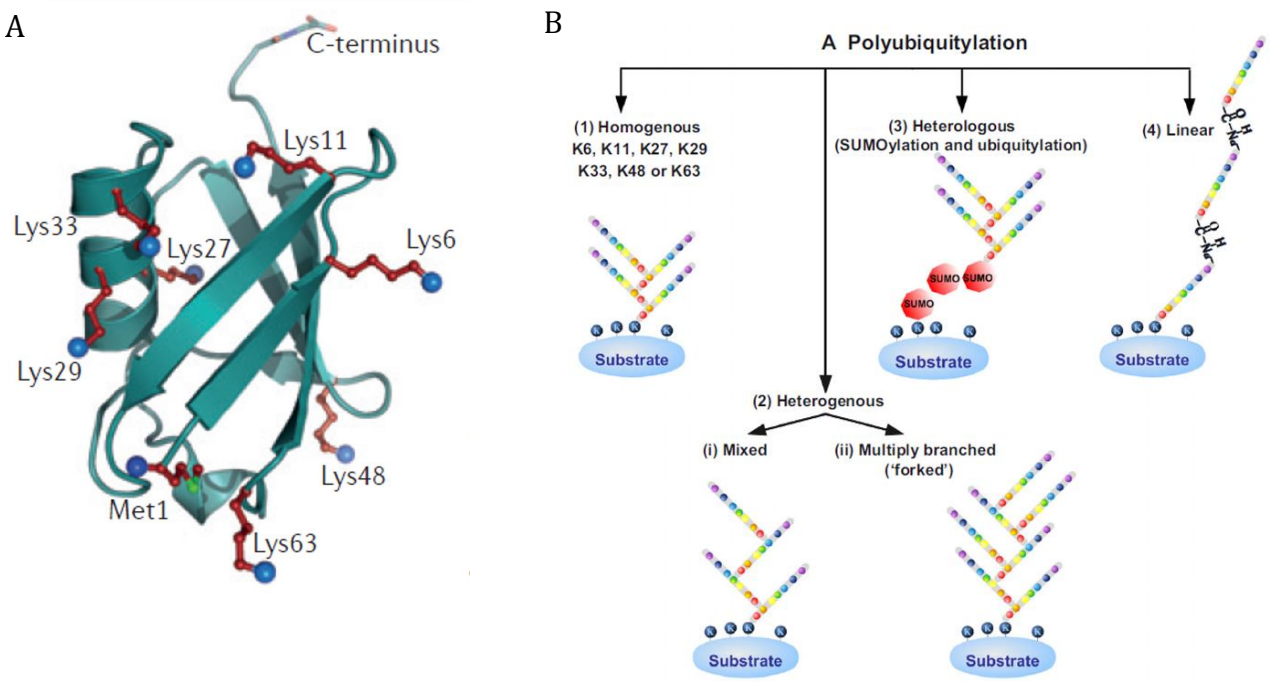

Figure 1-6 Ubiquitin structure and ubiquitination.

(A) Schematic representation of ubiquitin. Location of candidate residues for ubiquitination linkage were labelled. (Figure adapted from (Kulathu and Komander, 2012)) (B) Different types of ubiquitin chains (figure adapted from (Kravtsova-Ivantsiv and Ciechanover, 2012))

Ubiquitin-activating enzyme (E1) catalyses the adenosine triphosphate (ATP)-dependent first step of ubiquitination. It first catalyses ubiquitin C-terminal acyl adenylation (Tokgoz et al., 2006), and the catalytic cysteine of E1 forms a thioester bond with this ubiquitin (Schulman and Harper, 2009). A second ubiquitin molecule is then adenylated and bound to a different site of the same E1 enzyme. The E1 enzyme then transfers the first ubiquitin molecule to the ubiquitin-conjugating enzyme E2 through a transthioesterification reaction (Lee and Schindelin, 2008). The second ubiquitin does not form the same thioester complex with E1 and the significance of this second ubiquitin molecule remains largely unknown (Schulman and Harper, 2009).

The activated ubiquitin is transferred to the cysteine residue on a ubiquitin-conjugating enzyme (E2). Subsequently, the E2 binds to its specifically corresponding ubiquitin ligase (E3) via a structurally conserved binding region (Nandi et al., 2006). Whilst E3s are involved in substrate selection, E2s are the main determinants for the selection of ubiquitin chain varieties formed on the substrate, thereby directly control the cellular fate of the substrate. To date, there has been 35 active E2 enzymes described in human (van Wijk and Timmers, 2010).

The ubiquitin ligase (E3) is responsible for binding the target protein substrate and transferring the ubiquitin from the E2 cysteine to a lysine residue on the target protein, acting as both molecular matchmaker and catalyst (Berndsen and Wolberger, 2014). More than 600 human E3 ligases have been described to date due to the need for specifically targeting a broad range of diverse substrates (Li et al., 2008). These E3 ligases are classified into three groups according to their conserved structural domains and the mechanism whereby ubiquitin is transferred from the E2 to the substrate. The RING family binds both E2 and substrates simultaneously, and catalyses a direct transfer of ubiquitin from E2 to its substrate (Budhidarmo et al., 2012; Deshaies and Joazeiro, 2009). On the other hand, the homology to E6AP C terminus (HECT) and RBR E3 families adapt a two-step ubiquitin transfer, thereby the ubiquitin is transferred to an active cysteine residue on E3 by forming an thioester bond,

and then from the E3 to the substrate (Huibregtse et al., 1995; Wenzel and Klevit, 2012) (Figure 1-7).

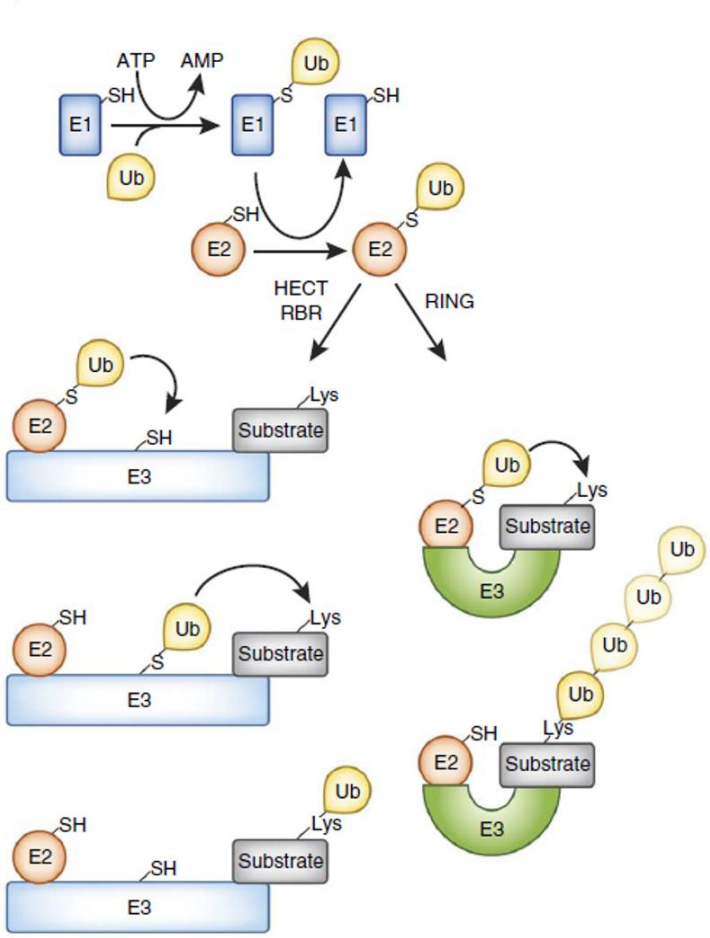

Figure 1-7 Mechanism of ubiquitination by different E3 ligase.

The mechanism by which ubiquitin molecule was transferred from E2 to E3 depends on the type of E3 ubiquitin ligases. (Figure adapted from (Berndsen and Wolberger, 2014)).

As described earlier, the types of ubiquitin chains determine how the ubiquitinated substrate is degraded. If the linkage to the target protein is via K48 on the ubiquitin, this will lead to a degradation of the polyubiquitinated protein by the proteasome. Of note, a minimum of four ubiquitins attached are required to trigger degradation (O'Neill, 2009). Non-degradative ubiquitination, on the other hand, has been observed in ubiquitinated proteins with ubiquitin chains other than K48-linked (Ikeda and Dikic, 2008). For instance, K63-linked polyubiquitination, the most studied atypical ubiquitination, directs ubiquitinated proteins to lysosome (Tan et al., 2008). It also mediates receptor endocytosis, NF-κB activation, DNA-repair process, and possibly mitophagy (Bennett and Harper, 2008; Geisler et al., 2010; Haglund and Dikic, 2005; Hayden and Ghosh, 2008; Narendra et al., 2010a; Nathan et al., 2013). K27-linked ubiquitination has been shown to inhibit TIEG1 nuclear translocation (Peng et al., 2011). Parkin-mediated mitophagy involves both K27- and K63-linked mitochondrial ubiquitination (Geisler et al., 2010). However K27-linked ubiquitination still facilitates the proteasomal degradation of Miro1 (Birsa et al., 2014). K29-/33-linked mixed chains have been implicated in blocking the activity of AMP-activated protein kinase (AMPK)-related kinase (Al-Hakim et al., 2008). Additionally, K29-linked ubiquitination has also been implicated in lysosomal protein degradation (Chastagner et al., 2006). These noncanonical ubiquitin chains represent new, albeit poorly understood, molecular signals.

1.3.3.2 Mitochondrial quality control

Mitochondria continuously undergo fission-fusion process to maintain the appropriate shape and function (Sheridan and Martin, 2010). When the damage reaches a level that the mitochondria can no longer be repaired by the fission/fusion process, it will be degraded by autophagy (Ashrafi and Schwarz, 2013). Parkin was first linked to mitochondrial function when the parkin-null Drosophila model was described. Parkin-null flies exhibited locomotor defects, reduced lifespan, male sterility, and mitochondrial pathology (swelling and disintegrated cristae) (Greene et al., 2003). This suggests that parkin plays a role in mitochondrial abnormalities. Similar mitochondrial dysfunction noted in autosomal recessive PD may result in selective neuronal loss (Greene et al., 2003; Pesah et al., 2004). This evidence is strengthened by the fact that parkin KO mice exhibit mild mitochondrial dysfunction, although these mitochondria appeared pathologically normal (Palacino et al., 2004). Fibroblasts from PD patients carrying parkin mutations display mitochondrial abnormalities including impaired mitochondrial function and morphology (Mortiboys et al., 2008), and decreased Complex I activity (Muftuoglu et al., 2004). Mitochondrial dysfunction in PINK1 null Drosophila model is complemented by Parkin (Clark et al., 2006; Park et al., 2006). Recent research further suggests that both parkin and PINK1 play a role in the selective degradation of damaged mitochondria by autophagy, a process called mitophagy (Deas et al., 2009).

It has been suggested that following mitochondrial depolarisation, full-length PINK1 accumulates to the OMM. This subsequently recruits and activates parkin to the mitochondrial surface where it ubiquitinates a number of OMM proteins, such as mitofusins 1 and 2 (Mfn1 and Mfn2) via K48- or K63-linked ubiquitination (Gegg et al., 2010; Glauser et al., 2011; Rakovic et al., 2011; Tanaka et al., 2010; Ziviani and Whitworth, 2010), and VDAC1 and Miro1 via formation of K27-linked polyubiquitination (Birsa et al., 2014; Geisler et al., 2010). A study conducted by quantitative diGly capture proteomics identified numerous mitochondrial proteins being ubiquitinated by Parkin upon mitochondrial depolarisation (Sarraf et al., 2013). Some of them, such as Mfn1/2

and Miro1/2, undergo rapid proteasomal turnover (Chan et al., 2011; Liu et al., 2012; Narendra et al., 2012; Tanaka et al., 2010; Wang et al., 2011b). It has been shown that proteasomal degradation of ubiquitinated Mfn1 and Mfn2 is a prerequisite for mitophagy (Anton et al., 2013; Gegg et al., 2010; Glauser et al., 2011; Leboucher et al., 2012; Wiedemann et al., 2013). Valosin-containing protein (VCP) was shown to relocalise to ubiquitinated mitochondria where it extracted ubiquitinated Mfns for further proteasomal degradation (Kim et al., 2013; Tanaka et al., 2010). The highly ubiquitinated mitochondria also recruit the autophagic adaptor proteins, such as p62 (Ding et al., 2010; Geisler et al., 2010; Narendra et al., 2010a; Okatsu et al., 2010; Seibenhener et al., 2013), which links ubiquitinated cargo to the autophagic machinery by binding both ubiquitin and membrane-bound LC3 II (Figure 1-8) (Deas et al., 2011b; Lim and Lim, 2011; Pankiv et al., 2007). However whether p62 is required in this step remains controversial, since fibroblasts from p62 KO mice demonstrate impairment only in mitochondrial perinuclear clustering but not mitophagy (Narendra et al., 2010a; Okatsu et al., 2010). On the other hand, the ubiquitin-binding deacetylase HDAC6 has been implicated in mitophagy by enhancing autophagosome-lysosome fusion via assembly of local actin network (Lee et al., 2010a; Lee et al., 2010b). Of note, fibroblasts from HDAC6 KO mice demonstrate impaired perinuclear mitochondrial clustering and mitophagy (Lee et al., 2010b). Nevertheless, the detailed molecular pathways associated with each step in mitophagy process remain to be fully elucidated.

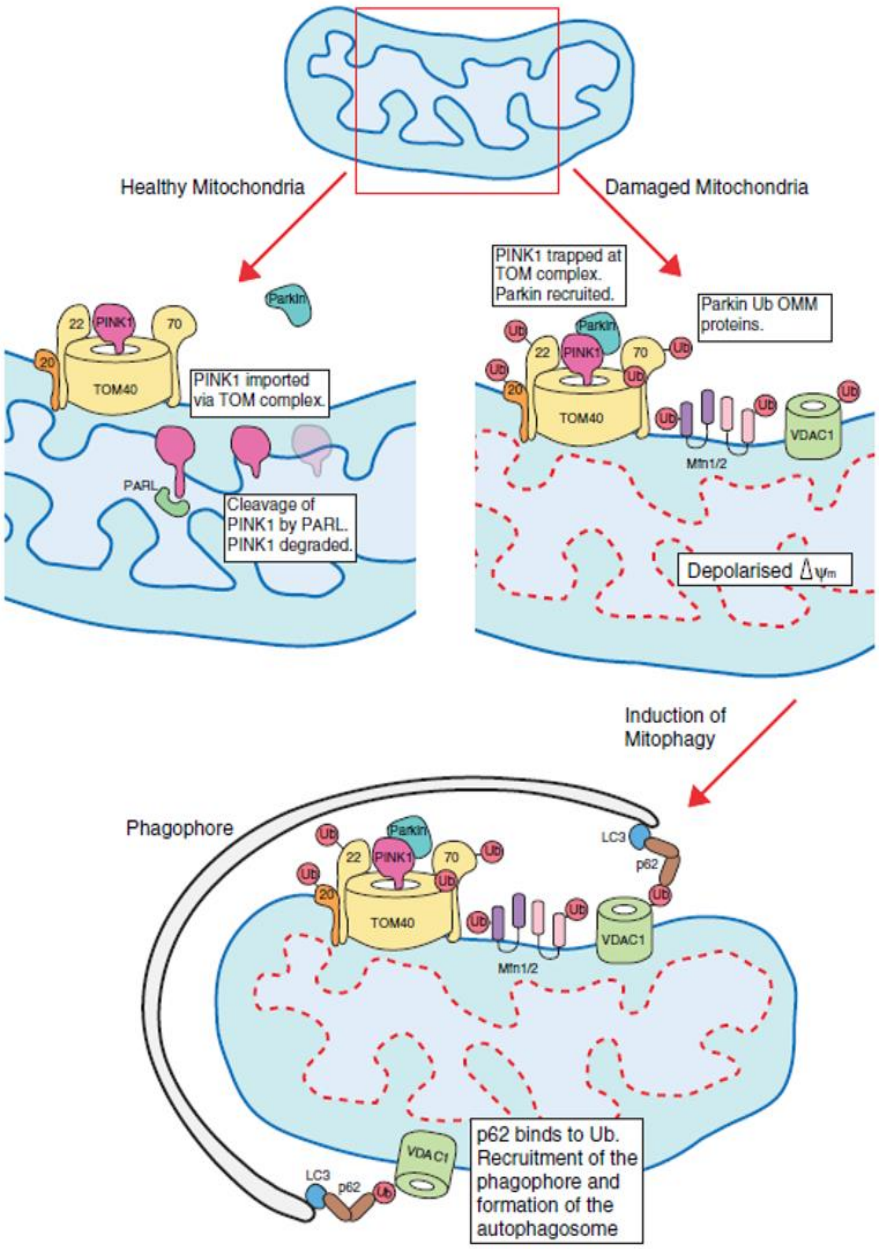

Figure 1-8 Mechanism of PINK1/Parkin-induced mitophagy.

Under normal cell homeostasis PINK1 is imported in a membrane potential dependent manner. It localises to the IMM where it is cleaved by PARL. Loss of membrane potential (dashed red line) ensures PINK1 cannot be imported and is trapped at the TOM complex. This recruits the E3 ubiquitin ligase Parkin which ubiquitinates proteins on the cytoplasmic surface of the mitochondria. Ubiquitination of VDAC1 recruits the adaptor protein p62/SQSTM1 which further binds LC3 and mediates recruitment of the phagophore. This mitochondrion is subsequently degraded by the autophagic pathway. (Figure adapted from (Kotiadis et al., 2014))

1.3.3.3 Neuronal protection

The absence of parkin and degeneration of dopaminergic neurons in patients carrying Parkin mutations suggest that Parkin has an important neuroprotective function (Shimura et al., 1999), which is also demonstrated in studies using cellular or animal models (Darios et al., 2003; Higashi et al., 2004; Jiang et al., 2004; Staropoli et al., 2003). Parkin mediates neuroprotection by activating the NF-κB (nuclear factor kappa-light-chain-enhancer of activated B cells) signalling pathway that plays a crucial role in neuronal integrity and synaptic plasticity (Henn et al., 2007; Karin and Lin, 2002). It was shown that the linear ubiquitin chain assembly complex (LUBAC) recruits Parkin upon cellular stress. Parkin then ubiquitinates IKKγ (IκB kinase γ)/NEMO (NF-κB essential modifier) complex, which leads to proteasomal degradation of NFκB inhibitor IκBα and release NFκB to further regulate transcription of target genes such as OPA1 (optic atrophy 1) that maintains mitochondrial integrity (Figure 1-9) (Winklhofer, 2014). Parkin has also been implicated in enhancing phosphoinositide 3-kinase (PI3K)/Akt signalling by reducing epidermal growth factor receptor (EGFR) internalisation (Fallon et al., 2006). It has also been shown that Parkin protects dopaminergic neurons from neurotoxins and oxidative stress by attenuating stress-activated protein kinase pathways (Hasegawa et al., 2008; Jiang et al., 2004; Petrucelli et al., 2002), although Parkin's cytosolic substrates associated with these stress-activated kinase pathways are yet to be identified (Details of Parkin substrates will be described in section 1.3.4). Therefore, Parkin is likely to protect the cells by enhancing neuroprotective signals such as NFκB or PI3K/Akt pathways, or by attenuating stress-activated signals such as the MAPK pathway.

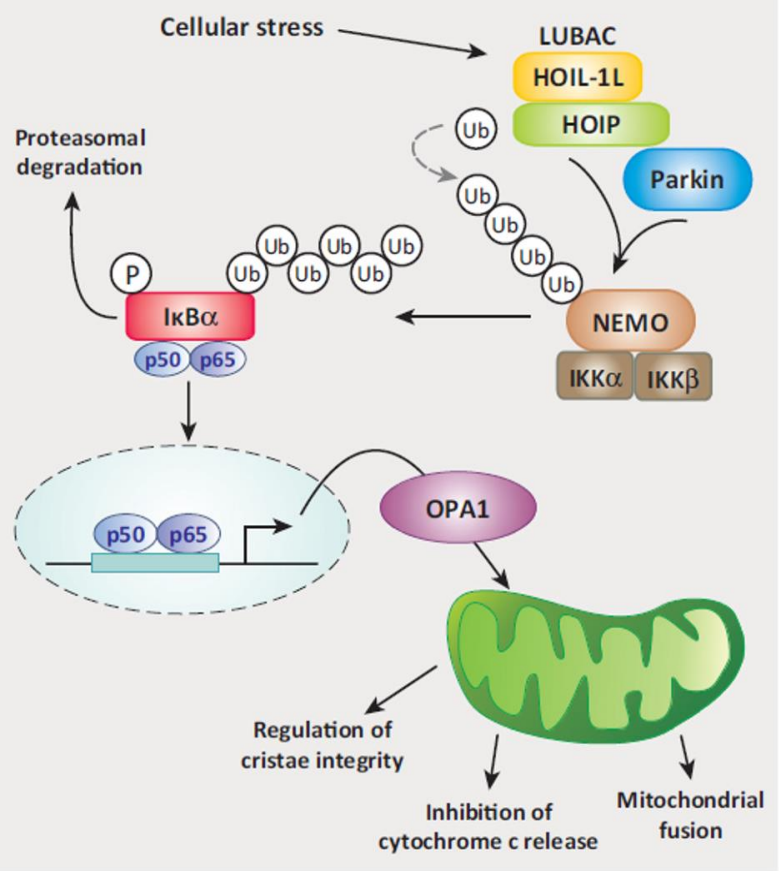

Figure 1-9 Parkin prevents stress-induced cell death by activating NF-κB signalling.

Upon cell stress, LUBAC recruits Parkin and this increases linear ubiquitination of NEMO, which leads to proteasomal degradation of NFκB inhibitor IκBα. NFκB is released to further regulate transcription of target genes such as OPA1 (optic atrophy 1) that maintains mitochondrial integrity. (Figure adapted from (Berndsen and Wolberger, 2014))

1.3.3.4 Tumour suppression

Parkin has been shown to display tumour suppressive function (Cesari et al., 2003; Denison et al., 2003b; Picchio et al., 2004; Wang et al., 2004), whereby whole exon deletions and duplications of this gene identified in ovarian and other cancers support this hypothesis (Denison et al., 2003a; Denison et al., 2003b). It may also negatively regulate the proliferation of breast cancer (Tay et al., 2010). More recently, *Parkin* somatic mutations and intragenic deletions have been identified by chromosomal microarray analysis in glioblastoma, colon cancer, and lung cancer (Figure 1-10) (Poulogiannis et al., 2010; Veeriah et al., 2010). Viotti and colleague demonstrated that p53-regulated Parkin transcription is decreased in oligodendroglioma, mixed glioma and glioblastoma (Viotti et al., 2014). Nevertheless, the *Parkin* gene spans a considerable length on the most fragile segment of chromosome 6, thereby is prone to mutations. Whether somatic mutations in Parkin are a primary cause of tumour requires further investigation.

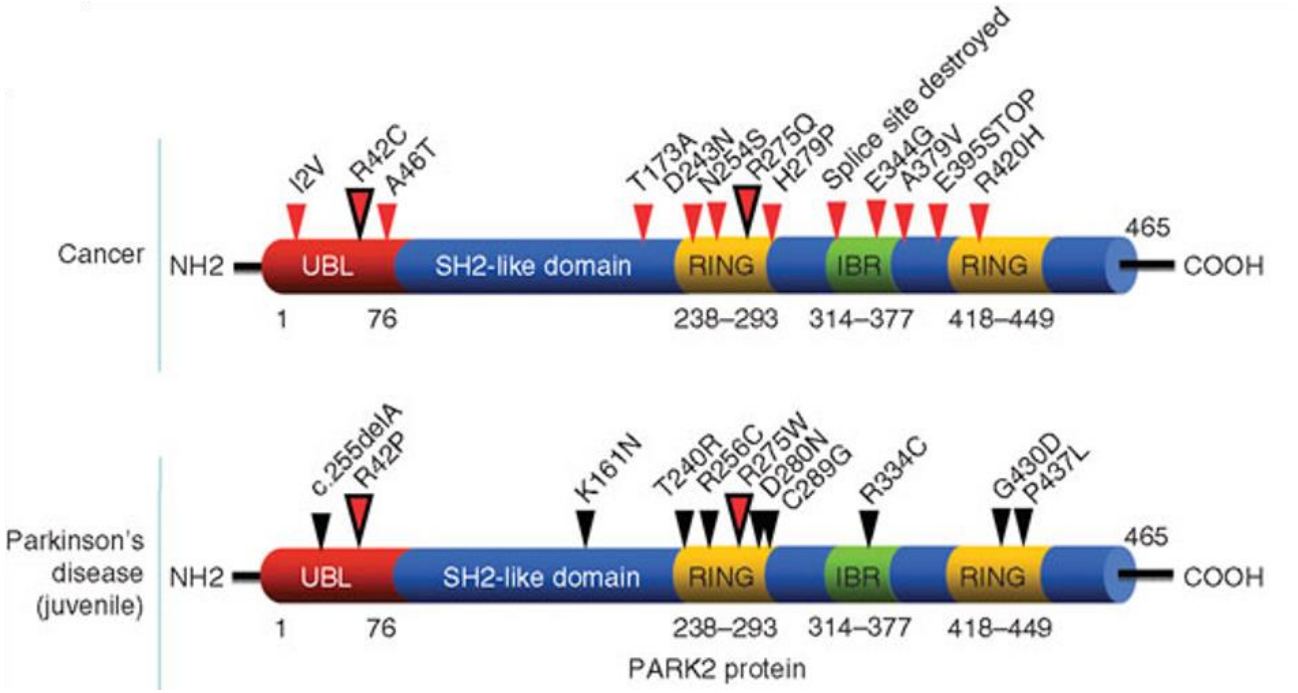

Figure 1-10 Mutations in Parkin gene in Cancer and EOPD.

Somatic mutations in *Parkin* gene (top panel) and PD pathogenic gene in *Parkin* gene (bottom panel) (Figure adapted from (Veeriah et al., 2010)).

1.3.4 Parkin substrates

Mutations in Parkin can alter its ubiquitin ligase function and subsequently impair degradation of its substrates. It is thought that the toxicity caused by the accumulation of Parkin substrates results in dopaminergic neuronal death in Parkin-related PD (Zhang et al., 2000). A number of Parkin substrates have been reported (Table 1-4), most of them are cytosolic. Whilst a robust *in vivo* evidence is still lacking in confirming any of the described cytosolic proteins is the true Parkin substrate, mounting evidences indicate that Parkin ubiquitinates numerous mitochondrial proteins in response to mitochondrial depolarisation (Figure 1-11) (Sarraf et al., 2013) by producing various ubiquitin chains (Ordureau et al., 2014). These data suggest Parkin conducts variable ubiquitinations on different substrates upon different stimulations. This argues the classical notion that Parkin substrates are to be K48-ubiquitinated and to accumulate in Parkin KO mice, in conditions where Parkin is inactivated and in sporadic PD (Dawson and Dawson, 2010). In conditions where the substrates are not ubiquitinated for the degradation purpose, their accumulation might not be detected.

Substrate	Physiological function	Ubiquitination	Degradation	Ref
Hsp70	Molecular chaperone	Mono	No	(Moore et al., 2008)
α-Sp22	Lewy body component	Poly	Yes	(Schlossmacher et al., 2002)
Synphilin-1	Interact with α-synuclein	Poly	No	(Chung et al., 2001)
PICK1	Synaptic scaffolding protein	Mono	No	(Joch et al., 2007)
Ataxin-3	Polyglutamine	Poly	Yes	(Tsai et al., 2003)
Ataxin-2	Polyglutamine	Poly	Yes	(Huynh et al., 2007)
CDCrel-1	Synaptic vesicle associated GTPase	Poly	Yes	(Zhang et al., 2000)
CDCrel-2a	Synaptic vesicle associated GTPase	Poly	Yes	(Choi et al., 2003)
SynaptotagminXI	Membrane trafficking protein	Poly	Yes	(Huynh et al., 2003)
AIMP2/p38	Aminoacyl t-RNA synthetase cofactor	Poly	Yes	(Corti et al., 2003)
FBP1	Regulates c-myc mRNA	Yes	Yes	(Ko et al., 2006)
Cyclin	E Cell cycle regulating protein	Poly	Yes	(Staropoli et al., 2003)
β-catenin	Component in Wnt signalling	Unknown	Yes	(Rawal et al., 2009)
RanBP2	Interact with nuclear pore complex	Poly	Yes	(Um et al., 2006)
PDCD2-1	Involved in apoptosis, inflammation and proliferation	Poly	Yes	(Fukae et al., 2009)
α/β-tubulin	Cytoskeletal components	Unknown	Yes	(Ren et al., 2003)
Lim	Kinase 1 Phosphorylates cofilin	Poly	Yes	(Lim et al., 2007)
Ικκγ	Component in NFκB signalling	Poly	No	(Henn et al., 2007)
TRAF2	Component in NFκB signalling	Yes	No	(Henn et al., 2007)
Pael-R	G-protein coupled receptor	Poly	Yes	(Imai et al., 2001)
PLCγ1	Hydrolyses lipids	Unknown	Yes	(Dehvari et al., 2009)
Eps15	Internalizes EGF-R	Mono	No	(Fallon et al., 2006)
VDAC	Mitochondrial ion channel	Poly	No	(Geisler et al., 2010)

Bcl-2	Anti-apoptotic protein	Mono	No	(Chen et al., 2010)
Mitofusin-1/-2	Mitochondrial fusion protein	Poly	Yes	(Tanaka et al., 2010)
Drp1	Mitochondrial fusion protein	Poly	Yes	(Wang et al., 2011a)
Miro	Mitochondrial anchor protein	Unknown	Yes	(Birsa et al., 2014; Wang et al., 2011b)

Table 1-4 Parkin substrates

(Adapted from (Sandebring A and A, 2012)).

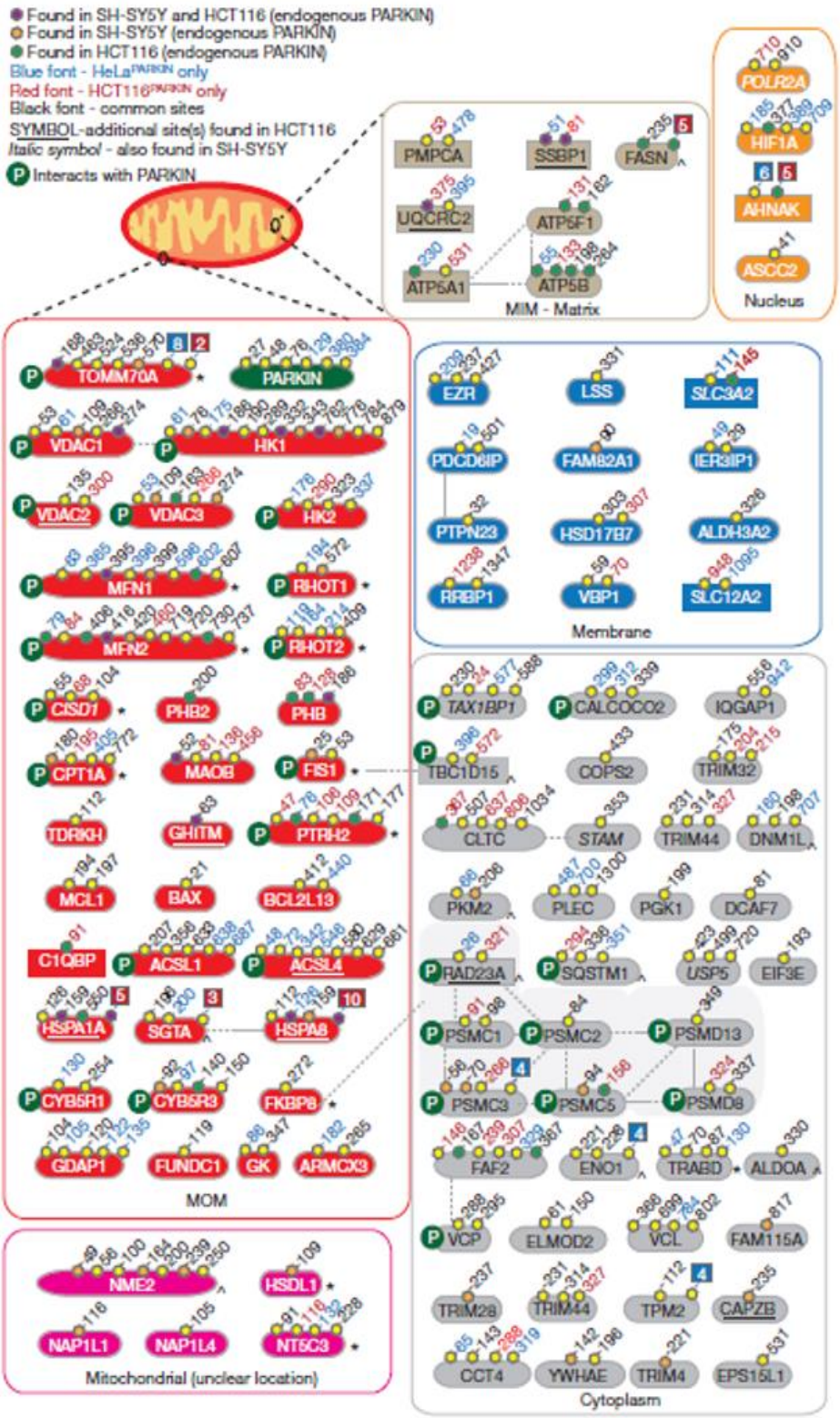

Figure 1-11 Possible Parkin substrates detected upon mitochondrial depolarisation.

Mitochondrial depolarisation related substrate (Figure adapted from (Sarraf et al., 2013))

1.3.5 Models for investigating Parkin function

1.3.5.1 Genetic animal models

A robust animal model for PD would recapitulate histopathological characteristics of progressive and significant loss of dopaminergic neurons, LB pathology, an onset during adulthood, presence of clinical symptoms of human disease, and improved motor features sensitive to dopamine treatment. None of the Parkin KO rodent models currently available fully recapitulate the above-mentioned principal clinical and neuropathological hallmarks of PD (Beal, 2010). Bacterial artificial chromosome (BAC) transgenic mice expressing C-terminal truncated human mutant Parkin (Parkin Q311X) in dopaminergic neurons exhibit progressive hypokinetic motor deficits and age-dependent dopaminergic neuron degeneration with α-synuclein accumulation (Lu et al., 2009). Nevertheless, this model suggests dominant toxic effect by the overexpressed C-terminal truncated Parkin but does not necessarily recapitulate the features caused by reduced Parkin function.

Parkin null *Drosophila*, on the other hand, exhibits lower body weight and reduced cell size, locomotor defects accompanied by mitochondrial structural abnormalities, a reduced life span, and male sterility, and dopaminergic neuronal loss (Greene et al., 2003; Pesah et al., 2004; Pienaar et al., 2010). Differences that contribute to interspecies variation between man and animals could explain the discrepancies of "PD phenotype" in rodents and flies.

1.3.5.2 Cell models

Many cell models have been used for studying Parkin function in normal and pathophysiological conditions. Most of them are human cancer cell lines. These rapidly-dividing cells are usually an easier and cheaper alternative as compared to animal models. Moreover they can easily be genetically manipulated. These genetic manipulations include overexpression and knockdown experiments.

1.3.5.3 Parkin-patient derived cell lines as potential models

Primary human dopaminergic neurons carrying pathological mutations would appear to be a very good model for studying parkin function. However, it is impossible to obtain such neurons directly from parkin patients. In 2007, Yamanaka and Thomson (Takahashi et al., 2007; Yu et al., 2007) first derived human induced pluripotent stem cells (iPSC) from skin fibroblasts using a cocktail of designated transcription factors. Parkin-iPSC and neuronal models derived from them would have the advantage of expressing endogenous Parkin carrying exactly the same mutations as patients. This Parkin-patient derived model would provide a great opportunity for observing a kinetic change of the parkin function through all stages of neuronal differentiation

1.3.6 Post-translational modification (PTM) of Parkin

1.3.6.1 S-nitrosylation

Nitric oxide (NO) produced by neuronal nitric oxide synthetase (nNOS) in neurons functions as an excitatory signalling molecule. However NO is also a free radical whose excessive production leads to oxidative stress. Upon inflammatory insult expression of the inducible isoform of NOS (iNOS) is enhanced, thereby producing excessive NO that in turn reacts with other free radicals such as superoxide anion to form a more reactive nitrogen species peroxynitrite. These free radicals can damage protein, lipid and DNA, which eventually leads to neuronal degeneration (Ischiropoulos and Beckman, 2003) It has been shown that nitrated protein aggregates are a prominent feature of brain tissue in PD patients (Giasson et al., 2000). Chung and colleague showed increased level of Parkin S-nitrosylation both *in vitro* and in the brain tissue of PD animal models and PD patients (Chung et al., 2004). S-nitrosylation is a process of adding NO to the sulfur residue of cysteine in proteins. The effect of Parkin S-nitrosylation remains controversial as S-nitrosylation of cysteine residues in the IBR and RING2 domains of Parkin inhibit its E3 ubiquitin ligase activity (Chung et al., 2004; Chung et al., 2005; Lipton et al., 2005; Sunico et al., 2013; Yao et al., 2004), whereas Cys323 S-nitrosylation has been demonstrated

to increase its activity (Ozawa et al., 2013). How this PTM is relevant to PD pathogenesis requires further investigation.

1.3.6.2 Dopamine modification

Dopamine is also a highly reactive molecule that is synthesized in the SNc and LC. It can oxidize to form dopamine quinone (Stokes et al., 1999), which is a reactive metabolite of dopamine that prone to bind reduced cysteine residues within polypeptides (Hastings et al., 1996; LaVoie and Hastings, 1999). Dopamine quinone has also been shown to bind to a number of proteins covalently *in vivo* or *in vitro* (Hastings et al., 1996; LaVoie and Hastings, 1999), and to inactivate thiol-dependent enzymes (Berman and Hastings, 1997; Berman et al., 1996; Kuhn and Arthur, 1998; Kuhn et al., 1999; Xu et al., 1998). LaVoie and colleagues demonstrated that dopamine quinone irreversibly binds to cysteine residues in Parkin RING domain, leading to conformational change that reduce Parkin's solubility and E3 ubiquitin ligase activity (Figure 1-12) (LaVoie et al., 2005).

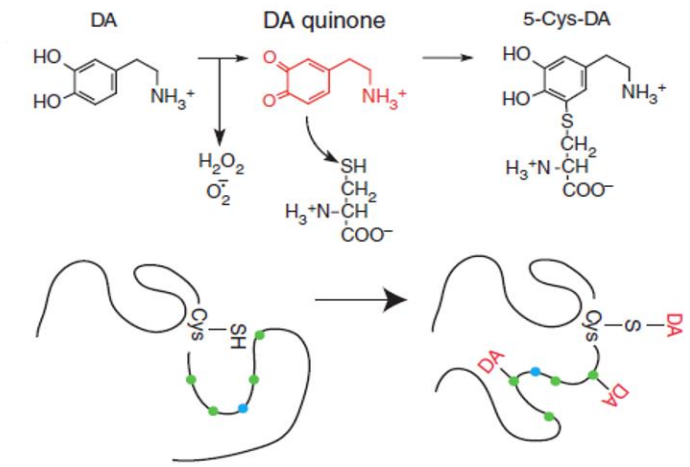

Figure 1-12 Schematic representation of the oxidated dopamine modifying amino acid cysteine.

Schematic of the oxidation of dopamine and the irreversible chemical reaction between the dopamine quinone and the amino acid cysteine. (Figure adapted from (LaVoie et al., 2005))

1.3.6.3 SUMOylation

Small ubiquitin-related modifier (SUMO) is a 97-amino acid protein that covalently binds to lysine residues on target proteins via a similar cascade to ubiquitin pathway (Geiss-Friedlander and Melchior, 2007). A number of studies have shown that the SUMO family of proteins plays a key role in neuronal function. For example, both tau and amyloid precursor protein were suggested to be regulated by SUMO (Dorval and Fraser, 2006; Gocke et al., 2005; Zhang and Sarge, 2008). LB from patient of dementia with LB (DLB) have been reported to stain positively for SUMO-1 (Pountney et al., 2005). Additionally, inclusion bodies from multiple system atrophy (MSA) have also been stained positively for SUMO-1 (Pountney et al., 2005). A non-covalent interaction between Parkin and SUMO-1 has been reported *in vitro* and *in vivo*, enhancing Parkin's E3 ligase activity (Um and Chung, 2006). However the significance of the reported SUMOylation in neurodegenerative diseases has not yet been fully established.

1.3.6.4 Neddylation

NEDD8 is another ubiquitin-like small molecule that regulates the function of target proteins by covalent conjugation, a process called neddylation that is via a cascade similar to ubiquitination (Huang et al., 2009; Kurz et al., 2008; Meyer-Schaller et al., 2009). Both PINK1 and Parkin have been shown to be modified by neddylation, resulting in stabilization of 55 kDa PINK1 cleaved fragment and increased Parkin's E3 ubiquitin ligase activity (Choo et al., 2012; Um et al., 2012). In addition, endogenous Parkin neddylation has also been detected in the brain of PD patient (Choo et al., 2012).

1.3.6.5 Phosphorylation

Another PTM, phosphorylation, has also been implicated in the pathogenesis of PD. Endoplasmic reticulum (ER) stress caused by increased unfolded protein has been shown to reduce parkin phosphorylation, which in turn has been shown to increase Parkin activity (Yamamoto et al., 2005). A number of Parkin

phosphorylation sites have been identified, mostly through *in vitro* methods (Figure 1-13). Several kinases are shown to phosphorylate parkin, including casein kinase-1 (CK-1), protein kinase A (PKA), cyclin-dependent kinase 5 (Cdk5), and c-Abl (Avraham et al., 2007; Ko et al., 2010; Yamamoto et al., 2005). *In vitro* kinase assays show that PKA phosphorylates parkin at S101, S131, and 136 (Yamamoto et al., 2005). CK-1 and Cdk5 are shown to phosphorylate parkin at S101 and S131 respectively *in vitro* and at overexpressed level in cell, and these two kinases enhance each other's ability to phosphorylate parkin. These *in vitro* studies reveal that Parkin phosphorylation increases its aggregation and reduces Parkin's ligase function (Avraham et al., 2007; Rubio de la Torre et al., 2009; Yamamoto et al., 2005). Another *in vitro* kinase assay has shown that the non-receptor tyrosine kinase c-Abl phosphorylates parkin on Y143. This phosphorylation event also decreases parkin E3 ubiquitin ligase activity, leading to the accumulation of Parkin putative substrates, and ultimately cell death. These data have been further confirmed using conditional c-Abl KO neurons (Ko et al., 2010), but no other group has yet reproduced this result.

PINK1 has also been observed to phosphorylate Parkin on T175 *in vitro*, and a non-phosphorylatable Parkin mutant (T175A) fails to translocate to depolarised mitochondria (Kim et al., 2008). However, Parkin T175 phosphorylation following CCCP-induced mitochondrial depolarisation was not observed *in vivo* by Kondapalli and colleagues (Kondapalli et al., 2012). On the other hand, they showed that Parkin S65 can be phosphorylated by PINK1 both *in vitro* and *in vivo* upon CCCP-induced mitochondrial depolarisation, which is also confirmed by another independent group (Kondapalli et al., 2012; Shiba-Fukushima et al., 2012). It is still not clear whether parkin is phosphorylated under pathological conditions. The kinase signalling pathways associated with parkin, the functional consequences of parkin phosphorylation, and the possible role of parkin phosphorylation in the selective death of dopaminergic neurons all remain to be determined.

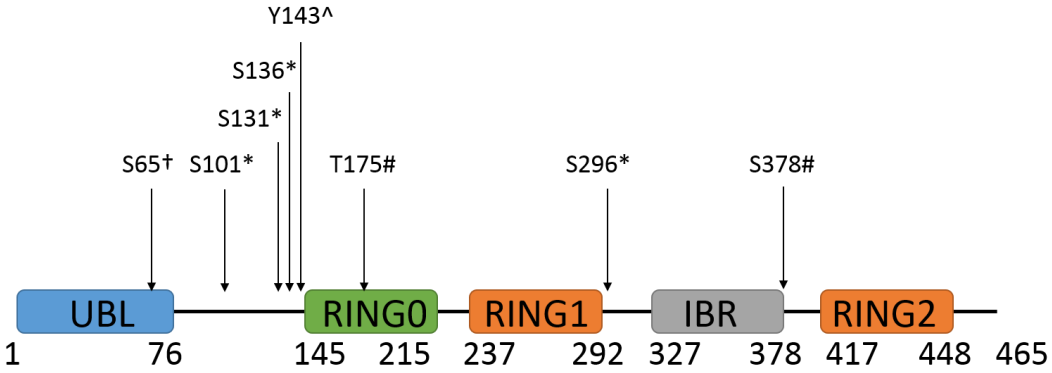

Figure 1-13 A schematic representation of reported Parkin phosphorylation sites.

Reported Parkin phosphorylation sites and the methods by which each site was assessed. **in vivo* phosphorylation assay. #*In vitro* phosphorylation assay. ^*In vitro* kinase assay. † *in vivo* phosphorylation assay following CCCP treatment.

1.3.7 Signalling pathways associated with Parkin regulation

1.3.7.1 Mitogen-activated protein kinase (MAPK) signalling pathways

The mammalian MAPK family consists of extracellular signal-related kinases (ERK), Jun N-terminal kinases (JNK), and p38 proteins (Chang and Karin, 2001). These highly conserved three-tiered signalling cascades are activated in response to a variety of stimuli, such as mitogens, stress, and pro-inflammatory cytokines to regulate important cellular processes including gene expression, cell proliferation, cell survival and cell death (Chang and Karin, 2001) (Figure 1-14).

A striatal overactivated ERK1/2 in PD animal model has been described to potentially relate to L-DOPA-associated dyskinesia (Fieblinger et al., 2014; Girault et al., 2007). Previous reports have shown that ERK1/2 signalling is dysregulated in PD patients (Kurup et al., 2015; Ren et al., 2009). ERK1/2 activation by microtubule depolymerising agents rotenone or colchicine can be attenuated by Parkin, and Parkin mutation such as exon 4 deletion results in activated ERK1/2 signal in various cell models (Ren et al., 2009). On the other hand, sporadic and autosomal recessive PD (mutation not described) patients show striatal accumulation of $STEP_{61}$ (striatal-enriched protein tyrosine phosphatase 61) and reduced phosphorylation of ERK1/2 and CREB (cAMP response element-binding protein), whereby synaptic function is disrupted (Kurup et al., 2015).

ETC Complex I toxin rotenone has been reported to induce apoptosis in SH-SY5Y neuroblastoma cells through the activation of JNK and p38 MAPKs (Newhouse et al., 2004). Upregulation of JNK and p38 signalling pathways has also been shown in the striatum of PD animal model treated with MPTP (Karunakaran et al., 2008). Overactivated JNK pathway has been described in Drosophila dopaminergic neurons expressing loss-of-function Parkin mutant (Cha et al., 2005). Activation of the p38 signalling pathway is involved in mediating cellular stress and inflammatory responses (Corrêa and Eales, 2012).

A previous report demonstrated that the p38 signalling induced by microtubule depolymerising agents in cell models can be attenuated by overexpressing Parkin (Ren et al., 2009).

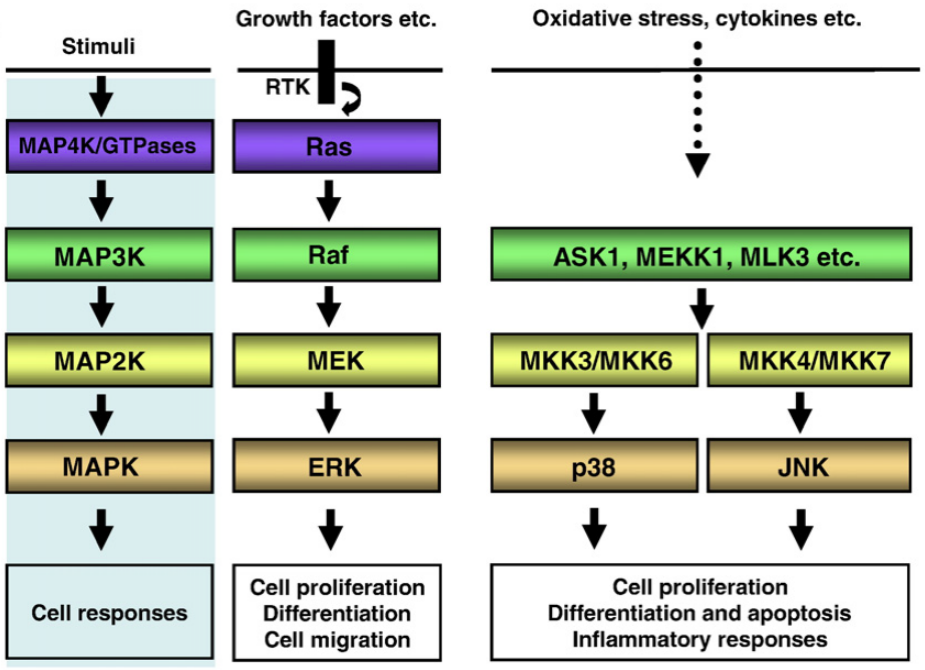

Figure 1-14 MAPK signalling pathways.

The mammalian MAPK family includes ERK, p38, and JNK. In the ERK signalling pathway, ERK1/2 is activated by MEK1/2, which is activated by Raf. Raf is activated by the Ras GTPase, whose activation is induced by RTKs such as the epidermal growth factor receptor. The p38 and JNK pathways consist of a MAP3K such as ASK1, MEKK1, or MLK3 as well as a MAP2K such as MKK3 or MKK6 for the p38 pathway or MKK4 or MKK7 for the JNK pathway. (Figure adapted from (Kim and Choi, 2010))

1.3.7.2 PI3K/Akt signalling pathway

The PI3K/Akt signalling pathway plays an important role in regulating cell growth, metabolism and survival (Sheppard et al., 2012). Akt is the major downstream target of PI3K (Kirkegaard et al., 2010) and activation of Akt by phosphorylation further activates mTOR (Bartolome et al., 2010). Activation of Akt has been reported as neuroprotective (Burke, 2007; Levy et al., 2009). A specific Akt haplotype also demonstrates neuroprotection against PD (Xiromerisiou et al., 2008). Both Parkin (Fallon et al., 2006) and DJ-1 (Kim et al., 2005; Yang et al., 2005) have been shown to enhance Akt signalling.

1.3.7.3 NF-κB signalling pathway

Nuclear factor kappa-light-chain-enhancer of activated B cells (NF-*κ*B) is a family of inducible transcription factors. Expression of NF-*κ*B has been described in a variety of cells and tissues, including microglia, astrocytes, and neurons. Of note, NF-*κ*B shows diverse functions in different cellular contexts. Whilst regulating inflammatory mediators production during inflammation in glial cells (Jenner, 1998; Qian and Flood, 2008; Zielasek and Hartung, 1996), activation of NF-*κ*B in neurons demonstrates neuroprotective function (Henn et al., 2007; Kaltschmidt and Kaltschmidt, 2009). It has been shown that PINK1-mediated Parkin phosphorylation activates catalysing K63-linked polyubiquitination and enhances Parkin-mediated ubiquitin signalling through the NF-κB pathway (Sha et al., 2010).

1.4 Objectives of this thesis

As described earlier in this chapter, mutations in Parkin are the most frequent cause of EOPD. However the upstream molecular pathways activating Parkin remain poorly understood. The overall objective of this thesis is to unravel the molecular pathways associated with Parkin activation in cell models overexpressing exogenous Parkin and in Parkin patient-derived cell model. The specific aims of my thesis are:

1. To validate the specificity of available Parkin antibodies.

2. To characterise Parkin patient fibroblasts and generate patient-derived iPSCs.

3. To investigate signalling pathways regulating Parkin phosphorylation.

4. To identify the role of Parkin phosphorylation in the mitophagy process.

Chapter 2 Materials and Methods

2.1 Materials

2.1.1 Bioinformatics

Human DNA sequence of PARK2 (MIM: 600116) and protein sequence of Parkin (gi: 3063388) were obtained from National Institute of Health (NIH) National Center for Biotechnology Information (NCBI) server. The protein sequence was first published in (Kitada et al., 1998).

2.1.1.1 Amino acid sequence homology

Amino acid sequences of Parkin of human, chimpanzee, macaque, cow, pig, chicken, mouse, and rat were obtained from NCBI database. The multiple sequence alignment result was produced by ClustralW2 or T-COFFEE online programmes on the following websites:

http://www.ebi.ac.uk/Tools/msa/clustalw2/

http://tcoffee.crg.cat/apps/tcoffee/do:regular

The conservation of amino acid sequence of Parkin is examined by these programmes as well.

2.1.1.2 Prediction of phosphorylation sites

Amino acid sequence of Parkin was examined for putative phosphorylation sites and corresponding kinase(s) using online algorithms KinasePhos2.0.

(http://kinasephos2.mbc.nctu.edu.tw/)

2.1.2 Reagents and consumables

2.1.2.1 Molecular biology

Buffers for competent *E. coli* (*Escherichia coli*) production:

TF buffer I (sterile filtered)

Final concentration		MW	For 1L
100mM	KCl	74.55	7.46g
50mM	RbCl	120.92	6.05g
10mM	CaCl2	110.99	1.11g
30mM	KAc	98.14	2.99g
15%	glycerin		

pH adjusted to 5.8 with acetic acid

TF buffer II (Sterile filtered)

Final concentration		MW	For 1L
10mM	MOPS	209.26	2.08g
10mM	RbCl2	120.92	1.21g
75mM	CaCl2	110.99	8.32g
15%	glycerin		

pH adjusted to 7.0 with NaOH

Bacterial growth medium: Luria broth (LB) powder (10 g/l tryptone, 5 g/l yeast extract, 5 g/l NaCl) was purchased from Sigma-Aldrich, diluted in distilled water according to the manufacturer's protocol and sterilised by autoclaving.

LB agar plates: LB-agar powder (as for LB broth plus 15 g/l agar powder) was purchased from Sigma-Aldrich, diluted in distilled water according to the

manufacturer's protocol and sterilised by autoclaving, Ampicillin sodium salt was purchased from Sigma-Aldrich, diluted in deionised water to a concentration of 100 mg/ml and sterilised by 0.22μm syringe filtered. LB-agar was allowed to cool to 50°C before addition of ampicillin to a final concentration of 100 μg/ml. The LB agar-ampicillin was then poured into 10 cm dishes and allowed to set at room temperature before storage at 4°C.

DNA constructs: All DNA constructs used in this thesis are shown in Table 2-1 below.

Name of construct	Vector backbone	Obtained from
FLAG-pcDNA3	pcDNA3	Helen Ardley (Leeds)
FLAG-Parkin	pcDNA3	Helen Ardley (Leeds)
FLAG-Parkin S101A	pcDNA3	This thesis
FLAG-Parkin S101D	pcDNA3	This thesis
FLAG-Parkin S378A	pcDNA3	This thesis
FLAG-Parkin S378D	pcDNA3	This thesis
FLAG-Parkin S65A	pcDNA3	This thesis
FLAG-Parkin S65D	pcDNA3	This thesis
FLAG-Parkin S65A/S101A	pcDNA3	This thesis
FLAG-Parkin S65D/S101D	pcDNA3	This thesis

Table 2-1 DNA constructs used in this thesis.

Kits: (all the following kits were purchased from Qiagen) QIAprep spin miniprep, QIAfilter plasmid maxiprep, QIAquick gel extraxtion, Qiashredder columns and RNease mini kits.

Electrophoresis regents: TBE (Tris-borate-ethylenediaminetetraacetic acid (EDTA)) buffer was prepared as follows: 89 mM Tris base, 89 mM boric acid, 2 mM EDTA (pH 8). 10x Orange G loading buffer was prepared by dissolving 2.5 g/l Orange G in 30% (v/v) glycerol. GelRed nucleic acid stain was purchased from Biotium (CA, USA). Agarose powder was purchased from Sigma-Aldrich.

Reverse transcription: (all reagents were purchased from Invitrogen)

Reagents and their category numbers are listed in Table 2-2 below.

dNTP mix	Cat No. 18427-013
Random primer	Cat No. 48190-011
5X FX buffer	P/N: Y02321
0.1M DTT	P/N : Y00147
RNase OUT	Cat No. 10777-019
SuperScript III	P/N : 56576

Table 2-2 Material for reverse transcription.

Site-direct mutagenesis: AccuPrime *Pfx* SuperMix and Dpn1 endonuclease were both purchased from Invitrogen.

Quantitative polymerase chain reaction (qPCR): Universal mastermix and TaqMan probes were purchased from Applied Biosystems. A FAM-labelled probe was used for Parkin (TagMan gene expression assay, Parkin: Hs00247755_m1), A VIC-labelled probe was used for GAPDH.

PCR primers:

Primers used for *Parkin* exon sequencing were listed in Table 2-3, for plasmid construct sequencing were listed in Table 2-4, for truncated cDNA amplification were listed in Table 2-5, and for site-direct mutagenesis were listed in Table 2-6.

PCR primers:	
Exon 1	PARK2EX1AF: GTAAAACGACGGCCAGTGAGGCCTGGAGGATTTAACC
	PARK2EX1AR: CAGGAAACAGCTATGACCGCCCCGTCATTGACAGTT
Exon 2	ParkinEX2F-M13: TGTAAAACGACGGCCAGTATGTTGCTATCACCATTTAAGGG
	ParkinEX2R-M13: CAGGAAACAGCTATGACCAGATTGGCAGCGCAGGCGGCATG
Exon 3	ParkinEX3F-M13: TGTAAAACGACGGCCAGTTCTCGCATTTCATGTTTGACA
	ParkinEX3R-M13: CAGGAAACAGCTATGACCTAAATATGCACCCGGTGAGG
	ParkinEx3FNew-M13: TGTAAAACGACGGCCAGTTGTGACCTGGATCAGCAGAG
Exon 4	ParkinEX4F-M13: TGTAAAACGACGGCCAGTACAAGCTTTTAAAGAGTTTCTTGT
	ParkinEX4R-M13: CAGGAAACAGCTATGACCAGGCAATGTGTTAGTACACA
Exon 5	ParkinEX5F-M13: TGTAAAACGACGGCCAGTTGGAAACATGTCTTAAGGAGTACA
	ParkinEX5R-M13: CAGGAAACAGCTATGACCTTCCTGGCAAACAGTGAAGA
Exon 6	ParkinEX6F-M13: TGTAAAACGACGGCCAGTAGAGATTGTTTACTGTGGAAACA
	ParkinEX6Rnew-M13: CAGGAAACAGCTATGACCGTCCGTGGAGGGAAGTGAC
Exon 7	ParkinEX7F-M13: TGTAAAACGACGGCCAGTTGCCTTTCCACACTGACAGGTACT
	ParkinEX7R-M13: CAGGAAACAGCTATGACCTCTGTTCTTCATTAGCATTAGAGA

Exon 8	ParkinEX8F-M13: TGTAAAACGACGGCCAGTTGATAGTCATAACTCTGTGTAAG
	ParkinEX8R-M13: CAGGAAACAGCTATGACCACTGTCTCATTAGCGTCTATCTT
Exon 9	ParkinEX9F-M13: TGTAAAACGACGGCCAGTTTGCAGTCAGTTTGAAAGCTC
	ParkinEX9R-M13: CAGGAAACAGCTATGACCAATATAATCCCAGCCCATGTGCA
Exon 10	Parkin10FC1-M13: TGTAAAACGACGGCCAGTTGTTATTGCCAAATGCAACC
	ParkinEX10R-M13: CAGGAAACAGCTATGACCGGAACTCTCCATGACCTCCAG
Exon 11	ParkinEX11F-M13: TGTAAAACGACGGCCAGTACAGGGAACATAAACTCTGATCC
	ParkinEX11R-M13: CAGGAAACAGCTATGACCCAACACACCAGGCACCTTCAGA
Exon 12	ParkinEX12F-M13: TGTAAAACGACGGCCAGTGTTTGGGAATGCGTGTTTT
	ParkinEX12R-M13: CAGGAAACAGCTATGACCAGAATTAGAAAATGAAGGTAGACA
M13 sequencing primers	M13F: TGTAAAACGACGGCCAGT
	M13R: CAGGAAACAGCTATGACC

Table 2-3 Primers for Parkin exon sequencing used in this thesis.

Primer name	Sequence	Tm (˚C)
Parkin HindIII Koz	5'-GCAAGCTTGCCACCATGATAGTGTTTGTCAGG-3'	69.5
PSq1	5'-GCTCA GTCCTCCCAGGAG-3'	60.5
PSq2	5'-GCACAGACGTCAGGAGC-3'	57.6
PSq3	5'-GTGGGTTTGCCTTCTGCCG-3'	61.0
Parkin stop BamHI rev	3'-CCCCTGGTGACCAAGCTGCACATCCCTAGGCG-5'	72.3

Table 2-4 Primers for plasmid construct sequencing used in this thesis.

cDNA amplicon range	Sequence (5'-3')	Tm (˚C)
Full length	p-FL-Fw: GCAGGGAAGGAGCTGAGGAATGACTG	68.0
	p-FL-Rv: CTGCACTCCCCTTCATGGTACGCTT	66.3
Exon 1-6	p-16-Fw: GACCATGATAGTGTT	42.4
	p-16-Rv: GATGTTCCGACTATTTGTTGCGATCAGGT	65.3
Exon 3-4	p-34-Fw: TGCAGAATTGTGACCTGGAT	55.3
	p-34-Rv: AAGATGGACCCTGGGTC	56.7
Exon 2-7	p-27-Fw: TGATAGTGTTTGTCAGGTTCAACTC	59.7
	p-27-Rv: GGACAGCCAGCCACACAAG	61.0

Table 2-5 Primers for truncated cDNA amplification.

Mutation	Sequence (5'-3')	Tm (˚C)
S101A	Fw: CGGGAGCCCCAGGCGTTGACTCGGGTG	>75
	Rv: CACCCGAGTCAACGCCTGGGGCTCCCG	>75
S101D	FW: GCGGGAGCCCCAGGACTTGACTCGGGTG	>75
	Rv: CACCCGAGTCAAGTCCTGGGGCTCCCGC	>75
S378A	Fw: CATGAAGGGGAGTGCGCTGCCGTATTTGAAGCC	73.2
	Rv: GGCTTCAAATACGGCAGCGCACTCCCCTTCATG	732.
S378D	Fw: CCATGAAGGGGAGTGCGATGCCGTATTTGAAGCC	73.1
	Rv: GGCTTCAAATACGGCATCGCACTCCCCTTCATGG	73.1
S65A	FW: CTGGATCAGCAGGCCATTGTTCACATTGTG	68.1
	RV: CACAATGTGAACAATGGCCTGCTGATCCAG	68.1
S65D	Fw: CTGGATCAGCAGGATATTGTTCACATTGTGCAG	68.2
	Rv: CTGCACAATGTGAACAATATCCTGCTGATCCAG	68.2

Table 2-6 Primers for site-direct mutagenesis used in this thesis.

MLPA (Multiplex ligation-dependent probe amplification): MLPA kits were provided by IoN Department of Neurogenetics Diagnostic Lab (purchased from MRC-Holland). Parkin MLPA used SALSA MLPA P052-C1 Parkinson mix 2 which was able to detect PARK2 6q25.2, UCHL1 4p14, GCH1 14q22.1, and LRRK2 12q12.

siRNA knockdown:

siRNA used in this thesis were listed in Table 2-7 below

SMARTpool: siGENOME PKN2 siRNA	M-004612-03
SMARTpool: siGENOME PINK1 siRNA	M-004030-02
siGENOME Non-Targeting siRNA Pool	D-001206-13

Table 2-7 List of siRNA used in this thesis.

Parkin shRNA knockdown:

The vector backbone pGIPZ was obtained from Open Biosystems. The parkin shRNA insert is a pool of three constructs (numbers 84517, 84518 and 84520) targeting the *Parkin* gene at different sites. The three hairpin sequences are listed in Table 2-8 below.

84517	CGAGAGAGTTCTCACATTTAAT
84520	AACGTTTAGAAATGATTTCAAA
84518	CACTCACTAGAATATTCCTTAT

Table 2-8 Parkin shRNA sequences used in this thesis.

2.1.2.2 Biochemistry

The growth media for cell lines and human primary fibroblasts used in this thesis were summarised in Table 2-9.

0.25% trypsin-EDTA and sterile phosphate buffered saline (PBS) were purchased from Sigma-Aldrich, UK. 4-hydroxytamoxifen (4OH-Tx) and insulin were purchased from Sigma Adrich (Poole, UK). Epidermal growth factor (EGF) was purchased from PeproTech (NJ, USA). CK1 inhibitors (LH846, D4476, IC261), CCCP, DMSO, puromycin and G418 were purchased from Sigma-Aldrich).

Transfection reagent: Effectene Kit was purchased from Qiagen. Lipofectamine 2000 Kit was purchased from Invitrogen. DharmaFECT was purchased from Thermo Scientific

Western blot: NuPAGE 4-12% Bis-Tris protein gels and Novex Sharp Standard protein ladder were purchased from Invitrogen. Immobilon-P transfer membrane was purchased from Millipore (Billerica, MA, USA). Amersham chemiluminescent substrate was purchased from GE Healthcare (Bucks, UK). CL-Xposure X-ray film was purchased from Thermo Scientific. RG Universal X-ray fixer and developer were purchased from Champion Photochemistry (Chelmsford, Essex, UK). All the antibody used in Western blot were list in Table 2-10.

Medium	Supplement	Cell types grown with this medium
Dulbecco's modified eagle medium (DMEM) containing high glucose and 2mM L-glutamine (Life Technology, UK)	10% heat inactivated foetal bovine serum (FBS; Gibco/Life Technology, UK)	All immortalised cell lines and mouse embryonic fibroblasts (MEFs) unless stated otherwise.
DMEM containing high glucose and 2mM L-glutamine (Life Technology, UK)	10% FBS (Gibco/Life Technology, UK) and G418 disulfate salt 750ug/ml (Sigma-Aldrich, UK).	SH-SY5Y, only for clonal selection.
DMEM containing high glucose and 2mM L-glutamine (Life Technology, UK)	10% donor calf serum (DCS; PAA).	NIH-3T3 cells lines
DMEM containing high glucose, sodium pyruvate, and GlutaMAX-1 (Life Technology, UK)	10% FBS (Gibco/Life Technology, UK),Penicillin 50I.U/ml, and Streptomycin 50 ug/ml (Sigma-Aldrich, UK).	Human skin fibroblasts. (Antibiotics were only supplemented when culturing chunks of skin biopsy, and were tapered after fibroblasts appeared.

Table 2-9 Growth medium used in this thesis and cells grown with them.

Protein	Species	Dilution	Obtained from
Parkin	Rabbit	1:1000	Abcam
Parkin	Rabbit	1:1000	Cell Signalling
Parkin	Mouse	1:1000	Cell Signalling
Parkin	Mouse	1:1000	Santa Cruz
Parkin	Rabbit	1:1000	Enzo Life Science
FLAG M2 peroxidase (HRP)	Mouse	1:5000	Sigma-Aldrich
FLAG	Rabbit	1:5000	Sigma-Aldrich
Phospho-Parkin (S101)	Rabbit	1:1000	AbD Serotec
Phospho-Parkin (S378)	Rabbit	1:1000	AbD Serotec
Phospho-Parkin (S131)	Rabbit	1:1000	AAT Bioquest
Phospho-Parkin (S65)	Sheep	1:1000	Dr Miratul Muqit (University of Dundee, UK)
PINK1	Rabbit	1:1000	Novus
Phospho-Akt (T308)	Rabbit	1:1000	Cell Signalling
Phospho-Akt (S473)	Rabbit	1:1000	Cell Signalling
phospho-ERK1/2 (Thr202/Tyr204	Mouse	1:1000	Cell Signalling
ERK1/2	Rabbit	1:1000	Cell Signalling
phospho-S6 ribosomal protein (Ser235/236)	Rabbit	1:1000	Cell Signalling
S6 ribosomal protein	Rabbit	1:1000	Cell Signalling
phospho-p38 (Thr180/Tyr182),	Rabbit	1:1000	Cell Signalling
p38	Rabbit	1:1000	Cell Signalling
phospho-JNK (Thr183/Tyr185)	Rabbit	1:1000	Cell Signalling

JNK	Rabbit	1:1000	Cell Signalling
Mitofusin 1	Mouse	1:1000	Abcam
Mitofusin 2	Mouse	1:1000	Abcam
MIRO1	Rabbit	1:1000	Atlas Antibodies
VDAC1	Mouse	1:1000	Meuro-Mab
Mono-/poly-linkage ubiquitin	Mouse	1:1000	Enzo Life Science
K48-linked ubiquitin	Rabbit	1:1000	Millipore
K63-linked ubiquitin	Rabbit	1:1000	Millipore
LC3	Rabbit	1:1000	Novus
HtrA2	Rabbit	1:1000	R&D Systems
GAPDH	Mouse	1:1000	Abcam
ApoTrack cocktail	Mouse	1:1000	MitoScience
ATP synthase β subunit	Mouse	1:1000	Abcam

Table 2-10 List of antibodies used in Western blotting.

When not stated, all chemicals were purchased from Sigma (UK)

1x NuPAGE gel sample buffer (Invitrogen) containing 10mM of DTT as cell lysis buffer.

2% CHAPS lysis buffer: 10mM Tris (pH8), 150 mM NaCl, 2% CHAPS. EDTA-free protease inhibitor cocktail tablets (Roche) were added immediately before use. Additional PhosSTOP phosphatase inhibitor cocktail tablets (Roche) were added if phosphorylated proteins were to be analysed.

RIPA lysis buffer: 50 nM Tris HCl (pH7.5), 1% Triton X-100, 0.5 % deoxycholic acid, 0.1 % SDS, 100 mM NaCl, 1mM EDTA.

Triton lysis buffer: 50 nM Tris HCl (pH7.5), 150 mM NaCl, 1% Triton X-100, 10% Glycerol.

NP-40 lysis buffer: 50 nM Tris HCl (pH7.5), 150 mM NaCl, 0.5% NP-40, 1mM EDTA

Sample loading buffer: NuPAGE 4x LDS sample buffer (Invitrogen) plus DTT to a final concentration of 10 mM.

PBS Tween-20 0.1%: PBS tablets x 2, ddH2O 1000 ml, Tween-20 0.1%.

Gel running buffer: NuPAGE MES SDS running buffer (Invitrogen)

Transfer buffer: Tris-Glycine (National Diagnostic, Georgia, USA), 20% methanol

PBST: 1x phosphate buffered solution (PBS) was made from tablets (Invitrogen) diluted in deionised ultrapure water containing 0.1% Tween-20 (Sigma, UK)

Skimmed milk: Marvel milk powder was dissolved in PBST to the appropriate concentration.

Immunoprecipitation: ANTI-FLAG® M2 Affinity Gel and FLAG® Peptide lyophilized powder were purchased from Sigma (UK).

Mitochondrial isolation:

Buffers for short protocol: **Mitochondrial isolation buffer**: 70 mM Tris base (mw 121.14), 0.25 M sucrose (mw 342.3) and 1 mM EDTA, pH 7.4. **MES buffer**: 19.8 mM EDTA, 0.25 M D-mannitol (mw 182.172) and 19.8 mM MES (mw 195.2), pH 7.4. Both buffers were used at 1:1 ratio when used.

Buffers for long protocol: 10 mM Tris·HCl (pH 7.4), 1 mM sodium EDTA, 250 mM sucrose. Protease inhibitors cocktail tablets and phosphatase inhibitor cocktail tablets were added to the ice-cold buffer shortly before use.

Immunofluorescence: Fix: 4% PFA (paraformaldihide) in PBS. Permeabilise: 0.5% Triton X-100 in PBS. ProLong® Gold Antifade Reagent with DAPI, Alexa Fluor® 568 Goat Anti-Mouse IgG (H+L), Alexa Fluor® 488 Goat Anti-Rabbit IgG (H+L) were purchased from Invitrogen. Coverslips and glass slides were purchased from VWR.

2.1.3 Cell models

2.1.3.1 Immortalised cell lines

Human embryonic kidney (HEK293T) cells and human neuroblastoma SH-SY5Y cells were obtained from the European Collection of Cell Cultures (ECACC).

SH-SY5Y cells stably expressing wild-type (WT) FLAG-Parkin were kind gifts from Dr Helen Ardley (University of Leeds, UK) (Ardley et al., 2003). SH-SY5Y cells stably expressing FLAG-pcDNA3.1 were generated within the laboratory by Dr Emma Deas (UCL, UK).

SH-SY5Y cells stably expressing FLAG-Parkin mutants (S101A, S101D, S378A, S378D, S65A, S65A/S101A) were generated in lab as a part of the work in this thesis.

HEK293T cells stably expressing ΔMEKK3:ER were generated by Dr Plun-Favreau (Plun-Favreau et al., 2007). NIH-3T3 cells stably expressing myrAkt:ER or ΔRaf-DD:ER were all obtained from Dr Julian Downward and Dr Almut Schulze (Cancer Research UK).

2.1.3.2 Mouse embryonic fibroblasts

Immortalised HtrA2 WT MEFs were obtained in collaboration with Dr Miguel Martins (Leicester University, UK).

Cell lysates of WT and Parkin KO mouse MEF were kindly provided by Dr Matthew Gegg in UCL Royal Free Hospital for characterisation of anti-Parkin antibody by Western blotting.

2.1.3.3 Human skin fibroblasts

Control human primary skin fibroblasts:

Fibroblasts were isolated by punch biopsy following informed consent from healthy volunteers at the Royal Free Hospital by Dr Jan-Willem Taanman (UCL, UK), using the protocol previously described by Sly and Grubb lab (Sly and Grubb, 1979).

Human primary skin fibroblasts from parkin-mutant patients:

Skin puncture biopsies were performed following informed consent from parkin-mutant patients by Dr Una-Marie Sheerin. Fibroblasts were subsequently isolated at the Queen Square as a part of the work in this thesis, following the protocol previously described by Sly and Grubb lab (Sly and Grubb, 1979).Human induced pluripotent stem cells.

The skin biopsy was immediately transferred to our lab in Institute of Neurology in sterile falcon tube filled with culture medium at room temperature. The skin was then cut into smaller pieces of about 0.5 mm^3 in size. Each skin piece was placed in one 6 cm petri dish for development of fibroblasts in the incubator at 37˚C. The fibroblasts started to grow in a single layer around the skin piece after 7 to 10 days

2.2 Methods

2.2.1 Molecular biology

2.2.1.1 Parkin patient genotyping

DNA extractions were performed using Flexi Gene DNA Kits (Qiagen). PCR primers (Table 2-3), provided by the diagnostic lab of Department of Neurogenetics, were used for analysing all 12 exons of the parkin gene. All PCR primers contained sequences of M13 sequencing primers (18mer). The sequences were analysed using Sequencher version 4.9.

2.2.1.2 Multiplex Ligation-dependent Probe Amplification (MLPA) for analysis of whole exon deletions/duplications

MLPA was performed in the diagnostic lab of Department of Neurogenetics, using SALSA MLPA kit for detecting familial PD (P052-Parkinson mix 2) from MRC-Holland (Amsterdam, the Netherlands) and following the manufacturer's protocol.

2.2.1.3 Quantitative PCR

RNA extraction:

After rinsed with cold PBS, cells were harvested by scraping down in PBS, transferred to an Eppendorf and pelleted by centrifugation at 16,000 *g* for 5 min in a benchtop centrifuge. The supernatant was removed and the cell pellet either stored at -80°C, or immediately lysed for RNA extraction by resuspension

in lysis buffer provided with the Qiagen RNeasy mini RNA extraction kit, according to the manufacturer's protocol. Lysates were homogenised using Qiagen QIAshredder columns before the RNA was further extracted using the RNA extraction kit.

Reverse transcription:

For production of cDNA, 1 µg extracted RNA was reverse transcribed using Superscript III reverse transcriptase, according to the manufacturer's protocol. Briefly, 1 ug RNA was combined with random hexamer primers (final concentration 2.5 µM) and dNTP mix (final concentration 0.5 mM) in an initial volume of 12 µl and incubated at 65°C for 5 min. The mixture was immediately ice-shocked and then incubated on ice for 1 min before addition of the provided First-Strand 5x buffer, 5 mM DTT and RNAse out. The tube was then incubated at 42°C for 2 min. Before the 2 min was up, add 200 U Superscript III reverse transcriptase, bringing the total reaction volume to 20 µl. The reaction was incubated at 42°C for further 70 min, then the reaction was inactivated at 70°C for 15 min. The RT reaction can be kept at 4°C for further concentration measurement or for storage at -20°C.

Quantitative real-time PCR (qPCR):

mRNA expression of Parkin in SH-SY5Y, SH-SY5Y stably expressing FLAG-Parkin, SH-SY5Y stably expression Parkin shRNA was measured using TaqMan quantitative PCR, performed on a Rotor-gene 6000 (Corbett). 10 ng cDNA was combined with 2X Taqman Universal Mastermix and 20X probe sets for the gene of interest and GAPDH in a total reaction volume of 6.5 µl. Assay conditions are shown in Table 2-11 below.

Step	Cycles	Temperature	Time
Initialisation	1	95 °C	10 min
Denaturing	35	95 °C	30 sec
Annealing		60 °C	45 sec

Table 2-11 Thermal cycling protocol for qPCR (TagMan).

Data were acquired on the green (FAM) and yellow (VIC) channels during the 60°C extension step (gain = 10). Data were analysed using the $2^{-\Delta\Delta CT}$ method (Livak and Schmittgen, 2001), using GAPDH as an internal standard.

2.2.1.4 Plasmid amplification and purification

Production of competent *E.coli*:

One vial of chemically competent Top10 *E. coli* was diluted in 5 ml LB and cultured overnight in a shaking incubator at 37°C and 220 rpm. Next morning 1 ml of this pre-culture was transferred into 200 ml LB and incubated with shaking for ~ 4 h until the bacteria were dividing exponentially (OD_{580} = 0.3-0.5). The bacteria were pelleted in a pre-cooled (4°C) centrifuge for 7 min at 5000 *g*, resuspended in 30 ml filter-sterilised TF buffer I and incubated on ice for 15 min. The bacteria were then pelleted for a second time at 5000 *g* for 7 min, resuspended in 7.5 ml filter-sterilised TF buffer II and incubated for 15 min on ice before aliquoting into pre-chilled autoclaved Eppendorfs. Aliquots of 50 µl were snap frozen in liquid nitrogen and stored at -80°C until needed.

Transformation/Re-transformation:

DNA (1 µg purified DNA for re-transformation) was added to 50 µl chemically competent Top10 *E. coli* on ice, mixed gently by flicking and incubated on ice for 30 min. Bacteria were heat-shocked at 42°C for 30 s before returning to ice for a further 5 min. 200 µl pre-warmed LB medium without antibiotic was added and the bacteria incubated for 1 h shaking at 37°C and 225 rpm. 50 to 100 µl bacteria (in the case of DNA re-transformation) were spread on pre-warmed LB-agar plates containing the appropriate antibiotic selection and incubated overnight at 37°C.

Glycerol stock storage:

Pick one colony from the LB-agar culture mentioned above and cultured in 3 ml LB broth for 6-8 h. Prepare sterilised 80% glycerol by autoclaving. Then in a

sterile 2 ml screw-cap tube add 0.5 ml of 80% glycerol and the same amount of bacteria stock from the 3 ml culture, to reach final concentration of 40% glycerol. Snap freeze the glycerol stock tubes in liquid nitrogen and then stored at -80°C until needed.

Utilisation of glycerol stock: Scrape the surface of the frozen glycerol stock, then streak out onto a fresh LB agar plate. Then in the next morning pick a single colony as usual. Alternatively thaw half of the glycerol stock and add it straight into a 200ml culture for further incubation.

Plasmid purification:

For preparation of small quantities of DNA (Miniprep), single bacterial colonies were picked using a sterile Gilson pipette tip into 4 ml LB broth containing the appropriate antibiotic selection and incubated at 37°C shaking at 220 rpm overnight. The resulting bacteria were pelleted by centrifugation at 16,000 *g* for 1 min in a 2 ml Eppendorf, resuspended in 250 µl Qiagen buffer P1 and DNA extracted using a QIAprep spin miniprep kit according to the manufacturer's instructions.

For the preparation of larger quantities of DNA (Maxiprep), bacterial colonies were picked as described above into 3 ml LB broth containing the appropriate antibiotic, and incubated at 37°C at 220 rpm for approximately 8 h. After this time, 1 ml bacterial culture was transferred into 200 ml LB containing antibiotic and incubated overnight at 37°C, shaking at 220 rpm. The resulting bacteria were pelleted by centrifugation at 6000 *g* for 15 min, resuspended in 10 ml Qiagen buffer P1, and DNA extracted using a QiaFilter Plasmid Maxiprep kit, according to the manufacturer's protocol. Upon elution of the DNA in buffer QF, DNA was precipitated using isopropanol according to the manufacturer's instruction, but at this point the recommended purification of DNA using 70% ethanol was replaced with sodium acetate precipitation. The precipitated DNA was resuspended in 100 µl deionised water and transferred to an Eppendorf containing 1 ml 100% ethanol and 40 µl 3 M NaAc (pH 5.2). The Eppendorf was

kept at -80°C overnight to facilitate precipitation of DNA. The DNA was pelleted by centrifugation at 16,000 *g* for 30 min in a cooled benchtop centrifuge. The supernatant was aspirated and the pellet allowed to air dry before resuspension in an appropriate volume of sterile deionised water. Plasmid concentration and quality was measured spectrophotometrically using a NanoDrop 2000.

2.2.1.5 Sequencing:

For each construct generated, 6-12 colonies were picked, mini-prepped and sent for Sanger sequencing at the UCL Scientific Support Service. Sequencing primers were designed across exon boundaries to exclude the possibility of genomic DNA contamination, at intervals of approximately 500 bp. The program Primer3 (*http://frodo.wi.mit.edu/*) was used to generate primer sequences, using an optimal primer length of 20 residues (acceptable range 18-27) and an optimal Tm of 60°C (acceptable range 57-63°C). All sequences returned were analysed by aligning the sequenced sense and antisense fragments with the expected sequence for *Parkin* using Sequencher software (GeneCodes, MI, USA). This compilation was analysed by eye to check for mutations or changes to the open reading frame.

2.2.1.6 Mutagenesis

Full-length human Parkin was inserted into FLAG-pcDNA3 as backbone unless otherwise specified. FLAG-pcDNA3 empty vector and FLAG-Parkin pcDNA3 were gifts from Dr Helen Ardley (Leeds Institute of Molecular Medicine) and have been previously described (Ardley et al., 2003). FLAG-Parkin S101A, S101D, S65A, S65D, S65A/S101A, S65D/S101D mutations were generated by site-direct mutagenesis on the FLAG-Parkin pcDNA3 backbone.

Mix the follow material for PCR reaction: 50ng of DNA, 1.25 ul of forward primer, 1.25 ul of reverse primer, 2.5ul DMSO, and add AccuPrime Pfx mastermix up to 25 ul as final volume. The mixtures were then subjected to PCR reaction.

The PCR thermal cycling protocol for mutagenesis is listed in Table 2-12 below:

Segment	Cycles	Temperature	Time
1	1	95 ˚C	30 sec
2	18	95 ˚C	30 sec
		55 ˚C	1 min
		68 ˚C	2 min/kb
3	Standby	4 ˚C	

Table 2-12 PCR thermal cycling protocol for mutagenesis.

The PCR reactions were than subjected to Dpn1 digestion for remove the methylated, non-mutated parental DNA templates. Add 1 ul of Dpn1 restriction enzyme to each PCR reaction product. Mix well and then spin down the mixture. Then incubate the mixture at 37 ˚C for 1 h. The products were then ready for subsequent plasmid amplification procedures.

2.2.2 Cellular biology

2.2.2.1 Cell culture and transfection

Target cells were obtained from European Collection of Cell Cultures (ECACC) and cultured in Dulbecco's Modified Eagle Medium (DMEM) containing 4.5 g/L glucose and L-glutamine, and supplemented with 10% heat-inactivated FBS in a humidified chamber at 37˚C with 5 % CO_2. SH-SY5Y cells stably expressing FLAG-Parkin WT or mutants were generated by transfecting the SH-SY5Y cells using Effectene reagent (Qiagen) following manufacturer's instruction. Transfected cells were selected by appropriate antibiotics (G418, 0.75 mg/ml or puromycin 2 μg/ml) 48 h after transfection. Monoclonal cell lines were obtained by limiting dilution procedure.

2.2.2.2 Stable cell line generation

Transfection reagent:

Effectene transfection reagent was used according to the manufacturer's instruction (Qiagen, UK). Appropriate amount of SH-SY5Y cells were seeded in 10 cm dishes the day before the transfection and incubated under normal growth condition, and the cells were transfected at 60% confluence (approximately).

Limiting dilution:

Forty-eight hours after transfection, the cells were subjected to 2μg/ml puromycin (or G418, depending on plasmid types) selection. After 10 days of antibiotics selection, the cells were trypsinised and seeded in 96-well plates at the concentration of ½ cell/well, 1 cell/well, and 2 cells/well. A month later single colonies were picked for further expansion. The colonies were successively seeded in 24-well, 12-well and then 6-well plate. Only the colonies with moderate expressing GFP were kept. The final clones were then subjected to Western blotting and q-PCR to confirm the knockdown.

2.2.2.3 Activation of ΔMEKK3:ER, myrAkt:ER or ΔRaf-DD:ER cell lines

ΔMEKK3:ER HEK293T cells, or myrAkt:ER or ΔRaf-DD:ER NIH3T3 cells were seeded in 6-well plates. Confluent cells were then starved overnight with serum free DMEM. These cells were then stimulated with 100 nM 4OH-Tx for the time indicated. 100% ethanol was added as a control vehicle. Finally cells were harvested and samples were prepared for Western blottings.

2.2.2.4 Activation of endogenous PI3K/Akt signalling pathway

HEK293t cells were seeded into 6-well plates and then transfected with FLAG-parkin and FLAG-pcDNA3 (vector control), respectively, using Effectene transfection reagent. The transfection continued for 60 hours before the media were replaced by serum free DMEM for another 16 hours. MEFs or control human primary fibroblasts were seeded in 6-well plates. Confluent cells were then starved overnight with serum free DMEM. All serum-starved cells were

then stimulated with 10 to 100 ng/ml of EGF and 50 to 100 nM insulin diluted in serum free DMEM.

2.2.2.5 iPSC generation

The viral packaging and fibroblast transduction protocol were simplified in Table 2-13 below.

Day 1	1. Coat 4x10cm dishes with 1.2ml Poly-d-lysine, incubate RT for 2 hours 2. Wash 3x PBS 3. Seed 3.6x10^6 Plat-A cells per plate in 12ml DMEM+FCS without antibiotics
Day 2	1. One hour before transduction, change medium to Optimem, 12ml/dish 2. Dilute 16ug DNA with 1.5ml Optimem 3. Dilute 60µl Lipofectamine 2000 in 1.5ml Optimem, incubate RT for 5 min 4. Mix DNA + Lipofectamine together, incubate RT for 20 min 5. Add mixture to appropriate dish
Day 3	1. Change medium to DMEM+FCS, 6ml per plate 2. Seed fibroblasts: 100,000 per well of 3 – 6/well
Day 4	1. Collect and combine 4 viral supernatants, filter 0.45um 2. Add to cells to be transduced (24ml total, ~4ml per well, 6 wells) 3. Supplement with 8 ug/ml polybrene per well 4. 2 of 3 wells of each target lines (3rd being untransfected control) 5. Replenish media on transfected cells
Day 5	1. Repeat steps 1-5 of day 4 2. Discard packaging cells 3. Seed feeders (irradiated SNL or MEF), 900,000 per 10cm dish x4
Day 6	1. Lift transduced fibs, with accutase (no need for ROCK inhibitor) 2. Count 3. Seed cells on 10cm dish of feeders (range 60,000 to 500,000 cells per dish) 4. Freeze down remainder
Day 7	1. Change media on plates to hES media + 0.5mM valproic acid + 20ng/µl bFGF 2. Replace media alternate days thereafter, until colonies form 3. Then, withdraw valproic acid and feed daily with hES media

Table 2-13 Viral packaging and fibroblast transduction protocol for iPSC generation.

2.2.3 Biochemistry

2.2.3.1 Harvesting cells and protein extraction from cultured cells

By sample buffer

The cells were kept on ice throughout the all the steps of the procedure. Growth media was removed and then the cells were washed once with cold PBS. PBS was removed and 1X NuPAGE sample loading buffer supplemented with 10mM DTT was added to the cells. Cells were then scraped to tubes, boiled for 10 min, and then sonicated briefly. The homogenates were then centrifuged at 4˚C at 13,000 rpm for 10 min, and the supernatants were transferred to new Eppendorf tubes for further western blot analysis,

By lysis buffer

The cells were kept on ice throughout the all the steps of the procedure. They were first washed with cold PBS, than harvested by adding appropriate lysis buffer (2% CHAPS buffer, RIPA buffer, NP-40 buffer, or Triton X-100 buffer. See material) supplemented with protease inhibitors and phosphatase inhibitors and scraped in to Eppendorf tubes. Lysates were snap frozen in liquid nitrogen or frozen in -80˚C overnight. They were then thawed on ice, incubated at 4˚C in a rotatory wheel for 1 h to ensure complete lysis. Insoluble cellular components were removed by centrifugation at 16,000 g for 10 min at 4˚C. The supernatant was transferred to a fresh Eppendorf tube and stored at -20˚C if not used immediately.

2.2.3.2 Mitochondrial isolation (short protocol)

To isolate mitochondria from cultured cells for the analysis of mitochondria-associated protein, a protocol was followed from (Samali et al., 1999). Briefly, the growth media was aspirated from the cells and the cell monolayer rinsed once with PBS. An appropriate volume of mitochondrial isolation buffer (100 µl for one well of a 6 well plate) was added directly to the cells, then an equal

volume of MES buffer with 0.2 mg/ml digitonin added and incubated at room temperature for 10 min. The cells were scraped into an Eppendorf and pelleted at 900 g for 2 min to remove intact cells and debris. The supernatant was then centrifuged at 16,000 g for 10 min to separate the mitochondrial pellet from the cytosolic fraction (the supernatant). The cytosolic fraction was removed and diluted directly in sample buffer for Western blot analysis, while the mitochondrial pellet was rinsed once with PBS, resuspended in diluted sample buffer and sonicated before loading.

2.2.3.3 Mitochondrial isolation from SH-SY5Y cells (long protocol)

Permeabilisation of the cells by digitonin in the previous method may strip loosely associated proteins (for example, Parkin) from the outer mitochondrial membrane. For this reason, an alternative protocol was followed from (Gegg et al., 2010) with few modification to reduce cross contamination. Harvest cells from one confluent 10-cm plate by aspirating the media, washing the plate with ice cold PBS, adding 1 ml mitochondrial homogenisation buffer (MHB) supplemented with freshly-added protease inhibitor and phosphatase inhibitor, and then freezing the plate in -80˚C freezer for at least 1 h. Then thaw the plates on ice, scrape the cells (in MHB) to 2 ml tubes, and store the tube in -80˚C freezer overnight. Next day, thaw the tubes on ice. Homogenise the cells by resuspending the mixture with p200 micropipettor carefully (20 pipetting per sample), then pellet nuclei, cell debris and unbroken cells by centrifugation at 1,500 g for 10 min at 4˚C. Transfer the supernatant to a new 2-ml tube, repeat centrifugation at 1,500 g for 10 min at 4˚C to remove any residual nuclei, cell debris and unbroken cells. Transfer the supernatant to a new 2-ml tube and pellet mitochondrial by centrifugation at 12,000 g for 20 min at 4˚C. Transfer the supernatant to a new 1.5 ml tube. Resuspend the mitochondrial pellet with 1 ml of MHB supplemented with protease inhibitors and phosphatase inhibitors and transfer all to a new 2-ml tube. Centrifuge both 1.5 ml and 2 ml tubes at 12,000 g for 30 min at 4˚C. From the 1.5-ml tube, transfer the supernatant (cleaned cytosolic fraction) to fresh 1.5 ml tube. For the 2 ml tube, remove and discard the supernatant carefully by pipette. The cleaned mitochondrial pellet

was resuspended in 100 ul 1x sample buffer supplemented with 10 uM DDT (mitochondria-enriched fraction) and sonicated for further Western blot analysis.

2.2.3.4 Western blotting

The cell lysates were loaded onto a 4-12% NuPAGE gel. Proteins were separated by electrophoresis at 80 to 100V and then were transferred to Polyvinylidene fluoride (PVDF) microporous membrane for 80 minutes at 80V at 4˚C. The membrane was blocked in 3% skimmed milk in PBS-Tween20 for 1 h at room temperature and further incubated with the primary antibody diluted in blocking buffer either overnight (16 h) at 4˚C or for 1 h at room temperature. The membrane was washed 6 times for a total 1 h in PBS-Tween 20, incubated with appropriate secondary antibody diluted in blocking buffer for 1 hr at the room temperature, and further washed 6 times for a total 1 h in PBS-Tween 20. Membrane was developed by incubation with 1 ml of ECL (enhanced chemiluminescence) (Pierce, UK) for 1 minute, and then exposed to X-ray film for an appropriate period of time to record the resultant chemiluminescence.

Proteins bands were scanned and the intensities were quantified and analysed using Image J software.

2.2.3.5 Immunoprecipitation:

Prepare CHAPS lysis buffer (CHAPS 2%, NaCl 150mM, Tris-HCl (pH8.0) 10mM), by adding protease inhibitors and phosphatase inhibitors freshly before use. After harvesting cells, resuspend each dry cell pallet with 1mL of icy cold CHAPS lysis buffer. Samples were incubated on a rotation mixer at 4°C for 1 h, and then centrifuged at 13,200 rpm for 10 min at 4°C. While centrifuge is occurring, prepare FLAG beads (ANTI-FLAG M2 Affinity Gel), Wash 25ul/sample of packed FLAG bead with CHAPS lysis buffer and remove the buffer carefully after wash. Resuspend the washed beads with equal volume (25ul/sample) of CHAPS lysis buffer (with protease inhibitor) to achieve 50% v/v bead suspension. Apply 50ul/sample of bead suspension to each fresh 1.5 mL Eppendorf for further use.

Transfer the supernatants (cell lysates) after centrifuge into fresh 1.5mL Eppendorfs. Transfer 9/10 of lysate into the 1.5mL Eppendorf containing 50ul of FLAG beads suspension ('IP samples'). The rest 1/10 can be stored as 'input' (later load 10 ul of each input sample for SDS-PAGE). The 'IP samples' were incubated on a rotation mixer at 4°C for a minimum of 2 h, to facilitate binding of the FLAG-tagged protein to the antibody. After reaction, the IP sample was centrifuged at 1,000 rpm for 2 min at 4°C, and the supernatant was removed carefully. The pelleted FLAG-beads were then washed by adding 1 ml/sample of CHAPS lysis buffer and gently inverting the tubes for 6 times. Then centrifuge IP samples at 1,000 rpm for 2 min at 4°C and remove supernatant carefully. The FLAG-beads were washed for total three times. Finally, elute FLAG-tagged protein from FLAG beads by FLAG-peptide. Prepare FLAG-peptide to working concentration of 150 ug/ml. Add 100 ul of 150 ug/ml FLAG-peptide to each sample. Agitate the sample by scratching the Eppendorfs against the tube rack for 30 min. Centrifuge at maximum speed (13,200 rpm) for 2 min. Transfer 80ul of eluted solution to a fresh Eppendorf. Load 10ul of eluted IP sample for SDS-PAGE.

2.2.3.6 Immunofluorescence and confocal imaging

Cells plated on 13mm glass coverslips were fixed with 4% Paraformaldehyde/phosphate buffered saline (PBS) solution for 20 min at room temperature, then permeabilised using 0.5% Triton X-100/PBS for 15 min. Samples were blocked for 30 min in 10% FBS/0.5% Triton X-100/PBS solution before addition of the primary antibody for 2 h in 10% FBS/PBS solution. The appropriate secondary antibodies were added in 10% FBS/PBS for 1 h and then the coverslips were mounted to glass slides using ProLong® Gold Antifade Reagent with DAPI (Life Technologies P36931). Primary antibodies were used as follows: rabbit anti-FLAG (Sigma F7425, 1:2,000), mouse anti-FLAG (Sigma F3165, 1:2,000), anti-Parkin (pSer101) (AbD AHP 1304, 1:1,000), anti-mono/poly-ubiquitinated conjugates (FK2) (Enzo Life Sciences PW8810, 1:1,000), anti-K48 polyubiquitinated protein (clone Apu2; Millipore 05-1307; 1:1000), anti-K63 polyubiquitinated protein (clone Apu3; Millipore 05-1308;

1:1000), anti-p62 (Abcam ab56416, 1:1,000), rabbit HtrA2 (R&D AF1458, 1:1,000), mouse anti-complex V β subunit (Abcam as4730, 1:2,000). Secondary antibodies were used as follows: Alexia Fluor® 568 anti-mouse (Life Technologies A-11004, 1:2,000), and Alexia Fluor® 488 anti-rabbit (Life Technologies A11008, 1:2,000). Confocal images were obtained with Zeiss 710 via CLSM equipped with a META detection system using 63x oil immersion objective, with excitation/emission at 495/515 nm for detecting primary antibodies raised in rabbit and 558/583 nm for primary antibodies raised in mouse. Images were processed with Zen software (Carl Zeiss) or Volocity image analysis software (PerkinElmer).

For quantification of Parkin mitochondrial translocation, mitochondrial ubiquitination, p62 recruitment and mitochondrial clearance, approximately 150 cells per coverslip were acquired. Cells were scored visually by one non-blinded and two blinded observers independently, and final cell numbers were calculated by the average of results by three observers. For Parkin mitochondrial translocation (or mitochondrial ubiquitination), cells were categorized into no, partial or complete Parkin translocation (or mitochondrial ubiquitination) according to the levels of Parkin (or ubiquitin) co-localizing with mitochondria. A cell with no Parkin (or ubiquitin) signal co-localized with mitochondria was classified as no Parkin translocation (or mitochondrial ubiquitination), and a cell with all Parkin (or ubiquitin) signals co-localized with all mitochondria, regardless of mitochondrial morphology, was complete Parkin translocation (or mitochondrial ubiquitination). Any cells that fail to fulfil the criteria for no or complete Parkin translocation (or mitochondrial ubiquitination) were categorized as partial. For p62 recruitment experiment, only cells with complete co-localization of p62 and mitochondria were scored as positive. For mitophagy experiment, only cells with no staining for the mitochondria were scored positive for mitochondria clearance. In all cases, a minimum of 150 cells were scored per coverslip and each experiment was performed at least three times.

2.2.3.7 Compaction index of mitochondrial calculation

Compaction index is defined by the ratio of the shortest possible perimeter of an object (which is a perimeter of a circle) with the same area as the object of interest divided by the actual perimeter of the object of interest. To measure the perimeter and area of mitochondria in an individual cell, the confocal images were exported as single-channel (CVβ) only images. CVβ channel was then converted into binary in ImageJ program (NIH). The individual cell was selected using the ''region of interest'' tool and the accumulated perimeter and area of mitochondrial within this selected cell were measured using ''analyse particles'' tool. Compaction index of mitochondria was calculated by the following formula (P: actual perimeter; A: area of object of interest):

$$(2\pi*((A/\pi)^{1/2}))/P.$$

At least six cells were selected per coverslip and the experiment was performed at least three times.

2.2.3.8 In-silico modelling of pS101 with human full-length Parkin structure

(This part of work was perform in collaboration with Dr Wolfdieter Springer's lab in Department of Neuroscience Mayo Clinic.)

Computational modelling: Modelling of the human full-length Parkin structure has been described elsewhere. Initial modelling for P-S101 was performed using the Schrödinger software suite (Schrödinger, LLC) (Loving et al., 2009; Schrödinger, 2013). The starting conformation of all residues within 12 Å of pS101 was obtained by the method of Polak-Ribière conjugate gradient (PRCG) energy minimization with the Optimized Potentials for Liquid Simulations (OPLS) 2005 force field (Jorgensen and Tiradorives, 1988) for 5000 steps, or until the energy difference between subsequent structures was less than 0.001 kJ/(mol-Å) (Mohamadi et al., 1990). Our methodology has been described previously (Caulfield and Devkota, 2012; Caulfield et al., 2011; Friesner et al.,

2006; Loving et al., 2009). Briefly, in order to generate the protein with the protein preparation wizard module, which uses Schrödinger's builder module for manipulation and modification of residues, we relaxed the region surrounding residues pS101 of Parkin at a distance of 12 Å following model building and minimization. Then, we prepared grids for the region surrounding pS101 for future Glide docking experiments scanning for small molecule binders in this region (Loving et al., 2009; Salam et al., 2009). Site hydroxyls, such as in serines and threonines, were allowed to move with rotational freedom. Hydrophobic patches were utilized within the Van der Waals (VdW) as an enhancement. Structural refinement with molecular dynamics**:** Yasara-based molecular dynamics was next implemented for refining the structure under the Amber04 force field (D.A. Pearlman, 1995; Krieger et al., 2009). Molecular modelling for importing and refining the X-ray structure and generation of pS101 modification, as well as, rendering of figure images were completed with Maestro, the built-in graphical user interface of the Schrödinger chemistry package (v. 5.6) (Schrödinger, 2013). Molecular dynamics was run for over 100 ns as previously described (Caulfield and Devkota, 2012; Zhang et al., 2013).

Chapter 3 Characterisation of Parkin fibroblasts and generation of induced pluripotent stem cell model from Parkin fibroblasts

3.1 Introduction

As described in Chapter 1, Parkin is an E3 ubiquitin ligase with multiple cellular functions (Clark et al., 2006; Darios et al., 2003; Henn et al., 2007; Higashi et al., 2004; Jiang et al., 2004; Park et al., 2006; Petrucelli et al., 2002; Poulogiannis et al., 2010; Staropoli et al., 2003; Tay et al., 2010; Veeriah et al., 2010). Parkin pathogenic mutations cause a loss of function of this protein in familial PD through various mechanisms (Dawson and Dawson, 2010). Deletions which span several exons usually eliminate normal protein function. Nonsense mutations result in a truncated protein, which may be degraded more easily, causing reduced or complete loss of function (Dawson and Dawson, 2010). Missense mutations may still produce full-length protein with substituted amino acids; however, the resulting mutant protein may have reduced stability, decreased solubility and therefore altered intracellular localisation, reduced enzyme activity, or aberrant ubiquitination (Hampe et al., 2006; Matsuda et al., 2006; McNaught et al., 2003; Wang et al., 2005b; Winklhofer et al., 2003). Furthermore, various environmental stresses have been reported to alter or inactivate Parkin functions in sporadic PD cases. These stress include

nitrosative stress, oxidative stress and dopaminergic stress (Chung et al., 2004; Yao et al., 2004).

How Parkin mutations cause PD remains poorly understood. Investigation of Parkin functions has been initiated in various cellular and animal models. However, most of the currently available Parkin animal models (described in 1.3.6) do not show robust phenotypes that simulate the human disease (Perez and Palmiter, 2005). As for the immortalised cancer cell lines, they do not fully recapitulate the physiological environment of Parkin mutations due to their cell cycle regulation and bioenergetics differs considerably from neuronal cells. Recent cellular biology breakthrough in generating induced pluripotent stem cells (iPSC) from patient's fibroblasts sheds light on the research for neurological diseases like PD wherein pathological neurons are almost impossible to be obtained for further investigation. This chapter aims to generate Parkin-mutant iPSC by reprogramming the skin fibroblasts from PD patients carrying mutations in the *Parkin* gene and apply this model for further investigation of Parkin molecular pathways. The work described in the first section of this chapter starts with validating antibodies against Parkin. A number of commercially available Parkin antibodies will be assessed for their specificity in detecting Parkin in cell lysates extracted from several cell lines by various lysis buffers.

According to UniProt database (http://www.uniprot.org/uniprot/O60260), the Parkin protein is widely expressed, more abundantly in the brain, heart, skeleton muscles and testis. Fibroblasts and peripheral leukocytes also demonstrate detectable Parkin protein (Kasap et al., 2009; Nakaso et al., 2006). Therefore, the patient's fibroblast itself can potentially be a good model for the research if the antibody is specific enough to detect endogenous Parkin. In the second section of this chapter, human fibroblasts from Parkin patients in UCL, Royal Free Hospital were validated to confirm the mutation as well as the protein expression level. Another skin biopsy from the Parkin patient in National Hospital for Neurology and Neurosurgery, Queen Square, was obtained and skin fibroblasts culture was set up on site in our lab before characterisation

of the fibroblast line. Finally, the attempt to generate Parkin-iPSC was described in the third section of this chapter.

3.2 Results

3.2.1 Characterisation of anti-Parkin antibody

Although a considerable amount of studies show the detection of endogenous Parkin by Western blotting using various anti-Parkin antibodies, non-specific bands in the blots were frequently observed in the many of these studies. With this in mind, I first assessed the specificity of several anti-Parkin antibodies.

3.2.1.1 Information of Parkin antibodies tested

A number of commercially available Parkin antibodies were purchased. Five antibodies were selected for further validation, namely Cell Signalling (mouse, CS4211), Cell Signalling (rabbit, CS2132), Abcam (rabbit, ab15954), Santa Cruz (mouse, SC-32282) and Enzo (rabbit, BML-PW9365). Their product informations are listed below (Table 3-1). The product category numbers were used throughout this thesis to specify the various antibodies.

Make	Spices	Cat No	Epitope	Applications
Cell Signalling	Mouse (Prk8)	CS4211	**Human** recombinant Parkin maps to the carboxy terminus of Parkin	WB, IP
Cell Signalling	Rabbit	CS2132	Synthetic peptide correspond to residues surrounding aa 400 of **human** Parkin	WB
Abcam	Rabbit	ab15954	Synthetic peptide corresponding to aa 304-322 of **mouse** Parkin.	WB, IP, IF
Santa Cruz	Mouse (Prk8)	SC-32282	**Human** recombinant Parkin maps to the carboxy terminus of Parkin	WB, IP, IF
Enzo	Rabbit	BML-PW9365	Synthetic peptide (PP9366) aa 399-412 of **human** Parkin	WB, IP, IF

Table 3-1 Information of Parkin antibodies tested.

Details of the five Parkin antibodies used in this project. Information of epitope were provided by manufacturer's datasheet. (Abbreviations: aa, amino acid. WB: Western blotting. IP: immunoprecipitation. IF: immunofluorescence.)

3.2.1.2 Validation of Parkin antibodies by transient knockdown of Parkin with siRNA in SH-SY5Y cells stably expressing FLAG-Parkin

In order to assess the specificity of the different antibodies, PARK2 (Psi) and scrambled (Ssi) small interfering RNA (siRNA) were used to transiently knockdown Parkin expression in SH-SY5Y neuroblastoma cells stably expressing FLAG-Parkin (Ardley et al., 2003). Untransfected SH-SY5Y cells and control human primary fibroblasts were used as controls for endogenous Parkin expression. Cells were harvest and lysed 72 h post transfection using RIPA buffer. The lysates were further analysed by SDS-PAGE and Western blotting (Figure 3-1). Anti-FLAG antibody detected strong FLAG-Parkin expression in untransfected and Ssi-transfected FLAG-Parkin SH-SY5Y cells, whereas FLAG-Parkin expression was almost completely inhibited in Psi-transfected cells, indicating a satisfactory knockdown efficiency. However, when probing with the ab15954 anti-Parkin antibody, Parkin knockdown appeared to be less efficient compared to the anti-FLAG antibody. The ab15954 antibody detected both FLAG-tagged and endogenous Parkin. Finally this preliminary experiment suggested that endogenous Parkin expressed at lower levels in control human primary fibroblasts as compared to SH-SY5Y cells.

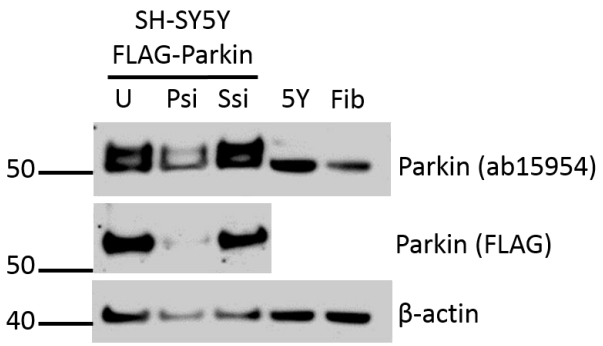

Figure 3-1 FLAG-Parkin knockdown by Parkin siRNA.

SH-SY5Y cells stably expression FLAG-Parkin were transfected with Parkin and non-targeting pool siRNA. The Western blotting membranes were probed with anti-Parkin (ab15954) and anti-FLAG antibodies, respectively. (Abbreviations: U, untransfected. Psi: Parkin siRNA. Ssi: non-targeting siRNA. 5Y: SH-SY5Y. Fib: control human fibroblast.)

3.2.1.3 Generation of stable Parkin knockdown SH-SY5Y cell lines by short hairpin RNA

Given that endogenous Parkin was detectable with the ab15954 antibody, I have then generated a stable Parkin knockdown cell line that can be used as a control and a model for investigating Parkin molecular pathways at the later stage of this project. Three human *Parkin* shRNAs were selected and mixed as a pool for transfection. The pGIPZ vector encodes a GFP marker that enables the identification of shRNA–expressing cells by fluorescence microscopy, and a puromycin resistance for further generation of stable knockdown cell lines. Stable cell lines transfected with empty pGPIZ vector or a non-targeting shRNA sequence (scrambled) were also generated as negative controls. Effectene transfection reagent was used in accordance with the manufacturer's protocol. Cells were selected by puromycin 48 h post transfection and clones were generated by limiting dilution protocol (See 2.2.2.1 for details). Finally, the clones were chosen under fluorescence microscope for their moderate GFP expression and similar cell duplication speed as to the untransfected SH-SY5Y cells.

3.2.1.4 Validation of Parkin antibodies by Parkin knockdown cell lines

Six knockdown (K1 to K6), five empty-vector (E1 to E5), and 3 scrambled shRNA (S1 o S3) clones were chosen for further validation of Parkin knockdown. Cells lysates from all the clones were collected for analysing protein expression by Western blotting (Figure 3-2 A). Parkin was knocked down in three of the six clones (K3, K4, K5). Due to limited number of wells in each gel, the two best knockdowns (K4, K5) as well as one empty-vector (E2) and one scrambled shRNA (S1) clones were analysed again with untransfected SH-SY5Y and FLAG-Parkin SH-SY5Y cells at the same protein amount (Figure 3-2 B). Although K5 still showed good knockdown, E2 also demonstrated reduced Parkin expression.

Real-time polymerase chain reaction (qPCR) was performed to further assess the knockdown. The three knockdown clones (K3, K4, and K5) showed 65% to

85% reduction of Parkin expression, with K4 and K5 clones giving the best knockdowns (Figure 3-2 C). Inexplicably, a slightly increased Parkin expression was observed in the E2 clone. The S1 clone, on the other hand, revealed mild (18%) but significant reduction of Parkin expression, suggesting possible non-specific inhibition caused by scrambled shRNAs.

K5 Parkin knockdown clone was then chosen for further Parkin antibody validation. Three different Parkin antibodies (CS4211, SC-32282 and ab15954) were used for testing four different cell lines (MEFs, untransfected SH-SY5Y, Parkin knockdown SH-SY5Y K5, and FLAG-Parkin SH-SY5Y). Two different protein amounts were loaded in order to better distinguish antibodies with higher specificity (Figure 3-3). The two Parkin antibodies raised in mouse (SC4211 and SC-32282) showed a strong sensitivity to FLAG-Parkin but detected no Parkin in MEFs. SC4211 apparently detected endogenous Parkin more efficiently in SH-SY5Ys as compared to SC-32282. The rabbit antibody (ab15954) apparently detected Parkin in all cell lines tested.

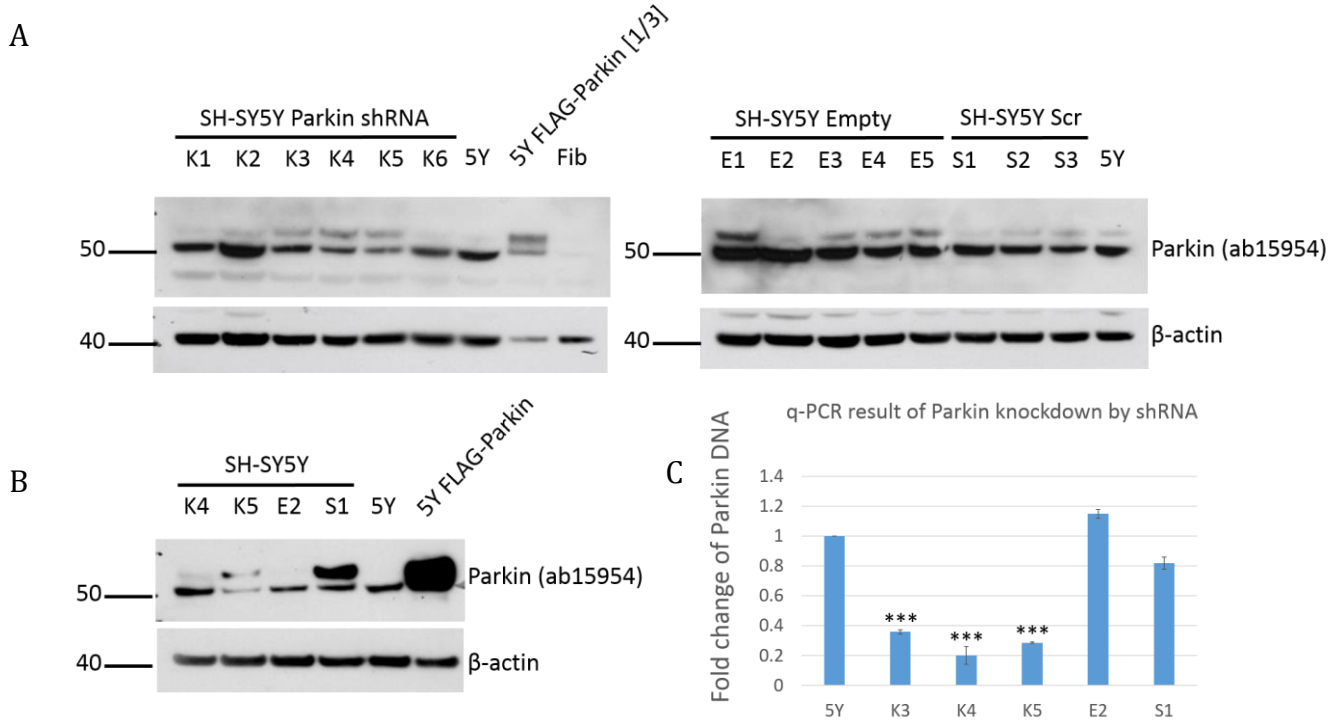

Figure 3-2 Endogenous Parkin knockdown by Parkin shRNA.

(A) SH-SY5Y cells transfected Parkin shRNA (K1 to K6), pGIPZ empty vector (Empty) (E1 to E5) and non-targeting shRNA (Scr) (S1 to S3) were compared with untransfected SH-SY5Y (5Y), SH-SY5Y stably expressing FLAG-Parkin (5Y FLAG-Parkin, 1/3 amount protein loaded) and control human primary fibroblasts (fib). (B) Selective Parkin knockdown lines and the negative controls were compared again with 5Y and 5Y FLAG-Parkin on the same Western blotting membrane. (C) q-PCR result of Parkin knockdown by shRNA. Histogram indicates mean±S.E.M. Significance was determined by *t*-test (*** indicates $p<0.001$) and one-way ANOVA with Bonferroni correction ($p<0.001$). N=3.

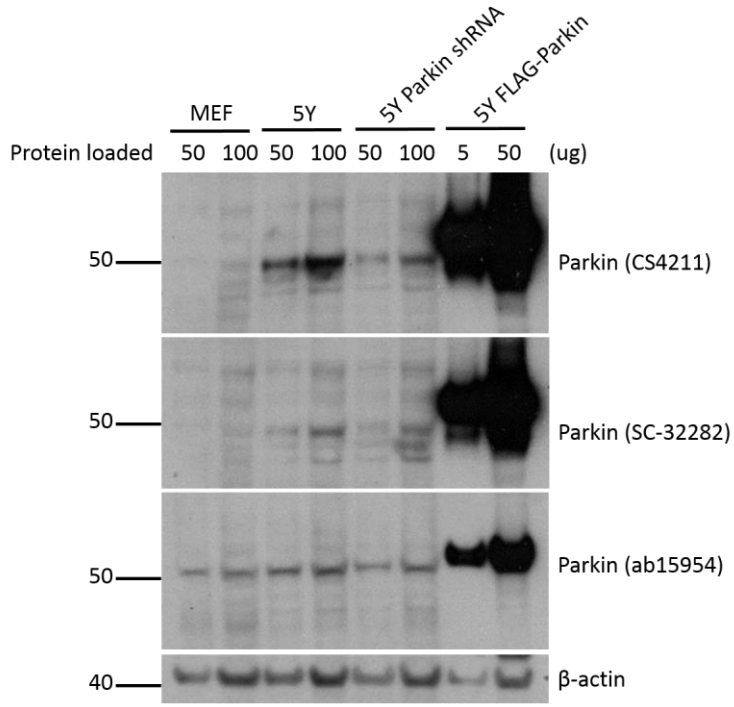

Figure 3-3 Validating Parkin antibodies by four cell lines at two different protein amounts.

Proteins from MEF, SH-SY5Y (5Y) and SH-SY5Y Parkin knockdown (5Y Parkin shRNA) at 50 or 100 ug, and from SH-SY5Y stably expressing FLAG-Parkin (5Y FLAG-Parkin) at 5 or 50 ug were loaded to the gel for validating four Parkin antibodies.

3.2.1.5 Validation of Parkin antibodies by Parkin KO MEFs

I then used WT and Parkin KO MEFs to further validate the antibodies. FLAG-Parkin SH-SY5Y and its empty-vector control (SH-SY5Y stably expressing FLAG-pcDNA3), untransfected SH-SY5Y, Parkin knockdown SH-SY5Y (K5) and its scrambled-shRNA control (S1) were used as controls (Figure 3-4). Two mouse antibodies (CS4211 and SC-32282) and two rabbit antibodies (ab15954 and BML-PW9365) against Parkin were assessed. However, whatever antibodies used, multiple bands around Parkin molecular weight size (52 kDa) were detected in Parkin KO MEFs, calling the specificity of the antibodies into question.

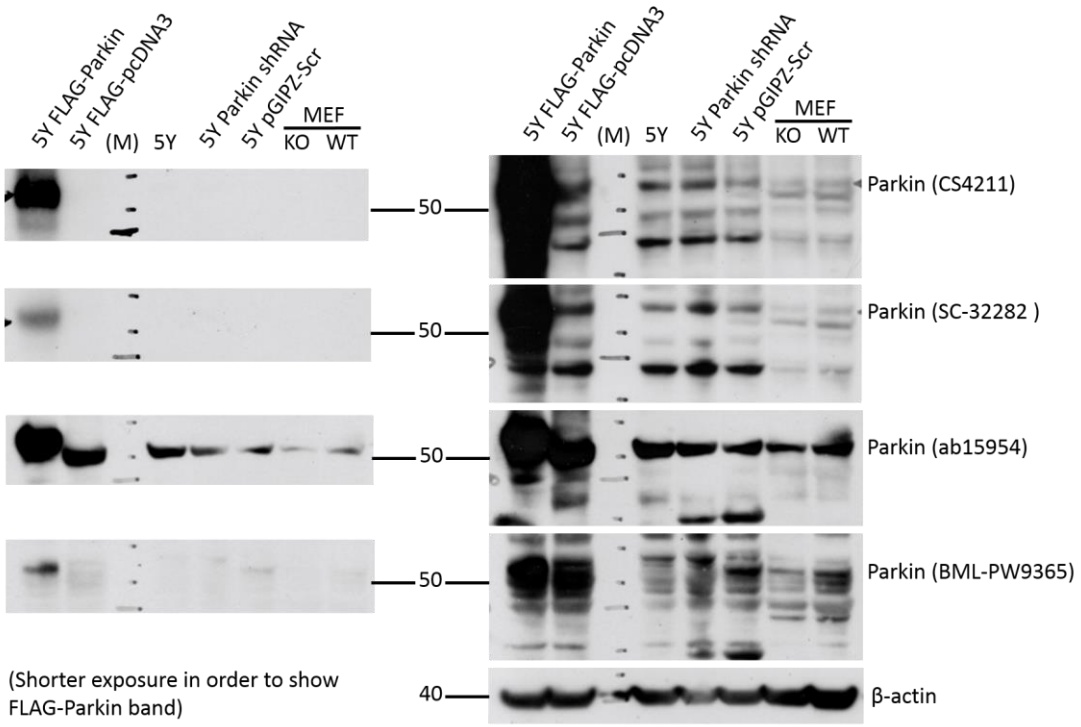

Figure 3-4 Four Parkin antibodies tested by WT and Parkin KO MEFs.

MEFs from WT and Parkin KO mice were utilised for validating four different Parkin antibodies. Untransfected 5Y, 5Y FLAG-Parkin, 5Y FLAG-pcDNA3, 5Y Parkin shRNA, and 5Y pGIPZ-Scr were tested along as controls. The Left panel showed images of shorter exposure to the blot corresponding to the images at the right panel. (M) indicates the molecular weight marker.

3.2.1.6 Validation of Parkin antibodies by control human primary fibroblasts harvested in various lysis buffers

I then test different lysis buffers to see whether antibody specificity would be improved. Control human primary fibroblasts were lysed in five different lysis buffer respectively. Untransfected SH-SY5Y and FLAG-Parkin SH-SY5Y (both in RIPA buffer) were used as controls (Figure 3-5). Parkin expression appeared almost identical when the cells were lysed in CHAPS, NP-40, RIPA, or Triton X-100, although two Parkin bands were observed. A single Parkin band was observed when cells were lysed in 1x LDS loading buffer and both SH-SY5Y cells lysed in RIPA.

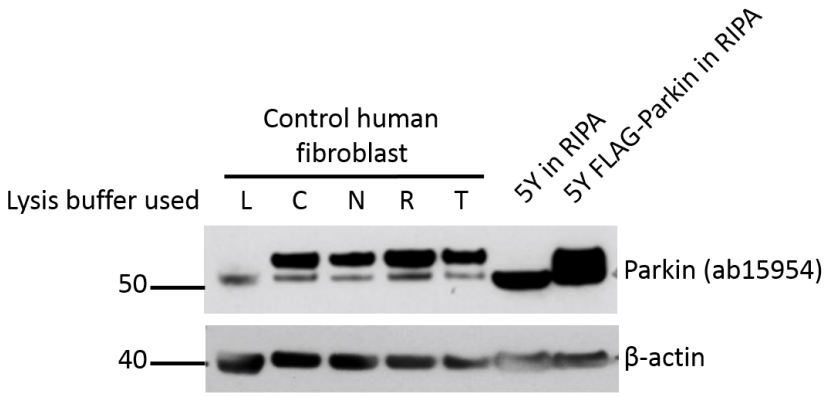

Figure 3-5 Validation of Parkin antibodies by control human primary fibroblasts harvested in various lysis buffers.

Control human primary fibroblasts were harvested by five different lysis buffers (L: LDS sample loading buffer. C: CHAPS lysis buffer. N: NP-40 buffer. R: RIPA buffer. T: Triton X-100 lysis buffer). 5Y and 5Y FLAG-Parkin (both harvested in RIPA buffer) were also used as control.

3.2.2 Characterisation of fibroblasts from PD patients carrying parkin mutations, sample P1, P2, P3, P6 and P7

We then took steps to establish fibroblast lines from patients carrying Parkin mutations. We first obtained five skin biopsies along with blood samples of patients carrying Parkin mutations. All of them carried either homozygous mutations or compound heterozygous mutations in the *Parkin* gene. The fibroblast culture was set up in UCL Royal Free Hospital by Dr Jan-Willem Taanman (Figure 3-6). Fibroblasts of early passage were then transferred to our lab for further use. Whilst waiting for the expansion of fibroblast culture, resequencing of all samples were performed using the DNA extracted from patients' blood samples.

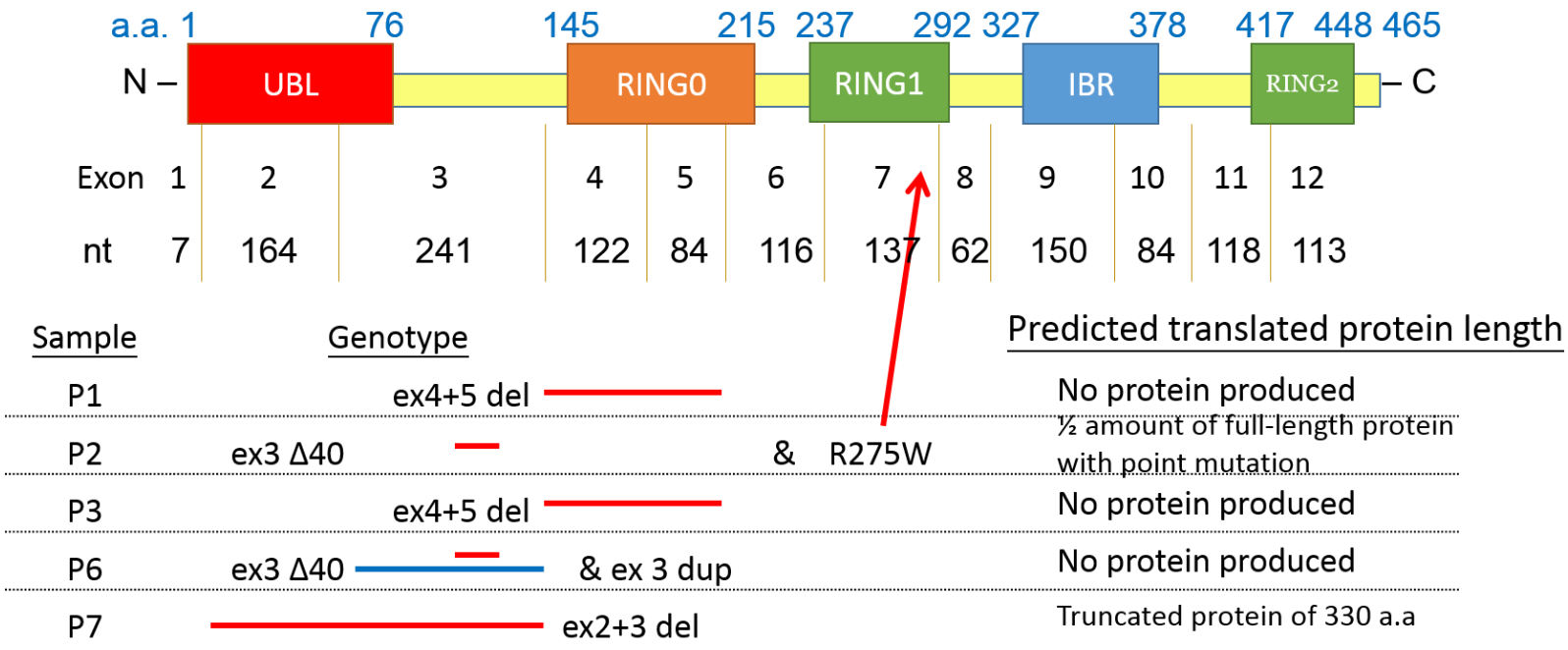

Figure 3-6 Parkin mutation details of five Parkin fibroblasts.

The mutation details of the five Parkin patients (refereed as P1, P2, P3, P6, and P7) were demonstrated as coloured bars (red: deletion; blue: duplication) at the corresponding locations of Parkin cDNA sequence. The predicted protein length translated by each of mutant *Parkin* were also described. (Abbreviations: ex, exon. del, deletion. dup, duplication. nt: nucleotide.)

110

3.2.2.1 Exon sequencing, sample P1, P2, P3, P6 and P7

Leukocytes DNA from these five patients' frozen blood samples were subjected to sequence analysis of all exons of the *parkin* gene. The exon sequencing results were summarised in Table 3-2. Exon sequencing detected a 40-bp deletion in exon 3 of P2 and P6 samples, as well as a c.823C>T (p.R275W) in P2. Therefore, only P2 can be confirmed as compound heterozygous mutations in Parkin by the sequencing result. No exon deletion can be detected by exon sequencing, raising the suspicion that Parkin mutations in the rest four samples might be heterozygous. In order to confirm the whole exon deletion/duplication in these samples, the DNA of these samples were subjected to multiplex ligation-dependent probe amplification (MLPA). MLPA result also supported this impression, as exon deletion was demonstrated in P1, P3 and P7, but the peak ratio is about 50% of normal, suggesting the deletion was not complete in these samples, most likely to be a loss of single allele. A possible duplication of exon 3 in P6, however, was also revealed by MLPA, confirming P6 sample is also a compound heterozygous Parkin mutation. As it's difficult to contact the original physician who's recorded the clinical data, further information about patients' family histories was unavailable. It could only be concluded that two samples (P2 and P6) carried compound heterozygous mutations in Parkin, whilst the rest three (P1, P3, P7) might be heterozygous Parkin mutation.

Parkin sample	Exon sequence analysis	MLPA (Peak ratio of exon DNA)	Conclusion of Parkin mutation after resequencing
P1	No mutations detected	Exon 4-5 deletion (exon 4: 0.546. exon 5: 0.510)	Exon 4-5 deletion. Heterozygous
P2	Deletion of 40 bp in the exon 3, heterozygous point mutation c.823C>T	No whole exon deletions/duplications detected	Exon 3 (40-bp deletion) / R275W. Compound heterozygous
P3	No mutations detected	Exon 4-5 deletion (exon 4: 0.507. exon 5: 0.454)	Exon 4-5 deletion. Heterozygous
P6	Deletion of 40 bp in the exon 3	Heterozygous duplication of exon 3 (exon 3: 1.329)	Exon 3 (40-bp deletion) / exon 3 duplication. Compound heterozygous
P7	No mutations detected	Exon 2-3 deletion (exon 2: 0.565. exon 3: 0.505)	Exon 2-3 deletion. Heterozygous

Table 3-2 Resequencing result of leukocyte DNA from the five Parkin patients

Leukocyte DNA of five Parkin patients were subjected to repeated exon sequencing and MLPA. The results from these two resequencing procedures were concluded in the first column at the right.

112

3.2.2.2 Protein expression by Western blotting, sample P1, P2, P3, P6 and P7

Fibroblasts of these five Parkin patients as well as one control were lysed in RIPA buffer. Western blotting with the ab15954 anti-Parkin antibody revealed two bands in all patient lines (Figure 3-7). P1, P3 and P6 fibroblasts were expected to produce no Parkin protein at all, whilst P7, whose deletion of exons 2-3 resulting in an in-frame mutation, was expected to produce a truncated protein of 330 amino acids. P2 was expected to produce a lower amount of non-functioning full-length Parkin. However, due to the presence of double bands in all Parkin samples, it was unable to conclude the Parkin protein expression. The discrepancies between sequencing and protein expression results limited the further use of these fibroblasts.

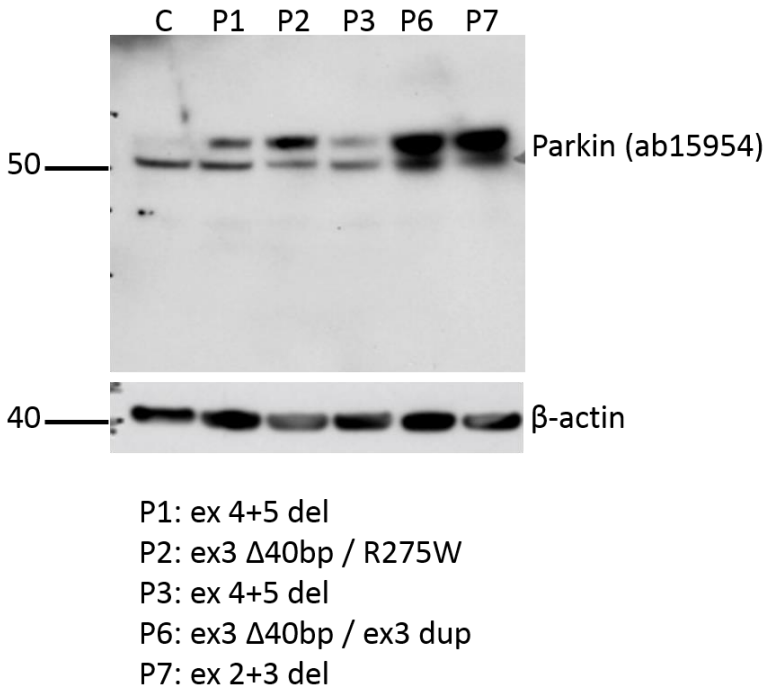

Figure 3-7 Characterisation of Parkin fibroblasts by protein expression level.

The Parkin protein expression level of the five Parkin fibroblasts and one control fibroblasts were validated by Western blotting. The mutation of each sample was denoted below the figure.

3.2.2.3 Establishing new Parkin fibroblasts culture from patient carry Parkin mutation (P8)

To try and make sense of the discrepancies between DNA and protein results, a new skin biopsy was requested from a patient carrying a homozygous deletion of exons 3 and 4. The homozygous in-frame exon deletion is preferable in view of that both sequencing and protein expression results should match indisputably. The biopsy was performed in National Hospital for Neurology and Neurosurgery (NHNN) with the consent from the patient. The skin biopsy was immediately transferred to our lab in Institute of Neurology for developing the culture. Fibroblasts started to grow in a single layer around the skin piece 7 to 10 days after the biopsy (Figure 3-8).

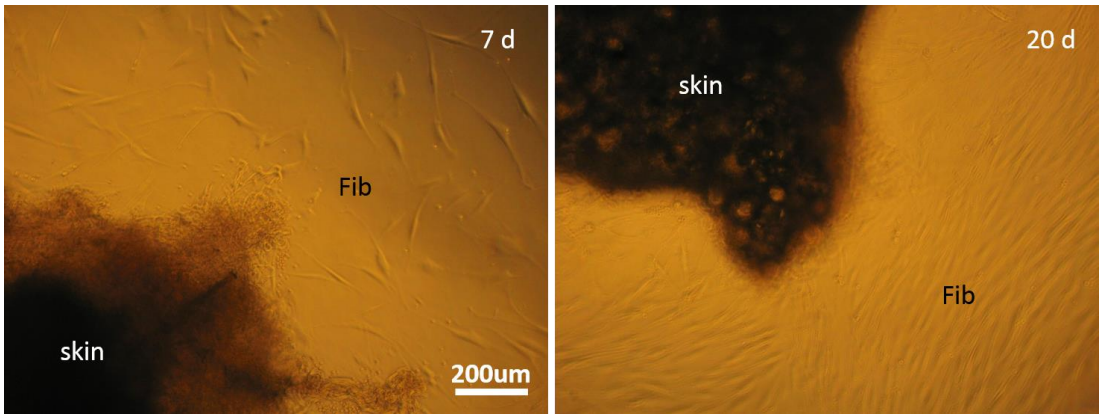

Figure 3-8 Establishing new Parking fibroblast culture from skin biopsy.

Light microscopy images of Parkin fibroblast (P8) culture established from skin biopsy. Fibroblasts (Fib) started to appear near the edge of skin approximately 7-10 days after the skin piece was place in the plate (left panel). The expanding fibroblasts formed a single layer around the skin piece after 20 days (right panel).

3.2.2.4 Characterisation of Parkin fibroblasts P8

Dried pellets of the fibroblasts (P8) and an age/sex-matched control were divided into three parts: one for DNA extraction, one for RNA extraction, and the last one for lysis in RIPA buffer and further protein expression analysis.

The whole genome DNA was extracted from P8 and control cell pellets and a PCR was performed, using primers for exons 3, 4 and 7. The PCR products were run out on an agarose gel alongside with a 1 Kb ladder (Figure 3-9A). The gel was checked under ultra-violet (UV) light, demonstrating no amplification of exons 3 and 4 in P8 fibroblasts, suggesting homozygous deletion of exons 3 and 4 by analysing the whole genome DNA.

RNA was extracted from both P8 and control fibroblast (C) for further generation of cDNA by the reversed transcription-PCR (RT-PCR). The cDNA products were first amplified by PCR with various combination of primers designed specially to recognise sequences at the boundary of neighbouring exons. The primer pairs and estimated sizes of their corresponding amplicons were depicted in Figure 3-9 B. The PCR of cDNA also supported the diagnosis of homozygous deletion of exons 3 and 4 in P8 fibroblasts.

As a deletion of exons 3 and 4 is an in-frame mutation, thereby a truncated mRNA will still be transcribed, and its cDNA product should demonstrate a linkage between 3' end of exon 2 and the 5' end of exon 5. To prove this, cDNA was sequenced by the forward primer recognising exons 1-2 boundary and reversed primer for exons 7-8 boundary. The result clearly demonstrated that exon 2 was followed by exon 5 in cDNA from P8 (Figure 3-10).

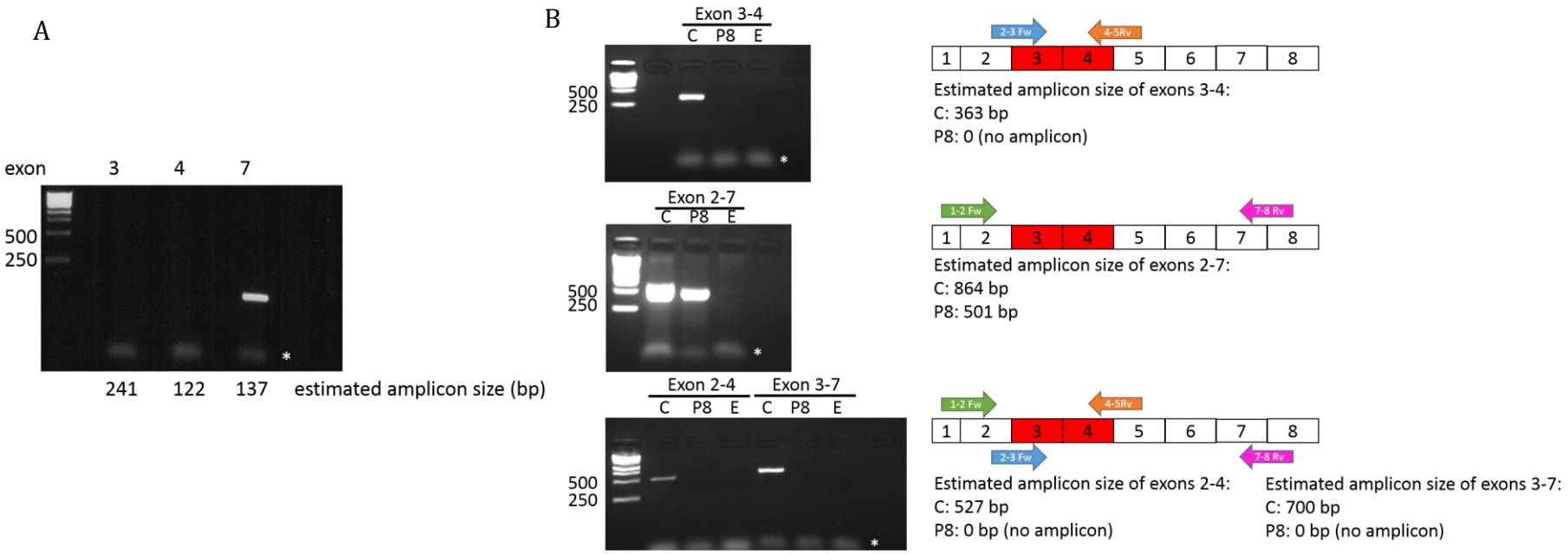

Figure 3-9 PCR results from (A) genomic DNA and (B) cDNA of P8 Parkin fibroblasts.

(* indicates bands formed by primer pairs)

Parkin exon 1, 2, 5 reference sequence

ATGATAGTGTTTGTCAGGTTCAACTCCAGCCATGGTTTCCCAGTGGAGGTCGATTCTGACACCAGCATCTTCCAGCTCAAGGAGG
TGGTTGCTAAGCGACAGGGGGTTCCGGCTGACCAGTTGCGTGTGATTTTCGCAGGGAAGGAGCTGAGGAATGACTGGACTGTG
CAGGGTCCATCTTGCTGGGATGATGTTTTAATTCCAAACCGGATGAGTGGTGAATGCCAATCCCCACACTGCCCTGGGACTAGTG
CA

Figure 3-10 Sequencing result of cDNA from P8 Parkin fibroblast.

The cDNA obtained from reversed transcription of P8 Parkin fibroblast RNA was subjected to sequencing using forward primer for exon 1-2 boundary and reversed primer for exon 7-8 boundary. The result was analysed by Sequencher and the segment demonstrating exon 2 and 5 boundary was showed at the bottom part of this figure. The reference sequence of exon 1 (in blue), exon 2 (in red), and exon 5 (in green) was shown at the top. The first six bases were highlighted to point out the boundary between exons 2 and 5.

117

With the mutation in P8 fibroblasts confirmed by genomic DNA PCR and cDNA sequence analysis, protein lysates from the control and P8 fibroblasts were subjected to Western blotting. Three Parkin antibodies (ab15954, BML-PW9365 and CS4211) as well as two phospho-Parkin antibodies (P-Parkin S101, P-Parkin S378) were used to characterise the protein expression of P8 fibroblasts (Figure 3-11 A&B). According to the cDNA sequencing result, a truncated protein of 330 a.a (approximately 35 kDa) would be produced in P8 fibroblasts. Surprisingly, all five antibodies labelled a band in P8 fibroblasts at around 50 kDa as control fibroblasts did. Of note, a smaller protein (approximately 35 kDa) was detected by ab15954. It presented in both control and Parkin fibroblasts, although this band was stronger in the latter. The two phospho-Parkin antibodies detected the protein at the same size (around 50-52 kDa) in both control and Parkin fibroblasts. However, a smaller protein of around 35 kDa was detected in P8 by both phospho-antibodies. Western blotting with the same lysates was repeated again using a non-gradient 12% Tris-Glycine gel in order to reveal details between 30 and 40 kDa (Figure 3-11 C). The smaller protein (approximately 35 kDa) in P8 was detected by ab15954. However, the possible full-length Parkin at around 50 kDa was also stronger in P8 Parkin fibroblasts. Once again, the result raise the issue of inadequate specificity of these Parkin antibodies.

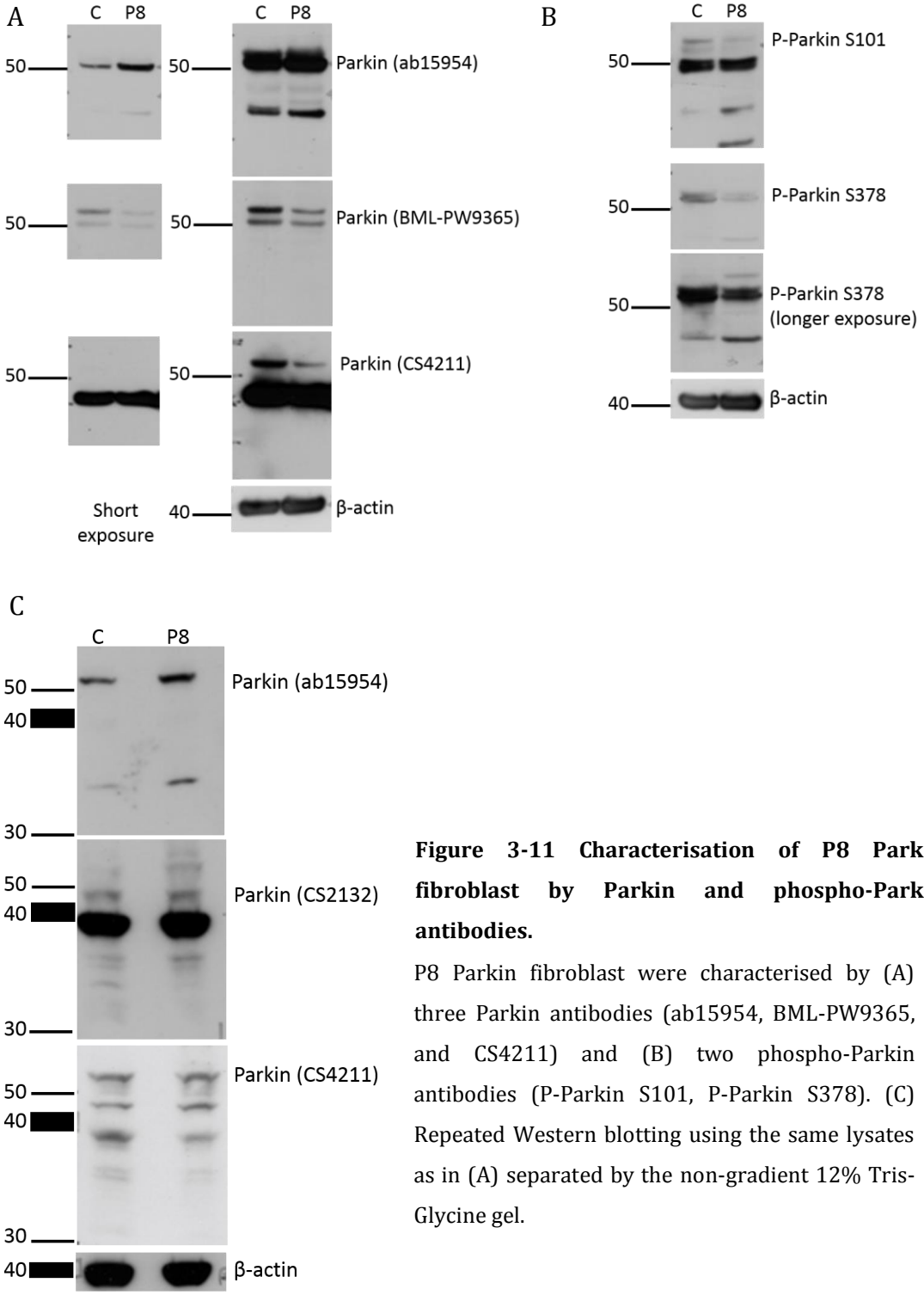

Figure 3-11 Characterisation of P8 Parkin fibroblast by Parkin and phospho-Parkin antibodies.

P8 Parkin fibroblast were characterised by (A) three Parkin antibodies (ab15954, BML-PW9365, and CS4211) and (B) two phospho-Parkin antibodies (P-Parkin S101, P-Parkin S378). (C) Repeated Western blotting using the same lysates as in (A) separated by the non-gradient 12% Tris-Glycine gel.

3.2.3 Parkin fibroblasts-derived induced pluripotent stem cells

3.2.3.1 Viral transduction to reprograme the target fibroblasts

The four mouse reprogramming factors were a generous gift from Dr Michael Devine and their use has been described before (Devine et al., 2011). Those factors were inserted into the pMXs vector backbone from Addgene (pMXs-cMyc #13375, pMXs-Klf4 #13370, pMXs-Oct4 #13366, pMXs-Sox2 #13367). The reprogramming method has also been described (Devine et al., 2011) (See chapter 2 for details). The P8 Parkin fibroblast and the age/sex-matched control fibroblast were subjected for reprogramming.

3.2.3.2 Maintenance of stem cell colony after reprogramming

Stem cell-like colonies in both transduced control and P8 fibroblasts started to appear approximately 3.5 weeks after viral transduction of reprogramming factors. Each colony was mechanically picked to the 24-well plates pre-coated with irradiated SNL fibroblast feeders (Figure 3-12). Differentiated cells at the edge of the colonies were also removed mechanically in order to avoid uncontrolled spontaneous differentiation of the entire colony. The colonies in each well were split on the conditions that daughter colonies counted more than six, presence of connecting colony edges, or rapid increasing of differentiated cells.

Further characterisation of stem cell colonies were not performed due to uncertainty of whether this model can be fully characterised on the grounds of poor Parkin antibody specificity. The colonies were thus frozen and this part of project would be continued provided Parkin antibody of high specificity can be obtained.

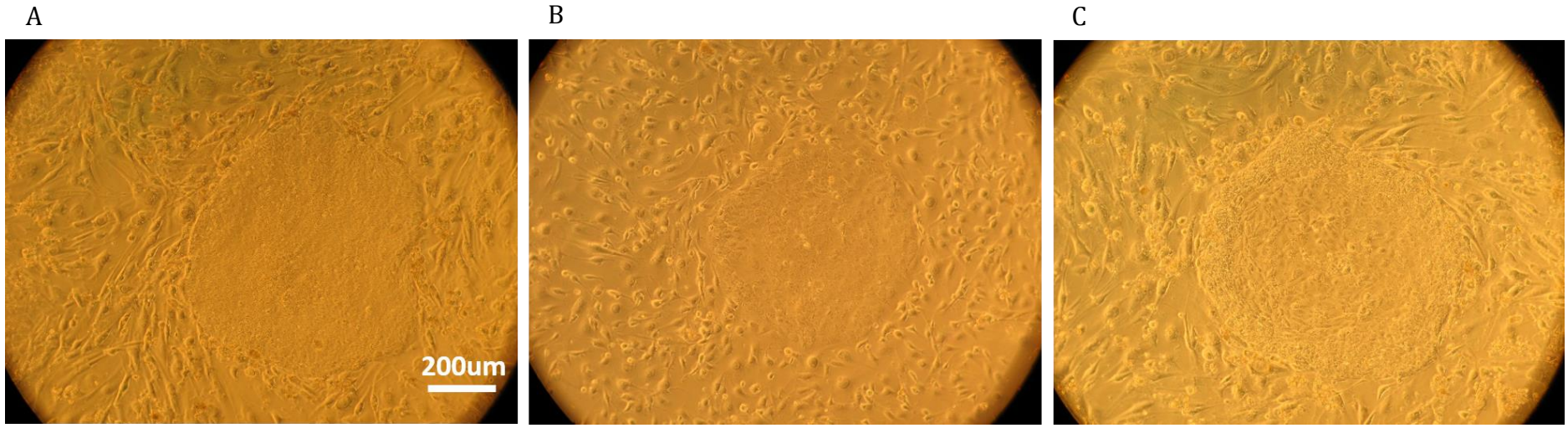

Figure 3-12 iPSC-like colonies derived from Parkin fibroblasts.

The stem cell-like colonies appeared approximately 3.5 weeks after viral transduction of reprogramming factors. (A) and (B) demonstrated colonies with primitive cell in major, whereas the colony in (C) revealed differentiated cells at its periphery. The cells surrounded the colonies were irradiated SNL fibroblast feeders.

3.3 Discussion

3.3.1 The sensitivity and specificity of Parkin antibody

Both sensitivity and specificity of Parkin antibodies to endogenous Parkin have been reported as very poor (Seibler et al., 2011; Vives-Bauza et al., 2010). Although a number of studies show endogenous Parkin detection in Western blotting by various anti-Parkin antibodies, non-specific bands are frequently observed. (LaVoie et al., 2007; Scuderi et al., 2014; Seibler et al., 2011; Um et al., 2009; Van Humbeeck et al., 2011; Vives-Bauza et al., 2010). In this project five Parkin antibodies as well as two phospho-Parkin antibodies were tested. None of them gave satisfactory results. Whenever tagged Parkin could be accurately detected in FLAG-Parkin overexpressing SH-SY5Y cells, endogenous Parkin was not reliably detected with any of the five antibodies tested, mainly due to the presence of multiple unspecific bands in Western blotting.

The protein extraction efficiency and the presence of unspecific bands on the Western blot were barely affected by the type of detergent used to lyse the cells. Harvesting cells directly in loading buffer appeared to resolve the issue of the unspecific bands, however this buffer was of limited utility as lysates harvested this way couldn't be used for subsequent protein assay or immunoprecipitation. The specificity of the five anti-Parkin antibodies was further questioned using Parkin siRNA knockdown SH-SY5Y cells or Parkin KO MEFs. Again a number of unspecific bands were detected in these cells that were meant to be devoid of full-length Parkin.

One possible reason to explain the low specificity of Parkin antibodies is the frequent alternative splicing in the *Parkin* gene. Sequencing from *Parkin* cDNA shows that it includes 12 exons (Kitada et al., 1998; Matsumine et al., 1997). It was once thought that only one transcript was encoded by these 12 exons. However, at least 21 *Parkin* alternative splice variants have been described to date (Table 3-3) (Beyer et al., 2008; Dagata and Cavallaro, 2004; Humbert et al., 2007; Ikeuchi et al., 2009; Kitada et al., 2000; Sunada et al., 1998; Tan et al.,

2005). Distinct *Parkin* transcripts can be found in different human tissues. For instance, exons 3-5, the exons most prone to deletion, have been shown to be alternative spliced in peripheral leukocytes (Scuderi et al., 2014; Sunada et al., 1998). It was further shown that every antibody recognised a pool of different isoforms (Table 3-4) (Scuderi et al., 2014). The anti-Parkin antibodies used in this project can be roughly divided into three groups according to this table. The ab15954 antibody recognises a slightly different amino acid sequence, as compared to the other four antibodies. Accordingly, my data showed a unique band pattern in Western blotting, when compared to the other four. A similar band pattern was observed by other groups using the same antibody (Geisler et al., 2010; Vives-Bauza et al., 2010).

New code identifier	GI	Protein accession number	Predicted MW	pI	aa sequence
H20	469609976	AGH62057.1	58,127	6,41	530 aa
H1	3063387	BAA25751.1 BAF43729.1	51,65	6,71	465 aa
	121308969	BAF85279.1 NP_004553.2			
	158258616	ABN46990.1			
	169790968				
	125630744				
H5	284468410	ADB90270.1	48,713	7,12	437 aa
	169790970	NP_054642.2			
H10	284468412	ADB90271.1	46,412	6,91	415 aa
H14	284516985	ADB91979.1	43,485	7,43	387 aa
H4	34191069	AAH22014.1	42,407	8,15	387 aa
H8	284468407	*	42,52	6,65	386 aa
H17	284516991	*	42,52	6,65	386 aa
H21	520845529	AGP25366.1	39,592	7,08	358 aa
H6	169790972	NP_054643.2	35,63	6,45	316 aa
H11	284516981	*	30,615	6,3	274 aa
H2	20385797	AAM21457.1	30,155	6,05	270 aa
H3	20385801	AAM21459.1	22,192	5,68	203 aa
H12	284516982	*	19,201	6,09	172 aa
H9	284468408	ADB90269.1	15,521	5,54	143 aa
H13	284516983	ADB91978.1	15,521	5,54	143 aa
H7	194378189	BAG57845.1	15,407	6,41	139 aa
H18	284516993	*	15,393	6,41	139 aa
H15	284516987	ADB91980.1	10,531	8,74	95 aa
H19	469609974	AGH62056.1	6,832	10,09	61 aa
H16	284516989	ADB91981.1	5,348	7,79	51 aa

Table 3-3 *Homo sapiens* Parkin isoform

Summary of all Parkin isoform described to date. H1 represents the canonical sequence cloned by Kitada et al. (Kitada et al., 1998). * indicates the protein accession number is not present in database. This table was adapted from (Scuderi et al., 2014).

Name	Target	Recognised Parkin isoforms	Potential isoforms pool recognised by Parkin antibodies used in this project
M73 (Shimura et al., 1999)	124–137	H1, H4, H5, H8, H9, H10, H13, H14, H17, H20, H21	
M74 (Shimura et al., 1999)	293–306	H1, H2, H3, H4, H5, H6, H8, H10, H11, H14, H17, H20, H21	ab15954 (304-322)
ParkA (Huynh et al., 2000)	96–109	H1, H2, H3, H4, H5, H6, H8, H9, H10, H11, H13, H14, H17, H20, H21	
ParkB (Huynh et al., 2000)	401-417	H1, H2, H5, H6, H7, H8, H10, H11, H12, H14, H17, H18, H20, H21	CS2132 (around 400), BML-PW9365 (399-412)
HP6A (Schlossmacher et al., 2002)	6–15	H1, H4, H5, H6, H9, H10, H13, H14, H16, H20	
HP7A (Schlossmacher et al., 2002)	51–62	H1, H4, H5, H6, H9, H10, H13, H14, H15, H20	
HP1A (Schlossmacher et al., 2002)	84–98	H1, H2, H3, H4, H5, H6, H8, H9, H10, H11, H13, H14, H17, H20, H21	
HP2A (Schlossmacher et al., 2002)	342–353	H1, H2, H3, H4, H5, H6, H7, H8, H11, H12, H17, H18, H20, H21	
HP5A (Schlossmacher et al., 2002)	453–465	H1, H2, H5, H6, H7, H8, H10, H11, H12, H14, H17, H18, H20, H21	CS4211 (C-terminus), SC-32282 (C-terminus)

Table 3-4 Parkin isoforms recognised by antibodies used by others and in this project

The Parkin isoform pools recognised by Parkin antibodies described in some studies. Based on the target amino acid sequence, antibodies used in this project were listed in the first column at the right showing the potential isoform pool that each antibody could recognise. A part of this table was adapted from (Scuderi et al., 2014).

3.3.2 Characterisation of Parkin fibroblasts

Although the *Parkin* contains only 12 exons, the gene spans more than 1.38 Mb in the long arm of chromosome 6 (6q25.2-q27) (Kitada et al., 1998). The long segment of introns between exons makes sequencing Parkin from the whole genome a challenging task. The original report of the mutations in the first five Parkin fibroblasts provided by the clinician indicated that all the fibroblasts had either homozygous mutation or compound heterozygous mutations in Parkin. However, repeated sequencing was not able to reproduce the original results. The exon sequencing done in our lab detected only the 40-bp deletion in 2 samples and one point mutation in one of them. No whole exon deletion was detected by the exon sequencing. Further MLPA also demonstrated that all exon deletions mentioned in the original report were possibly heterozygous, as the peak ratio of the deleted exon was only 50% less than the exons that were not deleted. Both exon sequencing and MLPA results suggested the exon deletions mentioned in P1, P3 and P7 fibroblasts were likely to be heterozygous. Nevertheless, the exon 3 duplication in one allele of P2 was confirmed by the MLPA done in the lab. In addition, data from the protein expression assay by Western blotting was not convincing enough to support the mutations described in the original report, owing to low sensitive of Parkin antibodies. Due to uncertainty in the mutation details, these five Parkin fibroblasts were not suitable to be used as target fibroblasts for the reprogramming. It was later when another Parkin fibroblast line with confirmed mutation was obtained then the reprogramming was commenced.

3.3.3 Reprogramming Parkin fibroblasts

This part of the project was delayed until another Parkin fibroblast with confirmed homozygous mutation was acquired. Several reprogramming strategies had been reported. The reprogramming factors can be delivered to the target cells by retroviral system such as retroviral (Takahashi et al., 2007) or lentiviral (Yu et al., 2007) transduction, or alternative methods including adenoviral transduction (Zhou and Freed, 2009), small molecule

compounds(Shi et al.), plasmids (Okita et al., 2008) or piggyBac transposon (Woltjen et al., 2009). Recombinant proteins (Zhou et al., 2009) or microRNAs (Judson et al., 2009) have also been shown to achieve iPSC generation. Generally, the retroviral or lentiviral system demonstrated higher efficiency than the rest of the methods to accomplish reprogramming. The disadvantage of retroviral/lentiviral transduction is the risk of mutagenesis of the target cells caused by the incorporation of viral genes into the host genome, namely insertional mutagenesis. Nevertheless the non-retroviral methods, though much safer, all come with a drawback of low reprogramming efficiency. Considering the time-frame issue, retroviral system was chosen for reprogramming the Parkin fibroblasts.

In addition to the original 'Yamanaka factors' (*Oct4, Sox2, Klf4, and c-myc*) (Takahashi et al., 2007), different combinations of transcription factors have also been described. For instance, the Thomson group used *Oct4*, *Sox2*, *Nanog*, and *Lin28* for reprogramming (Yu et al., 2007). Whilst *Oct4, Sox2* are both essential for reprogramming, *Klf4, c-myc*, *Nanog*, and *Lin28* have been described to increase the efficiency in the induction of pluripotency (Takahashi et al., 2007; Yu et al., 2007). Considering the viral system chosen for this project is retrovirus which has been described by Yamanaka group, therefore Yamanaka factors were also selected for pluripotency induction.

The transduced fibroblasts were transferred onto SNL fibroblast feeder layer three days after transduction. Formation of small colonies started to appear approximately three weeks after replating and a small amount of stem-cell like colonies were then stored in liquid nitrogen before characterisation. This project went parallel with the project investigating Parkin molecular pathway (Chapter 4). By the time the possible iPSC colonies appeared, all the rest experiments still suffered from low sensitivity of Parkin antibodies toward endogenous Parkin. Fearing that this potential Parkin-iPSC model will still be less useful if endogenous Parkin can't be recognised in it, the colonies were thus stored before further characterisation and application.

3.3.4 Experimental difficulties

Two major difficulties were encountered in this project. First, the original sequencing data from the first five Parkin fibroblast lines couldn't be reproduced in our lab. Second, the low sensitivity and specificity of anti-Parkin antibodies made characterisation of these fibroblasts at Parkin protein expression level almost impossible. For these reasons we didn't carry out full reprogramming of Parkin fibroblasts.

As mentioned in section 3.3.2, the *Parkin* gene spans a considerable length along the long arm of chromosome 6, thereby making sequencing the full length Parkin rather challenging. Although the primers for sequencing, provided by the genetic diagnostic lab in NHNN, had great fidelity ensured, the exon sequencing and the subsequent MLPA results mismatched mostly with the original mutation data provided by original clinician, namely the three lines with exons deletions. Unfortunately protein expression assay provided no better supportive evidence as the specificity of Parkin antibodies was also low. Therefore these five Parkin fibroblast lines could not be used until another new line was acquired and mutations were ascertained.

The low sensitivity and specificity of Parkin antibodies demonstrated in this project indicates that detecting endogenous Parkin remains challenging. Although the functional study can indirectly demonstrate the protein expression level, in this part of project it is essential to match the protein expression level to the corresponding Parkin mutation in order to select appropriate cell models as well as antibodies for the subsequent work. This leads to the reconsideration of using overexpressed Parkin in the following projects.

3.3.5 Conclusions

In this chapter, five anti-Parkin antibodies have been characterised using a neuroblastoma cell line (overexpressing Parkin, WT, transiently or stably Parkin knockdown), MEFs (WT or Parkin KO) and human primary fibroblasts. None of the antibodies tested showed strong enough sensitivity or specificity, possibly

due to the number of Parkin isoforms recognised by the antibodies. As a result, we decided to pursue our study of molecular pathways associated with Parkin using overexpression cell models.

The five Parkin fibroblasts originally used in this study were not further used due to conflicting sequencing data. The last Parkin fibroblast line was confirmed to carry a homozygous deletion of exons 3-4 and was then selected for Parkin-iPSC generation. Nevertheless, the iPSC colonies couldn't be characterised due to the Parkin protein detection problem.

3.3.6 Future perspectives

Few more experimental conditions can be further tested for anti-Parkin antibodies characterisation within timeframe available. For instance, Western blotting conditions such as different types of blocking reagents and lysis buffer salt concentrations can be assessed more systematically. Alternatively, immunoprecipitation of the endogenous Parkin for further analysis could possibly increase the quality. Another consideration is the utility of overexpressed Parkin.

Detecting a decreased Parkin activity can indirectly support the existence of mutations in Parkin fibroblasts. The Parkin fibroblast line with homozygous mutation (P8) has been used in a side project for evaluating Mfn1 and Mfn2 ubiquitination following mitochondrial depolarisation (Figure 3-13) and by a collaborating group for assessing Miro1 regulation in the mitophagy process (Birsa et al., 2014). As Parkin has been implicated in regulating mitophagy process, assessing mitochondrial physiology and metabolism by a live cell analysis is another alternative assay for evaluating Parkin fibroblasts dysfunction in the future work.

Parkin-iPSC, although yet to be characterised, is still a promising model for studying Parkin dysfunction. If one more step forward is taken to differentiate Parkin iPSC into Parkin iPSC-derived dopaminergic neurons, this can be the

most relevant disease-affected model of invaluable contribution for investigating Parkin molecular pathways. Another important contribution that this iPSC-derived neuronal model can provide in the future is the chance to observe both morphological and physiological changes of Parkin neurons during the developing and senescing process. It would also be ideal to further exploit the genome-editing technique by correcting the causal mutation in these patient-derived models, which is of great therapeutic potential.

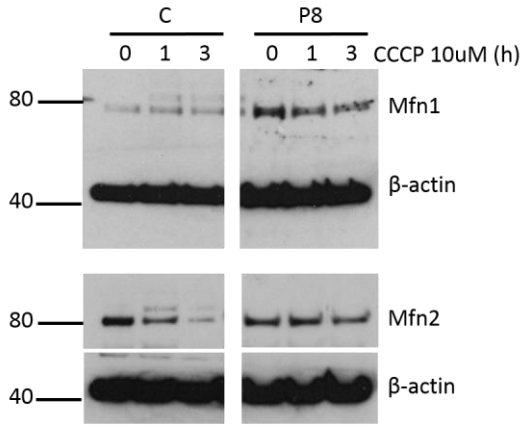

Figure 3-13 P8 Parkin fibroblast demonstrated decreased ubiquitination of Mfn1 and Mfn2 upon mitochondrial depolarisation.

Both Parkin (P8) and the age-sex matched control (C) fibroblasts were treated with carbonyl cyanide m-chlorophenyl hydrazone (CCCP). There was no ubiquitinated Mfn1 or Mfn2 in P8 comparing to C after CCCP-induced mitochondrial depolarisation. (Figure was provided by Dr Marta Delgado Camprubi)

Chapter 4 Investigation of molecular pathways associated with Parkin regulation

4.1 Introduction

Various PTM might play an important role in regulating Parkin's E3 ubiquitin ligase activity (Avraham et al., 2007; Birsa et al., 2014; Chung et al., 2004; Imam et al., 2011; Kazlauskaite et al., 2014; Kim et al., 2008; Ko et al., 2010; Kondapalli et al., 2012; LaVoie et al., 2005; Rubio de la Torre et al., 2009; Sha et al., 2010; Shiba-Fukushima et al., 2012; Yamamoto et al., 2005). However, the underlying molecular pathways that regulate these modifications are not clear. Of these PTMs, Parkin phosphorylation has gained increasing attention in the last decade. Several phosphorylation sites of Parkin have been recognised but the role of Parkin phosphorylation remains poorly understood (Avraham et al., 2007; Birsa et al., 2014; Imam et al., 2011; Kazlauskaite et al., 2014; Kim et al., 2008; Ko et al., 2010; Kondapalli et al., 2012; Rubio de la Torre et al., 2009; Sha et al., 2010; Shiba-Fukushima et al., 2012; Yamamoto et al., 2005).

Dysfunction of mitogen activated protein kinase (MAPK) or PI3K/Akt signalling pathways have been implicated in potential PD pathophysiology. A number of Parkin mutations have also been shown to associate with dysregulation of these signalling pathways. For instance, increased MAPK activity is observed in patients with Parkin mutations such as exon 4 deletion (Ren et al., 2009).

Drosophila dopaminergic neurons expressing loss-of-function Parkin mutations demonstrate highly activated JNK-1 (Cha et al., 2005; Kim and Choi, 2010). Parkin has been shown to promote class I PI3K/Akt signalling by interacting with ubiquitin-interacting motif (UIM) of Eps15, an epidermal growth factor receptor (EGFR) adaptor, thus delaying the internalisation and degradation of EGFR (Fallon et al., 2006). It is also suggested that Parkin binds to class III PI3K complex activator Ambra1 to induce mitophagy (Van Humbeeck et al., 2011).

Given that MAPK and Akt are serine/threonine protein kinases and most of putative parkin phosphorylation sites are serine residues, we sought to determine whether parkin can be phosphorylated following MAPK or Akt activation and to dissect the upstream molecular signalling pathway leading to parkin phosphorylation. Amid all the described Parkin phosphorylation sites, the N-terminal S101 is a highly conserved residue amongst many spices, whilst the C-terminal S378 is also conserved amongst primates (Figure 4-1). Phosphorylation at these two sites will be used as readout for this project. Cell lines expressing 4-hydroxytamoxifen (4OH-Tx)-inducible versions of MAP kinases/ERK kinase kinase kinase (MEKK3), Raf or Akt (ΔMEKK3:ER, ΔRaf – DD:ER or myrAkt:ER) (Figure 4-2), as well as activators that trigger these signalling cascades will be used. Wherever possible, selective inhibitors will be utilised for dissecting the Parkin regulatory pathway.

	|95 108|	|372 385|
Homo sapiens	CEREPQ**S**LTRVDLS	YHEGEC**S**AVFEASG
Pan troglodytes	CEREPQ**S**LTRVDLS	YHEGEC**S**ALFEASG
Macaca fascicularis	CEREPQ**S**LTRVDLS	YHEGEC**S**ALFEASG
Gallus gallus	LERVPE**S**LTRIDLS	YHEGEC**S**SFLSTQG
Bos taurus	SDREPE**S**LTRVDLS	YHEGDCGAVIEASG
Rattus norvegicus	SIWEPR**S**LTRVDLS	YHEGECDSMFEASG
Mus musculus	SIWESR**S**LTRVDLS	YHEGDCDSLLEPSG
Sus scrofa	AGREPA**S**LTRVDLS	YHEGEC**S**ALFEASA
	*	*

Figure 4-1 Alignment of Parkin homologues in different species.

Putative Parkin phosphorylation site S101 is highly conserved amongst different species. S378 is also conserved among primates, pigs and chickens.

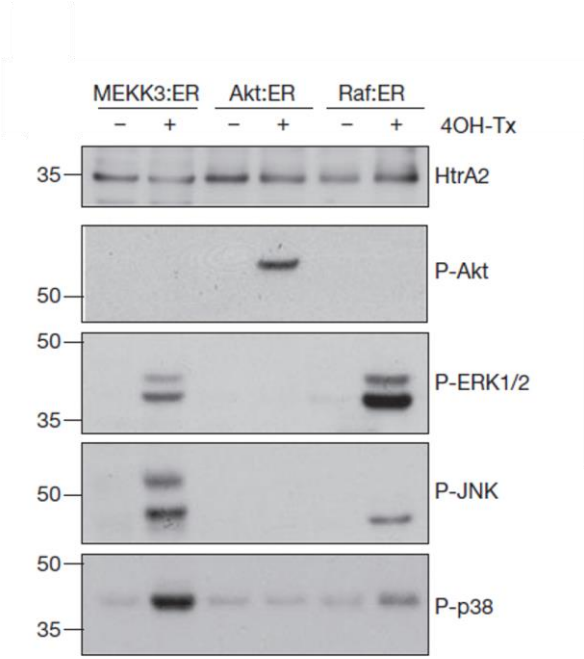

Figure 4-2 Kinases that can be activate upon 4OH-Tx treatment in ΔMEKK3:ER (MEKK3:ER), myrAkt:ER (Akt:ER) and ΔRaf-DD:ER (Raf: ER) stable cell lines.

Three cell lines stably expressing inducible kinases were used in this project. Upon treatment with 4OH-Tx, there is a strong phosohorylation of p38 and weaker phosphorylations of JNK and ERK1/2 in ΔMEKK3:ER cells, phosphorylation of Akt only in myrAkt:ER cells, and phosphorylation of ERK1/2 in ΔRaf-DD:ER cells. (Figure is adapted from (Plun-Favreau et al., 2007))

4.2 Results

4.2.1 Parkin phosphorylation is not detected upon activation of p38 signalling pathway

To study whether Parkin is phosphorylated following activation of p38 signalling pathway, full-length human Parkin inserted in FLAG-pcDNA3 vector (Ardley et al., 2003) and the empty vector control were transfected in to human embryonic kidney (HEK)293t cells stably expressing ΔMEKK3:ER for 48 h. ΔMEKK3:ER is a 4OH-Tx-inducible version of MEKK3 in which the kinase domain of human MEKK3 is fused in-frame to a modified hormone binding domain of oestrogen receptor (ER). Activation of ΔMEKK3:ER by treatment of 4OH-Tx results in strong activation of endogenous p38, weaker activation of JNK and ERK1/2, and no activation of Akt (Figure 4-2) (Plun-Favreau et al., 2007). The transiently transfected ΔMEKK3:ER cells, together with the untransfected control, were treated with 100 nM 4OH-Tx in order to induce the MEKK3 signalling pathway. The whole cell lysates were analysed by SDS-PAGE, followed by Western blotting and detection by total and phosphorylation site-specific antibodies of p38 and Parkin (Figure 4-3 A). Phosphorylation of p38 (P-p38) was equally strong in un-transfected, FLAG-Parkin transfected, or empty vector transfected ΔMEKK3:ER cells following 4OH-Tx treatment. Although the transfection efficiency of FLAG-Parkin was good, phospho-Parkin S101 (P-Parkin S101) was not detected at the predicted 52-kDa site, even with longer exposure time of the x-ray film to the membrane. On the other hand, Parkin was constitutively phosphorylated at S378 (P-Parkin S378), although several cross-reacting bands were also observed.

In order to ascertain whether Parkin was phosphorylated at 378, the experiment was repeated in FLAG-Parkin and empty vector-transfected ΔMEKK3:ER cells. After the cells were lysed, 90% of the whole cell lysate of each sample was subjected to immunoprecipitation (IP) by anti-FLAG antibody-coupled agarose beads and subsequently eluted by FLAG-peptide. Both original

lysates (input) and peptide-eluted samples (FLAG-IP) were separated by SDS-PAGE and analysed by Western blotting (Figure 4-3 B). P-p38 was observed upon treatment of 4OH-Tx in the input fraction. In the input P-Parkin S378 antibody detected bands in both FLAG-Parkin and empty vector-expressing cells, strongly arguing for the non-specificity of the antibody. In the FLAG-IP fraction, P-Parkin S378 was activated constitutively. These data suggest that Parkin phosphorylation at S378 can only be detected following IP, and that Parkin is constitutively phosphorylated at S378, independent of p38 activation.

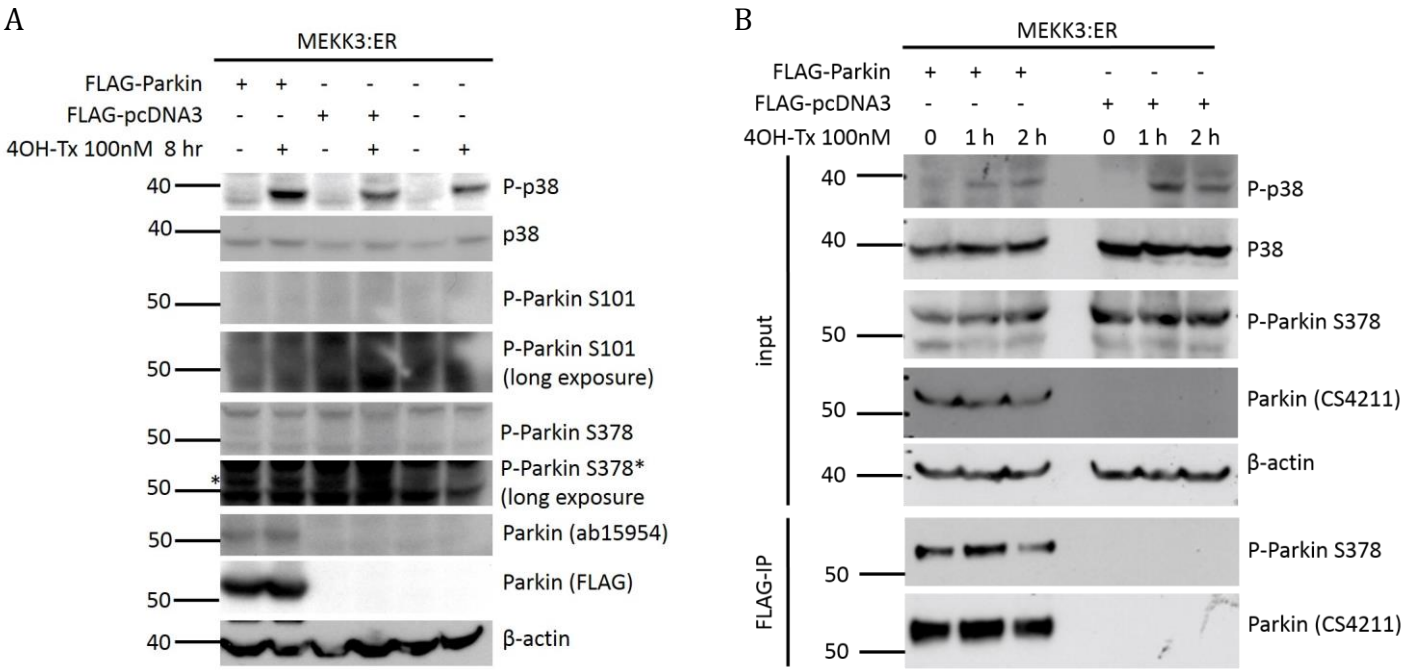

Figure 4-3 Parkin was not phosphorylated upon activation of p38 signalling pathway.

(A) ΔMEKK3:ER-expressing HEK293t cells were transiently transfected with FLAG-Parkin and FLAG-pcDNA3. Whilst phosphorylation of p38 (P-p38) was induced following 4OH-Tx treatment, no phosphorylation of Parkin at S101 or S378 was detected, even with longer exposure of Western blot membranes to x-ray films. (* represents possible phospho-Parkin at S378 (P-Parkin S378) located at the same molecular weight as FLAG-Parkin) (B) Same experiments were repeated and part of the lysates were subjected to immunoprecipitation with anti-FLAG antibody-coupled agarose beads (FLAG-IP). Parkin was constitutively phosphorylated at S378, independent of p38 signalling pathway activation.

137

4.2.2 Parkin phosphorylation is not detected upon activation of ERK1/2 signalling pathway

Next I tested whether Parkin can be phosphorylated following ERK1/2 signalling activation by using NIH-3T3 cells stably expressing ΔRaf-DD:ER. ΔRaf-DD:ER is a 4OH-Tx-inducible version of the human Raf protein kinase in which Raf is activated by deletion of its N terminus and substitution of aspirate (D) residues at Tyr-340 and -341, and fused in-frame to a modified hormone binding domain of oestrogen receptor (Bagowski et al., 2001; Bosch et al., 1997). Activation of ΔRaf-DD:ER by treatment of 4OH-Tx results in specific activation of endogenous ERK1/2 (Figure 4-2).

FLAG-Parkin and FLAG-pcDNA3 were transfected in ΔRaf-DD:ER cells for 48 h prior to Raf signalling pathway induction by 100 nM 4OH-Tx. Cells were lysed and each reaction was divided, with 90% subjected to FLAG-IP. Both the original lysates (input) and FLAG-peptide eluted lysates (FLAG-IP) were analysed by SDS-PAGE and Western blotting (Figure 4-4). Phosphorylated ERK1/2 (P-ERK1/2 T202/Y204) was detected upon treatment of 4OH-Tx in the input fraction, although it was slightly weaker in FLAG-Parkin expressing in ΔRaf-DD:ER cells. In the input the anti-P-Parkin S378 antibody detected several bands, most of which were likely to be non-specific. The weak FLAG-Parkin bands detected by anti-Parkin antibody suggested that the transfection efficiency of FLAG-Parkin in the ΔRaf-DD:ER cells was low, as NIH-3T3 cells were relatively resistant to the transfection of additional constructs comparing to ΔMEKK3:ER-expressing HEK293 cells. The expression of FLAG-Parkin was so low that it was only inconsistently detected in FLAG-IP fraction, whereas P-Parkin S378 was undetectable (FLAG-IP data not shown). Although the phosphorylation of ERK1/2 was slightly reduced in FLAG-Parkin-expressing ΔRaf-DD:ER cells, more studies with robust Parkin expression in the cells will be needed before this finding is to be confirmed. In conclusion, whether activation of ERK1/2 signalling pathway results in Parkin phosphorylation remains inconclusive.

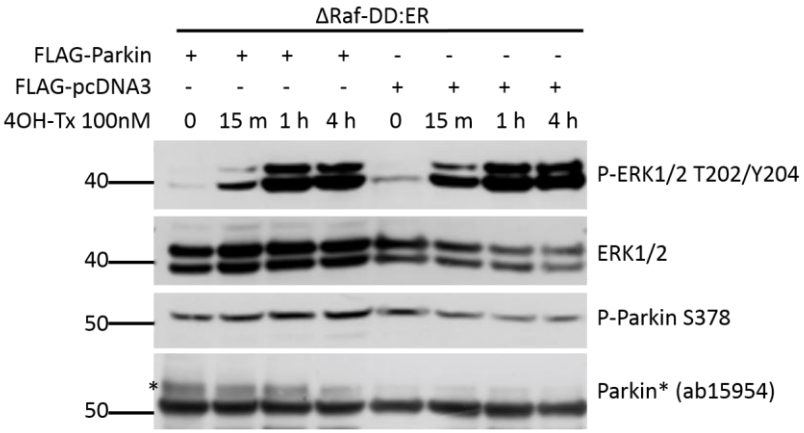

Figure 4-4 Parkin was not phosphorylated upon activation of ERK1/2 signalling pathway.

ΔRaf-DD:ER-expressing NIH-3T3 cells were transiently transfected with FLAG-Parkin and FLAG-pcDNA3. Phosphorylation of ERK1/2 (P-ERK1/2 T202/Y204) was induced by 4OH-Tx. Transfection efficiency of FLAG-Parkin was poor and no P-Parkin S378 was detectable upon ERK1/2 signalling activation. (* represents FLAG-Parkin bands detected by anti-Parkin antibody. The bands below FLAG-Parkin in all samples were likely to be non-specific.)

4.2.3 Parkin is weakly phosphorylated upon Akt activation

4.2.3.1 Investigating Parkin phosphorylation by using myrAkt:ER cell model

A weak Parkin phosphorylation at S378 upon activation of Akt signalling has been shown by the preliminary experiment in our lab (Figure 4-5 A). To further confirm this finding, NIH-3T3 cells stably expressing inducible myrAkt:ER were utilised. MyrAkt:ER is a constitutively active form of Akt (myrAkt) that fuses to the hormone binding domain of the oestrogen receptor. Treating myrAkt:ER cells with 4OH-Tx activates myrAkt directly, instead of activating the whole phosphatidylinositide 3-kinases (PI3K)/Akt signalling cascade like what happens in 4OH-Tx-treated ΔMEKK3:ER or ΔRaf-DD:ER cells. The activated myrAkt was detectable by anti-phospho-Akt S473 (P-Akt S473) antibody at 75 kDa (Figure 4-2).

FLAG-Parkin and FLAG-pcDNA3 were transfected into myrAkt:ER cells for 48 h prior to treatment with 100 nM 4OH-Tx. The Western blot of whole cell lysates demonstrated activated myrAkt detected by P-Akt S473 antibody at 75 kDa following 4OH-Tx treatment, equally in both FLAG-Parkin and empty-vector transfected myrAkt:ER cells (Figure 4-5 B). The expression of FLAG-Parkin in myrAkt:ER cells was weak and anti-P-Parkin S378 antibody only detected non-specific bands. Repeated experiments had been attempted several times in order to IP FLAG-Parkin but the transfection efficiency was extremely low that hardly any FLAG-Parkin was detectable in the FLAG-IP fraction (Data not shown). Due to poor transfection efficiency of FLAG-Parkin and low specificity of P-Parkin S378 antibody, whether Parkin can be phosphorylated upon Akt activation is inconclusive in this model.

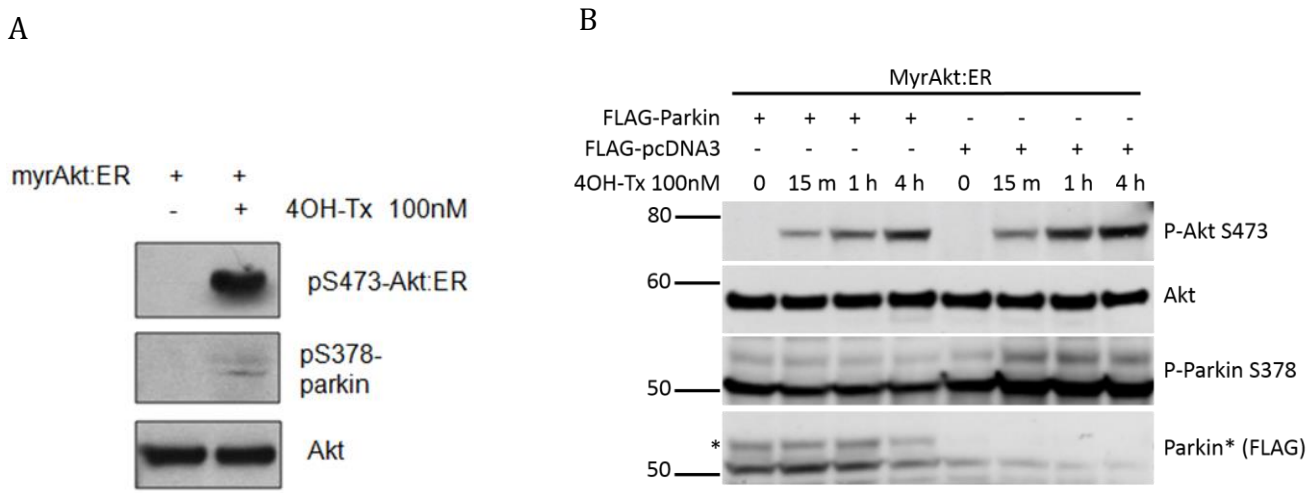

Figure 4-5 Parkin can be weakly phosphorylated upon activation of Akt signalling pathway.

(A) Preliminary data in our lab demonstrated a weak phosphorylation of Parkin at S378 in myrAkt:ER cells upon 4OH-Tx treatment (Dr Helene Plun Favreau, unpublished data). (B) MyrAkt:ER-expressing NIH-3T3 cells were transiently transfected with FLAG-Parkin and FLAG-pcDNA3. Activated myrAkt (detected by P-Akt S473) was induced by 4OH-Tx. Transfection efficiency of FLAG-Parkin was poor and P-Parkin S378 antibody detected several non-specific bands. (* represents FLAG-Parkin bands detected by anti-Parkin antibody. The bands below FLAG-Parkin in all samples were likely to be non-specific.)

4.2.3.2 FLAG-Parkin was not phosphorylated upon endogenous Akt activation in HEK293t cells

As a result of the low transfection efficiency of FLAG-Parkin into NIH-3T3 cells, I sought to activate the endogenous Akt signalling pathway in cells that are more transfectable. Endogenous Akt is the major effector in phosphatidylinositide 3-kinases (PI3K)/Akt signalling pathway, which can be activated by epidermal growth factor (EGF) (Ojeda et al., 2011) or insulin (Rafalski and Brunet, 2011).

HEK293t cells were transfected with FLAG-Parkin or FLAG-pcDNA3, serum starved, and then treated with 100 ng/ml EGF. The Western blotting of whole cell lysates showed Akt was phosphorylated at S473 after 5 min of EGF treatment (Figure 4-6). Although transfection efficiency of FLAG-Parkin was good in this model, P-Parkin S101 was undetectable. P-Parkin S378 antibody still detected multiple non-specific bands, although in one out of three experiments the strongest bands (at approximately 50 kDa) detected by P-Parkin S378 increased slightly following EGF stimulation. The whole cell lysates were not further subjected to FLAG-IP due to the consideration that EGF receptors are only weakly expressed in HEK293t cells. Although these experiments confirm endogenous Akt could be phosphorylated upon EGF treatment, whether Parkin is phosphorylated in this model remains inconclusive.

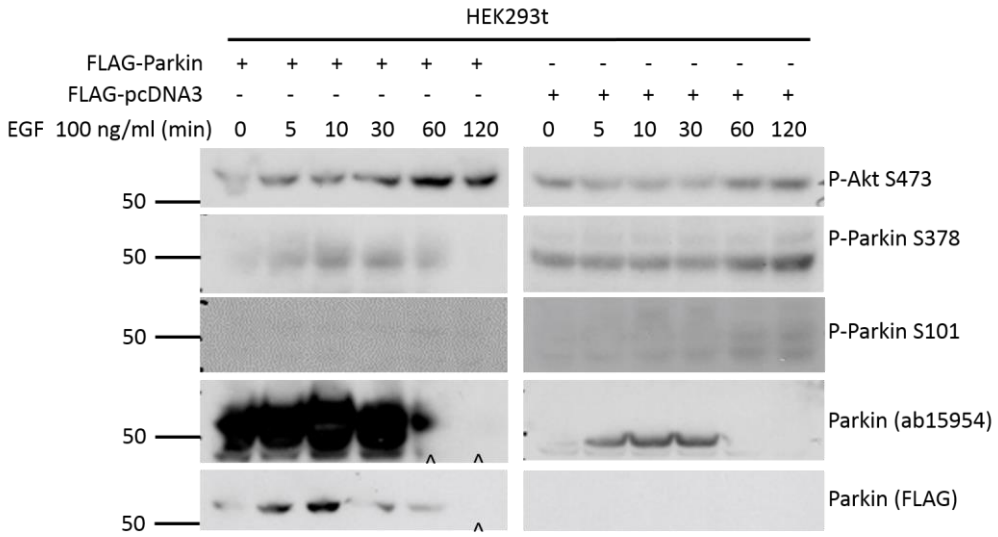

Figure 4-6 Parkin was not phosphorylated upon activation of Akt in HEK293t cells by epidermal growth factor (EGF).

HEK293t cells transfected with FLAG-Parkin or FLAG-pcDNA3 transiently were treated with EGF to activate endogenous Akt signalling pathway. Transfection efficiency of FLAG-Parkin was good. No phosphorylation of Parkin at S101 was observed. P-Parkin S378 antibody detected multiple non-specific bands in both transfected cells. (^ represents stripping process-related protein loss before reprobing the membrane with anti-Parkin and anti-FLAG antibodies respectively.)

4.2.3.3 FLAG-Parkin was not phosphorylated in SH-SY5Y cells upon activation of endogenous PI3K/Akt signalling pathway

The aforementioned experiments regarding Parkin phosphorylation following induction of the PI3K/Akt signalling pathway showed discrepancies in results obtained from different cell models. These cell models are less representative as PD pathology presents mainly in Dopaminergic neurons. Furthermore, phospho-Parkin was not reliably detected by commercially available antibodies at the endogenous level. As a result, the dopaminergic human neuroblastoma cell line SH-SY5Y stably expressing FLAG-Parkin or FLAG-pcDNA3 were then utilised to overcome the problems in the abovementioned cell models.

SH-SY5Y cells stably expressing were a gift from Dr Helen Ardley (Ardley et al., 2003) and SH-SY5Y cells stably expressing FLAG-pcDNA3 were produced in the lab by Dr Emma Deas. These cells were cultured in serum-free medium for 16 h before they were treated with 100 ng/ml EGF. The cells were lysed and each sample was divided by a 1:9 ratio, with 10% remained as input whilst 90% was subjected to IP with FLAG-beads. The latter fraction was then eluted by FLAG-peptide. Both fractions (input and FLAG-IP) were analysed by SDS-PAGE Western blotting (Figure 4-7). EGF induced a strong and early activation of PI3K/Akt and ERK1/2 signalling pathways in both FLAG-Parkin SH-SY5Y cells and the empty vector control, by the presence of P-Akt S473, P-S6 S235/S236, and P-ERK1/2 T202/Y204 in the input fraction. However, in the FLAG-IP fraction, Parkin was constitutively phosphorylated at either S101 or S378 following activation of these two pathways by EGF.

The experiment was repeated with the same cell model at the same condition except using 50 nM insulin to activate PI3K/Akt and ERK1/2 signalling pathways (Figure 4-8). In the input fraction, insulin activated PI3K/Akt signalling pathway at similar time point and same efficiency as EGF did, whilst insulin activated an overall weaker ERK1/2 phosphorylation than EGF did. Nevertheless, constitutive phosphorylations at S101 and S378 of Parkin were still observed in FLAG-IP fraction upon the treatment of insulin.

Although EGF or insulin used in this section activated endogenous PI3K/Akt signalling pathway in extremely high efficiency, phosphorylation of ERK1/2 was also observed in FLAG-Parkin 5Y as well empty vector control. Since Akt activated mTOR as its downstream effector in PI3K/Akt pathway, amino acid was then used to selectively activate mTOR and its downstream pathway. SH-SY5Y cells stably expressing FLAG-Parkin or FLAG-pcDNA3 were first serum starved for 16 h and then the medium were replaced by Earl's balanced solution (EBS) for amino acid-starvation for 2 h, followed by treating 20 ul/ml amino acid at designated durations. Western blotting showed that phosphorylation of mTOR at S2448 (P-mTOR S2488) was observed after 15 min of amino acid stimulation in the input fraction, whilst P-S6 S235/S236 was observed 1 h after stimulation (Figure 4-9). Phosphorylation of Akt but not ERK1/2 was observed upon amino acid treatment. In FLAG-IP fraction, constitutive phosphorylation of Parkin, however, was observed at either S101 or S378 following activation of mTOR signalling pathway by amino acid. These experiments suggest Parkin is not phosphorylated upon activation of Akt or ERK signalling pathways induced by EGF or insulin.

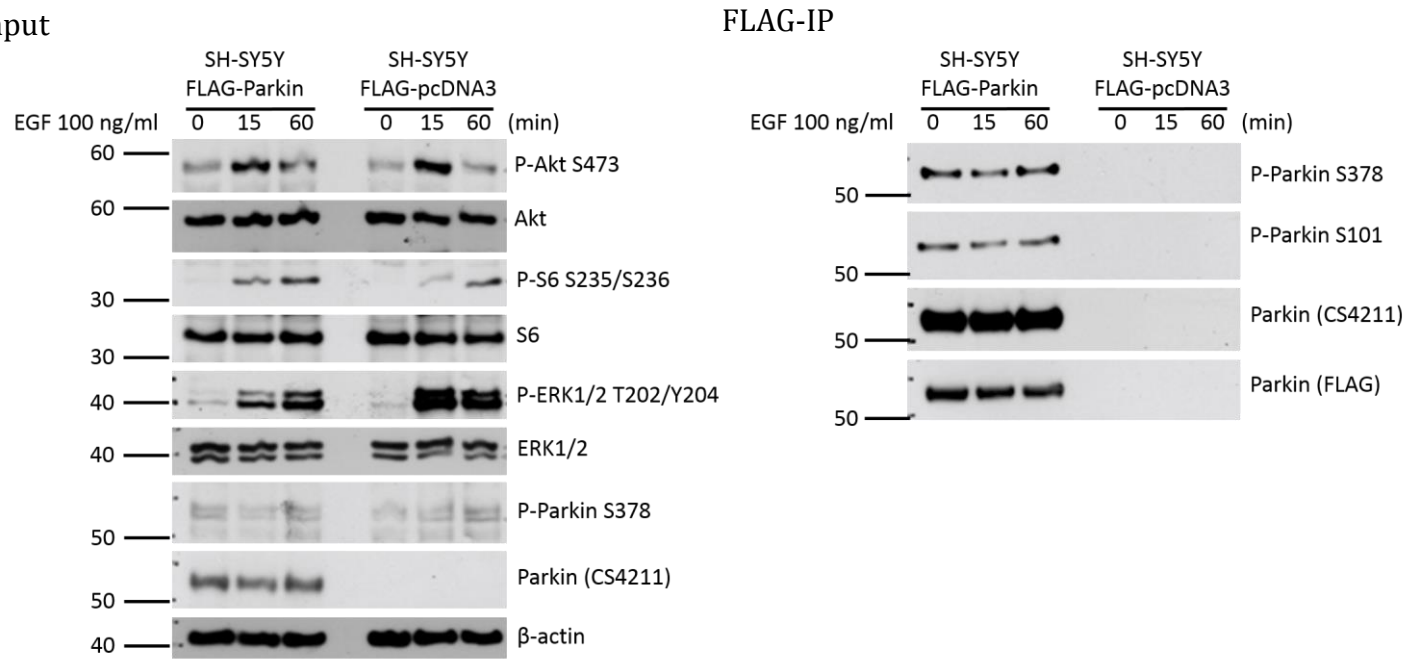

Figure 4-7 Immunoprecipitation of FLAG-Parkin from SH-SY5Y cells stably expressing FLAG-Parkin or FLAG-pcDNA3 following EGF treatment.

In the input fraction (left panel), Akt, S6, and ERK1/2 were phosphorylated upon treatment of EGF. The bands detected by P-Parkin S378 antibody were likely to be non-specific. The expression of FLAG-Parkin in the SH-SY5Y cells was good. Constitutive Parkin phosphorylation at S101 and S378 was detected in the FLAG-IP fraction (right panel), independent of EGF treatment.

146

Parkin **from**

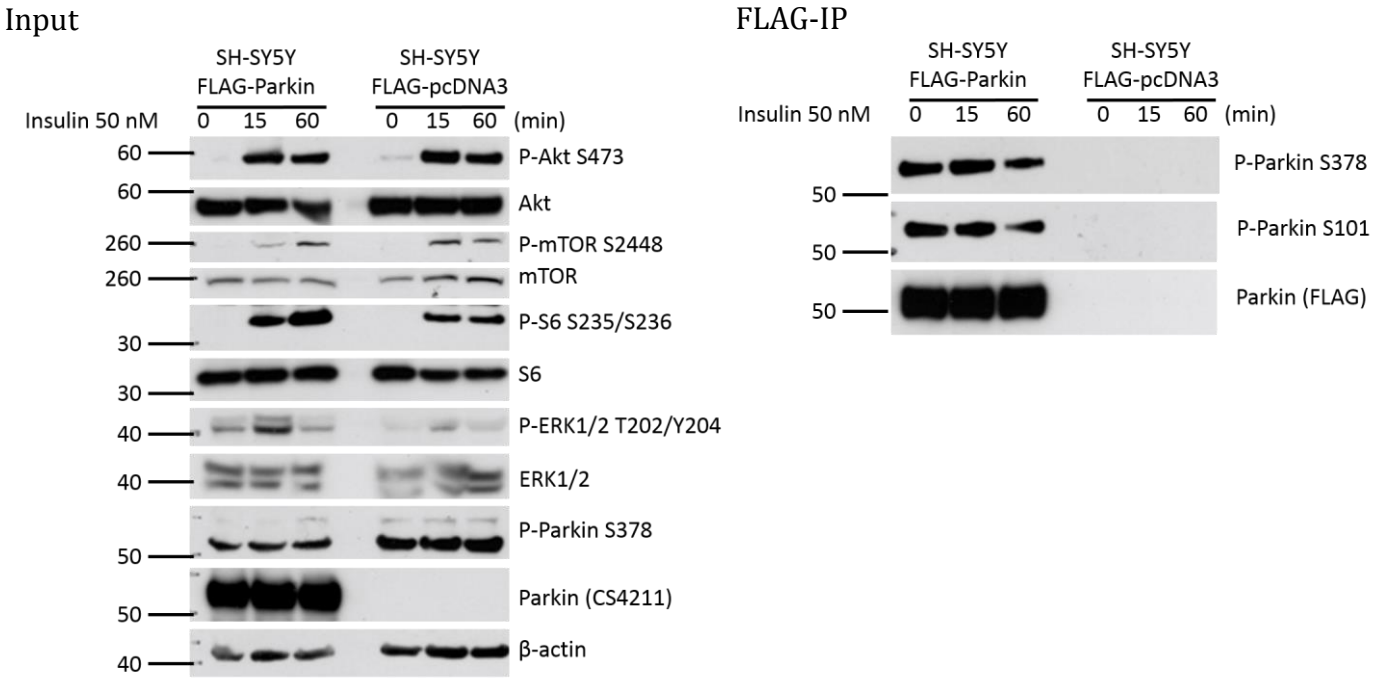

Figure 4-8 Immunoprecipitation of FLAG-Parkin from SH-SY5Y cells stably expressing FLAG-Parkin or FLAG-pcDNA3 following insulin treatment.

In the input fraction (left panel), Akt, S6, and ERK1/2 were phosphorylated upon treatment of insulin. P-Parkin S378 antibody detected only non-specific bands in the input fraction. Constitutive Parkin phosphorylation at S101 and S378 was detected in the FLAG-IP fraction (right panel), independent of insulin treatment.

147

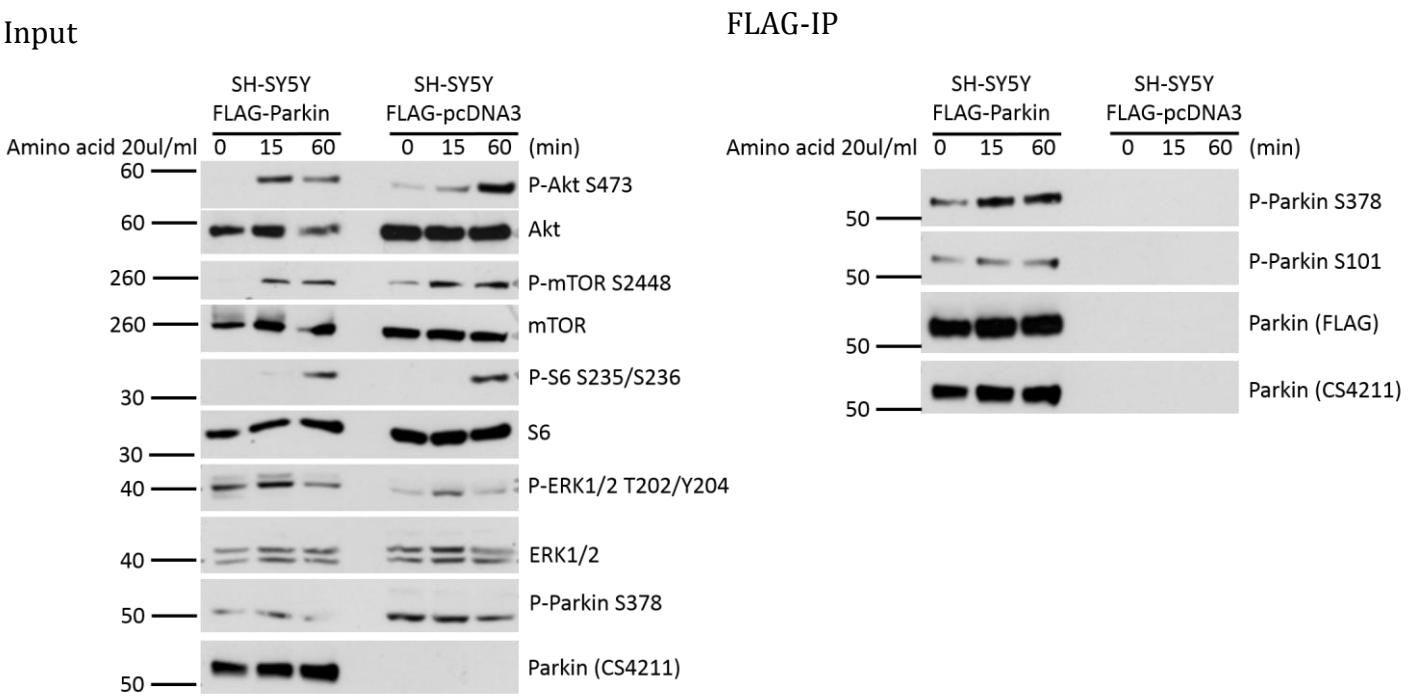

Figure 4-9 Immunoprecipitation of FLAG-Parkin from SH-SY5Y cells stably expressing FLAG-Parkin or FLAG-pcDNA3 following treatment with amino acid to activate mTOR.

In the input fraction (left panel), Akt and S6 were phosphorylated upon treatment of amino acid, whilst ERK1/ was not. P-Parkin S378 antibody detected only non-specific bands in the input fraction. Constitutive phosphorylation at S101 and S378 of Parkin was observed in the FLAG-IP fraction (right panel), independent of amino acid treatment.

148

4.3 Discussion

Several Parkin phosphorylation sites have been reported (Avraham et al., 2007; Imam et al., 2011; Kazlauskaite et al., 2014; Kim et al., 2008; Ko et al., 2010; Kondapalli et al., 2012; Rubio de la Torre et al., 2009; Sha et al., 2010; Shiba-Fukushima et al., 2012; Yamamoto et al., 2005), however the kinases that modulate these post-translational modifications of Parkin remain elusive. PINK1 has been shown to phosphorylate Parkin (Kazlauskaite et al., 2014; Kim et al., 2008; Kondapalli et al., 2012; Shiba-Fukushima et al., 2012), nevertheless the detailed signalling pathway leading to PINK1 phosphorylation of Parkin is still unclear. Previous reports suggest MAPK and PI3K/Akt signalling pathways are dysregulated in PD brain (Dzamko et al., 2014; Kim and Choi, 2010; Ren et al., 2009). The highly activated MAPK signal and attenuated Akt signal in PD pathology may increase the neurotoxicity (Dzamko et al., 2014). Thus these pathways were selected in this thesis for testing whether any of them involves Parkin regulation.

4.3.1 Parkin phosphorylation is not observed upon activation of MAPK signalling pathways

The mammalian MAPK family consists of JNK, p38 and ERK (Chang and Karin, 2001). The two cell lines with inducible mitogen-activated protein kinase kinase kinase (MAP3K) utilised in this part of work possess the advantage to activate either p38 or ERK1/2 specifically following induction. In theHEK293t cells expressing ΔMEKK3:ER, Parkin was constitutively phosphorylated at S378, independent of p38 signalling pathway activation. The anti-P-Parkin S101 antibody, on the other hand, was less sensitive in detecting FLAG-Parkin in either whole cell lysates or FLAG-peptide eluted Parkin from FLAG-IP samples in this model. Since the activation of p38 MAPK in this cell line is only induced upon 4OH-Tx treatment, the background p38 activity is low and less likely to cause Parkin S378 phosphorylation. Therefore, it can only be concluded here that Parkin S378 is constitutively phosphorylated and this phosphorylation is independent of p38 MAPK signalling pathway activation. Previous report demonstrated that the p38 signalling induced by microtubule depolymerising agents in cell models can be attenuated by overexpressing Parkin, suggesting Parkin might act upstream of p38 MAPK (Ren et al., 2009), instead of being activated by p38.

The ΔRaf-DD:ER-expressing NIH-3T3 cell model used in this project is more resistant to FLAG-Parkin transfection compared to ΔMEKK3:ER-expressing HEK293t cells. FLAG-Parkin is only weakly overexpressed in ΔRaf-DD:ER cells after trying various transfection reagents and conditions. Although the anti-P-Parkin S378 antibody detects several bands at various molecular weights and densities in the whole cell lysates, these bands are likely to be non-specific. In addition, the location of the strongest band detected by P-Parkin S378 antibody is slightly lower than the FLAG-Parkin band detected by anti-FLAG antibody. Not only Parkin phosphorylation at S378 is inconclusive, but the specificity of P-Parkin S378 antibody is questionable. The attempt to immunoprecipitate the samples with FLAG-beads does not seem to improve the FLAG-Parkin signal strength. Therefore it is not possible to conclude whether Parkin can be

phosphorylated upon ERK1/2 signalling pathway activation by ΔRaf-DD:ER-expressing NIH-3T3 cell model. That said, when endogenous ERK1/2 signalling pathway is activated in FLAG-Parkin-expressing SH-SY5Y cells, Parkin is not phosphorylated at either S101 or S378. This SH-SY5Y cell model demonstrates strong Parkin expression level, and in the FLAG-IP fraction the Parkin bands detected by antibodies against both total and phosphorylated Parkin are of the same molecular weight, suggesting a more reliable result in this SH-SY5Y model.

Previous reports have shown that ERK1/2 signalling is dysregulated in PD patients (Kurup et al., 2015; Ren et al., 2009). For instance, the ERK1/2 activation by microtubule depolymerising agent such as colchicine can be attenuated by Parkin, and mutation in Parkin results in activated ERK1/2 signal in cell models (Ren et al., 2009). On the contrary, Parkin mutant patients show striatal accumulation of $STEP_{61}$ (striatal-enriched protein tyrosine phosphatase) and reduced phosphorylation of ERK1/2 and CREB (cAMP response element-binding protein), whereby synaptic function is disrupted (Kurup et al., 2015). These reports suggest Parkin might act upstream of the ERK1/2 signalling pathway. The discrepancy of Parkin's influence on ERK1/2 activation in these reports, however, indicates Parkin could influence ERK1/2 signalling via diverse processes, resulting activation of different downstream effectors accordingly. In this project, P-ERK1/2 activation was slightly reduced in FLAG-Parkin-expressing ΔRaf-DD:ER NIH-3T3 cells, although the expression level of FLAG-Parkin was extremely low. In the SH-SY5Y cell model, on the other hand, P-ERK1/2 activation following EGF or insulin treatment was not altered by overexpression of FLAG-Parkin. This suggests different cell models might have different influences on how the signalling pathways are regulated.

These previous reports regarding Parkin dysfunction alters p38 or ERK1/2 signalling could explain why Parkin phosphorylation was not observed upon activation of p38 or ERK1/2 signalling pathway in this project. Nevertheless, overexpression of Parkin in the cell model used here did not alter the phosphorylation of p38 or ERK1/2 markedly, neither does the activation of p38 or ERK1/2 negatively affect the constitutive phosphorylation of Parkin S378.

4.3.2 Parkin might be phosphorylated upon activation of PI3K/Akt signalling pathway

A weak Parkin phosphorylation at S378 upon myrAkt activation in myrAkt:ER-expressing NIH-3T3 cells has been demonstrated in the preliminary experiment. I have since tried to verify this finding and dissect the associated pathways in various cell models, including myrAkt:ER-expressing NIH-3T3 cells (with or without overexpressing FLAG-Parkin), and SH-SY5Y (with or without overexpressing FLAG-Parkin). The attempt to reproduce the result in myrAkt:ER-expressing NIH-3T3 cells was unsuccessful. Despite trying various transfection reagents and protocols, the expression of FLAG-Parkin in myrAkt:ER-expressing NIH-3T3 cells is still low.

The alternative ways to activate endogenous Akt signal can be achieved by EGF or insulin (Galbaugh et al., 2006; Hermann et al., 2000; Lizcano and Alessi, 2002; Yip and Seow, 2012). An inconsistent, weak phosphorylation of Parkin S378 was detected in HEK293t cells expressing FLAG-Parkin transiently upon EGF stimulation. However, the phosphorylation of Akt is not as strong as expected, which might be explained by low expression of EGF receptor in HEK293t cells (Carter and Sorkin, 1998; Huang et al., 2008). Fibroblasts, on the other hand, have higher EGFR expression (Wells, 1999), but are less easy to be transfected. Activation of endogenous Akt and ERK1/2 in MEFs and human primary fibroblasts following treatment with EGF or insulin had been attempted (Data not shown), but Parkin phosphorylation was not detected at the endogenous level in MEFs. In control human fibroblasts, however, the signal intensity of the band detected by P-Parkin S378 antibody waxed and waned throughout the time of insulin stimulation, assuming the band observed was the true endogenous Parkin. The low sensitivity and specificity of these antibodies against phosphorylated/total Parkin at the endogenous level resulted in the difficulty in analysing the readout at this part of project.

In order to ensure a robust endogenous Akt signalling activation as well as a clear phosphorylated and total Parkin signal, neuroblastoma cells SH-SY5Y

stably expressing FLAG-Parkin were then utilised. This cell model also possesses the advantage that it mimics the *in vivo* environment of neurons better, as PD pathology present mainly in neurons. Both S101 and S378 seem to be constitutively phosphorylated in this model, independent of activation of Akt signalling pathway.

Activation of Akt signalling pathway is neuroprotective (Alessi et al., 1997; Thomas and Beal, 2007) and reduced Akt activity has been reported in PD pathology (Dzamko et al., 2014; Timmons et al., 2009; Yang et al., 2005). Despite molecular pathways remain elusive; compiling evidences demonstrate Parkin is also neuroprotective. Parkin overexpression increases resistance to cellular apoptosis and knocking down Parkin in SH-SY5Y cells causes apoptotic death of cells (Burke, 2008). By enhancing ubiquitination of TRAF2 (tumor necrosis factor (TNF) receptor-associated factor2) and IKKγ (IκB kinase γ)/NEMO (NF-κB essential modifier) complex, which leads to proteasomal degradation of NFκB (nuclear factor kappa-light-chain-enhancer of activated B cells) inhibitor IκBα, Parkin activates IKK/NFκB signalling that promotes the transcription of pro-survival genes (Henn et al., 2007; Sha et al., 2010). Parkin suppresses stress-activated protein kinase pathways (Hasegawa et al., 2008). Furthermore, Parkin is linked with Akt signalling with respect to neuroprotection function. Parkin can enhance Akt signalling by promoting ubiquitination of Eps15 UIM (ubiquitin-interacting motifs) and eventually delaying the endocytosis of EGF receptors (Fallon et al., 2006). This suggests Parkin might regulate Akt signalling pathway, which seems to discord with my hypothesis that Parkin could be regulated by Akt signalling via phosphorylation. Of note, EGF-induced Parkin-Eps15 interaction also reciprocally activates Parkin E3 ligase activity (Fallon et al., 2006). Additionally, the kinase prediction result by KinasePhos2.0 (http://kinasephos2.mbc.nctu.edu.tw/) shows Akt is one of the possible kinases that phosphorylate Parkin. However, all the models used in this part of work failed to demonstrate that Parkin can be phosphorylated at S101 or S378 following Akt signalling activation. Whether Akt can phosphorylate Parkin at serine sites other than S101 and S378 is yet to be confirmed.

4.3.3 Experimental difficulties and critical evaluation of study design

There has been two major difficulties while commencing this project: the low sensitivity and low specificity of commercial antibodies against endogenous total or phosphorylated Parkin, and the poor transfection efficiency in some of the cell models utilised.

It has been described in Chapter 3 that almost all anti-Parkin antibodies tested detect multiple bands in Western blotting. The bands possibly corresponding to Parkin located at variable positions between 50 and 55 kDa, depending on different antibody used. Additionally, the sensitivity of anti-P-Parkin S101 antibody was lower than the S378 one, as it hardly detected any band at the endogenous level, whilst the S378 one detected a weak band sandwiched between another two stronger bands at 50 and 60 kDa respectively.

The attempt to solve this protein detection issue was to overexpress Parkin in the cell models used in this experiment. This was where the second difficulty was encountered. The three cell models utilised in the first part of this project were the cells lines stably expressing inducible ΔMEKK3:ER, ΔRaf-DD:ER and myrAkt-ER. Whilst ΔMEKK3:ER is expressed in HEK293t cells, both ΔRaf-DD:ER and myrAkt-ER are expressed in NIH-3T3 cells. HEK293t cells can be transfected with 10-time higher efficiency than NIH-3T3 cells (Plautz et al., 2011). In this project, FLAG-Parkin expressed well inΔMEKK3:ER cells but was hardly detectable in ΔRaf-DD:ER and myrAkt-ER cells after attempting various transfection reagents and protocols.

The hypothesis of this study was initiated in view of the preliminary experiment showing Parkin was phosphorylated upon activation of Akt and the evidence supporting a number of signal pathways were dysregulated in PD pathology. At the time, the study was designed based on the abovementioned information. However in retrospect, it is useful to adjust the study design in accordance with the experimental outcomes as the project proceeded.

The PD-associated MAPK and PI3K/Akt signalling pathways were selected for testing whether any of them is associated with Parkin phosphorylation. Cell models expressing inducible ΔMEKK3:ER, ΔRaf-DD:ER and myrAkt-ER were readily available in lab. The advantage of using these cell models is to ensure a robust activation of the signalling pathways of interest. The generation of ΔMEKK1:ER-expressing stable NIH-3T3 cell line, in which P-JNK can be induced, has been attempted twice. However, no cells expressed adequate ΔMEKK1:ER level to resist the antibiotics selection following the transfection. Therefore, the experiments were only commenced in models with inducible p38, ERK1/2 or Akt signalling pathways. Nevertheless, the cellular backgrounds of these cell lines were not identical, as ΔMEKK3:ER was expressed in HEK293t cells whilst both ΔRaf-DD:ER and myrAkt-ER were in NIH-3T3 cells. The possible variations of the endogenous Parkin expression level in different cell lines could lead to misinterpretation of experimental readouts. Considering the time-consuming procedure it takes for generating stable cell lines of the same cellular background, it would be worth trying to do a preliminary experiment by transiently expressing the construct of inducible kinase in a single cell type to avoid background variation, and then generate the stable cell line from it if necessary. Activation of endogenous MAPK or Akt signalling pathways could be an alternative option. Although activating endogenous PI3K/Akt signalling pathway by EGF and insulin has been attempted, this project would be more completed if each endogenous MAPK signalling pathway (p38, ERK1/2 or JNK) can also be tested individually within timeframe available. Furthermore, it would be ideal to scale up the analysis to a high-throughput system, for instance RNAi-based screening.

The decision to detect Parkin at the endogenous level in some of the cell models utilised in this project is not ideal but alternative choices are little. As described in Chapter 3, the detection of endogenous Parkin remains challenging. Most of commercially available antibodies against phosphorylated or total Parkin used currently are not specific enough to detect a clear band at the correct molecular weight. A straightforward strategy to overcome this difficulty is thus to further

overexpress Parkin in the cell model with inducible kinase. However this is far from ideal, as this makes the cell model less physiological, and the susceptibility of each cell line toward a second construct transfection differs greatly in this project. It would be ideal to generate the models with the same cellular backgrounds by transfection methods of higher transfer rate, for instance the viral transduction. The alternative strategy taken in this project was to utilise the SH-SY5Y cells stably expressing FLAG-Parkin and FALG-pcDNA3. To avoid the difficulty of transfecting these cells with a second construct, endogenous signalling pathways were activated. In this project PI3K/Akt and ERK1/2 were activated by EGF or insulin at the dosage and duration optimised by preliminary experiments. As stated previously it would be interesting to test other signalling pathways at endogenous level within available timeframe or even scale up to a high-throughput assay to derive the architecture of possible Parkin-associated signalling pathway faster than traditional approaches.

Immunoprecipitating the lysates with anti-FLAG conjugated agarose beads was essential in this project because clear Parkin bands were only detectable in the FLAG-IP fraction. One possible bias when analysing the readout could be encountered with this method. Provided that P-Parkin antibodies were not specific enough against their phosphorylated protein targets, they might actually detect a higher fraction of total protein than the phosphorylated form since the FLAG-IP fraction contained a large amount of FLAG-Parkin, giving a false interpretation that these two serine sites (S101 and S378) were constitutively phosphorylated. Moreover, although these two serine sites are more conserved than others in Parkin, it would be ideal to test as many conserved sites as possible upon activation of selected signalling pathways. One of the alternative approaches to achieve this is to separate the lysates on the Phos-tag acrylamide gel (Kinoshita et al., 2006). Its Western blotting membrane is then probed with antibody against the protein of interest in order to obtain a shifted protein band which indicates a probable phosphorylation. The protein extracted from this shifted band can subsequently be subjected to the analysis by Mass Spectrometry for identification of the relevant phosphorylated site(s) in a more accurate way.

A final consideration is whether it was adequate to just observe the phosphorylation of Parkin following activation of selective signalling pathways. A number of previous reports implied dysregulation of these signalling pathways in models with Parkin dysfunction (Dzamko et al., 2014; Kim and Choi, 2010; Ren et al., 2009), pointing out the possibility that Parkin might actually act upstream of the target kinases observed in this project. However, there was no alteration of Akt or ERK1/2 activation observed in Parkin-expressing SH-SY5Y cells comparing to empty-vector controls or untransfected cells. The balanced signalling pathways might somehow be achieved by other compensatory mechanism following long-term expression of Parkin in the cells. The other way to observe the effect of Parkin dysfunction on these signalling pathways is to knock down Parkin in the cells. However due to the low specificity of antibody against endogenous Parkin, the knock-down of Parkin is even harder to be proved at the protein level, despite RT-qPCR could demonstrate efficient knockdown. Parkin patient fibroblasts might be a more reliable model comparing to knockdown cell lines. When protein expression data is unable to acquired, patient's clinical symptoms can offer another evidence of Parkin mutation on top of the genotyping result. It would also be very interesting to dissect these PD-associated signalling pathways using the human primary Parkin-mutant fibroblasts, iPSC derived from these fibroblasts, or even Parkin iPSC-derived dopaminergic neurons as the model if the timeframe permitted.

4.3.4 Conclusion

In this chapter, three PD-associated signalling pathways, p38, ERK1/2 and PI3K/Akt, were activated in order to detect possible Parkin phosphorylation. Although the preliminary experiment demonstrated weak Parkin phosphorylation at S378 upon activation of Akt signalling pathway, this result was not recapitulated in this project. By using the overexpressed Parkin in neuroblastoma cell model it is concluded that Parkin might not be phosphorylated upon Akt signalling pathway activation, provided that the specificity of P-Parkin antibodies are reliable. The difficulty to proceed this

project at the endogenous level of Parkin leads the next project to be commenced at the overexpressed level of Parkin (Chapter 5).

4.3.5 Future perspectives

The work presented in this chapter proceeded parallel to the project in Chapter 3, therefore the decision to work on Parkin at overexpressed level was made after several failed experiments in detecting Parkin at the endogenous level. Since Parkin could be detected more reliably in the SH-SY5Y cell stably expressing FLAG-Parkin, it would be reasonable to use this model to test all the PD-associated signalling pathways. Additional studies by treating the cells with specific activators to activate each pathways or even individual molecule will be needed before making the conclusion that Parkin is not phosphorylated upon activation of these signalling pathways.

In the meantime, the efficiency in detecting Parkin phosphorylation can be improved by methods other than site-specific phospho-Parkin antibodies in the future work. For instance, a robust evidence of Parkin phosphorylation can be supported by the Phos-tag gel system plus the subsequent Mass Spectrometry analysis, whereby a more specific and reliable information regarding phosphorylation sites over the full length of Parkin can be provided.

Although SH-SY5Y cell line is a neuronal cell model, it is not a differentiated neuron after all. A model with overexpressed Parkin in the relatively primitive neuronal cell is less likely to recapitulate the physiological condition. If the signalling pathway that regulates Parkin phosphorylation can be determined by the abovementioned methods, it is then worth reproducing the result in a more physiological model. The human skin fibroblasts from the patient carrying Parkin mutations and the cells derived from these fibroblasts could potentially be a more reliable cell model system. The Parkin iPSC-derived neurons should be a cell model that is closely resembling the physiological background. Any signalling pathway shown to regulate Parkin phosphorylation in this model will therefore have enormous therapeutic value.

Chapter 5 The role of Parkin phosphorylation in mitochondrial quality control

5.1 Introduction

Whilst studies of both sporadic and genetic cases of PD show that mitochondrial dysfunction is an important feature of pathogenesis (Burchell et al., 2010a, b; Narendra et al., 2010b), much of what is known about the disease process, in particular mitophagy, comes from the study of the rare genetic forms of the disease. In particular, two of the proteins associated with early-onset autosomal recessive PD, PINK1 (mitochondrial kinase) and Parkin (E3 ubiquitin ligase) (Kitada et al., 1998; Valente et al., 2004), act in a common pathway to regulate mitochondrial turnover (Youle and Narendra, 2011).

Under normal conditions, nuclear encoded PINK1 is imported into the inner membrane of healthy, polarised mitochondria via its mitochondrial targeting sequence, where it is cleaved by the protease Presenilins-associated rhomboid-like protein (PARL). Cleaved PINK1 is further released in the cytosol and degraded (Deas et al., 2011a; Narendra et al., 2010b). Upon mitochondrial depolarisation (Narendra et al., 2008; Narendra et al., 2010b; Vives-Bauza et al., 2010), accumulation of mitochondrial DNA mutations (Suen et al., 2010) or unfolded proteins in the mitochondrial matrix (Jin and Youle, 2013), PINK1 is no longer cleaved by PARL and full length PINK1 accumulates in the outer

mitochondrial membrane (OMM). This accumulation acts as a molecular sensor of damaged mitochondria to mediate the recruitment of Parkin (Narendra et al., 2008; Narendra et al., 2010b; Vives-Bauza et al., 2010). In addition to PINK1, a number of proteins have been shown to regulate Parkin translocation (Hasson et al., 2013; McCoy et al., 2014; Sato et al., 2006), in particular the F-box domain-containing protein Fbxo7, which is also associated with early-onset PD (Burchell et al., 2013; Di Fonzo et al., 2009a). Following its translocation to the surface of damaged mitochondria, Parkin ubiquitinates numerous OMM proteins (Chan et al., 2011; Sarraf et al., 2013), which in turn leads to proteasome and autophagy-associated degradation of damaged mitochondria (Jin and Youle, 2012).

Despite intensive research, several steps in the mitophagy process remain poorly understood. Some important questions needing to be addressed are: how is Parkin's E3 ubiquitin ligase activity regulated, and what is the precise mechanism by which Parkin is recruited to damaged mitochondria. Several studies suggest that Parkin is regulated via post-translational modifications such as phosphorylation (Avraham et al., 2007; Birsa et al., 2014; Imam et al., 2011; Kazlauskaite et al., 2014; Kim et al., 2008; Ko et al., 2010; Kondapalli et al., 2012; Rubio de la Torre et al., 2009; Sha et al., 2010; Shiba-Fukushima et al., 2012; Shiba-Fukushima et al., 2014; Yamamoto et al., 2005). In this project I show that Parkin is phosphorylated at S101 upon carbonyl cyanide m-chlorophenyl hydrazone (CCCP)-induced mitochondrial depolarisation, and the non-phosphorylatable S101 Parkin mutant decreases Parkin mitochondrial translocation, perinuclear clustering of mitochondria, OMM proteins ubiquitination, and autophagic mitochondrial clearance. This study reveals new insights into the regulation of Parkin function via phosphorylation at S101 that plays an important role in modulating mitophagy.

5.2 Results

5.2.1 Parkin is phosphorylated at S101 following mitochondrial depolarisation induced by CCCP

A number of Parkin phosphorylation sites have been identified *in vitro* (Avraham et al., 2007; Imam et al., 2011; Kim et al., 2008; Ko et al., 2010; Kondapalli et al., 2012; Rubio de la Torre et al., 2009; Sha et al., 2010; Shiba-Fukushima et al., 2012; Shiba-Fukushima et al., 2014; Yamamoto et al., 2005). In this study I focus on the S101 phosphorylation site, an evolutionary conserved residue amongst many species (Figure 4-1). S101 is located in a flexible linker domain between the ubiquitin-like (Ubl) domain and the first Really Interesting New Gene (RING) domain (RING0) of Parkin (Figure 5-1 A). I first investigated whether Parkin could be phosphorylated over a time course of CCCP treatment. Following CCCP-induced mitochondrial depolarisation, P-Parkin S101 was detected after FLAG-IP of Parkin from SH-SY5Y neuroblastoma cells stably expressing wild-type FLAG-Parkin (hereafter referred to as WT cells), but not in SH-SY5Y cells stably expressing FLAG-pcDNA3 (hereafter referred to as control) (Figure 5-1 B). Two other Parkin phosphorylation sites, S131 and S378, locating in the linker domain and in the in-between-RING (IBR) domain of Parkin, respectively (Wauer and Komander, 2013), were also phosphorylated. However, phosphorylation at these sites appeared to be constitutive, as opposed to CCCP-induced (Figure 5-1 C and D). Parkin phosphorylation at S101 was induced after 1 h of CCCP treatment, and decreased after 5 h.

Specificity of the P-Parkin S101 antibody was validated using SH-SY5Y cells stably expressing exogenous S101A (non-phosphorylatable, hereafter referred to as S101A cells) and S101D (phosphomimetic, hereafter referred to as S101D cells) FLAG-Parkin mutants, respectively (Figure 5-2 A). Consistent with previous reports, IP of FLAG-Parkin from cytosolic fraction (CF) and mitochondria-enriched fraction (MF) revealed that although Parkin localized predominantly in the cytosol, it is recruited to the mitochondria upon CCCP treatment. Parkin phosphorylation at S101 occurred in both the CF and the MF

(Figure 5-2 B). These data were further confirmed by immunofluorescence (IF), as P-Parkin S101 punctae staining co-localized with mitochondria in response to CCCP treatment in WT and S101D cells but not S101A cells (Figure 5-2 C).

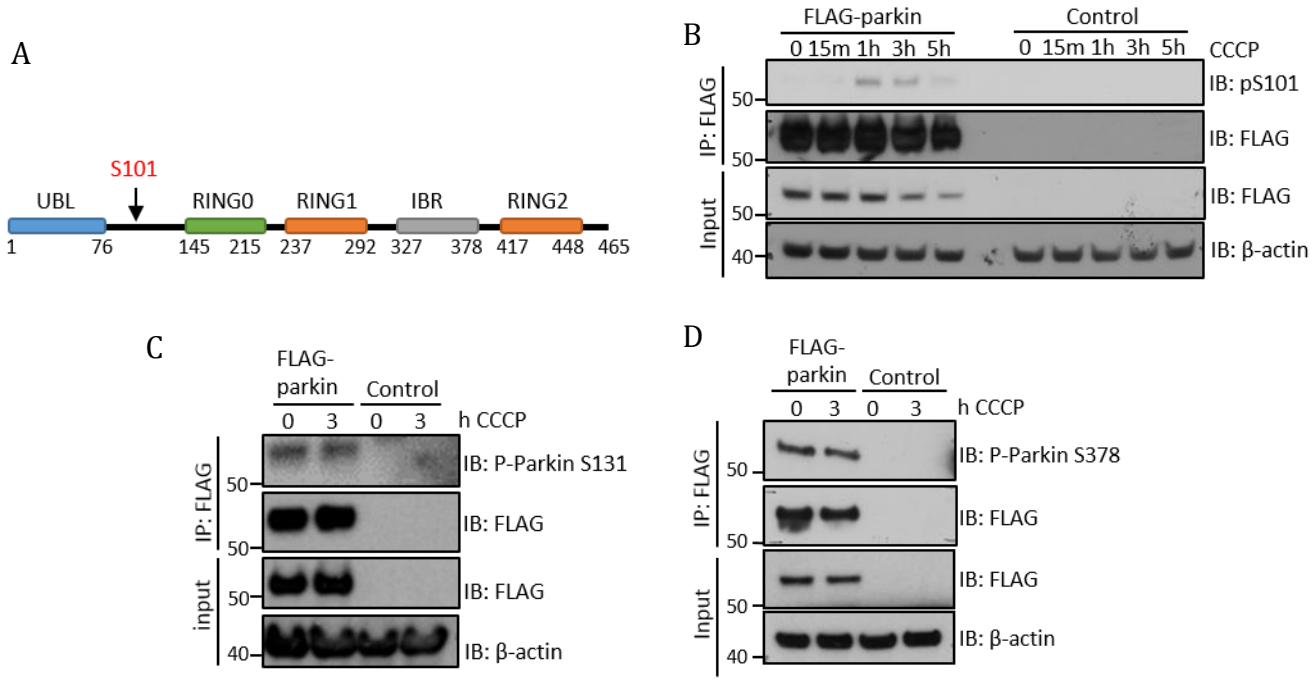

Figure 5-1 Parkin is phosphorylated at S101 following CCCP treatment.

(A) Diagram of Parkin structural domains, showing the location of the S101 phosphorylation site within the linker region. (Ubl: ubiquitin-like, RING: Really Interesting New Gene, IBR: in-between-RING) (B) Immunoblot (IB) of Parkin phosphorylation at S101 in FLAG-Parkin complexes immunoprecipitated (IP) from whole cell lysates of SH-SY5Y cells stably expressing FLAG-Parkin or FLAG-pcDNA3 (control) following 0, 1, 3 or 5 h treatment with CCCP (10 μM). (C and D) IB of Parkin phosphorylation at S131 (C) and S378 (D) in FLAG-Parkin complexes IP from whole cell lysates of FLAG-Parkin or control cells following 0 or 3 h treatment with CCCP (10 μM).

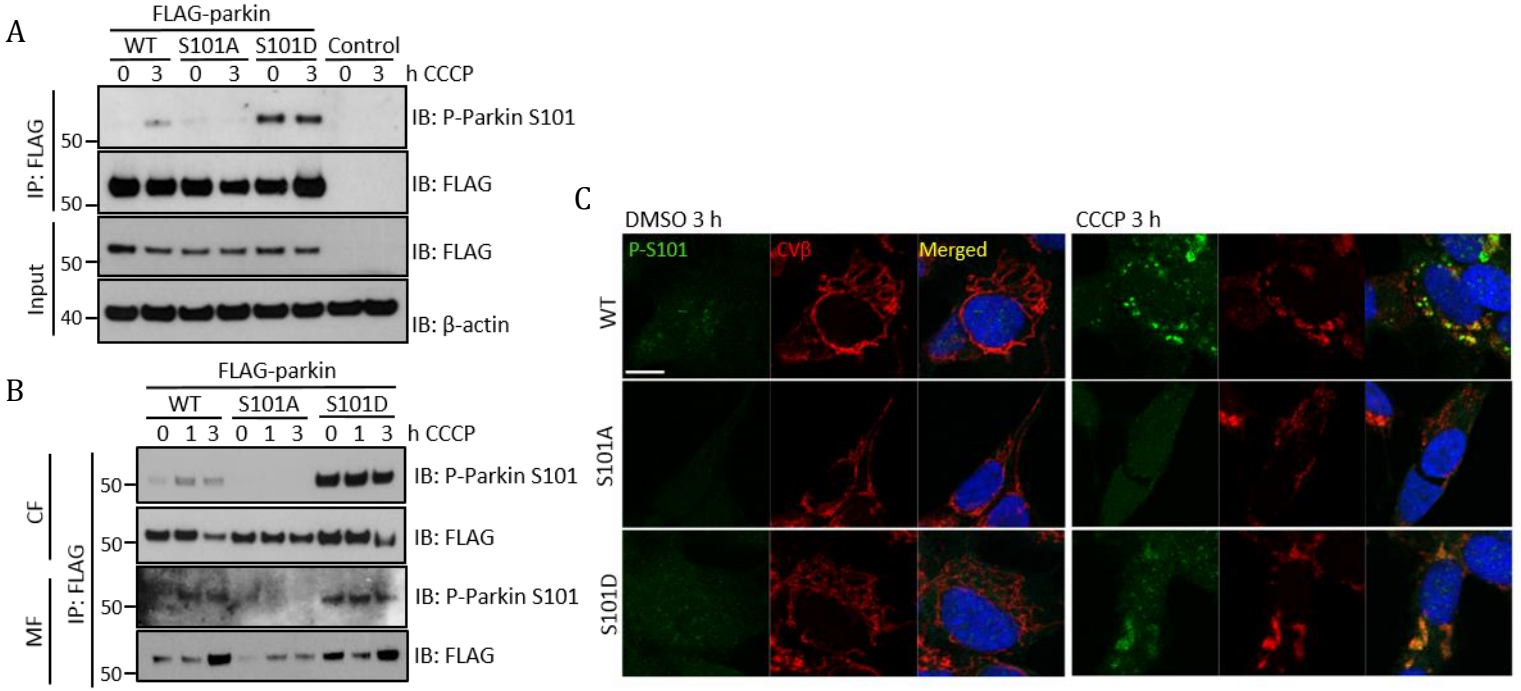

Figure 5-2 Parkin S101 phosphorylation is not detected in non-phosphorylatable mutant (S101A cells).

(A) Parkin is phosphorylated at S101 in FLAG-Parkin complexes IP from CCCP-treated (10 μM, 3 h) SH-SY5Y cells stably expressing wild-type (WT) or S101D FLAG-Parkin, but not S101A FLAG-Parkin or control. (B) Parkin is phosphorylated at S101 in FLAG-Parkin complexes IP from cytosolic fraction (CF) and mitochondria-enriched fraction (MF) of WT and S101D cells, but not S101A cells. IBs are representative of at least three independent experiments. (C) Immunofluorescence (IF) of SH-SY5Y cells stably expressing either WT, S101A or S101D FLAG-Parkin following 3 h treatment of CCCP (10 μM). Cells were immunostained for Parkin phosphorylated at S101 (P-S101), for mitochondria (Complex V β subunit, CVβ), and for nuclei (DAPI, blue). Scale bar, 10 μm.

5.2.2 S101 Phosphorylation modulates Parkin recruitment to depolarised mitochondria and affects mitochondrial perinuclear clustering

I next examined whether Parkin phosphorylation at S101 regulates its translocation to depolarised mitochondria. Over a time course of CCCP treatment, FLAG-Parkin level increased in the MF of WT and S101D cells, but to a lesser extent in the S101A cells. Parkin levels were consistently elevated in the two clonal populations of S101D cells we have generated (Figure 5-3 A and data not shown), suggesting that this mutation could impact on the protein stability. The reduction of FLAG-Parkin S101A mitochondrial recruitment was further supported by IF result. Consistently at 1 and 3 h CCCP treatment, the number of cells displaying partial and complete Parkin translocation to depolarised mitochondria was significantly reduced in S101A cells as compared to WT and S101D (Figure 5-3 B and C; see representative images of partial and complete Parkin translocation in Figure 5-3 D).

The reduction of Parkin translocation was associated with a disruption of the CCCP-induced perinuclear mitochondrial clustering in the S101A cells, as compared with the WT and S101D cells (see representative pictures in Figure 5-4 A). To evaluate the distribution of depolarised mitochondria within the cells, the fluorescence intensity peaks of FLAG-Parkin and mitochondria were analysed. These peaks overlapped around the edge of nuclei in both WT and S101D cells. However, in the S101A cells, Parkin and mitochondria fluorescence peaks showed variable degrees of overlapping and located at various distance from the edge of the nucleus, confirming that mitochondria are more scattered throughout the cytoplasm in S101A cells as compared to WT and S101D cells (Figure 5-4 B). In order to further confirm these data, the compaction index of mitochondria, as previously described by Narendra and colleagues (Narendra et al., 2010a), was calculated. In essence, for a given cellular mitochondrial network, the shorter the cumulative circumference the more compact/the less dispersed the mitochondria are (Figure 5-4 C). Consistent with above data, the compaction index of mitochondria was significantly reduced in S101A cells

(Figure 5-4 D). Altogether these data show that Parkin mitochondrial translocation and perinuclear mitochondrial clustering are decreased in S101A cells.

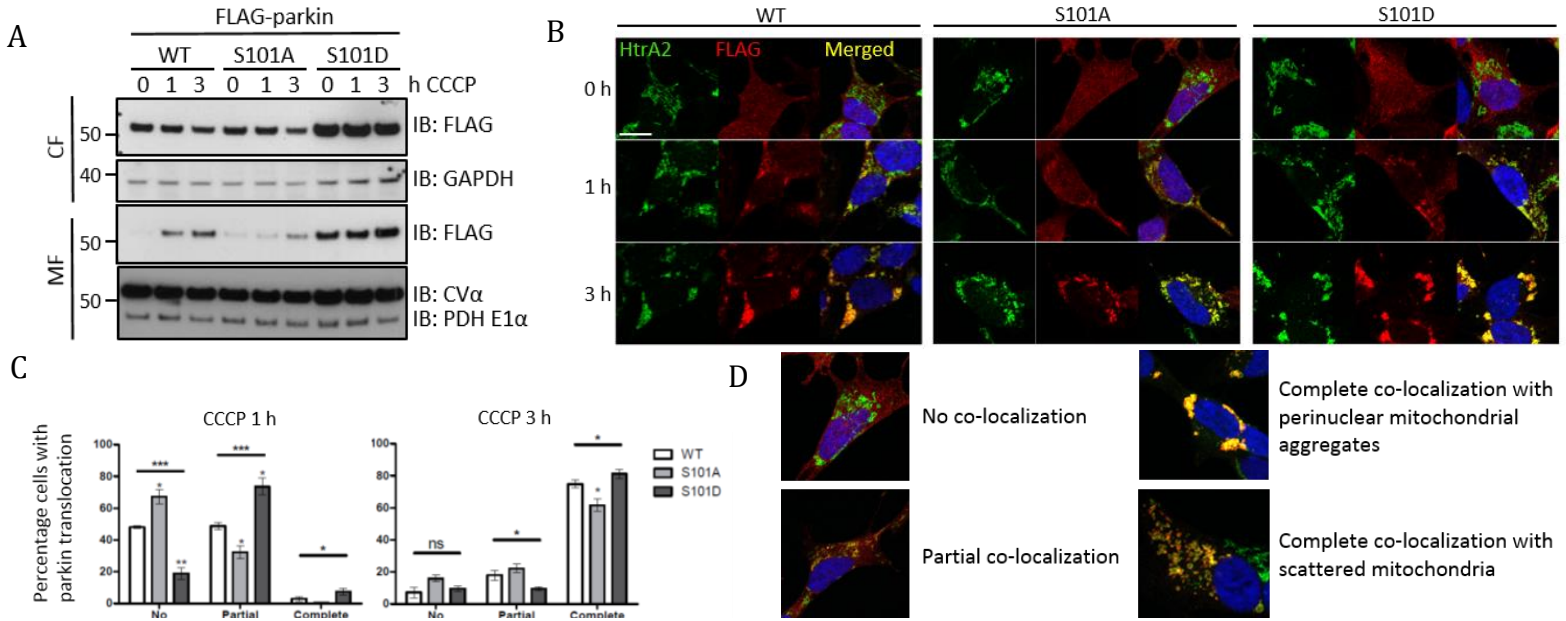

Figure 5-3 Mutation of S101 phosphorylation site alters Parkin translocation to depolarised mitochondria.

(A) Parkin translocation from the cytosolic fraction (CF) to the mitochondria-enriched fraction (MF) of S101A cells following 0, 1 or 3 h of 10 μM CCCP treatment is decreased as compared to WT and S101D cells. Complex V α subunit (CVα) and E1α subunit of pyruvate dehydrogenase (PDHE1α) are markers for mitochondria. Glyceraldehyde 3-phosphate dehydrogenase (GAPDH) is a cytosolic marker. IBs are representative of at least three independent experiments. (B) Mitochondrial translocation of FLAG-Parkin was assessed by IF in WT, S101A and S101D cells following 0, 1 or 3 h treatment with CCCP (10 μM). Nuclei were stained with DAPI (blue). Scale bar, 10μm. (C) Cells in (B) were scored for partial and complete co-localization of FLAG-Parkin with High temperature requirement protein A2 (HtrA2), a mitochondrial marker. Data are presented as mean of three experiments ± s.e.m. Significance was determined using two-tailed Student's t-test (asterisks above individual column) and one-way ANOVA with Bonferroni correction (asterisks above the bar) (* $p < 0.05$, ** $p < 0.01$, *** $p < 0.001$). (D) Representative images exhibiting the morphology of various levels of Parkin-mitochondria partial and complete co-localization following 3 h of CCCP treatment (10 μM).

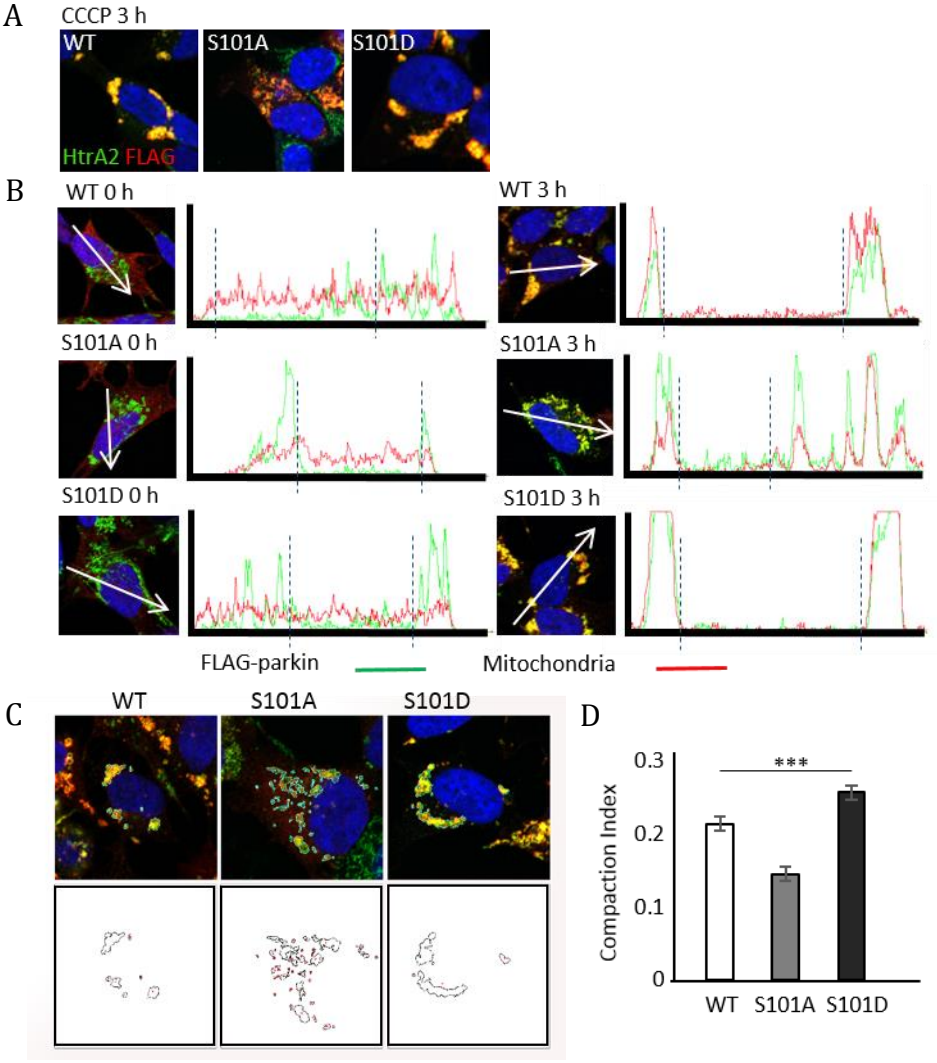

Figure 5-4 Mutation of S101 phosphorylation site alters mitochondrial perinuclear clustering.

(A) Representative IF images of FLAG-Parkin co-localization with mitochondria in WT, S101A and S101D cells following 3 h CCCP treatment (10 μM). (B) The relative intensity profiles of FLAG-Parkin (green) and mitochondria (red) fluorescence show that Parkin and mitochondria co-localize but are more scattered in S101A CCCP-treated cells (3 h, 10 μM), as compared to WT and S101D. (C) Compaction index of mitochondria was calculated by measuring mitochondrial area and perimeters within the cells after 3 h CCCP treatment. Representative drawings of mitochondrial aggregate perimeter of WT, S101A and S101D cells. (D) Data in (C) are presented as mean of three independent experiments (6 cells per experiment) ± s.e.m. Significance was determined by one-way ANOVA with Bonferroni correction (*** $p < 0.001$). N=3.

5.2.3 Parkin phosphorylation at S101 leads to conformational change

Parkin has long been regarded as a member of the RING-in-between-RING (RBR) E3 ligase family that consists of a Ubl domain, a linker, and four RING domains (Trempe et al., 2013). To gain additional structural insights, we used a full length human Parkin model (Caulfield et al., 2014) that has been built from several partial x-ray crystal structures (Riley et al., 2013; Trempe et al., 2013; Wauer and Komander, 2013). This all atom resolution model of human Parkin showed that the S101 site is buried within a cleft formed by the Ubl domain and the linker region (Figure 5-5 A). In-silico phosphorylation of S101 slightly perturbed the α-helix from residues 100-110 and resulted in a reorganization of the surrounding pocket to accommodate the interfacing residues nearby pS101 (Figure 5-5 B). Subsequent molecular dynamics simulations (MDS) revealed a hinge-like movement at residues 110-114 that allowed the α-helix containing S101 to move away from the Ubl domain over time (Figure 5-5 C and D). Of note, an adjusted orientation (Figure 5-5 E—H) revealed this movement also increased the distance between the REP (repressor element of Parkin) region and RING1, particularly at longer times of MDS (compare Figure 5-5 G and Figure 5-5 H). In the auto-inhibited state of Parkin, the REP region blocks the putative E2 ubiquitin conjugating enzyme binding site in RING1 (Trempe et al., 2013; Wauer and Komander, 2013). The noticeable increase in the distance between both domains upon phosphorylation of S101 would better allow for the accommodation of an E2 enzyme during activation of Parkin's E3 ubiquitin ligase functions.

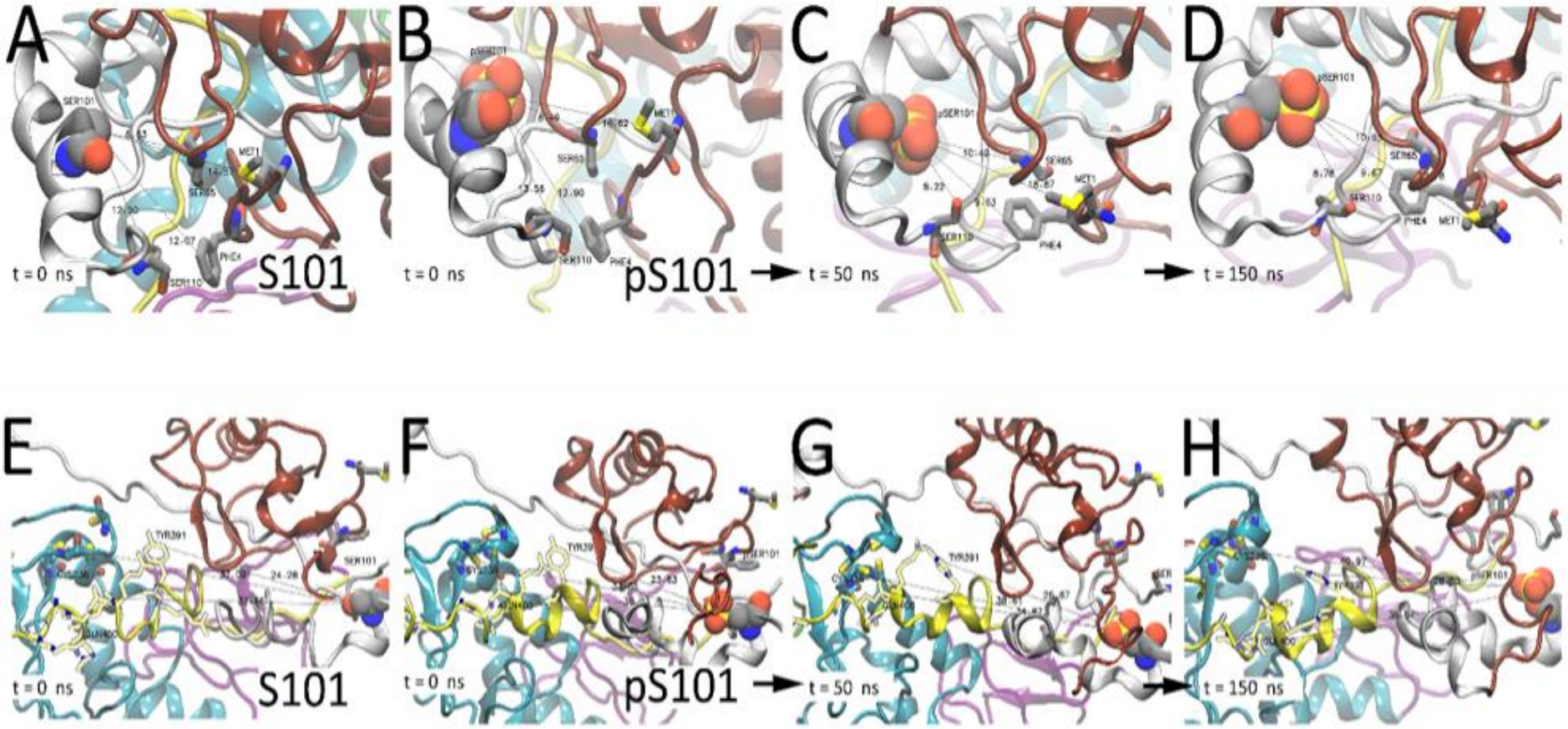
A
B
C
D
t = 0 ns
S101
t = 0 ns
pS101
t = 50 ns
t = 150 ns
E
F
G
H
t = 0 ns
S101
t = 0 ns
pS101
t = 50 ns
t = 150 ns

Figure 5-5 Effect of S101 phosphorylation on a structural model of human full-length Parkin.

Carbon, nitrogen, oxygen, and sulfur are coloured grey, blue, red and yellow, respectively. Domain structures are rendered in ribbon with colour by domain: Ubl is red, linker is white, RING0 is green, RING1 is cyan, IBR is purple, REP is yellow, and RING2 is pink. (A) Model for human Parkin with S101 is shown. S101 is rendered in Van der Waals (VdW) for emphasis. Methionine 1 (Met1), phenylalanine 4 (Phe4), serine 65 (Ser65), serine 110 (Ser110) are shown in licorice style. Distances are given in Å (ångström) between key residue pS101 sulfur to: Met1 sulfur, Phe4 carbon, Ser65 backbone, and Ser110 oxygen. (B—D) Model for human Parkin with pS101 modification is shown. Key residues are indicated as in panel (A) and with distances labelled. (B) Time equals zero, (C) 50 ns or (D) 150 ns of molecular dynamics simulation. (E) Model for human Parkin with S101 is shown. The orientation is rotated 90° in both X-/Y-plane allowing a view of the inhibitory REP region that blocks the E2 binding site in RING1. Cysteine 238 (Cys238), tyrosine 391 (Tyr391), and Glutamine 400 (Gln400) are shown in licorice style. Distances are given in Å between key residue pSer101 sulfur to: Cys328 sulfur, Tyr391 carbon, and Gln400 nitrogen. (F—H) Model for human Parkin with pS101 modification is shown. Key residues are indicated as in panel A and with distances labelled. (F) Time equals zero, (G) 50 ns or (H) 150 ns of molecular dynamics simulation. Experiment performed by Wolfdieter Spinger.

5.2.4 Parkin Phosphorylation S101 regulates ubiquitination of OMM proteins

We next assessed whether phosphorylation at S101 is important for ubiquitination of Parkin itself and OMM proteins. Self-ubiquitination of WT, S101A and S101D Parkin after CCCP treatment was assessed by FLAG-IP and subsequent immunoblotting. Total (mono/poly-) ubiquitinated Parkin in response to CCCP treatment was decreased in S101A cells compared to WT and S101D (Figure 5-6 A). Mitofusin1 (Mfn1) and mitofusin2 (Mfn2) have previously been shown to be target substrates of Parkin, and they are rapidly degraded following mitochondrial depolarisation (Chan et al., 2011; Gegg et al., 2010; Poole et al., 2010; Rakovic et al., 2011; Sarraf et al., 2013; Tanaka, 2010; Ziviani et al., 2010). Accordingly, treatment of SH-SY5Y cells with CCCP resulted in ubiquitination and degradation of mitofusins. Relative ubiquitination (Figure 5-6 B—D) and subsequent degradation (Figure 5-6 B, E and F) of Mfn1 and Mfn2 were significantly decreased in MF of S101A cells, compared to WT and S101D. Similarly, ubiquitination of Miro1, another Parkin substrate (Birsa et al., 2014; Geisler et al., 2010; Sarraf et al., 2013; Yoshii et al., 2011), was decreased in S101A cells, as compared to WT and S101D (Figure 5-7 A). Furthermore, Miro1 degradation was significantly reduced in S101A cells, as compared to WT and S101D (Figure 5-7 A and B).

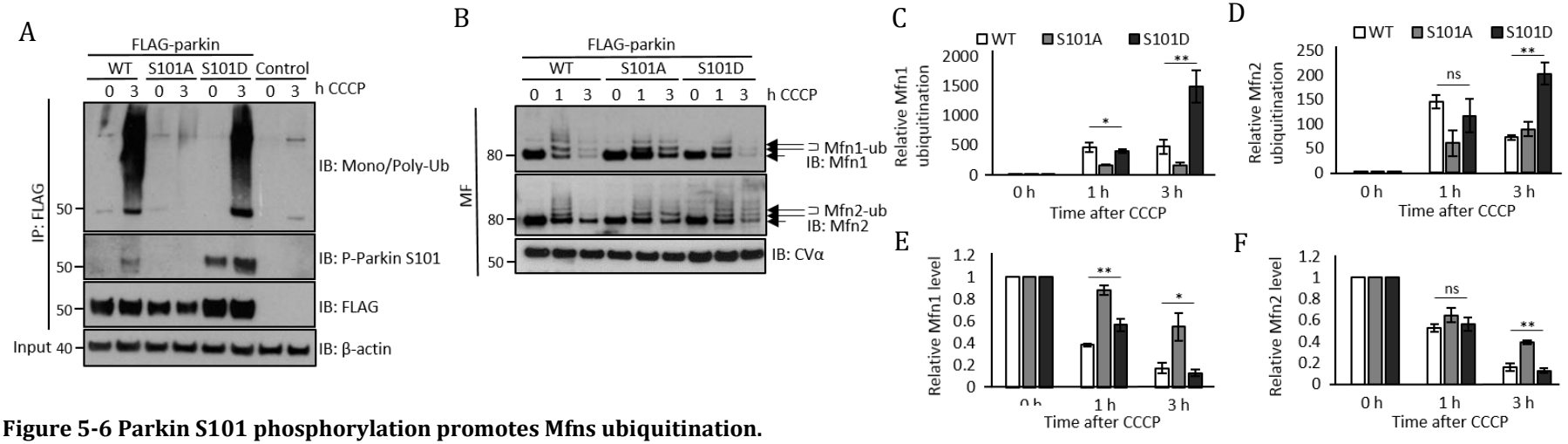

Figure 5-6 Parkin S101 phosphorylation promotes Mfns ubiquitination.

(A) Mono/poly- ubiquitination in FLAG-Parkin complexes immunoprecipitated (IP) from SH-SY5Y cells stably expressing S101A FLAG-Parkin (S101A cells) following 0 or 3 h CCCP treatment (10 μM) is considerably decreased, as compared to WT and S101D cells. IB, immunoblot. (B) Ubiquitination and degradation of Mitofusin (Mfn) 1 and 2 following 1 or 3 h of CCCP treatment (10 μM) are reduced in the mitochondria-enriched fractions (MF) of S101A cells compared to WT and S101D. Short and long arrows indicate non-ubiquitinated and ubiquitinated proteins, respectively. CVα is a marker for mitochondria. (C—F) Histograms show mean ± s.e.m. of densitometry analysis of relative Mfn1 (C) and Mfn2 (D) ubiquitination and relative Mfn1 (E) and Mfn2 (F). For relative ubiquitination, Mfn1 or Mfn2 ubiquitination bands of immunoblots in (B) were normalized to Mfn1 or Mfn2 levels. For each experiment results were then normalized to the 0 h CCCP response in WT cells. For relative Mfn1 and Mfn2 levels, data were normalized to CVα. For each experiment results were then normalized to the 0 h CCCP response in WT cells. Significance was determined by one-way ANOVA with Bonferroni correction (ns indicates not significant, * $p<0.05$, ** $p<0.01$). N=3.

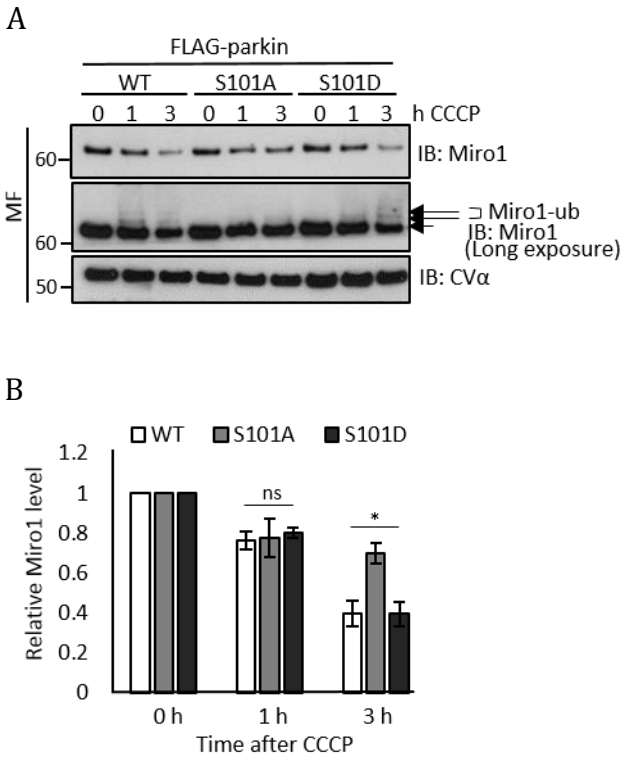

Figure 5-7 Parkin S101 phosphorylation promotes Miro1 ubiquitination.

(A) Ubiquitination and degradation of Miro1 following 0, 1 or 3 h of CCCP treatment (10 μM) in the mitochondria-enriched fractions (MF) of WT, S101A and S101D cells. Short and long arrows indicate non-ubiquitinated and ubiquitinated proteins, respectively. CVα is a marker for mitochondria. Immunoblot, IB. (B) Histogram shows mean of three independent experiments ± s.e.m. of densitometry analysis of Miro1 levels in immunoblots in (A). Data were normalized to CVα as a loading control then compared to the 0 h CCCP response in WT cells. Significance was determined by one-way ANOVA with Bonferroni correction (ns indicates not significant, * p<0.05). N=3.

5.2.5 Both K48- and K63- linked ubiquitinations were regulated by Parkin Phosphorylation S101

Previous reports have shown that Parkin recruitment to depolarised mitochondria leads to widespread K48- and K63-linked ubiquitination of the OMM (Chan et al., 2011; Sarraf et al., 2013). Therefore mono/poly-, K48- and K63-linked ubiquitination of mitochondria in WT, S101A and S101D SH-SY5Y cells was assessed by IF. Without CCCP treatment, the antibodies for mono/poly-, K48- and K63-linked chains displayed a diffuse cytosolic staining in WT, S101A and S101D cells (Figure 5-8 A—C, CCCP 0 h). In line with previous report (Okatsu et al., 2010), mono/poly-, K48- and K63- linked ubiquitination punctae staining co-localized with mitochondria in all cell lines following CCCP-induced depolarisation (Figure 5-8 A—C, CCCP 1 h;Fiugre 5-9, CCCP 3 h). However, mono/poly-, K48-linked and K63-linked ubiquitination of mitochondria were significantly reduced in S101A cells compared to WT and S101D (Figure 5-10 A—C; Figure 5-10 D—F). These experiments confirm that Parkin is important for both K48- and K63-linked ubiquitination of depolarised mitochondria following CCCP treatment. Yet in this project, K63-ubiquitination of mitochondria was more prominent than K48-ubiquitination upon CCCP-induced mitochondrial depolarisation (Figure 5-11 A—C), as shown per percentage of cells with complete mitochondrial ubiquitination.

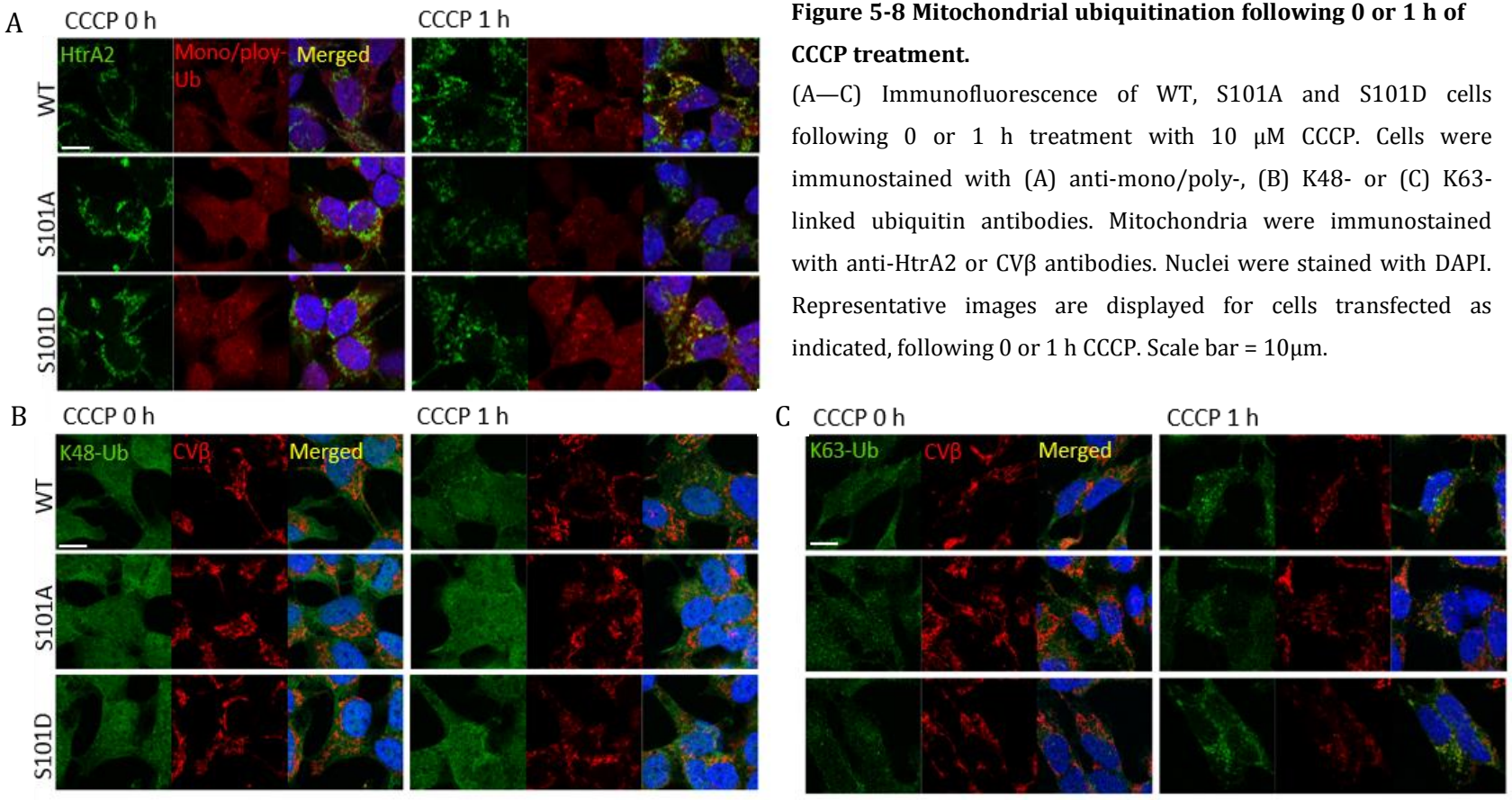

Figure 5-8 Mitochondrial ubiquitination following 0 or 1 h of CCCP treatment.

(A—C) Immunofluorescence of WT, S101A and S101D cells following 0 or 1 h treatment with 10 μM CCCP. Cells were immunostained with (A) anti-mono/poly-, (B) K48- or (C) K63-linked ubiquitin antibodies. Mitochondria were immunostained with anti-HtrA2 or CVβ antibodies. Nuclei were stained with DAPI. Representative images are displayed for cells transfected as indicated, following 0 or 1 h CCCP. Scale bar = 10μm.

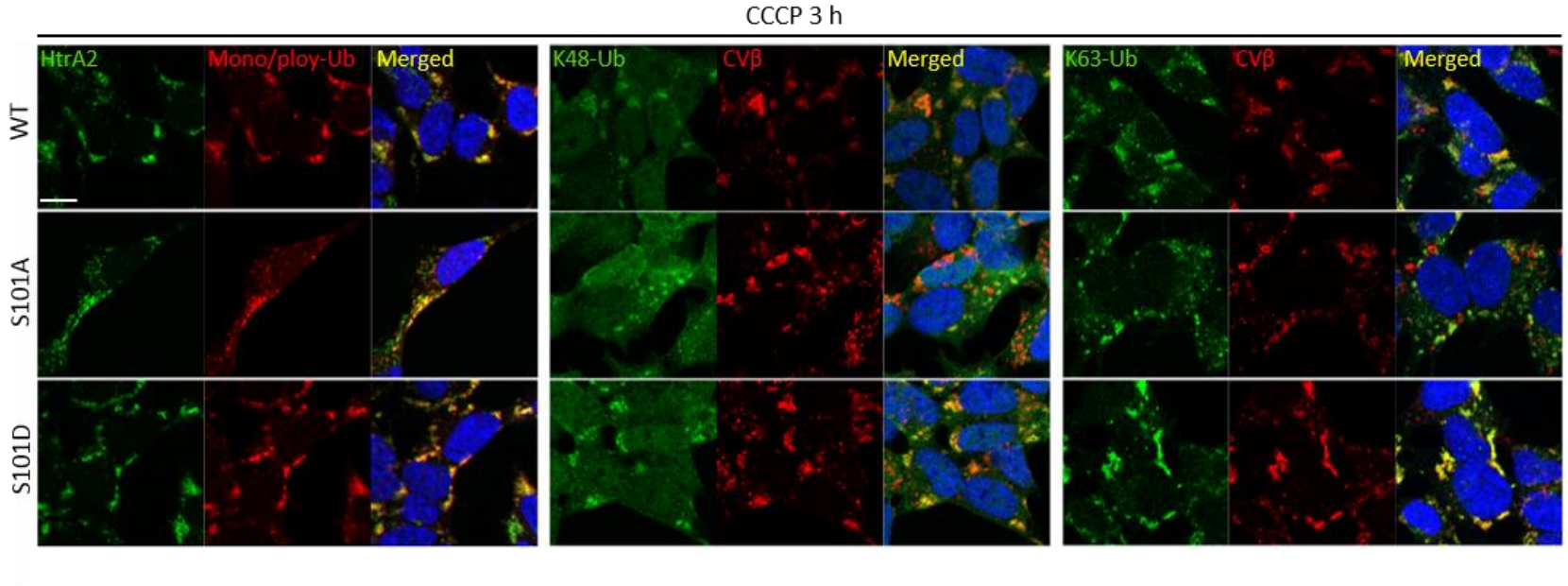

Figure 5-9 Mitochondrial ubiquitination following 3 h of CCCP treatment.

Mono/poly-, K48- and K63- ubiquitination of mitochondria, assessed by immunofluorescence (IF), is decreased in SH-SY5Y cells stably expressing S101A FLAG-Parkin (S101A cells) following 3 h CCCP treatment (10 μM), as compared to WT and S101D cells. Nuclei were stained with DAPI (blue). Scale bar, 10μm

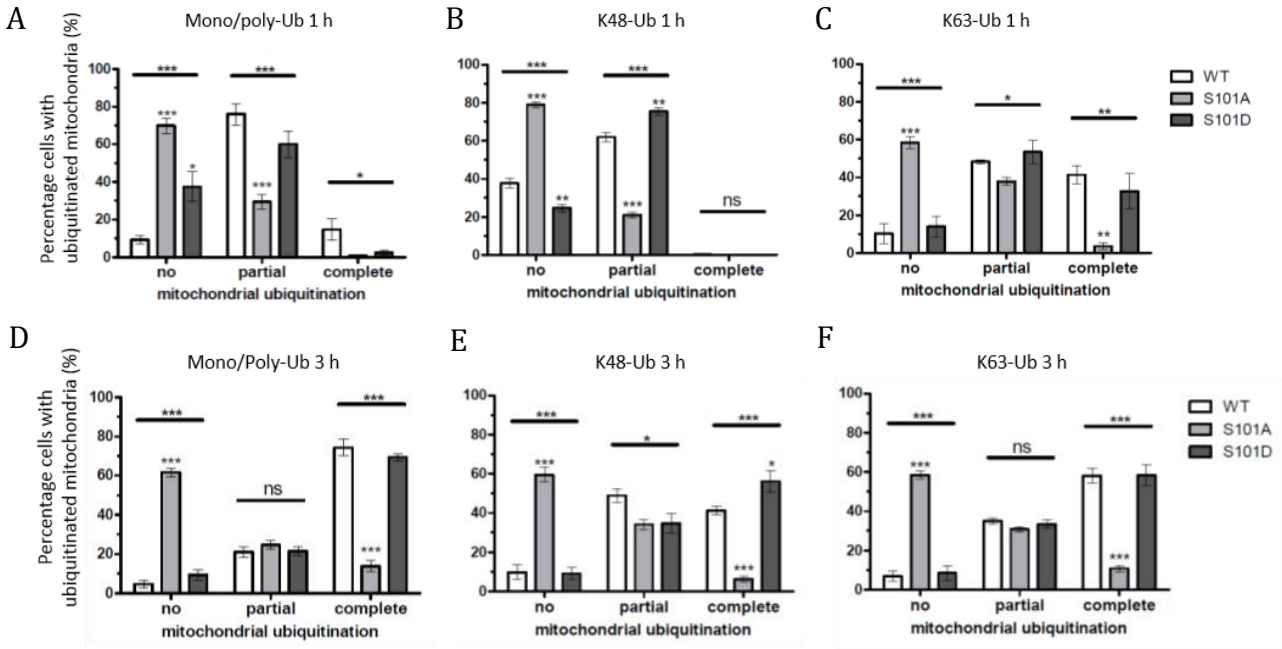

Figure 5-10 Parkin S101 phosphorylation promotes mitochondrial ubiquitination.

(A-C) Cells in Fig. 5-8 were scored for partial and complete co-localization of mono/poly-, K48- and K63- ubiquitination with HtrA2 or CVβ, two mitochondrial markers after 1 h of CCCP treatment (10 μM). Data are presented as mean of four independent experiments ± s.e.m. Significance was determined using two-tailed Student's *t*-test (asterisks above individual column) and one-way ANOVA with Bonferroni correction (asterisks above the bar) (* $p<0.05$, ** $p<0.01$, *** $p<0.001$). (D-F). Cells in Fig. 5-9 were scored for partial and complete co-localization of mono/poly-, K48- and K63- ubiquitination with HtrA2 or CVβ, two mitochondrial markers after 3 h of CCCP treatment. Data are presented as mean of four independent experiments ± s.e.m. Significance was determined using two-tailed Student's *t*-test (asterisks above individual column) and one-way ANOVA with Bonferroni correction (asterisks above the bar) (* $p<0.05$, *** $p<0.001$). N=3

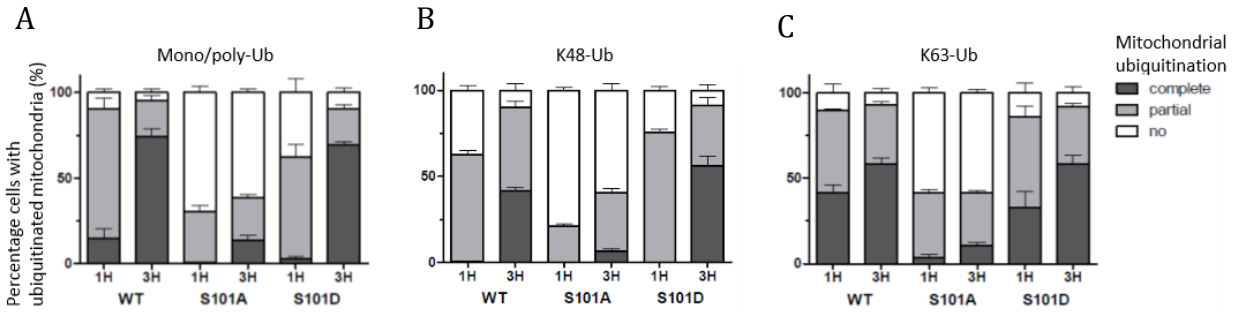

Figure 5-11 Parkin S101 phosphorylation promotes more K63- than K48-linked mitochondrial ubiquitination and S101A reduces both.

Histograms summarise mitochondrial ubiquitination results of 1 h (Fig. 5-10 A—C) and 3 h (Fig. 5-10 D—F) CCCP. Each column represents percentages of cells with no, partial or complete mitochondrial ubiquitination in each cell line at time point as indicated.

5.2.6 Parkin Phosphorylation at S101 modulates p62 recruitment to mitochondria and mitophagy

K63-linked ubiquitinated OMM substrates have been previously shown to recruit the autophagy adaptor p62 which in turn recruits autophagosomes, thus promoting lysosomal-mediated degradation of damaged mitochondria (Geisler et al., 2010; Lee et al., 2010b; Tanaka et al., 2010). In this project, the p62 recruitment to damaged mitochondria following 6 h CCCP treatment was considerably reduced in S101A cells, and significantly increased in S101D cells, as compared to WT cells (Figure 5-12 A and B). Finally to specifically investigate mitochondrial clearance (mitophagy), the proportion of FLAG-Parkin overexpressing SH-SY5Y cells with no remaining mitochondria after 24 h CCCP treatment was measured. In line with the p62 data, the percentage of cells containing no remaining mitochondria following CCCP treatment were significantly lower in S101A and higher in S101D cells, as compared to WT cells (Figure 5-13 A and B). Taken together, these data suggest that Parkin phosphorylation at S101 mediates p62 recruitment to depolarised mitochondria, and subsequent mitophagy.

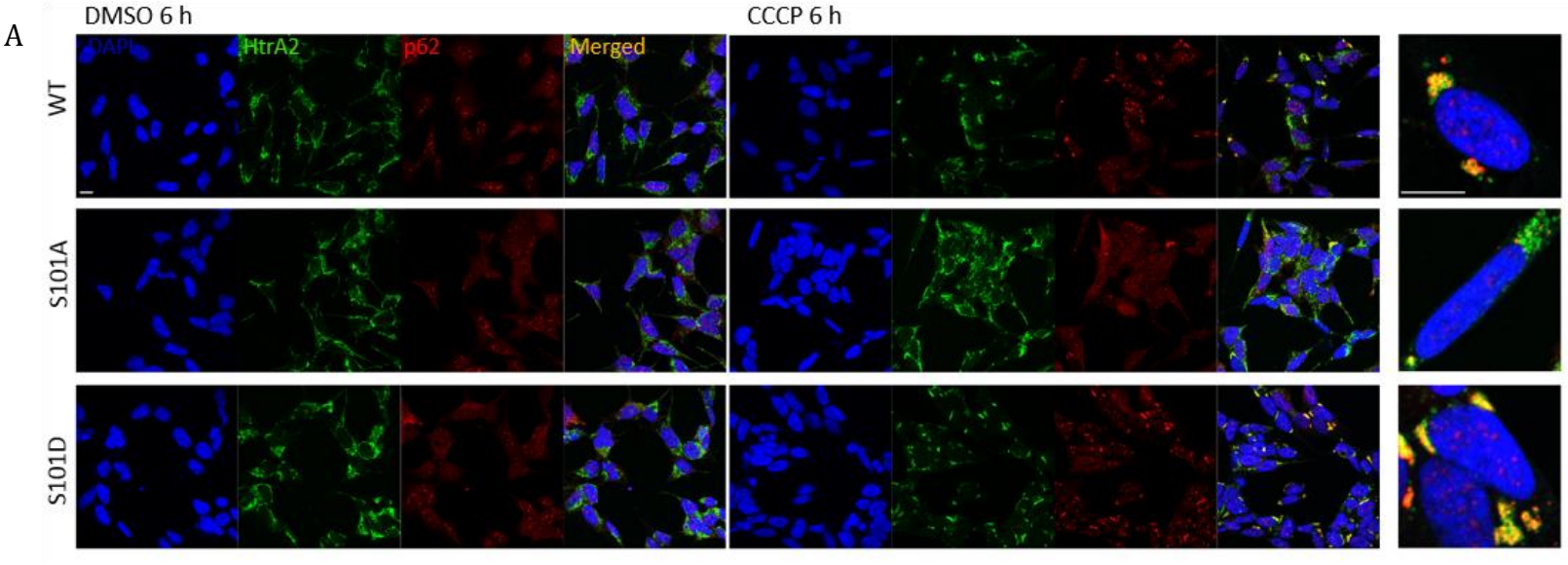

Figure 5-12 Parkin S101 phosphorylation modulates p62 recruitment to depolarised mitochondria.

(A) Mitochondrial translocation of p62 was assessed by immunofluorescence (IF) in WT, S101A and S101D cells following 6 h treatment with CCCP (10 μM). Cells were scored for co-localization of p62 with HtrA2, a mitochondrial marker. On the right hand side, representative images of magnified cells showing p62 recruitment to mitochondria. Nuclei were stained with DAPI (blue). Scale bar, 10μm. (B) Histogram shows the percentage of cells in which p62 co-localised to mitochondria. Data are presented as mean of three experiments ± s.e.m. Significance was determined by one-way ANOVA with Bonferroni correction (*** $p< 0.001$). N=3.

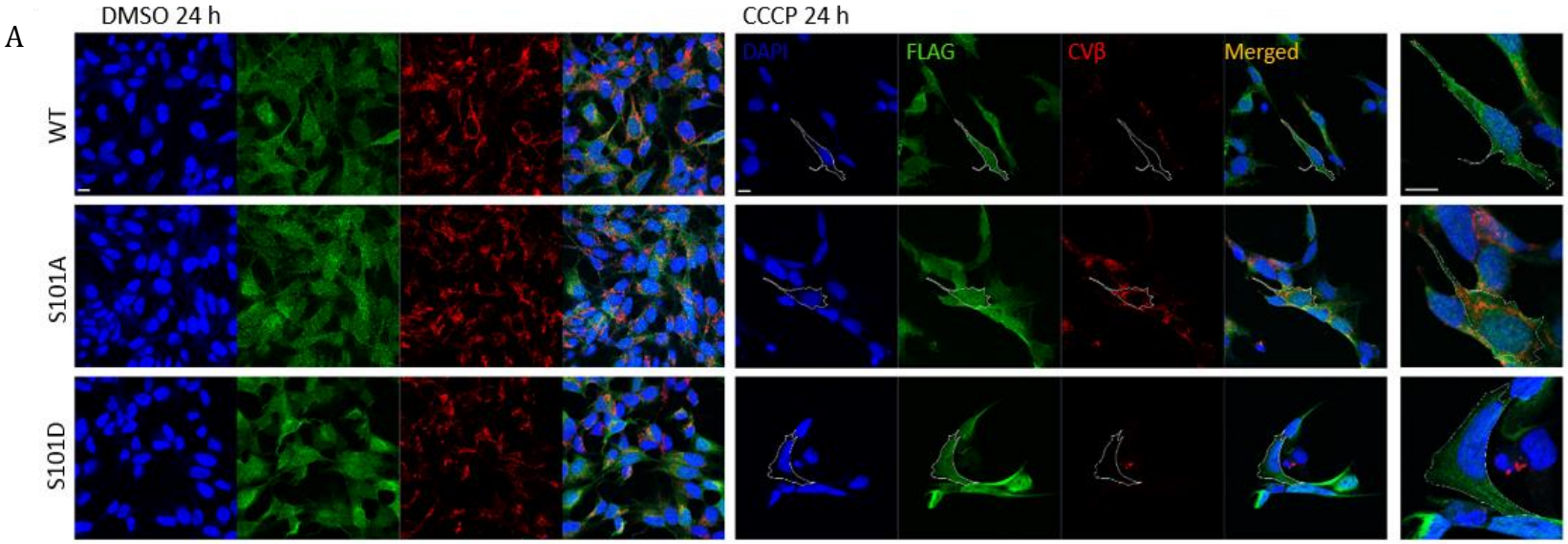

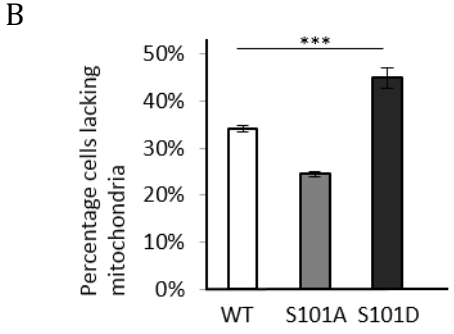

Figure 5-13 Parkin S101 phosphorylation is important for mitophagy.

(A) Mitophagy was analysed by IF in WT, S101A and S101D cells. On the right hand side, representative images of magnified cells undergoing mitophagy. CVβ was used as a mitochondrial marker. Nuclei were stained with DAPI (blue). Scale bar, 10μm. (D) Histogram indicates the percentage of cells with no remaining mitochondria following 24 h treatment with 10 μM CCCP. Data are presented as mean of three independent experiments ± s.e.m. Significance was determined by one-way ANOVA with Bonferroni correction (*** $p< 0.001$). N=3.

5.2.7 Phosphorylation at Parkin S101 is still detected in S65A mutant upon mitochondrial depolarisation

During my work on Parkin S101 phosphorylation, it was shown that S101 is located in the same cleft formed by the Ubl domain and the linker region as another reported Parkin phosphorylation site, S65 (Kondapalli et al., 2012; Shiba-Fukushima et al., 2012). MDS suggested that phosphorylation of either S65 or S101 would open this cleft to unfold Parkin (Caulfield et al., 2014). SH-SY5Y stably expressing FLAG-Parkin S65A (hereafter referred to as S65A cells) and S65A/S101A (hereafter referred to as S65A/S101A cells) were generated. The WT, S65A, S101A, and S65A/S101A cells were treated with CCCP. Phosphorylation of Parkin at S101 was detected in WT and S65A cells but not in S101A and S65A/S101A cells (Figure 5-14). These data further confirm the specificity of P-Parkin S101 antibody as it does not recognise the S65 site.

Figure 5-14 Parkin S101 phosphorylation can be detected inS65A cells.
Parkin is phosphorylated at S101 in FLAG-Parkin complexes IP from CCCP-treated (10 μM, 3 h) SH-SY5Y cells stably expressing WT or S65A FLAG-Parkin, but not S101A or S65A/S101A FLAG-Parkin.

5.2.8 Phosphorylation at Parkin S65 has only little additive effect on pS101 in regulating mitophagy process

To further investigate whether phosphorylation at these two sites had an additive effect on mitophagy process, Parkin mitochondrial translocation and mitophagy were assessed by IF. The FLAG-Parkin WT, S65A, S101A, and S65A/S101A cells were seeded on coverslips prior to CCCP treatment. The preliminary result for Parkin translocation following 3 h CCCP treatment revealed that the number of cells displaying partial and complete Parkin translocation to depolarised mitochondria was reduced in S101A and S65A/S101A cells to a similar extent (Figure 5-15 A). This result suggests that S65A has no additive effect on S101A.

Regulation of mitophagy following phosphorylation of these two sites were further assessed by treating the aforementioned cells with CCCP for 24 h. Similar to the result in 5.2.2, the percentage of cells containing no remaining mitochondria following CCCP treatment was significantly lower in S101A as compared to WT cells (Figure 5-15 B). Likewise, both S65A and S65A/S101A cells demonstrated significantly lower mitophagy as compared to WT cells. This suggests that these two serine sites are important for mitophagy, and S65A has a small additive effect on S101A.

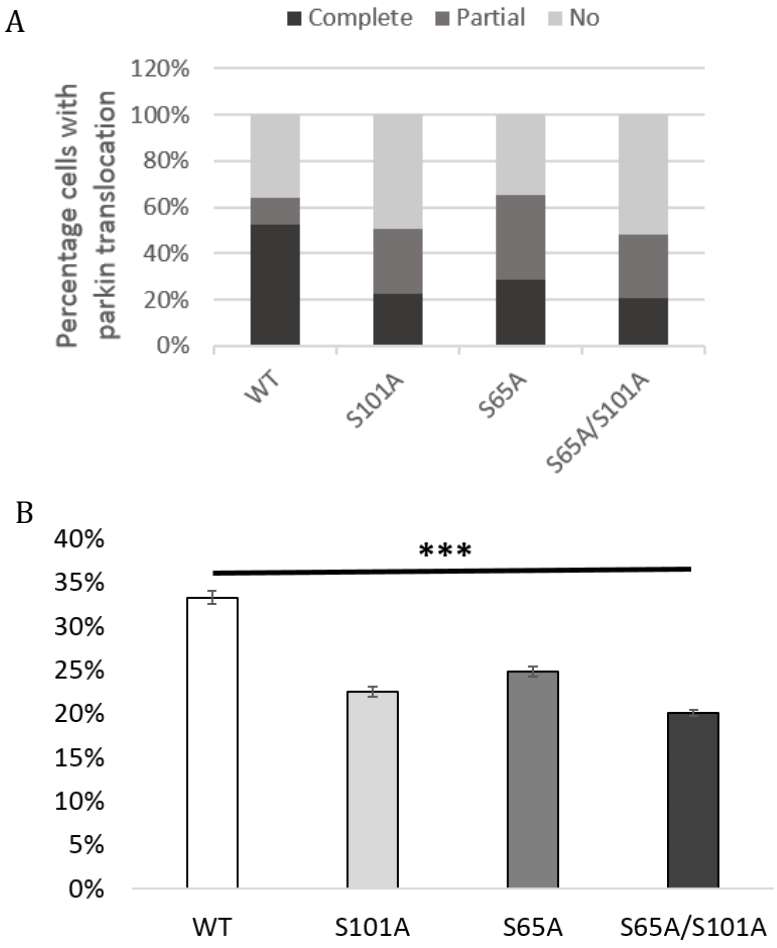

Figure 5-15 Parkin S101 and S65 phosphorylation are both important in modulating mitophagy process.

(A) Parkin translocation in SH-SY5Y cells transiently expressing WT, S101A, S65A and S65A/S101A FLAG-Parkin following 3 h of CCCP treatment was assessed by immunofluorescence (IF) (image not shown). Histogram shows the preliminary data of percentage of cells in which Parkin co-localised to mitochondria. (B) Mitophagy in abovementioned cells following 24 h of CCCP treatment was analysed by IF (image not shown). Histogram shows data presented as mean of three independent experiments ± s.e.m. Significance was determined by one-way ANOVA with Bonferroni correction (*** $p < 0.001$). N=3.

5.3 Discussion

In the last few years, mounting evidence has shown that PINK1 and Parkin, two proteins associated with autosomal recessive PD, act together to regulate mitophagy. Yet, a number of steps in this process remain poorly characterised. One important question is how Parkin mediates mitophagy? In this study I show that phosphorylation of Parkin at S101 can modulate Parkin recruitment to mitochondria, ubiquitination of OMM proteins, p62 recruitment and subsequent mitophagy.

5.3.1 Parkin phosphorylation at S101 modulates its translocation to depolarised mitochondria

Translocation of the non-phosphorylatable mutant S101A to depolarised mitochondria is decreased as opposed to abolished, suggesting that phosphorylation at S101 is important, but not indispensable, for Parkin translocation. Recently Parkin was shown to be activated by PINK1-dependent phosphorylation at S65 (Kondapalli et al., 2012; Shiba-Fukushima et al., 2012). Translocation of S65A Parkin to trifluoro carbonyl cyanide phenylhydrazone (FCCP)-induced depolarised mitochondria was delayed (Birsa et al., 2014), which is recapitulated in the S101A mutant. Both S101 and S65 phosphorylation sites locate within the same cleft formed by the Ubl and the linker domain of Parkin. Their close spatial relationship, together with our biochemistry data, suggests that Parkin may need to be phosphorylated at both sites in order to facilitate its mitochondrial translocation. We have assessed Parkin phosphorylation at S131 and S378 following CCCP treatment, however these sites appeared to be constitutively phosphorylated.

5.3.2 Parkin phosphorylation at S101 increases its E3 ligase activity

Previous studies have shown that *in vitro* phosphorylation of recombinant Parkin at S101 by casein kinase 1 (CK1) either reduces (Yamamoto et al., 2005) or has no significant effect (Rubio de la Torre et al., 2009) on Parkin's E3 ligase activity. In these experiments basal levels of Parkin auto-ubiquitination were

measured following inhibition of phosphoprotein phosphatase 1, 2A and 2B by okadaic acid using an *in vitro* auto-ubiquitination assay. Whilst these studies were performed *in vitro* using recombinant Parkin, our study measures CCCP-induced ubiquitination of Parkin and OMM proteins in SH-SY5Y cells. Our data strongly suggest that Parkin phosphorylation at S101 is associated with increased, rather than decreased, E3 ligase activity. The diversity in experimental models and conditions is likely to explain the discrepancies between the different studies. It remains to be clarified whether CK1 is the genuine kinase responsible for the phosphorylation of S101 in our model. Aside from S101, previous reports have suggested that phosphorylation at other sites, including S131 or Y143, could reduce Parkin's E3 ligase activity (Imam et al., 2011; Ko et al., 2010; Yamamoto et al., 2005). Conversely, Parkin phosphorylation at S65 (or its *Drosophila* Parkin analogue S94) or T175 by PINK1 has been shown to either increase Parkin's E3 ligase activity (S65 or *Drosophila* Parkin S94) or rescue the mitochondrial morphology in parkin-null *Drosophila* model (T175) (Birsa et al., 2014; Kazlauskaite et al., 2014; Kim et al., 2008; Kondapalli et al., 2012; Sha et al., 2010; Shiba-Fukushima et al., 2012; Shiba-Fukushima et al., 2014). All together these reports suggest that Parkin phosphorylation at various sites across the protein is important for modulating, either positively or negatively, its E3 ligase activity.

5.3.3 Parkin S101 phosphorylation results in conformational change of Parkin and enhances Parkin's E3 ligase activity

Recently, several studies have suggested a model in which Parkin may use a two-step mechanism to ligate ubiquitin to target proteins (Smit et al., 2012; Stieglitz et al., 2012; Wenzel et al., 2011; Winklhofer, 2014). This model suggests ubiquitin would first be transferred from an E2 conjugating enzyme to an acceptor cysteine on Parkin, most likely to be C431, thus forming a thioester bond in a similar mechanism used by HECT type E3 ligases. This ubiquitin would then be transferred to Parkin's substrate by forming an isopeptide bond, in a similar mechanism used by other RING E3 ubiquitin ligases (Lazarou et al., 2013; Riley et al., 2013; Wenzel et al., 2011). The mechanism by which Parkin

accomplishes this RING/HECT hybrid reaction remains yet to be described (Trempe et al., 2013; Wauer and Komander, 2013). However, X-ray crystallography has recently shed light on our understanding of how Parkin's biological function is determined by its structure. These studies modelled a low resolution structure of full-length rat Parkin (Trempe et al., 2013) and a higher resolution structure of RING0-RBR domains of human Parkin (Wauer and Komander, 2013; Wenzel et al., 2011). These studies suggest that the RING0:RING2 interaction buries the catalytic C431, and that the short linker (REP) between IBR and RING2 blocks the E2 binding site (beside Ubl binding site) on RING1 (Trempe et al., 2013; Wauer and Komander, 2013), keeping Parkin in an autoinhibited conformation. Of note, the linker domain, where S101 is located, is not visible in the model of full-length rat Parkin (Trempe et al., 2013). Our modelling, focusing on the linker domain, suggests that phosphorylation at S101 may induce a conformational change in Parkin structure that increases the accessibility of E2 enzyme binding site, thus enhancing its E3 ligase activity.

5.3.4 Phosphorylated Parkin ubiquitinates OMM proteins and facilitate their degradation

A number of studies, including ours, show that the ubiquitination of OMM proteins (e.g. mitofusins and Miro1) following mitochondrial depolarisation (Birsa et al., 2014; Gegg et al., 2010; Poole et al., 2010; Rakovic et al., 2011; Sarraf et al., 2013; Tanaka, 2010; Ziviani et al., 2010) is an important step for the arrest of damaged mitochondria, autophagosome formation and subsequent mitophagy (Geisler et al., 2010; Lee et al., 2010b; Tanaka et al., 2010; Wang et al., 2011b). Ubiquitinated mitofusins were shown to be degraded by the proteasome in a p97/valosin containing protein (VCP)-dependent manner (Kim et al., 2013; Tanaka et al., 2010). Damaged mitochondria now lacking mitofusins are less likely to fuse with the healthy mitochondrial network, and are instead sequestered and targeted for autophagy (Pallanck, 2010; Tanaka et al., 2010). As for Miro1, the adaptor that couples mitochondria to microtubules, its ubiquitination results in the arrest of damaged mitochondria by blocking

mitochondrial trafficking (Wang et al., 2011b). Our study shows that Parkin S101 phosphorylation can influence Mfn1, Mfn2 and Miro1 ubiquitination status, thus affecting the efficiency of subsequent mitochondria clearance.

5.3.5 Parkin linked proteasomal to lysosomal degradation system in mitophagy process by mediating mitochondrial ubiquitination

Parkin is known to carryout mono-ubiquitination (Hampe et al., 2006; Matsuda et al., 2006) as well as K6-, K11-, K27-, K29-, K48-, and K63-linked poly-ubiquitination (Chan et al., 2011; Doss-Pepe et al., 2005; Durcan et al., 2012; Durcan et al., 2011; Lim et al., 2013; Lim et al., 2005; Manzanillo et al., 2013; Olzmann and Chin, 2008). Parkin-dependent K27-, K48- and K63-ubiquitination of depolarised mitochondria supports a role for both proteasomal and lysosomal degradations of damaged mitochondria during the mitophagy process (Birsa et al., 2014; Chan et al., 2011; Geisler et al., 2010; Lazarou et al., 2013). Our study confirms that depolarised mitochondria are labelled with endogenous ubiquitin molecules in a variety of chain formations. We show that phosphorylation at S101 activates Parkin, catalysing both K48- and K63-linked ubiquitination during the mitophagy process. In line with previous reports, our data show more abundant K63-linked chains on mitochondrial substrates compared to K48-linked chains (Narendra et al., 2010a; Okatsu et al., 2010). One possible reason for this is that the K48-labeled OMM proteins are removed from mitochondria for further degradation, whilst K63-linked chains remain on mitochondria for further p62 recruitment. Overall our data show that both mono/poly-ubiquitination and K48-/K63-linked ubiquitination are significantly reduced in S101A cells, leading to reduction of OMM proteins degradation and p62 recruitment.

5.3.6 Parkin is essential in for depolarised mitochondria perinuclear clustering

Following 6 h CCCP treatment, S101A cells display a diffuse distribution of mitochondria throughout the cytoplasm, whilst depolarised mitochondria

cluster around the nucleus in WT and S101D cells. This is corroborated by a considerably smaller compaction index of mitochondria compared to the WT and S101D cells. This suggests that Parkin phosphorylation at S101 plays a role in perinuclear mitochondrial clustering. The mitochondrial network morphology in S101A cells resembles that seen in HeLa cells expressing exogenous pathogenic Parkin R275W, and in p62 KO mouse embryonic fibroblasts (MEFs) (Narendra et al., 2010a; Okatsu et al., 2010). Perinuclear mitochondrial clustering is markedly decreased in p62 KO MEFs, suggesting that p62 is required for mitochondrial positioning (Narendra et al., 2010a). In line with previous reports (Burchell et al., 2013; Geisler et al., 2010), our study shows that perinuclear mitochondrial clustering occurs before p62 recruitment, suggesting that factors other than p62 may be involved in mitochondria positioning. Phosphorylation and subsequent degradation of Miro1 were shown to be important for mitochondrial arrest and perinuclear mitochondrial clustering (Fransson et al., 2003, 2006; Liu et al., 2012; Wang et al., 2011b). Miro1 degradation is decreased in S101A cells and thus could partially explain mitochondrial mis-localisation in our model.

Mitophagy is thought to generally occur in the perinuclear (Vives-Bauza et al., 2010). However, whether perinuclear mitochondrial clustering is required for mitophagy is unclear. Although perinuclear mitochondrial clustering is impaired in p62 KO MEFs, similar levels of mitophagy are observed in these cells as compared to control (Narendra et al., 2010a). In our study, mitochondrial clustering is considerably reduced in S101A cells, however some mitophagy still remains. All together these data suggest that mitochondrial clustering is not indispensable for clearance of damaged mitochondria.

5.3.7 Parkin S101 phosphorylation modulates mitophagy

S101 and S65 are the only known sites to be phosphorylated upon CCCP-induced mitochondrial depolarisation. Our data demonstrates that converting S65 into non-phosphorylatable S65A mutant does not abolish S101 phosphorylation, suggesting S65 phosphorylation is not required for S101

phosphorylation in response to mitochondrial depolarisation. The S101 remodelling data in this project and S65 remodelling result described recently (Caulfield et al., 2014) suggest phosphorylation on either site is likely to induce similar conformational change that opens up the same cleft formed by Ubl and the linker domains. This can further explain why phosphorylation at S65 has no additive effect to S101 on Parkin translocation or only little additive effect on mitophagy. The double non-phosphorylatable mutant displays remaining Parkin activity, suggesting Parkin may be regulated by other PTMs.

5.3.8 Conclusion

In conclusion, our study suggests that Parkin phosphorylation at S101 releases the E3 ubiquitin ligase from its auto-inhibited state. We show that Parkin phosphorylation can further regulate its translocation to depolarised mitochondria, ubiquitination of OMM proteins, p62 recruitment and mitophagy. Modulating Parkin phosphorylation may open new avenues for potential therapeutics that may be beneficial for PD patients in the future.

5.3.9 Future perspectives

This work represents the first evidence that Parkin S101 can be phosphorylated upon mitochondrial depolarisation in cells. However few questions remain to be answered. For instance, which kinase is responsible for this phosphorylation remains to be determined. CK1 has been shown to phosphorylate Parkin at S101 by *in vitro* kinase assay from two independent groups (Rubio de la Torre et al., 2009; Yamamoto et al., 2005). However both groups suggested Parkin S101 phosphorylation reduced its ligase activity from the results of *in vitro* autoubiquitination assay or autoubiquitination of Parkin in okadaic acid-treated cells. Of note, the phosphomimetic S101E mutant from one of these two studies also showed a marked increase in autoubiquitination, pointing out the conflicting result in the *in vitro* observation of S101 phosphorylation. Our *in vivo* system demonstrates consistent outcomes amongst all readouts selected. Indeed, it would be ideal to further investigate whether Parkin S101 can be phosphorylated by CK1 in this *in vivo* model and what underlying molecular

pathway associates with this process. A preliminary experiment has been done and shown CCCP-induced Parkin S101 and S65 phosphorylation were both blocked by CK1δ inhibitor LH846 (Figure 5-16 A). However, further confirmation by repeating experiments with other inhibition methods, for example CK1 knockdown, is essential.

Our preliminary data show that Parkin phosphorylation at S101 is PINK1-dependent (Figure 5-16 B) (S65 is used as a positive control in the experiment). These data will need to be confirmed. To assess whether PINK1 directly phosphorylates Parkin at S101, an in vitro kinase assay will need to be done. Further dissecting the signalling pathways associated with phosphorylation of these two serine sites will be of great value to a better understanding of Parkin pathophysiology.

As described earlier, the data presented in this chapter earlier was generated using Parkin overexpressed in SH-SY5Y cells due to absence of good Parkin antibodies, making it difficult to reliably detect endogenous protein. Further studies would include the use of a human iPSC-derived neuronal model to investigate the S101 phosphorylation in a more physiological setting. A genome-editing technique can be used to customise a non-phosphorylatable mutation in the control iPSC-derived neurons (Ding et al., 2013) to create a model without the need of transfection. Investigating the potential alternation of S101 phosphorylation in Parkin iPSC-derived neurons of Parkin would further broaden the knowledge regarding how the particular Parkin mutation leads to PD.

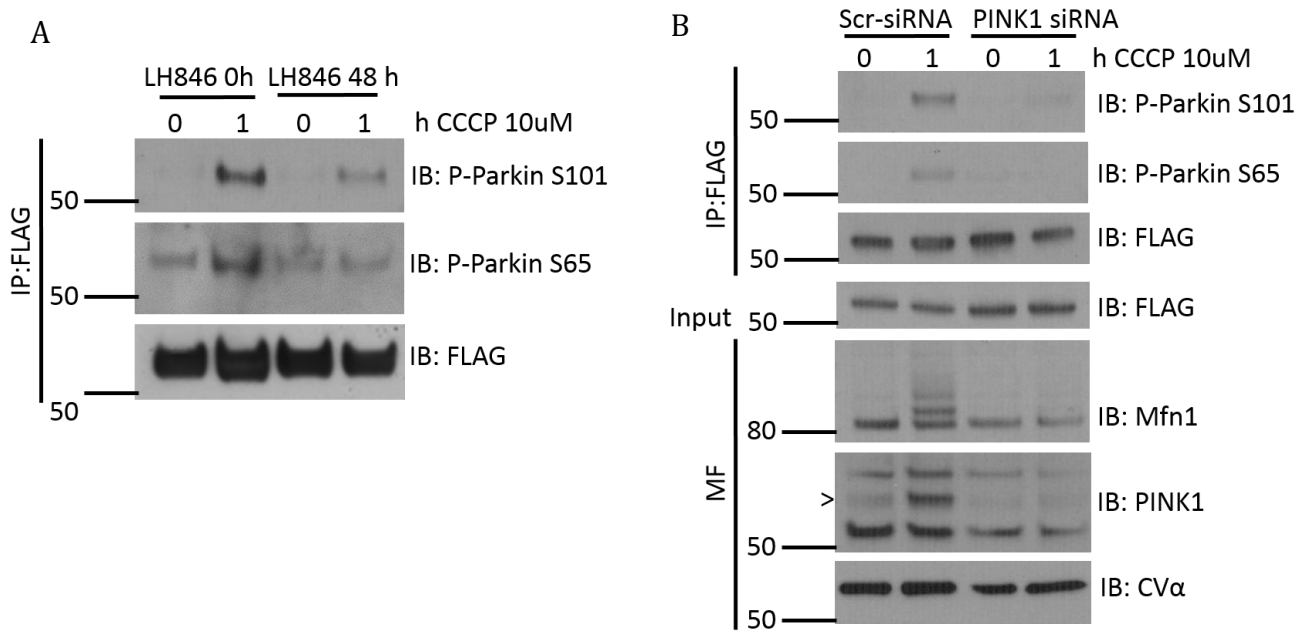

Figure 5-16 Both Parkin S101 and S65 phosphorylation upon CCCP treatment are diminished by CK1 inhibition or PINK1 knockdown.

(A) FLAG-Parkin complexes IP from SH-SY5Y cells stably expressing FLAG-Parkin following 0 or 1 h CCCP treatment (10 μM) in the presence or absence of 48 h CK1 inhibitor (LH846, 10 μM). IB, immunoblot. (B) FLAG-Parkin complexes IP, input and mitochondria-enriched fraction (MF) from SH-SY5Y cells stably expressing FLAG-Parkin, transiently expressing scrambled siRNA (Scr-siRNA) and PINK1 siRNA, followed by 0 or 1 h CCCP treatment (10 μM). > indicates full-length PINK1 at approximately 63 kDa. (Figure 5-16 (B) was provided by Dr Hélène Plun-Favreau)

193

Chapter 6 Discussion

This thesis investigated molecular mechanisms of Parkin regulation. The main conclusions from the data presented are: Firstly, Parkin is not phosphorylated upon activation of p38 or ERK1/2 MAPK signalling pathways, however Akt may have a small role in the regulation of S378 phosphorylation. Secondly, Parkin is phosphorylated at S101 and S65 upon mitochondrial depolarisation and this phosphorylation is likely to play a critical role in the regulation of the mitophagy pathway (Figure 6-1). The implications of these results have been discussed previously. This chapter seeks to address the broader implications related to this work.

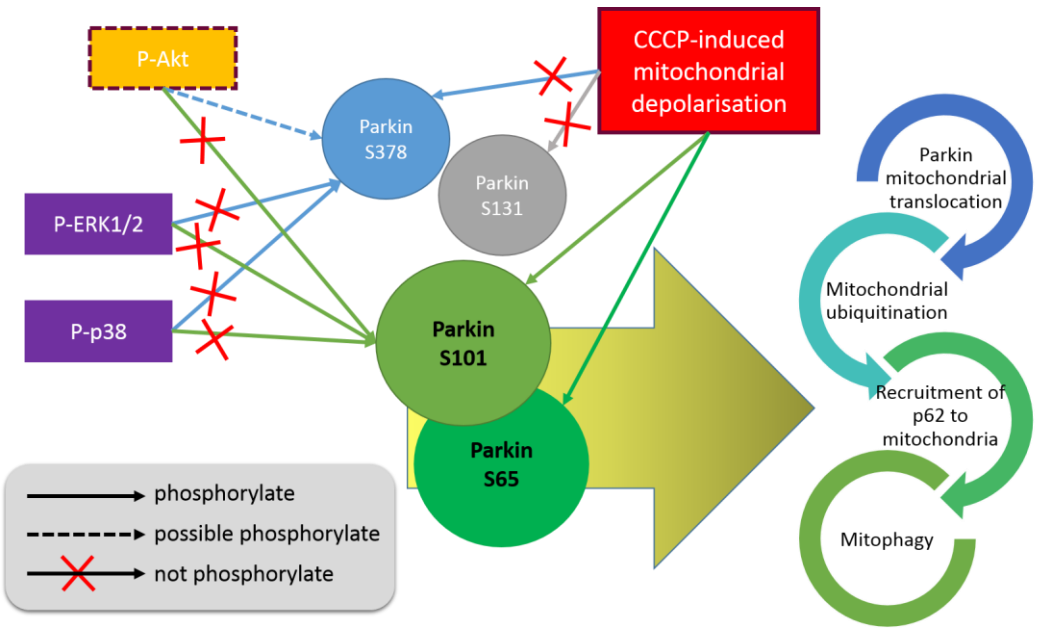

Figure 6-1 Summary of Parkin molecular pathways.

6.1 Implications of Parkin phosphorylation in the mitophagy pathway

Three mitophagy pathways have been described in mammalian cells (Ashrafi and Schwarz, 2013). Two of them occur in physiological conditions and involve the removal of all mitochondria in developing reticulocytes and sperm-derived mitochondria from fertilised oocytes (Figure 6-2). To date, the only known selective removal of damaged mitochondria in mammalian cells remains the PINK1/Parkin-regulated mitophagy pathway (Narendra et al., 2008; Poole et al., 2008). Several studies have shown Parkin activation is an essential step in the mitophagy process. it was recently shown that PINK1 phosphorylates Parkin at S65 to enhance Parkin mitochondrial translocation and its E3 ligase activity (Birsa et al., 2014; Kondapalli et al., 2012; Shiba-Fukushima et al., 2012). The regulatory role of Parkin phosphorylation at S101 on mitophagy however, until now, had not been described.

This thesis demonstrates that Parkin S101 phosphorylation can regulate the mitophagy pathway. To date no pathogenic mutations are reported at this S101. The closest pathogenic mutation to S101 is A82E (Wang et al., 2005b). The A82E pathogenic mutant appears to retain Parkin's catalytic activity and is not prone to form intracellular inclusions (Wang et al., 2005b). Furthermore, a Q100H polymorphism has been reported (Chen et al., 2003), however the effect on Parkin recruitment to damaged mitochondria and subsequent mitophagy remains to be determined.

As previously mentioned, PINK1 phosphorylates Parkin at S65. Our preliminary experiment shows that S101 phosphorylation is PINK1-dependent. However, whether S101 is also phosphorylated by PINK1 would require further investigations. Studies involving *in vitro* kinase assays using recombinant human full-length human PINK1 are technically challenging as this displays no significant kinase activity (Woodroof et al., 2011). As a result of this the majority of studies use the insect orthologue TcPINK1 as an alternative for PINK1 kinase assay (Woodroof et al., 2011). However recently an human full-length active

PINK1 has been purified and utilised in *in vitro* kinase assays (Aerts et al., 2015), allowing for the possibility of performing *in vitro* kinases using this kinase to study S101 in the future. Our data suggests that S101 phosphorylation takes place in the cytosol. Other cytosolic kinases, such as CK1 or Akt, may also be responsible for S101 phosphorylation however this has not been confirmed.

The work described in this thesis builds upon our previously published data showing that Parkin S101 phosphorylation and S65 (Birsa et al., 2014) can regulate mitophagy at various steps. These data show that non-phosphorylatable mutations at either or both sites do not completely disrupt Parkin mitochondrial translocation to depolarised mitochondria and subsequent mitophagy, suggesting other unknown factors contribute to this. Simulation of human Parkin phosphorylation at S101 (see section 5.2.3) and S65 (Caulfield et al., 2014) suggest that phosphorylation at either of the two sites induces similar conformational change, opening the cleft formed by Parkin's Ubl and linker domains. A number of studies suggest the removal of Parkin Ubl domain may disrupt its autoinhibited conformation thus activating Parkin E3 ligase activity (Chaugule et al., 2011; Spratt et al., 2013). Our work further suggests that phosphorylation at the linker domain is also important in activating Parkin E3 ligase activity. The 'priming' function of Parkin phosphorylation at the Ubl and the linker domain may be instrumental in initiating its E3 ubiquitin ligase activity, with additional regulatory mechanisms required for full activation.

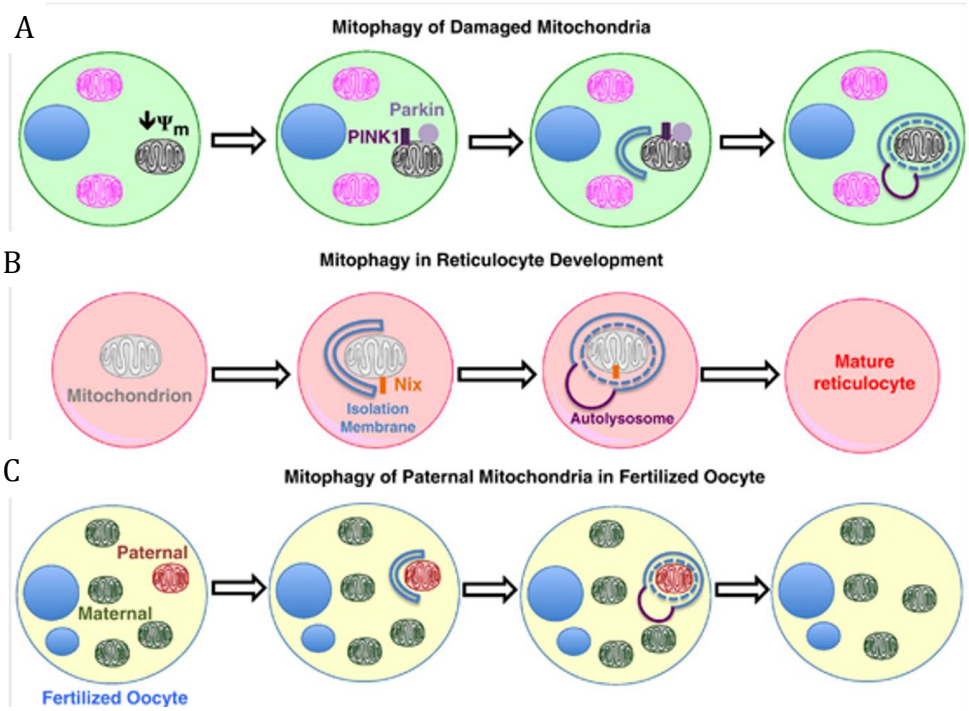

Figure 6-2 Mitophagy pathways in mammalian cells.

(A) Removal of damaged mitochondria upon cellular stress via PINK1/Parkin mitophagy pathway. (B) Mitophagy to remove all mitochondria during reticulocyte development. (C) Mitophagy to remove sperm-derived mitochondria in fertilised oocytes. (Figure adapted from (Ashrafi and Schwarz, 2013))

6.2 Model for Parkin molecular pathways investigation

The data presented in this thesis raises a number of interesting questions.

6.2.1 Primary neurons vs. cancer cell lines

Most of the PINK1/Parkin mitophagy studies have been performed in cancer cell lines, with a limited number of studies using human primary fibroblasts or mice neurons. However, none of these models recapitulate the main clinical features of the disease. (Gispert et al., 2009; Perez and Palmiter, 2005). Functional differences between neurons and non-neuronal cells includes their modes of energy production. Oxidative phosphorylation (OXPHOS) in the mitochondria and glycolysis in the cytosol are the two main pathways to generate ATP in mammalian cells. Under physiological conditions, the majority of healthy cells use the more energy-efficient OXPHOS as the main source of generating ATP. However neurons rely predominantly, if not exclusively, on OXPHOS, and are unable to upregulate glycolysis even during the time of metabolic stress (Almeida et al., 2001; Herrero-Mendez et al., 2009; Whalley, 2009). Neurons metabolise the majority of glucose through the pentose phosphate pathway (PPP), used to regenerate reduced glutathione that helps to protect neurons against oxidative stress, rather than energy production (Kletzien et al., 1994). It was shown that yeast readily undergo mitophagy under starved conditions (Kanki and Klionsky, 2008). However, when yeast cells are grown to depend on OXPHOS for energy production, mitophagy levels are considerably lowered, even under starved conditions. (McCoy et al., 2014; Van Laar et al., 2011). This may explain why mitophagy rates are low in OXPHOS-dependent neurons, and even overexpressed Parkin was unable to be recruited to depolarised mitochondrial in primary neurons (Van Laar et al., 2011).

6.2.2 Overexpressed vs. endogenous Parkin

The majority of studies relies on overexpressed Parkin to assess mitophagy, which is another limitation. In order to address this, Rokvic and colleagues used human control iPSC-derived neurons to compare mitophagy in the presence or

absence of overexpressed Parkin upon valinomycin treatment. The only observation they noted was the reduction of VDAC1 when Parkin is overexpressed, albeit mitophagy is not observed (Rakovic et al., 2013). The data presented in this thesis shows SH-SY5Y with endogenous levels of Parkin also show low mitophagy levels following CCCP. Interestingly, the overexpressed Parkin protein containing pathogenic mutants, such as R275W, translocates to damaged mitochondria (Narendra et al., 2010b) and retains the ability to induce mitophagy to the same level as overexpressed WT Parkin dose (Geisler et al., 2010). Taken together, these data suggests that endogenous Parkin levels are not sufficient to allow a detectable reduction in mitochondrial proteins upon depolarisation. Whether endogenous Parkin is recruited to depolarised mitochondria in neurons, and whether translocated endogenous Parkin promotes mitophagy or may even plays another role in neurons are important questions to be addressed. Improving methods will be essential to improve mitophagy detection in more physiological condition.

6.2.3 Physiological relevance on mitochondrial depolarising agent

The majority of studies investigating the roles of the PINK1/Parkin pathway employ chronic exposure of cells to a protonophore, such as CCCP to depolarise the mitochondria and study their subsequent clearance by mitophagy (Narendra et al., 2008). However other mitochondrial stressors, such as ionophores (valinomycin), complex I inhibitors (rotenone), complex II inhibitors (thenoyltrifluoroacetone, TTFA), complex III inhibitors (antimycin A), complex IV inhibitors (cyanide), or combination of antimycin A with ATP synthase inhibitors (oligomycin) have also been used (Ashrafi et al., 2014; Bartolome et al., 2013; Chen et al., 2007; Exner et al., 2012; Jin and Youle, 2012). These compounds cause profound mitochondrial depolarisation, but efficient Parkin translocation only occurs in cancer cell line models, not in primary neurons with endogenous level of Parkin (Van Laar et al., 2011). Additionally, primary neurons usually require higher concentrations and longer CCCP incubation times than cancer cell models (Imaizumi et al., 2012; Rakovic et al., 2013). Interestingly, recently an alternative physiological trigger of mitophagy

has been described. This system acts by activating the mitochondrial unfolded protein response (UPR^{mt}) pathway via the accumulation of the deletion mutant ornithine transcarbamylase (dOTC) within the mitochondrial matrix (Jin and Youle, 2013; Moisoi et al., 2014). This dOTC-induced mitochondrial stress causes PINK1 accumulation on polarised mitochondria and subsequent mitophagy (Jin and Youle, 2013). This study also described a combined transgenic animal model where dOTC is overexpressed in a PINK1 KO background, which demonstrates an accelerated neurodegeneration induced by the UPR^{mt} (Moisoi et al., 2014). Adapting a more physiological trigger for mitophagy research will enable a better understanding of PINK1/Parkin's role in PD pathogenesis.

6.3 Future perspectives

6.3.1 Future of Parkin mitophagy pathway research

There are still many unknown questions to be answered regarding the regulation of mitophagy. It would be imperative to further dissect the PINK/Parkin mitophagy pathway. This thesis describes the upstream pathway regulation of Parkin S101 phosphorylation is important in priming the damaged mitochondria for mitophagy process. It is essential to identify the true kinase(s) responsible for phosphorylating this site as well as other upstream modulators of this pathway. Other groups have attempted to address these issues of identifying both upstream and downstream molecules to improve knowledge linking the different steps of mitophagy. For instance, genome-wide RNAi (Hasson et al., 2013) or shRNA (McCoy et al., 2014) knockdown screen have identified several putative molecules that regulates Parkin translocation. For downstream pathways, quantitative proteomics studies have identified a number of regulators of Parkin-dependent ubiquitin chain synthesis on substrate proteins (Parkin ubiquilome) (Sarraf et al., 2013) and a feedforward mechanism for mitochondrial Parkin translocation and ubiquitin chain synthesis (Ordureau et al., 2014). The result from these assays will greatly

improve our mechanistic understanding that could be translated into future therapeutic targets.

As compelling evidence suggests Parkin is associated with a more general function such as neuroprotection, developing a more physiological mitophagy inducer is also crucial for a better understanding into how Parkin regulates mitophagy at the physiological level. Furthermore, an appropriate model that can recapitulate PD phenotypes and enable the detection of mitophagy with endogenous Parkin in neurons would provide an important step to identify genuine pathways more relevant to PD pathophysiology. Although iPSC-neurons are invaluable models for investigating neurodegenerative diseases, animal models presenting neurodegeneration will still provide reliable *in vivo* information of mitophagy research. Finally, by combining big genetic/proteomic/metabolomic databases will improve our understanding of new pathways regulating mitophagy. For example, lipogenesis pathway component sterol regulatory element binding transcription factor 1 (SREBF1) has been identified to regulate Parkin translocation (Ivatt et al., 2014), whereas Rab7L1 (RAB7, member RAS oncogene family-like 1), promoting the clearance of Golgi-derived vesicles through the autophagy–lysosome system, has been found as binding partner of LRRK2 (Beilina et al., 2014). These two examples provide strong evidence that supports a common pathway for both sporadic and familial PD.

6.3.2 Mitophagy pathway as a therapeutic target

6.3.2.1 Increasing Parkin expression or activity

As described in chapter 1, Parkin has been shown to display a wide range of neuroprotective functions. Parkin has also been shown to display tumour suppressive function (Cesari et al., 2003; Denison et al., 2003b; Picchio et al., 2004; Wang et al., 2004). A recent chemogenomic profiling analysis applied a genome-editing method to integrate a carefully-designed reporter pair for *Parkin* expression, and then a quantitative high-throughput screening assay to detect potential compounds that could enhance endogenous Parkin expression

(Hasson et al., 2015). If the target pathways found in this study can be further validated, this could potentially be a powerful drug screening system for developing a more effective therapy

6.3.2.2 Early disease detection

To date, PD diagnosis usually depends on clinical presentations and in most case early diagnosis is impossible. A better understanding of the signalling pathways important for the disease pathogenesis will be essential to help developing biomarkers and allow early diagnosis. This may also help delaying the disease progression, increasing the response to medical therapy, and, above all, improving patients' quality of life.

References

Abou-Sleiman, P.M., Healy, D.G., Quinn, N., Lees, A.J., and Wood, N.W. (2003). The role of pathogenic DJ-1 mutations in Parkinson's disease. Ann Neurol *54*, 283-286.

Aerts, L., Craessaerts, K., De Strooper, B., and Morais, V.A. (2015). PINK1 Kinase Catalytic Activity Is Regulated by Phosphorylation on Serines 228 and 402. Journal of Biological Chemistry *290*, 2798-2811.

Al-Hakim, A.K., Zagorska, A., Chapman, L., Deak, M., Peggie, M., and Alessi, D.R. (2008). Control of AMPK-related kinases by USP9X and atypical Lys(29)/Lys(33)-linked polyubiquitin chains. The Biochemical journal *411*, 249-260.

Alegre-Abarrategui, J., Christian, H., Lufino, M.M.P., Mutihac, R., Venda, L.L., Ansorge, O., and Wade-Martins, R. (2009). LRRK2 regulates autophagic activity and localizes to specific membrane microdomains in a novel human genomic reporter cellular model. Human Molecular Genetics *18*, 4022-4034.

Alessi, D.R., James, S.R., Downes, C.P., Holmes, A.B., Gaffney, P.R.J., Reese, C.B., and Cohen, P. (1997). Characterization of a 3-phosphoinositide-dependent protein kinase which phosphorylates and activates protein kinase Bα. Current Biology *7*, 261-269.

Almeida, A., Almeida, J., Bolaños, J.P., and Moncada, S. (2001). Different responses of astrocytes and neurons to nitric oxide: The role of glycolytically generated ATP in astrocyte protection. Proceedings of the National Academy of Sciences *98*, 15294-15299.

Anton, F., Dittmar, G., Langer, T., and Escobar-Henriques, M. (2013). Two Deubiquitylases Act on Mitofusin and Regulate Mitochondrial Fusion along Independent Pathways. Molecular Cell *49*, 487-498.

Ardley, H.C., Scott, G.B., Rose, S.A., Tan, N.G., Markham, A.F., and Robinson, P.A. (2003). Inhibition of proteasomal activity causes inclusion formation in neuronal and non-neuronal cells overexpressing Parkin. Mol Biol Cell *14*, 4541-4556.

Ascherio, A., Zhang, S.M., Hernan, M.A., Kawachi, I., Colditz, G.A., Speizer, F.E., and Willett, W.C. (2001). Prospective study of caffeine consumption and risk of Parkinson's disease in men and women. Ann Neurol *50*, 56-63.

Ashrafi, G., Schlehe, J.S., LaVoie, M.J., and Schwarz, T.L. (2014). Mitophagy of damaged mitochondria occurs locally in distal neuronal axons and requires PINK1 and Parkin. J Cell Biol *206*, 655-670.

Ashrafi, G., and Schwarz, T.L. (2013). The pathways of mitophagy for quality control and clearance of mitochondria. Cell Death Differ *20*, 31-42.

Avraham, E., Rott, R., Liani, E., Szargel, R., and Engelender, S. (2007). Phosphorylation of Parkin by the cyclin-dependent kinase 5 at the linker region modulates its ubiquitin-ligase activity and aggregation. J Biol Chem *282*, 12842-12850.

Bagowski, C.P., Xiong, W., and Ferrell, J.E. (2001). c-Jun N-terminal Kinase Activation in Xenopus laevis Eggs and Embryos: A POSSIBLE NON-GENOMIC ROLE FOR THE JNK SIGNALING PATHWAY. Journal of Biological Chemistry *276*, 1459-1465.

Banerjee, K., Sinha, M., Pham, C.L.L., Jana, S., Chanda, D., Cappai, R., and Chakrabarti, S. (2010). α-Synuclein induced membrane depolarization and loss of phosphorylation capacity of isolated rat brain mitochondria: Implications in Parkinson's disease. FEBS Letters *584*, 1571-1576.

Barbeau, A., Roy, M., Bernier, G., Campanella, G., and Paris, S. (1987). Ecogenetics of Parkinson's disease: prevalence and environmental aspects in rural areas. Can J Neurol Sci *14*, 36-41.

Baron, J.A. (1986). Cigarette smoking and Parkinson's disease. Neurology *36*, 1490-1496.

Bartolome, A., Guillen, C., and Benito, M. (2010). Role of the TSC1-TSC2 complex in the integration of insulin and glucose signaling involved in pancreatic beta-cell proliferation. Endocrinology *151*, 3084-3094.

Bartolome, F., Wu, H.C., Burchell, V.S., Preza, E., Wray, S., Mahoney, C.J., Fox, N.C., Calvo, A., Canosa, A., Moglia, C., *et al.* (2013). Pathogenic VCP Mutations Induce Mitochondrial Uncoupling and Reduced ATP Levels. Neuron *78*, 57-64.

Beal, M.F. (2010). Parkinson's disease: a model dilemma. Nature *466*, S8-S10.

Behari, M., Srivastava, A.K., Das, R.R., and Pandey, R.M. (2001). Risk factors of Parkinson's disease in Indian patients. J Neurol Sci *190*, 49-55.

Beilina, A., Rudenko, I.N., Kaganovich, A., Civiero, L., Chau, H., Kalia, S.K., Kalia, L.V., Lobbestael, E., Chia, R., Ndukwe, K., *et al.* (2014). Unbiased screen for interactors of leucine-rich repeat kinase 2 supports a common pathway for sporadic and familial Parkinson disease. Proceedings of the National Academy of Sciences *111*, 2626-2631.

Bender, A., Krishnan, K.J., Morris, C.M., Taylor, G.A., Reeve, A.K., Perry, R.H., Jaros, E., Hersheson, J.S., Betts, J., Klopstock, T., *et al.* (2006). High levels of mitochondrial DNA deletions in substantia nigra neurons in aging and Parkinson disease. Nat Genet *38*, 515-517.

Bennett, E.J., and Harper, J.W. (2008). DNA damage: ubiquitin marks the spot. Nature structural & molecular biology *15*, 20-22.

Berman, S.B., and Hastings, T.G. (1997). Inhibition of glutamate transport in synaptosomes by dopamine oxidation and reactive oxygen species. J Neurochem *69*, 1185-1195.

Berman, S.B., Zigmond, M.J., and Hastings, T.G. (1996). Modification of dopamine transporter function: effect of reactive oxygen species and dopamine. J Neurochem *67*, 593-600.

Berndsen, C.E., and Wolberger, C. (2014). New insights into ubiquitin E3 ligase mechanism. Nature structural & molecular biology *21*, 301-307.

Beyer, K., Domingo-Sabat, M., Humbert, J., Carrato, C., Ferrer, I., and Ariza, A. (2008). Differential expression of alpha-synuclein, parkin, and synphilin-1 isoforms in Lewy body disease. Neurogenetics *9*, 163-172.

Birsa, N., Norkett, R., Wauer, T., Mevissen, T.E., Wu, H.C., Foltynie, T., Bhatia, K., Hirst, W.D., Komander, D., Plun-Favreau, H., *et al.* (2014). Lysine 27 ubiquitination of the mitochondrial transport protein Miro is dependent on serine 65 of the Parkin ubiquitin ligase. J Biol Chem *289*, 14569-14582.

Bogaerts, V., Nuytemans, K., Reumers, J., Pals, P., Engelborghs, S., Pickut, B., Corsmit, E., Peeters, K., Schymkowitz, J., De Deyn, P.P., *et al.* (2008). Genetic variability in the mitochondrial serine protease HTRA2 contributes to risk for Parkinson disease. Hum Mutat *29*, 832-840.

Bonifati, V., Rizzu, P., van Baren, M.J., Schaap, O., Breedveld, G.J., Krieger, E., Dekker, M.C., Squitieri, F., Ibanez, P., Joosse, M., *et al.* (2003). Mutations in the DJ-1 gene associated with autosomal recessive early-onset parkinsonism. Science *299*, 256-259.

Bosch, E., Cherwinski, H., Peterson, D., and McMahon, M. (1997). Mutations of critical amino acids affect the biological and biochemical properties of oncogenic A-Raf and Raf-1. Oncogene *15*, 1021-1033.

Bras, J., Singleton, A., Cookson, M.R., and Hardy, J. (2008). Emerging pathways in genetic Parkinson's disease: Potential role of ceramide metabolism in Lewy body disease. FEBS J *275*, 5767-5773.

Bremm, A., Freund, S.M., and Komander, D. (2010). Lys11-linked ubiquitin chains adopt compact conformations and are preferentially hydrolyzed by the deubiquitinase Cezanne. Nature structural & molecular biology *17*, 939-947.

Bremm, A., and Komander, D. (2011). Emerging roles for Lys11-linked polyubiquitin in cellular regulation. Trends Biochem Sci *36*, 355-363.

Brooks, D.J. (2010). Imaging approaches to Parkinson disease. J Nucl Med *51*, 596-609.

Brooks, D.J., Frey, K.A., Marek, K.L., Oakes, D., Paty, D., Prentice, R., Shults, C.W., and Stoessl, A.J. (2003). Assessment of neuroimaging techniques as

biomarkers of the progression of Parkinson's disease. Exp Neurol *184 Suppl 1*, S68-79.

Broussolle, E., Lucking, C.B., Ginovart, N., Pollak, P., Remy, P., and Durr, A. (2000). [18 F]-dopa PET study in patients with juvenile-onset PD and parkin gene mutations. Neurology *55*, 877-879.

Budhidarmo, R., Nakatani, Y., and Day, C.L. (2012). RINGs hold the key to ubiquitin transfer. Trends Biochem Sci *37*, 58-65.

Burchell, V.S., Gandhi, S., Deas, E., Wood, N.W., Abramov, A.Y., and Plun-Favreau, H. (2010a). Targeting mitochondrial dysfunction in neurodegenerative disease: Part I. Expert Opinion on Therapeutic Targets *14*, 369-385.

Burchell, V.S., Gandhi, S., Deas, E., Wood, N.W., Abramov, A.Y., and Plun-Favreau, H. (2010b). Targeting mitochondrial dysfunction in neurodegenerative disease: Part II. Expert Opinion on Therapeutic Targets *14*, 497-511.

Burchell, V.S., Nelson, D.E., Sanchez-Martinez, A., Delgado-Camprubi, M., Ivatt, R.M., Pogson, J.H., Randle, S.J., Wray, S., Lewis, P.A., Houlden, H., *et al.* (2013). The Parkinson's disease-linked proteins Fbxo7 and Parkin interact to mediate mitophagy. Nat Neurosci *16*, 1257-1265.

Burke, R.E. (2007). Inhibition of mitogen-activated protein kinase and stimulation of Akt kinase signaling pathways: Two approaches with therapeutic potential in the treatment of neurodegenerative disease. Pharmacology & therapeutics *114*, 261-277.

Burke, R.E. (2008). Programmed cell death and new discoveries in the genetics of parkinsonism. J Neurochem *104*, 875-890.

Calì, T., Ottolini, D., Negro, A., and Brini, M. (2012). α-Synuclein Controls Mitochondrial Calcium Homeostasis by Enhancing Endoplasmic Reticulum-Mitochondria Interactions. Journal of Biological Chemistry *287*, 17914-17929.

Canet-Aviles, R.M., Wilson, M.A., Miller, D.W., Ahmad, R., McLendon, C., Bandyopadhyay, S., Baptista, M.J., Ringe, D., Petsko, G.A., and Cookson, M.R. (2004). The Parkinson's disease protein DJ-1 is neuroprotective due to cysteine-sulfinic acid-driven mitochondrial localization. Proc Natl Acad Sci U S A *101*, 9103-9108.

Carter, R.E., and Sorkin, A. (1998). Endocytosis of functional epidermal growth factor receptor-green fluorescent protein chimera. J Biol Chem *273*, 35000-35007.

Caulfield, T., and Devkota, B. (2012). Motion of transfer RNA from the A/T state into the A-site using docking and simulations. Proteins *80*, 2489-2500.

Caulfield, T.R., Devkota, B., and Rollins, G.C. (2011). Examinations of tRNA Range of Motion Using Simulations of Cryo-EM Microscopy and X-Ray Data. J Biophys *2011*, 219515.

Caulfield, T.R., Fiesel, F.C., Moussaud-Lamodière, E.L., Dourado, D.F.A.R., Flores, S.C., and Springer, W. (2014). Phosphorylation by PINK1 Releases the UBL Domain and Initializes the Conformational Opening of the E3 Ubiquitin Ligase Parkin. PLoS Comput Biol *10*, e1003935.

Cesari, R., Martin, E.S., Calin, G.A., Pentimalli, F., Bichi, R., McAdams, H., Trapasso, F., Drusco, A., Shimizu, M., Masciullo, V., *et al.* (2003). Parkin, a gene implicated in autosomal recessive juvenile parkinsonism, is a candidate tumor suppressor gene on chromosome 6q25-q27. Proc Natl Acad Sci U S A *100*, 5956-5961.

Cha, G.H., Kim, S., Park, J., Lee, E., Kim, M., Lee, S.B., Kim, J.M., Chung, J., and Cho, K.S. (2005). Parkin negatively regulates JNK pathway in the dopaminergic neurons of Drosophila. Proc Natl Acad Sci U S A *102*, 10345-10350.

Chan, N.C., Salazar, A.M., Pham, A.H., Sweredoski, M.J., Kolawa, N.J., Graham, R.L.J., Hess, S., and Chan, D.C. (2011). Broad activation of the ubiquitin-proteasome system by Parkin is critical for mitophagy. Human Molecular Genetics *20*, 1726-1737.

Chang, L., and Karin, M. (2001). Mammalian MAP kinase signalling cascades. Nature *410*, 37-40.

Chastagner, P., Israel, A., and Brou, C. (2006). Itch/AIP4 mediates Deltex degradation through the formation of K29-linked polyubiquitin chains. EMBO Rep *7*, 1147-1153.

Chaugule, V.K., Burchell, L., Barber, K.R., Sidhu, A., Leslie, S.J., Shaw, G.S., and Walden, H. (2011). Autoregulation of Parkin activity through its ubiquitin-like domain. EMBO J *advance online publication*.

Chen, D., Gao, F., Li, B., Wang, H., Xu, Y., Zhu, C., and Wang, G. (2010). Parkin mono-ubiquitinates Bcl-2 and regulates autophagy. J Biol Chem *285*, 38214-38223.

Chen, R., Gosavi, N.S., Langston, J.W., and Chan, P. (2003). Parkin mutations are rare in patients with young-onset parkinsonism in a US population. Parkinsonism & Related Disorders *9*, 309-312.

Chen, Y., McMillan-Ward, E., Kong, J., Israels, S.J., and Gibson, S.B. (2007). Mitochondrial electron-transport-chain inhibitors of complexes I and II induce autophagic cell death mediated by reactive oxygen species. Journal of Cell Science *120*, 4155-4166.

Cherra, S.J., Steer, E., Gusdon, A.M., Kiselyov, K., and Chu, C.T. (2013). Mutant LRRK2 Elicits Calcium Imbalance and Depletion of Dendritic Mitochondria in Neurons. The American Journal of Pathology *182*, 474-484.

Choi, P., Snyder, H., Petrucelli, L., Theisler, C., Chong, M., Zhang, Y., Lim, K., Chung, K.K., Kehoe, K., D'Adamio, L., *et al.* (2003). SEPT5_v2 is a parkin-binding protein. Brain Res Mol Brain Res *117*, 179-189.

Choo, Y.S., Vogler, G., Wang, D., Kalvakuri, S., Iliuk, A., Tao, W.A., Bodmer, R., and Zhang, Z. (2012). Regulation of parkin and PINK1 by neddylation. Human Molecular Genetics *21*, 2514-2523.

Chung, K.K., Thomas, B., Li, X., Pletnikova, O., Troncoso, J.C., Marsh, L., Dawson, V.L., and Dawson, T.M. (2004). S-nitrosylation of parkin regulates ubiquitination and compromises parkin's protective function. Science *304*, 1328-1331.

Chung, K.K., Zhang, Y., Lim, K.L., Tanaka, Y., Huang, H., Gao, J., Ross, C.A., Dawson, V.L., and Dawson, T.M. (2001). Parkin ubiquitinates the alpha-synuclein-interacting protein, synphilin-1: implications for Lewy-body formation in Parkinson disease. Nat Med *7*, 1144-1150.

Chung, K.K.K., Dawson, V.L., and Dawson, T.M. (2005). Response to Comment on "S-Nitrosylation of Parkin Regulates Ubiquitination and Compromises Parkin's Protective Function". Science *308*, 1870.

Clark, I.E., Dodson, M.W., Jiang, C., Cao, J.H., Huh, J.R., Seol, J.H., Yoo, S.J., Hay, B.A., and Guo, M. (2006). Drosophila pink1 is required for mitochondrial function and interacts genetically with parkin. Nature *441*, 1162-1166.

Cook, W.J., Jeffrey, L.C., Carson, M., Chen, Z., and Pickart, C.M. (1992). Structure of a diubiquitin conjugate and a model for interaction with ubiquitin conjugating enzyme (E2). J Biol Chem *267*, 16467-16471.

Cookson, M.R. (2010). The role of leucine-rich repeat kinase 2 (LRRK2) in Parkinson's disease. Nat Rev Neurosci *11*, 791-797.

Cookson, M.R., and Bandmann, O. (2010). Parkinson's disease: insights from pathways. Hum Mol Genet *19*, R21-27.

Cookson, M.R., Lockhart, P.J., McLendon, C., O'Farrell, C., Schlossmacher, M., and Farrer, M.J. (2003). RING finger 1 mutations in Parkin produce altered localization of the protein. Hum Mol Genet *12*, 2957-2965.

Corrêa, S.A.L., and Eales, K.L. (2012). The Role of p38 MAPK and Its Substrates in Neuronal Plasticity and Neurodegenerative Disease. Journal of Signal Transduction *2012*, 12.

Corti, O., Hampe, C., Koutnikova, H., Darios, F., Jacquier, S., Prigent, A., Robinson, J.-C., Pradier, L., Ruberg, M., Mirande, M., *et al.* (2003). The p38 subunit of the aminoacyl-tRNA synthetase complex is a Parkin substrate: linking protein biosynthesis and neurodegeneration. Human Molecular Genetics *12*, 1427-1437.

Cunningham, C.N., Baughman, J.M., Phu, L., Tea, J.S., Yu, C., Coons, M., Kirkpatrick, D.S., Bingol, B., and Corn, J.E. (2015). USP30 and parkin homeostatically regulate atypical ubiquitin chains on mitochondria. Nat Cell Biol *17*, 160-169.

D.A. Pearlman, D.A.C., J.W. Caldwell, W.R. Ross, T.E. Cheatham, III, S. DeBolt, D. Ferguson, G. Seibel and P. Kollman. (1995). AMBER, a computer program for

applying molecular mechanics, normal mode analysis, molecular dynamics and free energy calculations to elucidate the structures and energies of molecules. *Comp Phys Commun 91*, 1-41.

Dagata, V., and Cavallaro, S. (2004). Parkin transcript variants in rat and human brain. Neurochem Res *29*, 1715-1724.

Daniels, V., Vancraenenbroeck, R., Law, B.M., Greggio, E., Lobbestael, E., Gao, F., De Maeyer, M., Cookson, M.R., Harvey, K., Baekelandt, V., *et al.* (2011). Insight into the mode of action of the LRRK2 Y1699C pathogenic mutant. J Neurochem *116*, 304-315.

Darios, F., Corti, O., Lucking, C.B., Hampe, C., Muriel, M.P., Abbas, N., Gu, W.J., Hirsch, E.C., Rooney, T., Ruberg, M., *et al.* (2003). Parkin prevents mitochondrial swelling and cytochrome c release in mitochondria-dependent cell death. Hum Mol Genet *12*, 517-526.

Datta, A.B., Hura, G.L., and Wolberger, C. (2009). The structure and conformation of Lys63-linked tetraubiquitin. Journal of molecular biology *392*, 1117-1124.

Dawson, T.M., and Dawson, V.L. (2010). The role of parkin in familial and sporadic Parkinson's disease. Mov Disord *25 Suppl 1*, S32-39.

de Lau, L.M.L., and Breteler, M.M.B. (2006). Epidemiology of Parkinson's disease. The Lancet Neurology *5*, 525-535.

Deas, E., Plun-Favreau, H., Gandhi, S., Desmond, H., Kjaer, S., Loh, S.H.Y., Renton, A.E.M., Harvey, R.J., Whitworth, A.J., Martins, L.M., *et al.* (2011a). PINK1 cleavage at position A103 by the mitochondrial protease PARL. Human Molecular Genetics *20*, 867-879.

Deas, E., Plun-Favreau, H., and Wood, N.W. (2009). PINK1 function in health and disease. EMBO Mol Med *1*, 152-165.

Deas, E., Wood, N.W., and Plun-Favreau, H. (2011b). Mitophagy and Parkinson's disease: the PINK1-parkin link. Biochim Biophys Acta *1813*, 623-633.

Dehvari, N., Sandebring, A., Flores-Morales, A., Mateos, L., Chuan, Y.C., Goldberg, M.S., Cookson, M.R., Cowburn, R.F., and Cedazo-Minguez, A. (2009). Parkin-mediated ubiquitination regulates phospholipase C-gamma1. J Cell Mol Med *13*, 3061-3068.

Denison, S.R., Callahan, G., Becker, N.A., Phillips, L.A., and Smith, D.I. (2003a). Characterization of FRA6E and its potential role in autosomal recessive juvenile parkinsonism and ovarian cancer. Genes, chromosomes & cancer *38*, 40-52.

Denison, S.R., Wang, F., Becker, N.A., Schule, B., Kock, N., Phillips, L.A., Klein, C., and Smith, D.I. (2003b). Alterations in the common fragile site gene Parkin in ovarian and other cancers. Oncogene *22*, 8370-8378.

Deshaies, R.J., and Joazeiro, C.A. (2009). RING domain E3 ubiquitin ligases. Annu Rev Biochem *78*, 399-434.

Devi, L., Raghavendran, V., Prabhu, B.M., Avadhani, N.G., and Anandatheerthavarada, H.K. (2008). Mitochondrial Import and Accumulation of α-Synuclein Impair Complex I in Human Dopaminergic Neuronal Cultures and Parkinson Disease Brain. Journal of Biological Chemistry *283*, 9089-9100.

Devine, M.J., and Lewis, P.A. (2008). Emerging pathways in genetic Parkinson's disease: tangles, Lewy bodies and LRRK2. FEBS J *275*, 5748-5757.

Devine, M.J., Ryten, M., Vodicka, P., Thomson, A.J., Burdon, T., Houlden, H., Cavaleri, F., Nagano, M., Drummond, N.J., Taanman, J.-W., *et al.* (2011). Parkinson's disease induced pluripotent stem cells with triplication of the α-synuclein locus. Nature Communications *2*, 440.

Di Fonzo, A., Chien, H.F., Socal, M., Giraudo, S., Tassorelli, C., Iliceto, G., Fabbrini, G., Marconi, R., Fincati, E., Abbruzzese, G., *et al.* (2007). ATP13A2 missense mutations in juvenile parkinsonism and young onset Parkinson disease. Neurology *68*, 1557-1562.

Di Fonzo, A., Dekker, M.C., Montagna, P., Baruzzi, A., Yonova, E.H., Correia Guedes, L., Szczerbinska, A., Zhao, T., Dubbel-Hulsman, L.O., Wouters, C.H., *et al.* (2009a). FBXO7 mutations cause autosomal recessive, early-onset parkinsonian-pyramidal syndrome. Neurology *72*, 240-245.

Di Fonzo, A., Fabrizio, E., Thomas, A., Fincati, E., Marconi, R., Tinazzi, M., Breedveld, G.J., Simons, E.J., Chien, H.F., Ferreira, J.J., *et al.* (2009b). GIGYF2 mutations are not a frequent cause of familial Parkinson's disease. Parkinsonism Relat Disord *15*, 703-705.

Di Fonzo, A., Wu-Chou, Y.H., Lu, C.S., van Doeselaar, M., Simons, E.J., Rohe, C.F., Chang, H.C., Chen, R.S., Weng, Y.H., Vanacore, N., *et al.* (2006). A common missense variant in the LRRK2 gene, Gly2385Arg, associated with Parkinson's disease risk in Taiwan. Neurogenetics *7*, 133-138.

Dickson, D.W., Braak, H., Duda, J.E., Duyckaerts, C., Gasser, T., Halliday, G.M., Hardy, J., Leverenz, J.B., Del Tredici, K., Wszolek, Z.K., *et al.* (2009). Neuropathological assessment of Parkinson's disease: refining the diagnostic criteria. Lancet Neurol *8*, 1150-1157.

Ding, Q., Lee, Y.-K., Schaefer, E.A.K., Peters, D.T., Veres, A., Kim, K., Kuperwasser, N., Motola, D.L., Meissner, T.B., Hendriks, W.T., *et al.* (2013). A TALEN genome editing system to generate human stem cell-based disease models. Cell stem cell *12*, 238-251.

Ding, W.X., Ni, H.M., Li, M., Liao, Y., Chen, X., Stolz, D.B., Dorn, G.W., 2nd, and Yin, X.M. (2010). Nix is critical to two distinct phases of mitophagy, reactive oxygen species-mediated autophagy induction and Parkin-ubiquitin-p62-mediated mitochondrial priming. J Biol Chem *285*, 27879-27890.

Dorval, V., and Fraser, P.E. (2006). Small Ubiquitin-like Modifier (SUMO) Modification of Natively Unfolded Proteins Tau and α-Synuclein. Journal of Biological Chemistry *281*, 9919-9924.

Doss-Pepe, E.W., Chen, L., and Madura, K. (2005). α-Synuclein and Parkin Contribute to the Assembly of Ubiquitin Lysine 63-linked Multiubiquitin Chains. Journal of Biological Chemistry *280*, 16619-16624.

Durcan, T.M., Kontogiannea, M., Bedard, N., Wing, S.S., and Fon, E.A. (2012). Ataxin-3 Deubiquitination Is Coupled to Parkin Ubiquitination via E2 Ubiquitin-conjugating Enzyme. Journal of Biological Chemistry *287*, 531-541.

Durcan, T.M., Kontogiannea, M., Thorarinsdottir, T., Fallon, L., Williams, A.J., Djarmati, A., Fantaneanu, T., Paulson, H.L., and Fon, E.A. (2011). The Machado-Joseph disease-associated mutant form of ataxin-3 regulates parkin ubiquitination and stability. Hum Mol Genet *20*, 141-154.

Dzamko, N., Zhou, J., Huang, Y., and Halliday, G. (2014). Parkinson's disease-implicated kinases in the brain; insights into disease pathogenesis. Frontiers in Molecular Neuroscience *7*.

Eddins, M.J., Varadan, R., Fushman, D., Pickart, C.M., and Wolberger, C. (2007). Crystal structure and solution NMR studies of Lys48-linked tetraubiquitin at neutral pH. Journal of molecular biology *367*, 204-211.

Exner, N., Lutz, A.K., Haass, C., and Winklhofer, K.F. (2012). Mitochondrial dysfunction in Parkinson's disease: molecular mechanisms and pathophysiological consequences. The EMBO Journal *31*, 3038-3062.

Exner, N., Treske, B., Paquet, D., Holmstrom, K., Schiesling, C., Gispert, S., Carballo-Carbajal, I., Berg, D., Hoepken, H.H., Gasser, T., *et al.* (2007). Loss-of-function of human PINK1 results in mitochondrial pathology and can be rescued by parkin. J Neurosci *27*, 12413-12418.

Fall, P.A., Fredrikson, M., Axelson, O., and Granerus, A.K. (1999). Nutritional and occupational factors influencing the risk of Parkinson's disease: a case-control study in southeastern Sweden. Mov Disord *14*, 28-37.

Fallon, L., Belanger, C.M.L., Corera, A.T., Kontogiannea, M., Regan-Klapisz, E., Moreau, F., Voortman, J., Haber, M., Rouleau, G., Thorarinsdottir, T., *et al.* (2006). A regulated interaction with the UIM protein Eps15 implicates parkin in EGF receptor trafficking and PI(3)K-Akt signalling. Nat Cell Biol *8*, 834-842.

Fieblinger, T., Sebastianutto, I., Alcacer, C., Bimpisidis, Z., Maslava, N., Sandberg, S., Engblom, D., and Cenci, M.A. (2014). Mechanisms of Dopamine D1 Receptor-Mediated ERK1/2 Activation in the Parkinsonian Striatum and Their Modulation by Metabotropic Glutamate Receptor Type 5. The Journal of Neuroscience *34*, 4728-4740.

Finney, N., Walther, F., Mantel, P.Y., Stauffer, D., Rovelli, G., and Dev, K.K. (2003). The cellular protein level of parkin is regulated by its ubiquitin-like domain. J Biol Chem *278*, 16054-16058.

Fitzgerald, J.C., Camprubi, M.D., Dunn, L., Wu, H.C., Ip, N.Y., Kruger, R., Martins, L.M., Wood, N.W., and Plun-Favreau, H. (2012). Phosphorylation of HtrA2 by cyclin-dependent kinase-5 is important for mitochondrial function. Cell Death Differ *19*, 257-266.

Fitzgerald, J.C., and Plun-Favreau, H. (2008). Emerging pathways in genetic Parkinson's disease: autosomal-recessive genes in Parkinson's disease--a common pathway? FEBS J *275*, 5758-5766.

Foroud, T., Uniacke, S.K., Liu, L., Pankratz, N., Rudolph, A., Halter, C., Shults, C., Marder, K., Conneally, P.M., and Nichols, W.C. (2003). Heterozygosity for a mutation in the parkin gene leads to later onset Parkinson disease. Neurology *60*, 796-801.

Fransson, Å., Ruusala, A., and Aspenström, P. (2003). Atypical Rho GTPases Have Roles in Mitochondrial Homeostasis and Apoptosis. Journal of Biological Chemistry *278*, 6495-6502.

Fransson, Å., Ruusala, A., and Aspenström, P. (2006). The atypical Rho GTPases Miro-1 and Miro-2 have essential roles in mitochondrial trafficking. Biochemical and Biophysical Research Communications *344*, 500-510.

Friesner, R.A., Murphy, R.B., Repasky, M.P., Frye, L.L., Greenwood, J.R., Halgren, T.A., Sanschagrin, P.C., and Mainz, D.T. (2006). Extra precision glide: docking and scoring incorporating a model of hydrophobic enclosure for protein-ligand complexes. Journal of medicinal chemistry *49*, 6177-6196.

Fukae, J., Sato, S., Shiba, K., Sato, K.-i., Mori, H., Sharp, P.A., Mizuno, Y., and Hattori, N. (2009). Programmed cell death-2 isoform1 is ubiquitinated by parkin and increased in the substantia nigra of patients with autosomal recessive Parkinson's disease. FEBS Letters *583*, 521-525.

Galbaugh, T., Cerrito, M.G., Jose, C.C., and Cutler, M.L. (2006). EGF-induced activation of Akt results in mTOR-dependent p70S6 kinase phosphorylation and inhibition of HC11 cell lactogenic differentiation. BMC Cell Biol *7*, 34.

Gandhi, S., Muqit, M.M., Stanyer, L., Healy, D.G., Abou-Sleiman, P.M., Hargreaves, I., Heales, S., Ganguly, M., Parsons, L., Lees, A.J., *et al.* (2006). PINK1 protein in normal human brain and Parkinson's disease. Brain *129*, 1720-1731.

Gasser, T. (2001). Genetics of Parkinson's disease. Journal of Neurology *248*, 833-840.

Gasser, T., Muller-Myhsok, B., Wszolek, Z.K., Oehlmann, R., Calne, D.B., Bonifati, V., Bereznai, B., Fabrizio, E., Vieregge, P., and Horstmann, R.D. (1998). A susceptibility locus for Parkinson's disease maps to chromosome 2p13. Nat Genet *18*, 262-265.

Gegg, M.E., Cooper, J.M., Chau, K.-Y., Rojo, M., Schapira, A.H.V., and Taanman, J.-W. (2010). Mitofusin 1 and mitofusin 2 are ubiquitinated in a PINK1/parkin-dependent manner upon induction of mitophagy. Human Molecular Genetics *19*, 4861-4870.

Geisler, S., Holmstrom, K.M., Skujat, D., Fiesel, F.C., Rothfuss, O.C., Kahle, P.J., and Springer, W. (2010). PINK1/Parkin-mediated mitophagy is dependent on VDAC1 and p62/SQSTM1. Nat Cell Biol *12*, 119-131.

Geiss-Friedlander, R., and Melchior, F. (2007). Concepts in sumoylation: a decade on. Nat Rev Mol Cell Biol *8*, 947-956.

Giasson, B.I., Duda, J.E., Murray, I.V.J., Chen, Q., Souza, J.M., Hurtig, H.I., Ischiropoulos, H., Trojanowski, J.Q., and -Y. Lee, V.M. (2000). Oxidative Damage Linked to Neurodegeneration by Selective α-Synuclein Nitration in Synucleinopathy Lesions. Science *290*, 985-989.

Girault, J.A., Valjent, E., Caboche, J., and Herve, D. (2007). ERK2: a logical AND gate critical for drug-induced plasticity? Current opinion in pharmacology *7*, 77-85.

Gispert, S., Ricciardi, F., Kurz, A., Azizov, M., Hoepken, H.-H., Becker, D., Voos, W., Leuner, K., Müller, W.E., Kudin, A.P., *et al.* (2009). Parkinson Phenotype in Aged PINK1-Deficient Mice Is Accompanied by Progressive Mitochondrial Dysfunction in Absence of Neurodegeneration. PLoS ONE *4*, e5777.

Glauser, L., Sonnay, S., Stafa, K., and Moore, D.J. (2011). Parkin promotes the ubiquitination and degradation of the mitochondrial fusion factor mitofusin 1. Journal of Neurochemistry *118*, 636-645.

Gocke, C.B., Yu, H., and Kang, J. (2005). Systematic identification and analysis of mammalian small ubiquitin-like modifier substrates. J Biol Chem *280*, 5004-5012.

Gorrell, J.M., DiMonte, D., and Graham, D. (1996). The role of the environment in Parkinson's disease. Environ Health Perspect *104*, 652-654.

Greene, J.C., Whitworth, A.J., Kuo, I., Andrews, L.A., Feany, M.B., and Pallanck, L.J. (2003). Mitochondrial pathology and apoptotic muscle degeneration in Drosophila parkin mutants. Proc Natl Acad Sci U S A *100*, 4078-4083.

Greggio, E., and Cookson, M.R. (2009). Leucine-rich repeat kinase 2 mutations and Parkinson's disease: three questions. ASN neuro *1*.

Greggio, E., Jain, S., Kingsbury, A., Bandopadhyay, R., Lewis, P., Kaganovich, A., van der Brug, M.P., Beilina, A., Blackinton, J., Thomas, K.J., *et al.* (2006). Kinase activity is required for the toxic effects of mutant LRRK2/dardarin. Neurobiol Dis *23*, 329-341.

Haglund, K., and Dikic, I. (2005). Ubiquitylation and cell signaling. EMBO J *24*, 3353-3359.

Hampe, C., Ardila-Osorio, H., Fournier, M., Brice, A., and Corti, O. (2006). Biochemical analysis of Parkinson's disease-causing variants of Parkin, an E3 ubiquitin-protein ligase with monoubiquitylation capacity. Hum Mol Genet *15*, 2059-2075.

Hamza, T.H., Zabetian, C.P., Tenesa, A., Laederach, A., Montimurro, J., Yearout, D., Kay, D.M., Doheny, K.F., Paschall, J., Pugh, E., *et al.* (2010). Common genetic variation in the HLA region is associated with late-onset sporadic Parkinson's disease. Nat Genet *42*, 781-785.

Haque, M.E., Thomas, K.J., D'Souza, C., Callaghan, S., Kitada, T., Slack, R.S., Fraser, P., Cookson, M.R., Tandon, A., and Park, D.S. (2008). Cytoplasmic Pink1 activity protects neurons from dopaminergic neurotoxin MPTP. Proc Natl Acad Sci U S A *105*, 1716-1721.

Hardy, J. (2010). Genetic analysis of pathways to Parkinson disease. Neuron *68*, 201-206.

Hasegawa, T., Treis, A., Patenge, N., Fiesel, F.C., Springer, W., and Kahle, P.J. (2008). Parkin protects against tyrosinase-mediated dopamine neurotoxicity by suppressing stress-activated protein kinase pathways. J Neurochem *105*, 1700-1715.

Hasson, S.A., Fogel, A.I., Wang, C., MacArthur, R., Guha, R., Heman-Ackah, S., Martin, S., Youle, R.J., and Inglese, J. (2015). Chemogenomic profiling of endogenous PARK2 expression using a genome-edited coincidence reporter. ACS Chemical Biology.

Hasson, S.A., Kane, L.A., Yamano, K., Huang, C.-H., Sliter, D.A., Buehler, E., Wang, C., Heman-Ackah, S.M., Hessa, T., Guha, R., *et al.* (2013). High-content genome-wide RNAi screens identify regulators of parkin upstream of mitophagy. Nature *504*, 291-295.

Hastings, T.G., Lewis, D.A., and Zigmond, M.J. (1996). Role of oxidation in the neurotoxic effects of intrastriatal dopamine injections. Proc Natl Acad Sci U S A *93*, 1956-1961.

Hayden, M.S., and Ghosh, S. (2008). Shared principles in NF-kappaB signaling. Cell *132*, 344-362.

Hedrich, K., Djarmati, A., Schafer, N., Hering, R., Wellenbrock, C., Weiss, P.H., Hilker, R., Vieregge, P., Ozelius, L.J., Heutink, P., *et al.* (2004). DJ-1 (PARK7) mutations are less frequent than Parkin (PARK2) mutations in early-onset Parkinson disease. Neurology *62*, 389-394.

Hedrich, K., Marder, K., Harris, J., Kann, M., Lynch, T., Meija-Santana, H., Pramstaller, P.P., Schwinger, E., Bressman, S.B., Fahn, S., *et al.* (2002). Evaluation of 50 probands with early-onset Parkinson's disease for Parkin mutations. Neurology *58*, 1239-1246.

Henn, I.H., Bouman, L., Schlehe, J.S., Schlierf, A., Schramm, J.E., Wegener, E., Nakaso, K., Culmsee, C., Berninger, B., Krappmann, D., *et al.* (2007). Parkin

mediates neuroprotection through activation of IkappaB kinase/nuclear factor-kappaB signaling. J Neurosci *27*, 1868-1878.

Henn, I.H., Gostner, J.M., Lackner, P., Tatzelt, J., and Winklhofer, K.F. (2005). Pathogenic mutations inactivate parkin by distinct mechanisms. J Neurochem *92*, 114-122.

Hermann, C., Assmus, B., Urbich, C., Zeiher, A.M., and Dimmeler, S. (2000). Insulin-Mediated Stimulation of Protein Kinase Akt: A Potent Survival Signaling Cascade for Endothelial Cells. Arteriosclerosis, Thrombosis, and Vascular Biology *20*, 402-409.

Herrero-Mendez, A., Almeida, A., Fernandez, E., Maestre, C., Moncada, S., and Bolanos, J.P. (2009). The bioenergetic and antioxidant status of neurons is controlled by continuous degradation of a key glycolytic enzyme by APC/C-Cdh1. Nat Cell Biol *11*, 747-752.

Hershko, A., and Ciechanover, A. (1998). THE UBIQUITIN SYSTEM. Annual Review of Biochemistry *67*, 425-479.

Higashi, Y., Asanuma, M., Miyazaki, I., Hattori, N., Mizuno, Y., and Ogawa, N. (2004). Parkin attenuates manganese-induced dopaminergic cell death. J Neurochem *89*, 1490-1497.

Hilker, R., Klein, C., Ghaemi, M., Kis, B., Strotmann, T., Ozelius, L.J., Lenz, O., Vieregge, P., Herholz, K., Heiss, W.D., *et al.* (2001). Positron emission tomographic analysis of the nigrostriatal dopaminergic system in familial parkinsonism associated with mutations in the parkin gene. Ann Neurol *49*, 367-376.

Hochstrasser, M. (1996). Ubiquitin-dependent protein degradation. Annu Rev Genet *30*, 405-439.

Huang, D.T., Ayrault, O., Hunt, H.W., Taherbhoy, A.M., Duda, D.M., Scott, D.C., Borg, L.A., Neale, G., Murray, P.J., Roussel, M.F., *et al.* (2009). E2-RING expansion of the NEDD8 cascade confers specificity to cullin modification. Mol Cell *33*, 483-495.

Huang, L., Verstrepen, L., Heyninck, K., Wullaert, A., Revets, H., De Baetselier, P., and Beyaert, R. (2008). ABINs inhibit EGF receptor-mediated NF-kappaB activation and growth of EGF receptor-overexpressing tumour cells. Oncogene *27*, 6131-6140.

Hughes, A.J., Daniel, S.E., Kilford, L., and Lees, A.J. (1992). Accuracy of clinical diagnosis of idiopathic Parkinson's disease: a clinico-pathological study of 100 cases. J Neurol Neurosurg Psychiatry *55*, 181-184.

Huibregtse, J.M., Scheffner, M., Beaudenon, S., and Howley, P.M. (1995). A family of proteins structurally and functionally related to the E6-AP ubiquitin-protein ligase. Proc Natl Acad Sci U S A *92*, 2563-2567.

Humbert, J., Beyer, K., Carrato, C., Mate, J.L., Ferrer, I., and Ariza, A. (2007). Parkin and synphilin-1 isoform expression changes in Lewy body diseases. Neurobiol Dis *26*, 681-687.

Huynh, D.P., Dy, M., Nguyen, D., Kiehl, T.-R., and Pulst, S.M. (2001). Differential expression and tissue distribution of parkin isoforms during mouse development. Developmental Brain Research *130*, 173-181.

Huynh, D.P., Nguyen, D.T., Pulst-Korenberg, J.B., Brice, A., and Pulst, S.-M. (2007). Parkin is an E3 ubiquitin-ligase for normal and mutant ataxin-2 and prevents ataxin-2-induced cell death. Experimental neurology *203*, 531-541.

Huynh, D.P., Scoles, D.R., Ho, T.H., Del Bigio, M.R., and Pulst, S.-M. (2000). Parkin is associated with actin filaments in neuronal and nonneural cells. Annals of Neurology *48*, 737-744.

Huynh, D.P., Scoles, D.R., Nguyen, D., and Pulst, S.M. (2003). The autosomal recessive juvenile Parkinson disease gene product, parkin, interacts with and ubiquitinates synaptotagmin XI. Hum Mol Genet *12*, 2587-2597.

Ikeda, F., and Dikic, I. (2008). Atypical ubiquitin chains: new molecular signals. 'Protein Modifications: Beyond the Usual Suspects' review series. EMBO Rep *9*, 536-542.

Ikeuchi, K., Marusawa, H., Fujiwara, M., Matsumoto, Y., Endo, Y., Watanabe, T., Iwai, A., Sakai, Y., Takahashi, R., and Chiba, T. (2009). Attenuation of proteolysis-mediated cyclin E regulation by alternatively spliced Parkin in human colorectal cancers. Int J Cancer *125*, 2029-2035.

Imai, Y., Soda, M., Inoue, H., Hattori, N., Mizuno, Y., and Takahashi, R. (2001). An unfolded putative transmembrane polypeptide, which can lead to endoplasmic reticulum stress, is a substrate of Parkin. Cell *105*, 891-902.

Imaizumi, Y., Okada, Y., Akamatsu, W., Koike, M., Kuzumaki, N., Hayakawa, H., Nihira, T., Kobayashi, T., Ohyama, M., Sato, S., *et al.* (2012). Mitochondrial dysfunction associated with increased oxidative stress and alpha-synuclein accumulation in PARK2 iPSC-derived neurons and postmortem brain tissue. Mol Brain *5*, 35.

Imam, S.Z., Zhou, Q., Yamamoto, A., Valente, A.J., Ali, S.F., Bains, M., Roberts, J.L., Kahle, P.J., Clark, R.A., and Li, S. (2011). Novel regulation of parkin function through c-Abl-mediated tyrosine phosphorylation: implications for Parkinson's disease. J Neurosci *31*, 157-163.

Irrcher, I., Aleyasin, H., Seifert, E.L., Hewitt, S.J., Chhabra, S., Phillips, M., Lutz, A.K., Rousseaux, M.W.C., Bevilacqua, L., Jahani-Asl, A., *et al.* (2010). Loss of the Parkinson's disease-linked gene DJ-1 perturbs mitochondrial dynamics. Human Molecular Genetics *19*, 3734-3746.

Ischiropoulos, H., and Beckman, J.S. (2003). Oxidative stress and nitration in neurodegeneration: Cause, effect, or association? The Journal of Clinical Investigation *111*, 163-169.

Ivatt, R.M., Sanchez-Martinez, A., Godena, V.K., Brown, S., Ziviani, E., and Whitworth, A.J. (2014). Genome-wide RNAi screen identifies the Parkinson disease GWAS risk locus SREBF1 as a regulator of mitophagy. Proceedings of the National Academy of Sciences of the United States of America *111*, 8494-8499.

Jenner, P. (1998). Oxidative mechanisms in nigral cell death in Parkinson's disease. Mov Disord *13 Suppl 1*, 24-34.

Jensen, L.D., Vinther-Jensen, T., Kahns, S., Sundbye, S., and Jensen, P.H. (2006). Cellular parkin mutants are soluble under non-stress conditions. Neuroreport *17*, 1205-1208.

Jiang, H., Ren, Y., Zhao, J., and Feng, J. (2004). Parkin protects human dopaminergic neuroblastoma cells against dopamine-induced apoptosis. Hum Mol Genet *13*, 1745-1754.

Jin, S.M., and Youle, R.J. (2012). PINK1- and Parkin-mediated mitophagy at a glance. Journal of Cell Science *125*, 795-799.

Jin, S.M., and Youle, R.J. (2013). The accumulation of misfolded proteins in the mitochondrial matrix is sensed by PINK1 to induce PARK2/Parkin-mediated mitophagy of polarized mitochondria. Autophagy *9*, 1750-1757.

Joch, M., Ase, A.R., Chen, C.X., MacDonald, P.A., Kontogiannea, M., Corera, A.T., Brice, A., Seguela, P., and Fon, E.A. (2007). Parkin-mediated monoubiquitination of the PDZ protein PICK1 regulates the activity of acid-sensing ion channels. Mol Biol Cell *18*, 3105-3118.

Jones, J.M., Datta, P., Srinivasula, S.M., Ji, W., Gupta, S., Zhang, Z., Davies, E., Hajnoczky, G., Saunders, T.L., Van Keuren, M.L., *et al.* (2003). Loss of Omi mitochondrial protease activity causes the neuromuscular disorder of mnd2 mutant mice. Nature *425*, 721-727.

Jorgensen, W.L., and Tiradorives, J. (1988). The Opls Potential Functions for Proteins - Energy Minimizations for Crystals of Cyclic-Peptides and Crambin. J Am Chem Soc *110*, 1657-1666.

Judson, R.L., Babiarz, J.E., Venere, M., and Blelloch, R. (2009). Embryonic stem cell-specific microRNAs promote induced pluripotency. Nat Biotech *27*, 459-461.

Kachergus, J., Mata, I.F., Hulihan, M., Taylor, J.P., Lincoln, S., Aasly, J., Gibson, J.M., Ross, O.A., Lynch, T., Wiley, J., *et al.* (2005). Identification of a Novel LRRK2 Mutation Linked to Autosomal Dominant Parkinsonism: Evidence of a Common Founder across European Populations. American journal of human genetics *76*, 672-680.

Kaltschmidt, B., and Kaltschmidt, C. (2009). NF-κB in the Nervous System. Cold Spring Harbor Perspectives in Biology *1*.

Kamp, F., Exner, N., Lutz, A.K., Wender, N., Hegermann, J., Brunner, B., Nuscher, B., Bartels, T., Giese, A., Beyer, K., *et al.* (2010). Inhibition of mitochondrial fusion by α-synuclein is rescued by PINK1, Parkin and DJ-1, Vol 29.

Kanki, T., and Klionsky, D.J. (2008). Mitophagy in Yeast Occurs through a Selective Mechanism. Journal of Biological Chemistry *283*, 32386-32393.

Karin, M., and Lin, A. (2002). NF-kappaB at the crossroads of life and death. Nat Immunol *3*, 221-227.

Karunakaran, S., Saeed, U., Mishra, M., Valli, R.K., Joshi, S.D., Meka, D.P., Seth, P., and Ravindranath, V. (2008). Selective activation of p38 mitogen-activated protein kinase in dopaminergic neurons of substantia nigra leads to nuclear translocation of p53 in 1-methyl-4-phenyl-1,2,3,6-tetrahydropyridine-treated mice. J Neurosci *28*, 12500-12509.

Kasap, M., Akpinar, G., Sazci, A., Idrisoglu, H.A., and Vahaboğlu, H. (2009). Evidence for the presence of full-length PARK2 mRNA and Parkin protein in human blood. Neuroscience Letters *460*, 196-200.

Kazlauskaite, A., Kelly, V., Johnson, C., Baillie, C., Hastie, C.J., Peggie, M., Macartney, T., Woodroof, H.I., Alessi, D.R., Pedrioli, P.G.A., *et al.* (2014). Phosphorylation of Parkin at Serine65 is essential for activation: elaboration of a Miro1 substrate-based assay of Parkin E3 ligase activity. Open Biology *4*, 130213.

Kim, E.K., and Choi, E.J. (2010). Pathological roles of MAPK signaling pathways in human diseases. Biochim Biophys Acta *1802*, 396-405.

Kim, Nam C., Tresse, E., Kolaitis, R.-M., Molliex, A., Thomas, Ruth E., Alami, Nael H., Wang, B., Joshi, A., Smith, Rebecca B., Ritson, Gillian P., *et al.* (2013). VCP Is Essential for Mitochondrial Quality Control by PINK1/Parkin and this Function Is Impaired by VCP Mutations. Neuron *78*, 65-80.

Kim, R.H., Peters, M., Jang, Y., Shi, W., Pintilie, M., Fletcher, G.C., DeLuca, C., Liepa, J., Zhou, L., Snow, B., *et al.* (2005). DJ-1, a novel regulator of the tumor suppressor PTEN. Cancer Cell *7*, 263-273.

Kim, Y., Park, J., Kim, S., Song, S., Kwon, S.K., Lee, S.H., Kitada, T., Kim, J.M., and Chung, J. (2008). PINK1 controls mitochondrial localization of Parkin through direct phosphorylation. Biochem Biophys Res Commun *377*, 975-980.

Kinoshita, E., Kinoshita-Kikuta, E., Takiyama, K., and Koike, T. (2006). Phosphate-binding Tag, a New Tool to Visualize Phosphorylated Proteins. Molecular & Cellular Proteomics *5*, 749-757.

Kirkegaard, T., Witton, C.J., Edwards, J., Nielsen, K.V., Jensen, L.B., Campbell, F.M., Cooke, T.G., and Bartlett, J.M. (2010). Molecular alterations in AKT1, AKT2

and AKT3 detected in breast and prostatic cancer by FISH. Histopathology *56*, 203-211.

Kitada, T., Asakawa, S., Hattori, N., Matsumine, H., Yamamura, Y., Minoshima, S., Yokochi, M., Mizuno, Y., and Shimizu, N. (1998). Mutations in the parkin gene cause autosomal recessive juvenile parkinsonism. Nature *392*, 605-608.

Kitada, T., Asakawa, S., Minoshima, S., Mizuno, Y., and Shimizu, N. (2000). Molecular cloning, gene expression, and identification of a splicing variant of the mouse parkin gene. Mammalian Genome *11*, 417-421.

Klein, C., Lohmann-Hedrich, K., Rogaeva, E., Schlossmacher, M.G., and Lang, A.E. (2007). Deciphering the role of heterozygous mutations in genes associated with parkinsonism. Lancet Neurol *6*, 652-662.

Kletzien, R.F., Harris, P.K., and Foellmi, L.A. (1994). Glucose-6-phosphate dehydrogenase: a "housekeeping" enzyme subject to tissue-specific regulation by hormones, nutrients, and oxidant stress. FASEB J *8*, 174-181.

Ko, H.S., Kim, S.W., Sriram, S.R., Dawson, V.L., and Dawson, T.M. (2006). Identification of far upstream element-binding protein-1 as an authentic Parkin substrate. J Biol Chem *281*, 16193-16196.

Ko, H.S., Lee, Y., Shin, J.H., Karuppagounder, S.S., Gadad, B.S., Koleske, A.J., Pletnikova, O., Troncoso, J.C., Dawson, V.L., and Dawson, T.M. (2010). Phosphorylation by the c-Abl protein tyrosine kinase inhibits parkin's ubiquitination and protective function. Proc Natl Acad Sci U S A *107*, 16691-16696.

Komander, D., Reyes-Turcu, F., Licchesi, J.D., Odenwaelder, P., Wilkinson, K.D., and Barford, D. (2009). Molecular discrimination of structurally equivalent Lys 63-linked and linear polyubiquitin chains. EMBO Rep *10*, 466-473.

Kondapalli, C., Kazlauskaite, A., Zhang, N., Woodroof, H.I., Campbell, D.G., Gourlay, R., Burchell, L., Walden, H., Macartney, T.J., Deak, M., *et al.* (2012). PINK1 is activated by mitochondrial membrane potential depolarization and stimulates Parkin E3 ligase activity by phosphorylating Serine 65. Open Biology *2*, 120080.

Kotiadis, V.N., Duchen, M.R., and Osellame, L.D. (2014). Mitochondrial quality control and communications with the nucleus are important in maintaining mitochondrial function and cell health. Biochimica et Biophysica Acta (BBA) - General Subjects *1840*, 1254-1265.

Kravtsova-Ivantsiv, Y., and Ciechanover, A. (2012). Non-canonical ubiquitin-based signals for proteasomal degradation. J Cell Sci *125*, 539-548.

Krieger, E., Joo, K., Lee, J., Raman, S., Thompson, J., Tyka, M., Baker, D., and Karplus, K. (2009). Improving physical realism, stereochemistry, and side-chain accuracy in homology modeling: Four approaches that performed well in CASP8. Proteins *77 Suppl 9*, 114-122.

Kruger, R., Kuhn, W., Muller, T., Woitalla, D., Graeber, M., Kosel, S., Przuntek, H., Epplen, J.T., Schols, L., and Riess, O. (1998). Ala30Pro mutation in the gene encoding alpha-synuclein in Parkinson's disease. Nat Genet *18*, 106-108.

Kubo, S.-i., Kitami, T., Noda, S., Shimura, H., Uchiyama, Y., Asakawa, S., Minoshima, S., Shimizu, N., Mizuno, Y., and Hattori, N. (2001). Parkin is associated with cellular vesicles. Journal of Neurochemistry *78*, 42-54.

Kuhn, D.M., and Arthur, R., Jr. (1998). Dopamine inactivates tryptophan hydroxylase and forms a redox-cycling quinoprotein: possible endogenous toxin to serotonin neurons. J Neurosci *18*, 7111-7117.

Kuhn, D.M., Arthur, R.E., Jr., Thomas, D.M., and Elferink, L.A. (1999). Tyrosine hydroxylase is inactivated by catechol-quinones and converted to a redox-cycling quinoprotein: possible relevance to Parkinson's disease. J Neurochem *73*, 1309-1317.

Kulathu, Y., and Komander, D. (2012). Atypical ubiquitylation - the unexplored world of polyubiquitin beyond Lys48 and Lys63 linkages. Nat Rev Mol Cell Biol *13*, 508-523.

Kurup, P.K., Xu, J., Videira, R.A., Ononenyi, C., Baltazar, G., Lombroso, P.J., and Nairn, A.C. (2015). STEP61 is a substrate of the E3 ligase parkin and is upregulated in Parkinson's disease. Proceedings of the National Academy of Sciences.

Kurz, T., Chou, Y.C., Willems, A.R., Meyer-Schaller, N., Hecht, M.L., Tyers, M., Peter, M., and Sicheri, F. (2008). Dcn1 functions as a scaffold-type E3 ligase for cullin neddylation. Mol Cell *29*, 23-35.

Langston, J.W., Irwin, I., Langston, E.B., and Forno, L.S. (1984). Pargyline prevents MPTP-induced parkinsonism in primates. Science *225*, 1480-1482.

Lautier, C., Goldwurm, S., Durr, A., Giovannone, B., Tsiaras, W.G., Pezzoli, G., Brice, A., and Smith, R.J. (2008). Mutations in the GIGYF2 (TNRC15) gene at the PARK11 locus in familial Parkinson disease. Am J Hum Genet *82*, 822-833.

LaVoie, M.J., Cortese, G.P., Ostaszewski, B.L., and Schlossmacher, M.G. (2007). The effects of oxidative stress on parkin and other E3 ligases. Journal of Neurochemistry *103*, 2354-2368.

LaVoie, M.J., and Hastings, T.G. (1999). Dopamine quinone formation and protein modification associated with the striatal neurotoxicity of methamphetamine: evidence against a role for extracellular dopamine. J Neurosci *19*, 1484-1491.

LaVoie, M.J., Ostaszewski, B.L., Weihofen, A., Schlossmacher, M.G., and Selkoe, D.J. (2005). Dopamine covalently modifies and functionally inactivates parkin. Nat Med *11*, 1214-1221.

Lazarou, M., Narendra, D.P., Jin, S.M., Tekle, E., Banerjee, S., and Youle, R.J. (2013). PINK1 drives Parkin self-association and HECT-like E3 activity upstream of mitochondrial binding. The Journal of Cell Biology *200*, 163-172.

Leboucher, Guillaume P., Tsai, Yien C., Yang, M., Shaw, Kristin C., Zhou, M., Veenstra, Timothy D., Glickman, Michael H., and Weissman, Allan M. (2012). Stress-induced phosphorylation and proteasomal degradation of mitofusin 2 facilitates mitochondrial fragmentation and apoptosis. Molecular Cell *47*, 547-557.

Lee, I., and Schindelin, H. (2008). Structural insights into E1-catalyzed ubiquitin activation and transfer to conjugating enzymes. Cell *134*, 268-278.

Lee, J.-Y., Koga, H., Kawaguchi, Y., Tang, W., Wong, E., Gao, Y.-S., Pandey, U.B., Kaushik, S., Tresse, E., Lu, J., *et al.* (2010a). HDAC6 controls autophagosome maturation essential for ubiquitin-selective quality-control autophagy. EMBO J *29*, 969-980.

Lee, J.Y., Nagano, Y., Taylor, J.P., Lim, K.L., and Yao, T.P. (2010b). Disease-causing mutations in parkin impair mitochondrial ubiquitination, aggregation, and HDAC6-dependent mitophagy. J Cell Biol *189*, 671-679.

Lees, A.J. (2007). Unresolved issues relating to the Shaking Palsy on the celebration of James Parkinson's 250th birthday. Movement Disorders *22*, S327-S334.

Leroy, E., Boyer, R., Auburger, G., Leube, B., Ulm, G., Mezey, E., Harta, G., Brownstein, M.J., Jonnalagada, S., Chernova, T., *et al.* (1998). The ubiquitin pathway in Parkinson's disease. Nature *395*, 451-452.

Levy, O.A., Malagelada, C., and Greene, L.A. (2009). Cell death pathways in Parkinson's disease: proximal triggers, distal effectors, and final steps. Apoptosis *14*, 478-500.

Lewis, P.A., Greggio, E., Beilina, A., Jain, S., Baker, A., and Cookson, M.R. (2007). The R1441C mutation of LRRK2 disrupts GTP hydrolysis. Biochem Biophys Res Commun *357*, 668-671.

Li, J.Q., Tan, L., and Yu, J.T. (2014). The role of the LRRK2 gene in Parkinsonism. Mol Neurodegener *9*, 47.

Li, W., Bengtson, M.H., Ulbrich, A., Matsuda, A., Reddy, V.A., Orth, A., Chanda, S.K., Batalov, S., and Joazeiro, C.A.P. (2008). Genome-Wide and Functional Annotation of Human E3 Ubiquitin Ligases Identifies MULAN, a Mitochondrial E3 that Regulates the Organelle's Dynamics and Signaling. PLoS One *3*, e1487.

Li, X., Tan, Y.C., Poulose, S., Olanow, C.W., Huang, X.Y., and Yue, Z. (2007). Leucine-rich repeat kinase 2 (LRRK2)/PARK8 possesses GTPase activity that is altered in familial Parkinson's disease R1441C/G mutants. J Neurochem *103*, 238-247.

Li, Y.J., Scott, W.K., Hedges, D.J., Zhang, F., Gaskell, P.C., Nance, M.A., Watts, R.L., Hubble, J.P., Koller, W.C., Pahwa, R., *et al.* (2002). Age at onset in two common neurodegenerative diseases is genetically controlled. Am J Hum Genet *70*, 985-993.

Lim, G.G.Y., Chew, K.C.M., Ng, X.-H., Henry-Basil, A., Sim, R.W.X., Tan, J.M.M., Chai, C., and Lim, K.-L. (2013). Proteasome Inhibition Promotes Parkin-Ubc13 Interaction and Lysine 63-Linked Ubiquitination. PLoS ONE *8*, e73235.

Lim, K.-L., and Lim, G.G.Y. (2011). K63-linked ubiquitination and neurodegeneration. Neurobiology of Disease *43*, 9-16.

Lim, K.L., Chew, K.C.M., Tan, J.M.M., Wang, C., Chung, K.K.K., Zhang, Y., Tanaka, Y., Smith, W., Engelender, S., Ross, C.A., *et al.* (2005). Parkin Mediates Nonclassical, Proteasomal-Independent Ubiquitination of Synphilin-1: Implications for Lewy Body Formation. The Journal of Neuroscience *25*, 2002-2009.

Lim, M.K., Kawamura, T., Ohsawa, Y., Ohtsubo, M., Asakawa, S., Takayanagi, A., and Shimizu, N. (2007). Parkin interacts with LIM Kinase 1 and reduces its cofilin-phosphorylation activity via ubiquitination. Exp Cell Res *313*, 2858-2874.

Lipton, S.A., Nakamura, T., Yao, D., Shi, Z.-Q., Uehara, T., and Gu, Z. (2005). Comment on "S-Nitrosylation of Parkin Regulates Ubiquitination and Compromises Parkin's Protective Function". Science *308*, 1870.

Liu, S., Sawada, T., Lee, S., Yu, W., Silverio, G., Alapatt, P., Millan, I., Shen, A., Saxton, W., Kanao, T., *et al.* (2012). Parkinson's disease-associated kinase PINK1 regulates Miro protein level and axonal transport of mitochondria. PLoS Genet *8*, e1002537.

Lizcano, J.M., and Alessi, D.R. (2002). The insulin signalling pathway. Current Biology *12*, R236-R238.

Loving, K., Salam, N.K., and Sherman, W. (2009). Energetic analysis of fragment docking and application to structure-based pharmacophore hypothesis generation. Journal of computer-aided molecular design *23*, 541-554.

Lu, X.H., Fleming, S.M., Meurers, B., Ackerson, L.C., Mortazavi, F., Lo, V., Hernandez, D., Sulzer, D., Jackson, G.R., Maidment, N.T., *et al.* (2009). Bacterial artificial chromosome transgenic mice expressing a truncated mutant parkin exhibit age-dependent hypokinetic motor deficits, dopaminergic neuron degeneration, and accumulation of proteinase K-resistant alpha-synuclein. J Neurosci *29*, 1962-1976.

Lucking, C.B., Durr, A., Bonifati, V., Vaughan, J., De Michele, G., Gasser, T., Harhangi, B.S., Meco, G., Denefle, P., Wood, N.W., *et al.* (2000). Association between early-onset Parkinson's disease and mutations in the parkin gene. N Engl J Med *342*, 1560-1567.

Manzanillo, P.S., Ayres, J.S., Watson, R.O., Collins, A.C., Souza, G., Rae, C.S., Schneider, D.S., Nakamura, K., Shiloh, M.U., and Cox, J.S. (2013). The ubiquitin ligase parkin mediates resistance to intracellular pathogens. Nature *501*, 512-516.

Manzoni, C., Mamais, A., Dihanich, S., McGoldrick, P., Devine, M.J., Zerle, J., Kara, E., Taanman, J.-W., Healy, D.G., Marti-Masso, J.-F., *et al.* (2013). Pathogenic Parkinson’s disease mutations across the functional domains of LRRK2 alter the

autophagic/lysosomal response to starvation(). Biochemical and Biophysical Research Communications *441*, 862-866.

Marder, K.S., Tang, M.X., Mejia-Santana, H., Rosado, L., Louis, E.D., Comella, C.L., Colcher, A., Siderowf, A.D., Jennings, D., Nance, M.A., *et al.* (2010). Predictors of parkin mutations in early-onset Parkinson disease: the consortium on risk for early-onset Parkinson disease study. Arch Neurol *67*, 731-738.

Marsden, C.D. (1990). Parkinson's disease. The Lancet *335*, 948-949.

Martin, I., Dawson, V.L., and Dawson, T.M. (2011). Recent advances in the genetics of Parkinson's disease. Annual Review of Genomics and Human Genetics *12*, 301-325.

Martins, L.M., Iaccarino, I., Tenev, T., Gschmeissner, S., Totty, N.F., Lemoine, N.R., Savopoulos, J., Gray, C.W., Creasy, C.L., Dingwall, C., *et al.* (2002). The serine protease Omi/HtrA2 regulates apoptosis by binding XIAP through a reaper-like motif. J Biol Chem *277*, 439-444.

Martins, L.M., Morrison, A., Klupsch, K., Fedele, V., Moisoi, N., Teismann, P., Abuin, A., Grau, E., Geppert, M., Livi, G.P., *et al.* (2004). Neuroprotective role of the Reaper-related serine protease HtrA2/Omi revealed by targeted deletion in mice. Mol Cell Biol *24*, 9848-9862.

Matsuda, N., Kitami, T., Suzuki, T., Mizuno, Y., Hattori, N., and Tanaka, K. (2006). Diverse effects of pathogenic mutations of Parkin that catalyze multiple monoubiquitylation in vitro. J Biol Chem *281*, 3204-3209.

Matsumine, H., Saito, M., Shimoda-Matsubayashi, S., Tanaka, H., Ishikawa, A., Nakagawa-Hattori, Y., Yokochi, M., Kobayashi, T., Igarashi, S., Takano, H., *et al.* (1997). Localization of a gene for an autosomal recessive form of juvenile Parkinsonism to chromosome 6q25.2-27. American Journal of Human Genetics *60*, 588-596.

Matsumoto, M.L., Wickliffe, K.E., Dong, K.C., Yu, C., Bosanac, I., Bustos, D., Phu, L., Kirkpatrick, D.S., Hymowitz, S.G., Rape, M., *et al.* (2010). K11-linked polyubiquitination in cell cycle control revealed by a K11 linkage-specific antibody. Mol Cell *39*, 477-484.

McCoy, M.K., Kaganovich, A., Rudenko, I.N., Ding, J., and Cookson, M.R. (2014). Hexokinase activity is required for recruitment of parkin to depolarized mitochondria. Human Molecular Genetics *23*, 145-156.

McNaught, K.S., Belizaire, R., Isacson, O., Jenner, P., and Olanow, C.W. (2003). Altered proteasomal function in sporadic Parkinson's disease. Exp Neurol *179*, 38-46.

Meyer-Schaller, N., Chou, Y.C., Sumara, I., Martin, D.D., Kurz, T., Katheder, N., Hofmann, K., Berthiaume, L.G., Sicheri, F., and Peter, M. (2009). The human Dcn1-like protein DCNL3 promotes Cul3 neddylation at membranes. Proc Natl Acad Sci U S A *106*, 12365-12370.

Mizuno, Y., Hattori, N., Yoshino, H., Hatano, Y., Satoh, K., Tomiyama, H., and Li, Y. (2006). Progress in familial Parkinson's disease. J Neural Transm Suppl, 191-204.

Mohamadi, F., Richard, N.G.J., Guida, W.C., Liskamp, R., Lipton, M., Caufield, C., Chang, G., Hendrickson, T., and Still, W.C. (1990). Macromodel—an integrated software system for modeling organic and bioorganic molecules using molecular mechanics. J Comput Chem *11*, 440-467.

Moisoi, N., Fedele, V., Edwards, J., and Martins, L.M. (2014). Loss of PINK1 enhances neurodegeneration in a mouse model of Parkinson's disease triggered by mitochondrial stress(). Neuropharmacology *77*, 350-357.

Moore, D.J., West, A.B., Dikeman, D.A., Dawson, V.L., and Dawson, T.M. (2008). Parkin mediates the degradation-independent ubiquitination of Hsp70. J Neurochem *105*, 1806-1819.

Mortiboys, H., Thomas, K.J., Koopman, W.J., Klaffke, S., Abou-Sleiman, P., Olpin, S., Wood, N.W., Willems, P.H., Smeitink, J.A., Cookson, M.R., *et al.* (2008). Mitochondrial function and morphology are impaired in parkin-mutant fibroblasts. Ann Neurol *64*, 555-565.

Muftuoglu, M., Elibol, B., Dalmizrak, O., Ercan, A., Kulaksiz, G., Ogus, H., Dalkara, T., and Ozer, N. (2004). Mitochondrial complex I and IV activities in leukocytes from patients with parkin mutations. Mov Disord *19*, 544-548.

Muqit, M.M., Davidson, S.M., Payne Smith, M.D., MacCormac, L.P., Kahns, S., Jensen, P.H., Wood, N.W., and Latchman, D.S. (2004). Parkin is recruited into aggresomes in a stress-specific manner: over-expression of parkin reduces aggresome formation but can be dissociated from parkin's effect on neuronal survival. Hum Mol Genet *13*, 117-135.

Nakamura, K., Nemani, V.M., Azarbal, F., Skibinski, G., Levy, J.M., Egami, K., Munishkina, L., Zhang, J., Gardner, B., Wakabayashi, J., *et al.* (2011). Direct Membrane Association Drives Mitochondrial Fission by the Parkinson Disease-associated Protein α-Synuclein. Journal of Biological Chemistry *286*, 20710-20726.

Nakaso, K., Adachi, Y., Yasui, K., Sakuma, K., and Nakashima, K. (2006). Detection of compound heterozygous deletions in the parkin gene of fibroblasts in patients with autosomal recessive hereditary parkinsonism (PARK2). Neurosci Lett *400*, 44-47.

Nandi, D., Tahiliani, P., Kumar, A., and Chandu, D. (2006). The ubiquitin-proteasome system. Journal of biosciences *31*, 137-155.

Narendra, D., Kane, L.A., Hauser, D.N., Fearnley, I.M., and Youle, R.J. (2010a). p62/SQSTM1 is required for Parkin-induced mitochondrial clustering but not mitophagy; VDAC1 is dispensable for both. Autophagy *6*, 1090-1106.

Narendra, D., Tanaka, A., Suen, D.F., and Youle, R.J. (2008). Parkin is recruited selectively to impaired mitochondria and promotes their autophagy. J Cell Biol *183*, 795-803.

Narendra, D., Walker, J.E., and Youle, R. (2012). Mitochondrial quality control mediated by PINK1 and Parkin: links to parkinsonism. Cold Spring Harbor Perspectives in Biology *4*.

Narendra, D.P., Jin, S.M., Tanaka, A., Suen, D.F., Gautier, C.A., Shen, J., Cookson, M.R., and Youle, R.J. (2010b). PINK1 is selectively stabilized on impaired mitochondria to activate Parkin. PLoS Biol *8*, e1000298.

Nathan, J.A., Tae Kim, H., Ting, L., Gygi, S.P., and Goldberg, A.L. (2013). Why do cellular proteins linked to K63-polyubiquitin chains not associate with proteasomes?, Vol 32.

Newhouse, K., Hsuan, S.L., Chang, S.H., Cai, B., Wang, Y., and Xia, Z. (2004). Rotenone-induced apoptosis is mediated by p38 and JNK MAP kinases in human dopaminergic SH-SY5Y cells. Toxicological sciences : an official journal of the Society of Toxicology *79*, 137-146.

O'Neill, L.A.J. (2009). Regulation of Signaling by Non-degradative Ubiquitination. Journal of Biological Chemistry *284*, 8209.

Ojeda, L., Gao, J., Hooten, K.G., Wang, E., Thonhoff, J.R., Dunn, T.J., Gao, T., and Wu, P. (2011). Critical Role of PI3K/Akt/GSK3β in Motoneuron Specification from Human Neural Stem Cells in Response to FGF2 and EGF. PLoS ONE *6*, e23414.

Okatsu, K., Saisho, K., Shimanuki, M., Nakada, K., Shitara, H., Sou, Y.S., Kimura, M., Sato, S., Hattori, N., Komatsu, M., *et al.* (2010). p62/SQSTM1 cooperates with Parkin for perinuclear clustering of depolarized mitochondria. Genes Cells *15*, 887-900.

Okita, K., Nakagawa, M., Hyenjong, H., Ichisaka, T., and Yamanaka, S. (2008). Generation of Mouse Induced Pluripotent Stem Cells Without Viral Vectors. Science *322*, 949-953.

Olzmann, J.A., and Chin, L.S. (2008). Parkin-mediated K63-linked polyubiquitination: a signal for targeting misfolded proteins to the aggresome-autophagy pathway. Autophagy *4*, 85-87.

Ordureau, A., Sarraf, S.A., Duda, D.M., Heo, J.M., Jedrychowski, M.P., Sviderskiy, V.O., Olszewski, J.L., Koerber, J.T., Xie, T., Beausoleil, S.A., *et al.* (2014). Quantitative proteomics reveal a feedforward mechanism for mitochondrial PARKIN translocation and ubiquitin chain synthesis. Mol Cell *56*, 360-375.

Ozawa, K., Komatsubara, A.T., Nishimura, Y., Sawada, T., Kawafune, H., Tsumoto, H., Tsuji, Y., Zhao, J., Kyotani, Y., Tanaka, T., *et al.* (2013). S-nitrosylation regulates mitochondrial quality control via activation of parkin. Sci Rep *3*.

Paisan-Ruiz, C., Bhatia, K.P., Li, A., Hernandez, D., Davis, M., Wood, N.W., Hardy, J., Houlden, H., Singleton, A., and Schneider, S.A. (2009). Characterization of PLA2G6 as a locus for dystonia-parkinsonism. Ann Neurol *65*, 19-23.

Paisán-Ruiz, C., Guevara, R., Federoff, M., Hanagasi, H., Sina, F., Elahi, E., Schneider, S.A., Schwingenschuh, P., Bajaj, N., Emre, M., *et al.* (2010). Early-onset L-dopa-responsive parkinsonism with pyramidal signs due to ATP13A2, PLA2G6, FBXO7 and spatacsin mutations. Movement Disorders *25*, 1791-1800.

Paisan-Ruiz, C., Jain, S., Evans, E.W., Gilks, W.P., Simon, J., van der Brug, M., Lopez de Munain, A., Aparicio, S., Gil, A.M., Khan, N., *et al.* (2004). Cloning of the gene containing mutations that cause PARK8-linked Parkinson's disease. Neuron *44*, 595-600.

Palacino, J.J., Sagi, D., Goldberg, M.S., Krauss, S., Motz, C., Wacker, M., Klose, J., and Shen, J. (2004). Mitochondrial dysfunction and oxidative damage in parkin-deficient mice. J Biol Chem *279*, 18614-18622.

Pallanck, L.J. (2010). Culling sick mitochondria from the herd. The Journal of Cell Biology *191*, 1225-1227.

Pan, T., Kondo, S., Le, W., and Jankovic, J. (2008). The role of autophagy-lysosome pathway in neurodegeneration associated with Parkinson's disease. Brain *131*, 1969-1978.

Pankiv, S., Clausen, T.H., Lamark, T., Brech, A., Bruun, J.-A., Outzen, H., Øvervatn, A., Bjørkøy, G., and Johansen, T. (2007). p62/SQSTM1 Binds Directly to Atg8/LC3 to Facilitate Degradation of Ubiquitinated Protein Aggregates by Autophagy. Journal of Biological Chemistry *282*, 24131-24145.

Pankratz, N., Nichols, W.C., Uniacke, S.K., Halter, C., Rudolph, A., Shults, C., Conneally, P.M., and Foroud, T. (2002). Genome screen to identify susceptibility genes for Parkinson disease in a sample without parkin mutations. Am J Hum Genet *71*, 124-135.

Park, J., Lee, S.B., Lee, S., Kim, Y., Song, S., Kim, S., Bae, E., Kim, J., Shong, M., Kim, J.M., *et al.* (2006). Mitochondrial dysfunction in Drosophila PINK1 mutants is complemented by parkin. Nature *441*, 1157-1161.

Peng, D.-J., Zeng, M., Muromoto, R., Matsuda, T., Shimoda, K., Subramaniam, M., Spelsberg, T.C., Wei, W.-Z., and Venuprasad, K. (2011). Noncanonical K27-Linked Polyubiquitination of TIEG1 Regulates Foxp3 Expression and Tumor Growth. Journal of immunology (Baltimore, Md : 1950) *186*, 5638-5647.

Perez, F.A., and Palmiter, R.D. (2005). Parkin-deficient mice are not a robust model of parkinsonism. Proc Natl Acad Sci U S A *102*, 2174-2179.

Periquet, M., Latouche, M., Lohmann, E., Rawal, N., De Michele, G., Ricard, S., Teive, H., Fraix, V., Vidailhet, M., Nicholl, D., *et al.* (2003). Parkin mutations are frequent in patients with isolated early-onset parkinsonism. Brain *126*, 1271-1278.

Pesah, Y., Pham, T., Burgess, H., Middlebrooks, B., Verstreken, P., Zhou, Y., Harding, M., Bellen, H., and Mardon, G. (2004). Drosophila parkin mutants have decreased mass and cell size and increased sensitivity to oxygen radical stress. Development *131*, 2183-2194.

Petrucelli, L., O'Farrell, C., Lockhart, P.J., Baptista, M., Kehoe, K., Vink, L., Choi, P., Wolozin, B., Farrer, M., Hardy, J., *et al.* (2002). Parkin Protects against the Toxicity Associated with Mutant α-Synuclein: Proteasome Dysfunction Selectively Affects Catecholaminergic Neurons. Neuron *36*, 1007-1019.

Picchio, M.C., Martin, E.S., Cesari, R., Calin, G.A., Yendamuri, S., Kuroki, T., Pentimalli, F., Sarti, M., Yoder, K., Kaiser, L.R., *et al.* (2004). Alterations of the tumor suppressor gene Parkin in non-small cell lung cancer. Clin Cancer Res *10*, 2720-2724.

Pickart, C.M., and Fushman, D. (2004). Polyubiquitin chains: polymeric protein signals. Curr Opin Chem Biol *8*, 610-616.

Pienaar, I.S., Gotz, J., and Feany, M.B. (2010). Parkinson's disease: insights from non-traditional model organisms. Prog Neurobiol *92*, 558-571.

Plautz, S.A., Boanca, G., Riethoven, J.J., and Pannier, A.K. (2011). Microarray analysis of gene expression profiles in cells transfected with nonviral vectors. Mol Ther *19*, 2144-2151.

Plun-Favreau, H., Klupsch, K., Moisoi, N., Gandhi, S., Kjaer, S., Frith, D., Harvey, K., Deas, E., Harvey, R.J., McDonald, N., *et al.* (2007). The mitochondrial protease HtrA2 is regulated by Parkinson's disease-associated kinase PINK1. Nat Cell Biol *9*, 1243-1252.

Polymeropoulos, M.H., Lavedan, C., Leroy, E., Ide, S.E., Dehejia, A., Dutra, A., Pike, B., Root, H., Rubenstein, J., Boyer, R., *et al.* (1997). Mutation in the alpha-synuclein gene identified in families with Parkinson's disease. Science *276*, 2045-2047.

Poole, A.C., Thomas, R.E., Andrews, L.A., McBride, H.M., Whitworth, A.J., and Pallanck, L.J. (2008). The PINK1/Parkin pathway regulates mitochondrial morphology. Proc Natl Acad Sci U S A *105*, 1638-1643.

Poole, A.C., Thomas, R.E., Yu, S., Vincow, E.S., and Pallanck, L. (2010). The Mitochondrial Fusion-Promoting Factor Mitofusin Is a Substrate of the PINK1/Parkin Pathway. PLoS One *5*, e10054.

Poulogiannis, G., McIntyre, R.E., Dimitriadi, M., Apps, J.R., Wilson, C.H., Ichimura, K., Luo, F., Cantley, L.C., Wyllie, A.H., Adams, D.J., *et al.* (2010). PARK2 deletions occur frequently in sporadic colorectal cancer and accelerate adenoma development in Apc mutant mice. Proc Natl Acad Sci U S A *107*, 15145-15150.

Pountney, D.L., Chegini, F., Shen, X., Blumbergs, P.C., and Gai, W.P. (2005). SUMO-1 marks subdomains within glial cytoplasmic inclusions of multiple system atrophy. Neurosci Lett *381*, 74-79.

Pridgeon, J.W., Olzmann, J.A., Chin, L.-S., and Li, L. (2007). PINK1 Protects against Oxidative Stress by Phosphorylating Mitochondrial Chaperone TRAP1. PLoS Biology *5*, e172.

Qian, L., and Flood, P.M. (2008). Microglial cells and Parkinson's disease. Immunologic research *41*, 155-164.

Quik, M. (2004). Smoking, nicotine and Parkinson's disease. Trends Neurosci *27*, 561-568.

Quinn, N., Critchley, P., and Marsden, C.D. (1987). Young onset Parkinson's disease. Movement Disorders *2*, 73-91.

Rafalski, V.A., and Brunet, A. (2011). Energy metabolism in adult neural stem cell fate. Progress in Neurobiology *93*, 182-203.

Rajput, A.H., and Uitti, R.J. (1988). Neurological disorders and services in Saskatchewan--a report based on provincial health care records. Neuroepidemiology *7*, 145-151.

Rajput, A.H., Uitti, R.J., Stern, W., and Laverty, W. (1986). Early onset Parkinson's disease in Saskatchewan--environmental considerations for etiology. Can J Neurol Sci *13*, 312-316.

Rakovic, A., Grünewald, A., Kottwitz, J., Brüggemann, N., Pramstaller, P.P., Lohmann, K., and Klein, C. (2011). Mutations in PINK1 and Parkin impair ubiquitination of Mitofusins in human fibroblasts. PLoS One *6*, e16746.

Rakovic, A., Shurkewitsch, K., Seibler, P., Grünewald, A., Zanon, A., Hagenah, J., Krainc, D., and Klein, C. (2013). Phosphatase and Tensin Homolog (PTEN)-induced Putative Kinase 1 (PINK1)-dependent Ubiquitination of Endogenous Parkin Attenuates Mitophagy: STUDY IN HUMAN PRIMARY FIBROBLASTS AND INDUCED PLURIPOTENT STEM CELL-DERIVED NEURONS. Journal of Biological Chemistry *288*, 2223-2237.

Ramirez, A., Heimbach, A., Grundemann, J., Stiller, B., Hampshire, D., Cid, L.P., Goebel, I., Mubaidin, A.F., Wriekat, A.L., Roeper, J., *et al.* (2006). Hereditary parkinsonism with dementia is caused by mutations in ATP13A2, encoding a lysosomal type 5 P-type ATPase. Nat Genet *38*, 1184-1191.

Rawal, N., Corti, O., Sacchetti, P., Ardilla-Osorio, H., Sehat, B., Brice, A., and Arenas, E. (2009). Parkin protects dopaminergic neurons from excessive Wnt/beta-catenin signaling. Biochem Biophys Res Commun *388*, 473-478.

Ren, Y., Jiang, H., Yang, F., Nakaso, K., and Feng, J. (2009). Parkin protects dopaminergic neurons against microtubule-depolymerizing toxins by attenuating microtubule-associated protein kinase activation. J Biol Chem *284*, 4009-4017.

Ren, Y., Zhao, J., and Feng, J. (2003). Parkin binds to alpha/beta tubulin and increases their ubiquitination and degradation. J Neurosci *23*, 3316-3324.

Riley, B.E., Lougheed, J.C., Callaway, K., Velasquez, M., Brecht, E., Nguyen, L., Shaler, T., Walker, D., Yang, Y., Regnstrom, K., *et al.* (2013). Structure and function of Parkin E3 ubiquitin ligase reveals aspects of RING and HECT ligases. Nat Commun *4*, 1982.

Ross, O.A., Braithwaite, A.T., Skipper, L.M., Kachergus, J., Hulihan, M.M., Middleton, F.A., Nishioka, K., Fuchs, J., Gasser, T., Maraganore, D.M., *et al.* (2008a). Genomic investigation of alpha-synuclein multiplication and parkinsonism. Ann Neurol *63*, 743-750.

Ross, O.A., Gosal, D., Stone, J.T., Lincoln, S.J., Heckman, M.G., Irvine, G.B., Johnston, J.A., Gibson, J.M., Farrer, M.J., and Lynch, T. (2007). Familial genes in sporadic disease: common variants of alpha-synuclein gene associate with Parkinson's disease. Mech Ageing Dev *128*, 378-382.

Ross, O.A., Wu, Y.R., Lee, M.C., Funayama, M., Chen, M.L., Soto, A.I., Mata, I.F., Lee-Chen, G.J., Chen, C.M., Tang, M., *et al.* (2008b). Analysis of Lrrk2 R1628P as a risk factor for Parkinson's disease. Ann Neurol *64*, 88-92.

Rubio de la Torre, E., Luzon-Toro, B., Forte-Lago, I., Minguez-Castellanos, A., Ferrer, I., and Hilfiker, S. (2009). Combined kinase inhibition modulates parkin inactivation. Hum Mol Genet *18*, 809-823.

Salam, N.K., Nuti, R., and Sherman, W. (2009). Novel method for generating structure-based pharmacophores using energetic analysis. Journal of chemical information and modeling *49*, 2356-2368.

Samali, A., Cai, J., Zhivotovsky, B., Jones, D.P., and Orrenius, S. (1999). Presence of a pre-apoptotic complex of pro-caspase-3, Hsp60 and Hsp10 in the mitochondrial fraction of Jurkat cells. EMBO J *18*, 2040-2048.

Sandebring A, and A, C.-M. (2012). Parkin-an E3 ubiquitin ligase with multiple substrates. J Alzhemers Dis Parkinsonism *S10*.

Sarraf, S.A., Raman, M., Guarani-Pereira, V., Sowa, M.E., Huttlin, E.L., Gygi, S.P., and Harper, J.W. (2013). Landscape of the PARKIN-dependent ubiquitylome in response to mitochondrial depolarization. Nature *496*, 372-376.

Satake, W., Nakabayashi, Y., Mizuta, I., Hirota, Y., Ito, C., Kubo, M., Kawaguchi, T., Tsunoda, T., Watanabe, M., Takeda, A., *et al.* (2009). Genome-wide association study identifies common variants at four loci as genetic risk factors for Parkinson's disease. Nat Genet *41*, 1303-1307.

Sato, S., Chiba, T., Sakata, E., Kato, K., Mizuno, Y., Hattori, N., and Tanaka, K. (2006). 14-3-3eta is a novel regulator of parkin ubiquitin ligase. EMBO J *25*, 211-221.

Schapira, A.H., Cooper, J.M., Dexter, D., Clark, J.B., Jenner, P., and Marsden, C.D. (1990). Mitochondrial complex I deficiency in Parkinson's disease. J Neurochem *54*, 823-827.

Schapira, A.H.V. (2006). Etiology of Parkinson’s disease. Neurology *66*, S10-S23.

Schapira, A.H.V., Cooper, J.M., Dexter, D., Jenner, P., Clark, J.B., and Marsden, C.D. (1989). MITOCHONDRIAL COMPLEX I DEFICIENCY IN PARKINSON'S DISEASE. The Lancet *333*, 1269.

Schlossmacher, M.G., Frosch, M.P., Gai, W.P., Medina, M., Sharma, N., Forno, L., Ochiishi, T., Shimura, H., Sharon, R., Hattori, N., *et al.* (2002). Parkin localizes to the Lewy bodies of Parkinson disease and dementia with Lewy bodies. Am J Pathol *160*, 1655-1667.

Schrödinger (2013). Biologics Suite. In BioLuminate, version 11, Schrodinger, ed. (New York, NY, 2013: Schrödinger, LLC).

Schulman, B.A., and Harper, J.W. (2009). Ubiquitin-like protein activation by E1 enzymes: the apex for downstream signalling pathways. Nat Rev Mol Cell Biol *10*, 319-331.

Scuderi, S., La Cognata, V., Drago, F., Cavallaro, S., and D'Agata, V. (2014). Alternative Splicing Generates Different Parkin Protein Isoforms: Evidences in Human, Rat, and Mouse Brain. BioMed Research International *2014*, 14.

Seibenhener, M.L., Du, Y., Diaz-Meco, M.-T., Moscat, J., Wooten, M.C., and Wooten, M.W. (2013). A role for sequestosome 1/p62 in mitochondrial dynamics, import and genome integrity. Biochimica et Biophysica Acta (BBA) - Molecular Cell Research *1833*, 452-459.

Seibler, P., Graziotto, J., Jeong, H., Simunovic, F., Klein, C., and Krainc, D. (2011). Mitochondrial Parkin recruitment is impaired in neurons derived from mutant PINK1 induced pluripotent stem cells. J Neurosci *31*, 5970-5976.

Sha, D., Chin, L.S., and Li, L. (2010). Phosphorylation of parkin by Parkinson disease-linked kinase PINK1 activates parkin E3 ligase function and NF-kappaB signaling. Hum Mol Genet *19*, 352-363.

Sheppard, K., Kinross, K.M., Solomon, B., Pearson, R.B., and Phillips, W.A. (2012). Targeting PI3 kinase/AKT/mTOR signaling in cancer. Critical reviews in oncogenesis *17*, 69-95.

Sheridan, C., and Martin, S.J. (2010). Mitochondrial fission/fusion dynamics and apoptosis. Mitochondrion *10*, 640-648.

Shi, Y., Desponts, C., Do, J.T., Hahm, H.S., Schöler, H.R., and Ding, S. Induction of Pluripotent Stem Cells from Mouse Embryonic Fibroblasts by Oct4 and Klf4 with Small-Molecule Compounds. Cell Stem Cell *3*, 568-574.

Shiba-Fukushima, K., Imai, Y., Yoshida, S., Ishihama, Y., Kanao, T., Sato, S., and Hattori, N. (2012). PINK1-mediated phosphorylation of the Parkin ubiquitin-like domain primes mitochondrial translocation of Parkin and regulates mitophagy. Sci Rep *2*, 1002.

Shiba-Fukushima, K., Inoshita, T., Hattori, N., and Imai, Y. (2014). PINK1-mediated phosphorylation of parkin boosts parkin activity in drosophila. PLoS Genet *10*, e1004391.

Shimura, H., Hattori, N., Kubo, S., Mizuno, Y., Asakawa, S., Minoshima, S., Shimizu, N., Iwai, K., Chiba, T., Tanaka, K., *et al.* (2000). Familial Parkinson disease gene product, parkin, is a ubiquitin-protein ligase. Nat Genet *25*, 302-305.

Shimura, H., Hattori, N., Kubo, S., Yoshikawa, M., Kitada, T., Matsumine, H., Asakawa, S., Minoshima, S., Yamamura, Y., Shimizu, N., *et al.* (1999). Immunohistochemical and subcellular localization of Parkin protein: absence of protein in autosomal recessive juvenile parkinsonism patients. Ann Neurol *45*, 668-672.

Shojaee, S., Sina, F., Banihosseini, S.S., Kazemi, M.H., Kalhor, R., Shahidi, G.A., Fakhrai-Rad, H., Ronaghi, M., and Elahi, E. (2008). Genome-wide linkage analysis of a Parkinsonian-pyramidal syndrome pedigree by 500 K SNP arrays. Am J Hum Genet *82*, 1375-1384.

Shulman, J.M., De Jager, P.L., and Feany, M.B. (2011). Parkinson's Disease: Genetics and Pathogenesis. Annual Review of Pathology: Mechanisms of Disease *6*, 193-222.

Shults, C.W. (2006). Lewy bodies. Proc Natl Acad Sci U S A *103*, 1661-1668.

Sidransky, E., Nalls, M.A., Aasly, J.O., Aharon-Peretz, J., Annesi, G., Barbosa, E.R., Bar-Shira, A., Berg, D., Bras, J., Brice, A., *et al.* (2009). Multicenter analysis of glucocerebrosidase mutations in Parkinson's disease. N Engl J Med *361*, 1651-1661.

Simon-Sanchez, J., Schulte, C., Bras, J.M., Sharma, M., Gibbs, J.R., Berg, D., Paisan-Ruiz, C., Lichtner, P., Scholz, S.W., Hernandez, D.G., *et al.* (2009). Genome-wide association study reveals genetic risk underlying Parkinson's disease. Nat Genet *41*, 1308-1312.

Singleton, A.B., Farrer, M., Johnson, J., Singleton, A., Hague, S., Kachergus, J., Hulihan, M., Peuralinna, T., Dutra, A., Nussbaum, R., *et al.* (2003). alpha-Synuclein locus triplication causes Parkinson's disease. Science *302*, 841.

Skowyra, D., Craig, K.L., Tyers, M., Elledge, S.J., and Harper, J.W. (1997). F-box proteins are receptors that recruit phosphorylated substrates to the SCF ubiquitin-ligase complex. Cell *91*, 209-219.

Sly, W.S., and Grubb, J. (1979). Isolation of fibroblasts from patients. Methods Enzymol *58*, 444-450.

Smit, J.J., Monteferrario, D., Noordermeer, S.M., van Dijk, W.J., van der Reijden, B.A., and Sixma, T.K. (2012). The E3 ligase HOIP specifies linear ubiquitin chain assembly through its RING-IBR-RING domain and the unique LDD extension. EMBO J *31*, 3833-3844.

Spillantini, M.G., Schmidt, M.L., Lee, V.M., Trojanowski, J.Q., Jakes, R., and Goedert, M. (1997). Alpha-synuclein in Lewy bodies. Nature *388*, 839-840.

Spratt, D.E., Julio Martinez-Torres, R., Noh, Y.J., Mercier, P., Manczyk, N., Barber, K.R., Aguirre, J.D., Burchell, L., Purkiss, A., Walden, H., *et al.* (2013). A molecular

explanation for the recessive nature of parkin-linked Parkinson's disease. Nat Commun *4*, 1983.

Sriram, S.R., Li, X., Ko, H.S., Chung, K.K., Wong, E., Lim, K.L., Dawson, V.L., and Dawson, T.M. (2005). Familial-associated mutations differentially disrupt the solubility, localization, binding and ubiquitination properties of parkin. Hum Mol Genet *14*, 2571-2586.

Staropoli, J.F., McDermott, C., Martinat, C., Schulman, B., Demireva, E., and Abeliovich, A. (2003). Parkin is a component of an SCF-like ubiquitin ligase complex and protects postmitotic neurons from kainate excitotoxicity. Neuron *37*, 735-749.

Stieglitz, B., Morris-Davies, A.C., Koliopoulos, M.G., Christodoulou, E., and Rittinger, K. (2012). LUBAC synthesizes linear ubiquitin chains via a thioester intermediate. EMBO Rep *13*, 840-846.

Stokes, A.H., Hastings, T.G., and Vrana, K.E. (1999). Cytotoxic and genotoxic potential of dopamine. J Neurosci Res *55*, 659-665.

Strauss, K.M., Martins, L.M., Plun-Favreau, H., Marx, F.P., Kautzmann, S., Berg, D., Gasser, T., Wszolek, Z., Muller, T., Bornemann, A., *et al.* (2005). Loss of function mutations in the gene encoding Omi/HtrA2 in Parkinson's disease. Hum Mol Genet *14*, 2099-2111.

Suen, D.-F., Narendra, D.P., Tanaka, A., Manfredi, G., and Youle, R.J. (2010). Parkin overexpression selects against a deleterious mtDNA mutation in heteroplasmic cybrid cells. Proceedings of the National Academy of Sciences *107*, 11835-11840.

Sun, M., Latourelle, J.C., Wooten, G.F., Lew, M.F., Klein, C., Shill, H.A., Golbe, L.I., Mark, M.H., Racette, B.A., Perlmutter, J.S., *et al.* (2006). Influence of heterozygosity for parkin mutation on onset age in familial Parkinson disease: the GenePD study. Arch Neurol *63*, 826-832.

Sunada, Y., Saito, F., Matsumura, K., and Shimizu, T. (1998). Differential expression of the parkin gene in the human brain and peripheral leukocytes. Neurosci Lett *254*, 180-182.

Sunico, C., Nakamura, T., Rockenstein, E., Mante, M., Adame, A., Chan, S., Newmeyer, T., Masliah, E., Nakanishi, N., and Lipton, S. (2013). S-Nitrosylation of parkin as a novel regulator of p53-mediated neuronal cell death in sporadic Parkinson's disease. Molecular Neurodegeneration *8*, 29.

Takahashi, K., Tanabe, K., Ohnuki, M., Narita, M., Ichisaka, T., Tomoda, K., and Yamanaka, S. (2007). Induction of pluripotent stem cells from adult human fibroblasts by defined factors. Cell *131*, 861-872.

Tan, E.K., Shen, H., Tan, J.M., Lim, K.L., Fook-Chong, S., Hu, W.P., Paterson, M.C., Chandran, V.R., Yew, K., Tan, C., *et al.* (2005). Differential expression of

splice variant and wild-type parkin in sporadic Parkinson's disease. Neurogenetics *6*, 179-184.

Tan, J.M.M., Wong, E.S.P., Kirkpatrick, D.S., Pletnikova, O., Ko, H.S., Tay, S.-P., Ho, M.W.L., Troncoso, J., Gygi, S.P., Lee, M.K., *et al.* (2008). Lysine 63-linked ubiquitination promotes the formation and autophagic clearance of protein inclusions associated with neurodegenerative diseases. Human Molecular Genetics *17*, 431-439.

Tanaka, A. (2010). Parkin-mediated selective mitochondrial autophagy, mitophagy: Parkin purges damaged organelles from the vital mitochondrial network. FEBS Lett *584*, 1386-1392.

Tanaka, A., Cleland, M.M., Xu, S., Narendra, D.P., Suen, D.F., Karbowski, M., and Youle, R.J. (2010). Proteasome and p97 mediate mitophagy and degradation of mitofusins induced by Parkin. J Cell Biol *191*, 1367-1380.

Tanner, C.M., and Goldman, S.M. (1996). Epidemiology of Parkinson's disease. Neurol Clin *14*, 317-335.

Tay, S.P., Yeo, C.W., Chai, C., Chua, P.J., Tan, H.M., Ang, A.X., Yip, D.L., Sung, J.X., Tan, P.H., Bay, B.H., *et al.* (2010). Parkin enhances the expression of cyclin-dependent kinase 6 and negatively regulates the proliferation of breast cancer cells. J Biol Chem *285*, 29231-29238.

Thomas, B., and Beal, M.F. (2007). Parkinson's disease. Hum Mol Genet *16 Spec No. 2*, R183-194.

Thomas, K.J., McCoy, M.K., Blackinton, J., Beilina, A., van der Brug, M., Sandebring, A., Miller, D., Maric, D., Cedazo-Minguez, A., and Cookson, M.R. (2011). DJ-1 acts in parallel to the PINK1/parkin pathway to control mitochondrial function and autophagy. Human Molecular Genetics *20*, 40-50.

Timmons, S., Coakley, M.F., Moloney, A.M., and C, O.N. (2009). Akt signal transduction dysfunction in Parkinson's disease. Neurosci Lett *467*, 30-35.

Tokgoz, Z., Bohnsack, R.N., and Haas, A.L. (2006). Pleiotropic effects of ATP.Mg2+ binding in the catalytic cycle of ubiquitin-activating enzyme. J Biol Chem *281*, 14729-14737.

Trempe, J.-F., Sauvé, V., Grenier, K., Seirafi, M., Tang, M.Y., Ménade, M., Al-Abdul-Wahid, S., Krett, J., Wong, K., Kozlov, G., *et al.* (2013). Structure of Parkin Reveals Mechanisms for Ubiquitin Ligase Activation. Science *340*, 1451-1455.

Tsai, Y.C., Fishman, P.S., Thakor, N.V., and Oyler, G.A. (2003). Parkin facilitates the elimination of expanded polyglutamine proteins and leads to preservation of proteasome function. J Biol Chem *278*, 22044-22055.

Twelves, D., Perkins, K.S., and Counsell, C. (2003). Systematic review of incidence studies of Parkinson's disease. Mov Disord *18*, 19-31.

Um, J.W., and Chung, K.C. (2006). Functional modulation of parkin through physical interaction with SUMO-1. J Neurosci Res *84*, 1543-1554.

Um, J.W., Han, K.A., Im, E., Oh, Y., Lee, K., and Chung, K.C. (2012). Neddylation positively regulates the ubiquitin E3 ligase activity of parkin. J Neurosci Res *90*, 1030-1042.

Um, J.W., Min, D.S., Rhim, H., Kim, J., Paik, S.R., and Chung, K.C. (2006). Parkin Ubiquitinates and Promotes the Degradation of RanBP2. Journal of Biological Chemistry *281*, 3595-3603.

Um, J.W., Stichel-Gunkel, C., Lubbert, H., Lee, G., and Chung, K.C. (2009). Molecular interaction between parkin and PINK1 in mammalian neuronal cells. Mol Cell Neurosci *40*, 421-432.

Valente, E.M., Abou-Sleiman, P.M., Caputo, V., Muqit, M.M., Harvey, K., Gispert, S., Ali, Z., Del Turco, D., Bentivoglio, A.R., Healy, D.G., *et al.* (2004). Hereditary early-onset Parkinson's disease caused by mutations in PINK1. Science *304*, 1158-1160.

Van Humbeeck, C., Cornelissen, T., Hofkens, H., Mandemakers, W., Gevaert, K., De Strooper, B., and Vandenberghe, W. (2011). Parkin interacts with Ambra1 to induce mitophagy. The Journal of Neuroscience *31*, 10249-10261.

Van Laar, V.S., Arnold, B., Cassady, S.J., Chu, C.T., Burton, E.A., and Berman, S.B. (2011). Bioenergetics of neurons inhibit the translocation response of Parkin following rapid mitochondrial depolarization. Hum Mol Genet *20*, 927-940.

van Wijk, S.J.L., and Timmers, H.T.M. (2010). The family of ubiquitin-conjugating enzymes (E2s): deciding between life and death of proteins. The FASEB Journal *24*, 981-993.

Veeriah, S., Taylor, B.S., Meng, S., Fang, F., Yilmaz, E., Vivanco, I., Janakiraman, M., Schultz, N., Hanrahan, A.J., Pao, W., *et al.* (2010). Somatic mutations of the Parkinson's disease-associated gene PARK2 in glioblastoma and other human malignancies. Nat Genet *42*, 77-82.

Verhagen, A.M., Silke, J., Ekert, P.G., Pakusch, M., Kaufmann, H., Connolly, L.M., Day, C.L., Tikoo, A., Burke, R., Wrobel, C., *et al.* (2002). HtrA2 promotes cell death through its serine protease activity and its ability to antagonize inhibitor of apoptosis proteins. J Biol Chem *277*, 445-454.

Viotti, J., Duplan, E., Caillava, C., Condat, J., Goiran, T., Giordano, C., Marie, Y., Idbaih, A., Delattre, J.Y., Honnorat, J., *et al.* (2014). Glioma tumor grade correlates with parkin depletion in mutant p53-linked tumors and results from loss of function of p53 transcriptional activity. Oncogene *33*, 1764-1775.

Virdee, S., Ye, Y., Nguyen, D.P., Komander, D., and Chin, J.W. (2010). Engineered diubiquitin synthesis reveals Lys29-isopeptide specificity of an OTU deubiquitinase. Nat Chem Biol *6*, 750-757.

Vives-Bauza, C., Zhou, C., Huang, Y., Cui, M., de Vries, R.L., Kim, J., May, J., Tocilescu, M.A., Liu, W., Ko, H.S., *et al.* (2010). PINK1-dependent recruitment of Parkin to mitochondria in mitophagy. Proc Natl Acad Sci U S A *107*, 378-383.

Wang, C., Ko, H.S., Thomas, B., Tsang, F., Chew, K.C., Tay, S.P., Ho, M.W., Lim, T.M., Soong, T.W., Pletnikova, O., *et al.* (2005a). Stress-induced alterations in parkin solubility promote parkin aggregation and compromise parkin's protective function. Hum Mol Genet *14*, 3885-3897.

Wang, C., Tan, J.M., Ho, M.W., Zaiden, N., Wong, S.H., Chew, C.L., Eng, P.W., Lim, T.M., Dawson, T.M., and Lim, K.L. (2005b). Alterations in the solubility and intracellular localization of parkin by several familial Parkinson's disease-linked point mutations. J Neurochem *93*, 422-431.

Wang, F., Denison, S., Lai, J.P., Philips, L.A., Montoya, D., Kock, N., Schule, B., Klein, C., Shridhar, V., Roberts, L.R., *et al.* (2004). Parkin gene alterations in hepatocellular carcinoma. Genes, chromosomes & cancer *40*, 85-96.

Wang, H., Song, P., Du, L., Tian, W., Yue, W., Liu, M., Li, D., Wang, B., Zhu, Y., Cao, C., *et al.* (2011a). Parkin ubiquitinates Drp1 for proteasome-dependent degradation: implication of dysregulated mitochondrial dynamics in Parkinson disease. Journal of Biological Chemistry *286*, 11649-11658.

Wang, X., Winter, D., Ashrafi, G., Schlehe, J., Wong, Yao L., Selkoe, D., Rice, S., Steen, J., LaVoie, Matthew J., and Schwarz, Thomas L. (2011b). PINK1 and Parkin target Miro for phosphorylation and degradation to arrest mitochondrial motility. Cell *147*, 893-906.

Wauer, T., and Komander, D. (2013). Structure of the human Parkin ligase domain in an autoinhibited state. EMBO J *32*, 2099-2112.

Weissman, A.M. (1997). Regulating protein degradation by ubiquitination. Immunol Today *18*, 189-198.

Wells, A. (1999). EGF receptor. Int J Biochem Cell Biol *31*, 637-643.

Wenzel, D.M., and Klevit, R.E. (2012). Following Ariadne's thread: a new perspective on RBR ubiquitin ligases. BMC Biol *10*, 24.

Wenzel, D.M., Lissounov, A., Brzovic, P.S., and Klevit, R.E. (2011). UBCH7 reactivity profile reveals parkin and HHARI to be RING/HECT hybrids. Nature *474*, 105-108.

West, A., Periquet, M., Lincoln, S., Lucking, C.B., Nicholl, D., Bonifati, V., Rawal, N., Gasser, T., Lohmann, E., Deleuze, J.F., *et al.* (2002). Complex relationship between Parkin mutations and Parkinson disease. Am J Med Genet *114*, 584-591.

West, A.B., Moore, D.J., Biskup, S., Bugayenko, A., Smith, W.W., Ross, C.A., Dawson, V.L., and Dawson, T.M. (2005). Parkinson's disease-associated mutations in leucine-rich repeat kinase 2 augment kinase activity. Proceedings of the National Academy of Sciences of the United States of America *102*, 16842-16847.

Whalley, K. (2009). Neuronal metabolism: A question of balance. Nat Rev Neurosci *10*, 472-473.

Wider, C., Ross, O.A., and Wszolek, Z.K. (2010). Genetics of Parkinson disease and essential tremor. Current opinion in neurology *23*, 388-393.

Wiedemann, N., Stiller, Sebastian B., and Pfanner, N. (2013). Activation and Degradation of Mitofusins: Two Pathways Regulate Mitochondrial Fusion by Reversible Ubiquitylation. Molecular Cell *49*, 423-425.

Wilkinson, K.D. (1995). Roles of ubiquitinylation in proteolysis and cellular regulation. Annu Rev Nutr *15*, 161-189.

Winklhofer, K.F. (2007). The parkin protein as a therapeutic target in Parkinson's disease. Expert Opin Ther Targets *11*, 1543-1552.

Winklhofer, K.F. (2014). Parkin and mitochondrial quality control: toward assembling the puzzle. Trends Cell Biol *24*, 332-341.

Winklhofer, K.F., Henn, I.H., Kay-Jackson, P.C., Heller, U., and Tatzelt, J. (2003). Inactivation of parkin by oxidative stress and C-terminal truncations: a protective role of molecular chaperones. J Biol Chem *278*, 47199-47208.

Woltjen, K., Michael, I.P., Mohseni, P., Desai, R., Mileikovsky, M., Hamalainen, R., Cowling, R., Wang, W., Liu, P., Gertsenstein, M., *et al.* (2009). piggyBac transposition reprograms fibroblasts to induced pluripotent stem cells. Nature *458*, 766-770.

Wong, E.S., Tan, J.M., Wang, C., Zhang, Z., Tay, S.P., Zaiden, N., Ko, H.S., Dawson, V.L., Dawson, T.M., and Lim, K.L. (2007). Relative sensitivity of parkin and other cysteine-containing enzymes to stress-induced solubility alterations. J Biol Chem *282*, 12310-12318.

Woodroof, H.I., Pogson, J.H., Begley, M., Cantley, L.C., Deak, M., Campbell, D.G., van Aalten, D.M.F., Whitworth, A.J., Alessi, D.R., and Muqit, M.M.K. (2011). Discovery of catalytically active orthologues of the Parkinson's disease kinase PINK1: analysis of substrate specificity and impact of mutations, Vol 1.

Xie, W., and Chung, K.K.K. (2012). Alpha-synuclein impairs normal dynamics of mitochondria in cell and animal models of Parkinson’s disease. Journal of Neurochemistry *122*, 404-414.

Xiromerisiou, G., Hadjigeorgiou, G.M., Papadimitriou, A., Katsarogiannis, E., Gourbali, V., and Singleton, A.B. (2008). Association between AKT1 gene and Parkinson's disease: a protective haplotype. Neurosci Lett *436*, 232-234.

Xu, Y., Stokes, A.H., Roskoski, R., Jr., and Vrana, K.E. (1998). Dopamine, in the presence of tyrosinase, covalently modifies and inactivates tyrosine hydroxylase. J Neurosci Res *54*, 691-697.

Yamamoto, A., Friedlein, A., Imai, Y., Takahashi, R., Kahle, P.J., and Haass, C. (2005). Parkin phosphorylation and modulation of its E3 ubiquitin ligase activity. J Biol Chem *280*, 3390-3399.

Yang, Y., Gehrke, S., Haque, M.E., Imai, Y., Kosek, J., Yang, L., Beal, M.F., Nishimura, I., Wakamatsu, K., Ito, S., *et al.* (2005). Inactivation of Drosophila DJ-1 leads to impairments of oxidative stress response and phosphatidylinositol 3-kinase/Akt signaling. Proc Natl Acad Sci U S A *102*, 13670-13675.

Yang, Y., Gehrke, S., Imai, Y., Huang, Z., Ouyang, Y., Wang, J.W., Yang, L., Beal, M.F., Vogel, H., and Lu, B. (2006). Mitochondrial pathology and muscle and dopaminergic neuron degeneration caused by inactivation of Drosophila Pink1 is rescued by Parkin. Proc Natl Acad Sci U S A *103*, 10793-10798.

Yang, Y., Ouyang, Y., Yang, L., Beal, M.F., McQuibban, A., Vogel, H., and Lu, B. (2008). Pink1 regulates mitochondrial dynamics through interaction with the fission/fusion machinery. Proc Natl Acad Sci U S A *105*, 7070-7075.

Yao, D., Gu, Z., Nakamura, T., Shi, Z.Q., Ma, Y., Gaston, B., Palmer, L.A., Rockenstein, E.M., Zhang, Z., Masliah, E., *et al.* (2004). Nitrosative stress linked to sporadic Parkinson's disease: S-nitrosylation of parkin regulates its E3 ubiquitin ligase activity. Proc Natl Acad Sci U S A *101*, 10810-10814.

Yip, W.K., and Seow, H.F. (2012). Activation of phosphatidylinositol 3-kinase/Akt signaling by EGF downregulates membranous E-cadherin and β-catenin and enhances invasion in nasopharyngeal carcinoma cells. Cancer Letters *318*, 162-172.

Yoshii, S.R., Kishi, C., Ishihara, N., and Mizushima, N. (2011). Parkin mediates proteasome-dependent protein degradation and rupture of the outer mitochondrial membrane. Journal of Biological Chemistry *286*, 19630-19640.

Youle, R.J., and Narendra, D.P. (2011). Mechanisms of mitophagy. Nat Rev Mol Cell Biol *12*, 9-14.

Yu, J., Vodyanik, M.A., Smuga-Otto, K., Antosiewicz-Bourget, J., Frane, J.L., Tian, S., Nie, J., Jonsdottir, G.A., Ruotti, V., Stewart, R., *et al.* (2007). Induced pluripotent stem cell lines derived from human somatic cells. Science *318*, 1917-1920.

Zarranz, J.J., Alegre, J., Gomez-Esteban, J.C., Lezcano, E., Ros, R., Ampuero, I., Vidal, L., Hoenicka, J., Rodriguez, O., Atares, B., *et al.* (2004). The new mutation, E46K, of alpha-synuclein causes Parkinson and Lewy body dementia. Ann Neurol *55*, 164-173.

Zhang, Y., Gao, J., Chung, K.K., Huang, H., Dawson, V.L., and Dawson, T.M. (2000). Parkin functions as an E2-dependent ubiquitin- protein ligase and promotes the degradation of the synaptic vesicle-associated protein, CDCrel-1. Proc Natl Acad Sci U S A *97*, 13354-13359.

Zhang, Y.J., Caulfield, T., Xu, Y.F., Gendron, T.F., Hubbard, J., Stetler, C., Sasaguri, H., Whitelaw, E.C., Cai, S., Lee, W.C., *et al.* (2013). The dual functions of the

extreme N-terminus of TDP-43 in regulating its biological activity and inclusion formation. Hum Mol Genet.

Zhang, Y.Q., and Sarge, K.D. (2008). Sumoylation of amyloid precursor protein negatively regulates Abeta aggregate levels. Biochem Biophys Res Commun *374*, 673-678.

Zhou, H., Wu, S., Joo, J.Y., Zhu, S., Han, D.W., Lin, T., Trauger, S., Bien, G., Yao, S., Zhu, Y., *et al.* (2009). Generation of induced pluripotent stem cells using recombinant proteins. Cell Stem Cell *4*, 381-384.

Zhou, W., and Freed, C.R. (2009). Adenoviral Gene Delivery Can Reprogram Human Fibroblasts to Induced Pluripotent Stem Cells. STEM CELLS *27*, 2667-2674.

Zhou, W., Zhu, M., Wilson, M.A., Petsko, G.A., and Fink, A.L. (2006). The oxidation state of DJ-1 regulates its chaperone activity toward alpha-synuclein. Journal of molecular biology *356*, 1036-1048.

Zielasek, J., and Hartung, H.P. (1996). Molecular mechanisms of microglial activation. Advances in neuroimmunology *6*, 191-122.

Zimprich, A., Biskup, S., Leitner, P., Lichtner, P., Farrer, M., Lincoln, S., Kachergus, J., Hulihan, M., Uitti, R.J., Calne, D.B., *et al.* (2004). Mutations in LRRK2 cause autosomal-dominant parkinsonism with pleomorphic pathology. Neuron *44*, 601-607.

Ziviani, E., Tao, R.N., and Whitworth, A.J. (2010). Drosophila parkin requires PINK1 for mitochondrial translocation and ubiquitinates mitofusin. Proc Natl Acad Sci U S A *107*, 5018-5023.

Ziviani, E., and Whitworth, A.J. (2010). How could Parkin-mediated ubiquitination of mitofusin promote mitophagy? Autophagy *6*, 660-662.